NTNU – Trondheim
Norwegian University of
Science and Technology

Evaluation of a North Sea oil platform using exergy analysis

Knut Jøssang

NTNU

Norwegian University
of Science and Technology

Department of Energy
and Process Engineering

EPT-M-2013-64

MASTER THESIS

for

student Knut Jøssang

Spring 2013

Evaluation of a North Sea oil platform using exergy analysis
Vurdering av oljeplattform i Nordsjøen ved eksergianalyse

Background and objective

The typical power consumption at a Norwegian continental shelf platform rages from approx. 10 MW to several 100 MW. Most platforms generate their own power with gas turbines and diesel engines. In 2008, gas turbines and diesel engines on oil platforms caused 21 % of Norway's total CO_2 emissions. Reduction in power consumption at the continental shelf is therefore an important challenge.

There is a need for a tool to evaluate the performance of such offshore platforms. CO_2 per produced oil is often used. However, different platforms have different operating conditions. Exergy efficiency is an alternative performance parameter where operating conditions are taken into account. Also, by doing an exergy analysis, one can indicate the potential for reduction in power consumption in the process.

The master thesis work, continuing the specialization project from autumn 2012, is connected to an ongoing PhD thesis project at NTNU, on the same topic (other platforms). The project is in collaboration with Statoil.

The following tasks are to be considered:

- When relevant, update the conducted literature study of exergy analysis and its use for oil and gas platforms and other process plants.
- Refining and extending the existing HYSYS model of the oil and gas processes of an offshore oil platform, including the power turbines, hot oil system and cooling water system.
- In cooperation with supervisors, select cases to be studied based on available data.
- Conduct exergy analyses of the cases, determining the exergy exchanges, efficiencies and irreversibilities of the processes. Discussion of the results.

-- " --

Within 14 days of receiving the written text on the master thesis, the candidate shall submit a research plan for his project to the department.

When the thesis is evaluated, emphasis is put on processing of the results, and that they are presented in tabular and/or graphic form in a clear manner, and that they are analyzed carefully.

The thesis should be formulated as a research report with summary both in English and Norwegian, conclusion, literature references, table of contents etc. During the preparation of the text, the candidate should make an effort to produce a well-structured and easily readable report. In order to ease the evaluation of the thesis, it is important that the cross-references are correct. In the making of the report, strong emphasis should be placed on both a thorough discussion of the results and an orderly presentation.

The candidate is requested to initiate and keep close contact with his/her academic supervisor(s) throughout the working period. The candidate must follow the rules and regulations of NTNU as well as passive directions given by the Department of Energy and Process Engineering.
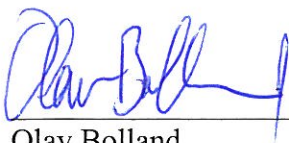
Risk assessment of the candidate's work shall be carried out according to the department's procedures. The risk assessment must be documented and included as part of the final report. Events related to the candidate's work adversely affecting the health, safety or security, must be documented and included as part of the final report. If the documentation on risk assessment represents a large number of pages, the full version is to be submitted electronically to the supervisor and an excerpt is included in the report.

Pursuant to "Regulations concerning the supplementary provisions to the technology study program/Master of Science" at NTNU §20, the Department reserves the permission to utilize all the results and data for teaching and research purposes as well as in future publications.

The final report is to be submitted digitally in DAIM. An executive summary of the thesis including title, student's name, supervisor's name, year, department name, and NTNU's logo and name, shall be submitted to the department as a separate pdf file. Based on an agreement with the supervisor, the final report and other material and documents may be given to the supervisor in digital format.

☐ Work to be done in lab (Water power lab, Fluids engineering lab, Thermal engineering lab)
☐ Field work

Department of Energy and Process Engineering, 14 January 2013

Olav Bolland
Department Head

Ivar S. Ertesvåg
Academic Supervisor

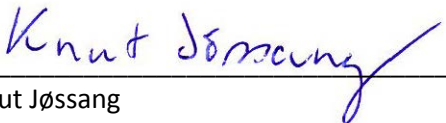Co-supervisor: Mari Voldsund, PhD candidate, Department of Chemistry

Preface

This report is the result of my master thesis for the department of Energy and Process Engineering under the faculty of Engineering Science and Technology at the Norwegian University of Science and Technology, NTNU. The thesis is connected to an ongoing PhD thesis project at NTNU, on the same topic, and is in collaboration with Statoil.

The purpose of this thesis is to evaluate a particular North Sea oil platform using an exergy analysis.

I wish to take the opportunity to thank my supervisor Ivar Ståle Ertesvåg and my co-supervisor Mari Voldsund. I would especially like to thank you, Ivar, for invaluable help and feedback on the structure and contents of the report and discussions on reasonable assumptions and I would like to thank you, Mari, for excellent supervision on the HYSYS modeling and not least innumerable good discussions and answers during the project period.

Trondheim, June 2013

Knut Jøssang

Preface

Abstract

The motivation is to explore the applicability of exergy analysis as an evaluation and monitoring tool for an offshore platform. The focus should be turned from energy efficiency to exergy efficiency, because to use an efficiency that does not account for the quality of the energy may be misleading for the improvement potential. The exergy efficiency contains the improvement potential, while current commonly used performance parameters only focus on power consumption. An exergy analysis is a good method to detect, locate and quantify the theoretical potential for savings and it is more useful the more complex and advanced the system to be analyzed is. Exergy efficiency can be used together with industries' own standard measures, such as specific CO_2-emissions. An exergy analysis is seldom systematically used in the industry yet, but the more details we have on the use of exergy, the more opportunities we have to foster environmental friendly technologies.

This thesis contains an exergy analysis of the oil and gas processing plant and the power generation system and distribution systems at a particular North Sea offshore platform. In the oil and gas processing a mix of reservoir petroleum and water is separated into oil, gas and water. The oil is exported through a 212 km long pipeline to an onshore terminal, gas and water are reinjected into the reservoir and some of the gas is used for gaslift. Gas can also be imported through a 50 km long pipeline from a nearby gas center to cover the need for gas injection. A fraction of the gas is combusted in power turbines and in pilot flames in the flare system. The oil and gas processing can be divided into six sub-processes; the production manifolds, the separation train, the recompression train, the reinjection train, the export system and the fuel gas system. The power generation system consists of three gas turbines, one mechanical drive and two generator drive. They cover the power demand at the platform. A seawater distribution system and a hot water distribution system supplies consumers with cold and hot water, respectively.

A process flowsheet of the oil and gas processing plant, power generation system and distribution systems is simulated in the chemical process simulator HYSYS. The exergy loss in the whole oil and gas processing process, the power generation system and the distribution system, in each sub-process and in each process unit, is calculated. This was done for two dates, with two years in between. In addition, the possibility for installing a combined cycle is studied. The exergy analysis of the oil and gas processing platform is also compared to another exergy analysis of a North Sea oil platform performed by Voldsund et al. [1].

The specific power consumption was 28 kWh/Sm^3/ 35 kWh/Sm^3 and the exergetic efficiency was 30.3 %/ 30.3 % for the whole oil and gas processing process at the platform. The highest losses were related to compression and cooling of gas in the recompression train and the reinjection train and throttling in the production manifolds. Also heating and cooling in the separation train and export system contributed a lot, respectively. The exhaust gas from the mechanical drive turbine does not have enough heat to cover the electricity demand via a steam cycle. However, if one utilizes the heat from one of the generator drive gas compressors at part load in addition, the electricity demand is covered. The total exergy destruction is reduced with 5.8 MW/ 10.0 MW.

We see the advantage of analyzing exergy destruction and exergetic efficiency of the process. These parameters show other features of the processes, in addition to the industry's own measures of performance.

Abstract

Sammendrag

Motivasjonen er å utforske anvendbarheten av en eksergianalyse som et evaluerings- og overvåkingsverktøy for en offshore plattform. Fokus bør rettes fra energivirkningsgrad til eksergivirkningsgrad, da bruken av en virkningsgrad som ikke tar hensyn til energikvalitet kan være misledende for forbedringspotensialet. Eksergivirkningsgraden inneholder forbedringspotensialet, mens nåværende vanlig brukte ytelsesparametere kun retter fokus mot kraftforbruk. En eksergianalyse er en god metode for å oppdage, lokalisere og kvantifisere det teoretiske potensialet for besparinger og er mer anvendbart desto mer komplekst og avansert systemet som skal analyseres er. Eksergivirkningsgrad kan bli brukt sammen med industriens egne parametere, slik som spesifikt CO_2-utslipp. Eksergianalyse er sjeldent systematisk brukt i industrien enda, men jo flere detaljer vi har på bruken av eksergi, jo flere muligheter har vi til å skape miljøvennlige teknologier.

Denne rapporten inneholder en eksergianalyse av olje- og gassprosesserings anlegget, kraftanlegg og distribusjonssystemer på en bestemt offshore plattform i Nordsjøen. I olje- og gassprosesseringen blir en blanding av reservoarpetroleum og vann separert til olje, gass og vann. Oljen blir eksportert gjennom en 212 km lang rørledning til en landbasert terminal, gass og vann blir reinjisert i reservoaret og noe gass blir brukt til gassløft. Gass kan også bli importert gjennom en 50 km lang rørledning fra et nærliggende gassenter for å dekke behovet for gassinjeksjon. En fraksjon av gassen blir forbrent i kraftturbiner og pilotflammer i fakkelsystemet. Olje- og gassprosesseringen kan deles inn i seks underprosesser; produksjonsmanifolder, separasjonstoget, rekompresjonstoget, reinjeksjonstoget, eksportsystemet og brenngassytemet. Kraftanlegget består av tre gassturbiner, en som driver en mekanisk aksling og to som driver generatorer. De dekker kraftbehovet på plattformen. Et sjøvannsdistribusjonssystem og et varmtvannsdistribusjonssystem forsyner forbrukere med henholdsvis kaldt og varmt vann.

Et prosessflytskjema av olje- og gassprosesseringsanlegget, kraftanlegget og distribusjonssystemene er simulert i den kjemiske prosess-simulatoren HYSYS. Eksergitapet i hele olje- og gassprosesseringsprosessen, kraftanlegget og distribusjonssystemet, i hver underprosess og i hver prosessenhet er beregnet. Dette er gjort for to datoer, med to års mellomrom. I tillegg er muligheten for å installere kombikraft studert. Eksergianalysen av olje- og gassprosesseringsplattformen er også sammenliknet med en annen eksergianalyse av en plattform i Nordsjøen gjort av Voldsund et al. [1].

Det spesifikke kraftforbruket var 28 kWh/Sm^3/ 35 kWh/Sm^3 og eksergivirkningsgraden for hele olje- og gassprosesseringen på plattformen var 30,3 %/ 30,3 %. De høyeste tapene var relatert til kompresjon og kjøling av gass i rekompresjonstoget og reinjeksjonstoget og struping i produksjonsmanifoldene. Oppvarming og kjøling i henholdsvis separasjonstoget og eksportsystemet bidro også en del. Eksosgassen fra gassturbinen som driver en mekanisk aksling, har ikke nok varme til å dekke elektrisitetsbehovet via en dampsyklus. Utnytter man derimot i tillegg varmen fra en av gassturbinene som driver en generator på dellast, er elektrisitetsbehovet dekket. Den totale eksergidestruksjonen er redusert med 5,8 MW/ 10,0 MW.

Vi ser fordelen av å analysere ekserginedbrytning og -virkningsgrad for prosessen. Disse parameterne viser andre egenskaper ved prosessen, i tillegg til industriens egne parametere for ytelse.

Sammendrag

Nomenclature

Roman symbols

AF	Air fuel ratio	[-]
API	American Petroleum Institute gravity	[-]
e	Specific exergy transfer accompanying to mass flow	[J/kg]
e_f	Specific flow exergy	[J/kg]
$e_f{}^{ph+k+p}$	Specific physical, kinetic and potential flow exergy	[J/kg]
$\bar{e}^{ch}$	Specific chemical exergy on molar basis	[J/mol]
$\dot{E}$	Exergy	[W]
$\dot{E}_{ch}$	Chemical exergy	[W]
$\dot{E}_p$	Potential exergy	[W]
$\dot{E}_{ph}$	Physical exergy	[W]
$\dot{E}_k$	Kinetic exergy	[W]
E_D	Exergy destruction	[W]
E_L	Exergy loss	[W]
E_P	Product exergy	[W]
E_U	Utilized exergy	[W]
f_i	f-value	[-]
g	Acceleration of gravity	[m/s^2]
h	Specific enthalpy	[J/kg]
H	Enthalpy	[J]
k_{ij}	Interaction parameter	[-]
LHV	Lower heating value	[J/kg]
$\dot{m}$	Mass flow	[kg/s]
n	Mole	[mol]
$\dot{n}_F$	Molar flow rate of fuel	[mol/s]
p	Pressure	[Pa]
$\dot{Q}_{CV}$	Net rate of energy transfer by heat across the boundary of the control volume	[W]
$\dot{Q}_j$	Rate of heat transfer at the location on the boundary where the instantaneous temperature is T_j	[W]
R	Universal gas constant	[J/mol K]
s	Specific entropy	[J/kg K]
SEC	Specific exergy consumption	[-]
SED	Specific exergy destruction	[-]
SG	Specific gravity	[-]
SPC	Specific power consumption	[kWh/Sm^3]
T_j	Instantaneous temperature at boundary	[K]
T_0	Temperature	[K]
u	Specific internal energy	[J/kg]
U	Internal energy	[J]
v	Specific volume	[m^3/kg]
V	Velocity or molar volume	[m/s] [m^3/mol]
$\dot{V}_{export}$	Volume flow rate of exported oil	[Sm^3]
$\dot{W}_{CV}$	Net rate of energy transfer by work across the	[W]

Nomenclature

	boundary of the control volume	
x_i	Mole fraction of component i	[-]
y_i	Mole fraction of component i	[-]
z	Elevation	[m]
Z	Compressibility factor	[-]

Greek symbols

α	Molar flow rate of the accompanying substance per molar flow rate of the fuel	[-]
β	Molar flow rate of the accompanying substance per molar flow rate of the fuel or chemical exergy correction factor	[-]
γ	Molar flow rate of the accompanying substance per molar flow rate of the fuel	[-]
δ_i	Efficiency defect	[-]
ε	Efficiency	[-]
λ	Theoretical air	
η_{th}	Thermal efficiency	[-]
θ	Relative irreversibility	[-]
$\dot{\sigma}_{CV}$	Entropy production	[W/K]
ψ	Efficiency	[-]
ω	Acentric factor	[-]

Subscripts and superscripts

air	Air
$avoidable$	Avoidable
c	Critical value
CV	Control volume
$"c-p"$	Consumed-produced
$dead$	Dead state
ex	Exit
$env.$	Environmental state
f	Formation
$Fuel$	Fuel
i	Index for sub-process, component etc.
ID	Ideal gas
in	Inlet
$intrinsic$	Intrinsic
$int.rev.$	Internal reversible
$"i-o"$	Input-output
j	Index for control volume etc.
net	Net
out	Out
r	Reduced value
ref	Reference
$stoich$	Stoichiometric
$total$	Total
$\bar{}$	Property is on molar basis
$\dot{}$	Property is on rate basis

Nomenclature

0	Reference state in equilibrium with environment

Abbreviations

$COSTALD$	Corresponding states liquid density
DLE	Dry low emissions
GG	Gas generator
HP	High pressure
$HSPT$	High speed power turbine
$HVAC$	Heating, ventilation and air conditioning
LM	Land and marine applications
LP	Low pressure
PGT	Propulsion gas turbine
pp	%-points
$PR\ EOS$	Peng Robinson Equation of State
SAC	Standard annular combustion
TIT	Turbine inlet temperature

Nomenclature

X

Contents

Contents

List of Tables

List of Figures

Contents

Contents

1 Introduction

1.1 Motivation

From 2007 the emissions from oil and gas processing have been the largest source to greenhouse gas emissions in Norway. In national context, this caused 21 % of Norway's total CO_2-emissions in 2008 [2] and the petroleum industries were responsible for 29 % of the CO_2-emissions in 2010 [3]. The emissions from offshore activities have shown a promising trend the few latest years, but still much has to be done to reach the 20-20-20 targets. The goal is a reduction in EU greenhouse gas emissions of at least 20 % below 1990 levels, 20 % of EU energy consumption should come from renewable resources, and there should be a 20 % reduction in primary energy use compared with projected levels, to be achieved by improving energy efficiency, each by 2020 [4].

Many offshore installations use gas turbines for power production and shaft power. The reasons for this domination are because of the high power to weight ratio, availability of fuel gas and reliability. Gas turbines accounted for 78.9 % of the CO_2-emissions in the petroleum sector. The NO_x-emissions from the oil and gas processing sector are significant as it contributed with 27.2 % of the total NO_x-emissions in 2009 [5].

For oil and gas processing platforms a challenge is to maintain a high performance over lifetime. Due to variations of reservoir properties, such as pressure and temperature, composition changes and variations in production flow rates, some equipment run at off-design conditions. One example is the need for anti-surge recycling in the compression stages. This leads to performance loss over lifetime. As the oil production decreases over time, water and gas injections are needed to enhance oil recovery from the reservoir. This is an energy intensive process. An overview of the oil and gas processing process is presented in Figure 1.1. The power demand for gas compression and water injection was focused upon by Svalheim and King [6], [7], and they recommended applying energy best practices, like gas turbine operation near design load and integration of waste heat recovery. In 1999 the first offshore combined cycle was installed at a platform in the North Sea [3]. Kloster [8], [9] argued in favor of this practice saying that it contribute to significant energy savings and reduction of CO_2-emissions. Maragone et al. [2] requested parameters that provide information on the magnitude of thermodynamic efficiencies of the whole platform and the impact of each subsystem on the overall performance.

A tool to reach this target is an exergy analysis. The motivation for this study is to explore the applicability of exergy analysis as an evaluation and monitoring tool for an offshore platform. The focus should be turned from energy efficiency to exergy efficiency, because to use an efficiency that does not account for the quality of the energy may be misleading for the improvement potential. Energy efficiency is based on the concept of wasting as little energy as possible relative to energy inputs, while exergetic efficiency focus on wasting and destructing as little available work as possible from the input of work. The exergy efficiency contains the improvement potential, while current commonly used performance parameters only focus on energy consumption. To obtain much exergy from energy is the real goal of any energy conversion [10]. An exergy analysis is a way to characterize the thermodynamic performance and identify different techniques to increase the overall performance of the whole system. The exergy analysis is a good method to evaluate the exergy

efficiency and the exergy destroyed in each set of equipment, e. g. separators, pumps, turbines, compressors and heaters for an oil and gas platform [11]. One should be aware of that there is not any direct link between exergy and cost. It may even be a conflict concerning reducing exergy loss and reducing investment cost. An exergy analysis is seldom systematically used in the industry yet, but the more details we have on the use of exergy, the more opportunities we have to foster environmentally friendly technologies.

Heat loss is seldom difficult to locate and detect, and therefore given much attention and resources in order to prevent. Irreversibilities, or work loss, are not often exposed in the same manner, but there is a major economic cost related to this kind of loss [12].

An exergy analysis is a good method to detect, locate and quantify the theoretical potential for savings. An exergy analysis is more useful the more complex and advanced the system to be analyzed is. Exergy efficiency can be used together with the industries own standard measurements, such as specific CO_2-emissions. One can also imagine that the authorities may impose minimum exergy efficiency on equipment used in the public sector.

Today the most frequently used performance parameter in the oil and gas industry is the specific CO_2-emissions. It supports good energy efficiency and the use of renewable energy sources. For platforms that use renewable energy sources, and thus not only use oil and gas as their energy sources, CO_2-emissions will no longer be proportional to the power consumption. Then the CO_2-emissions do not say anything about how decent the process is. After the introduction of the CO_2-tax in 1991, many energy conservation measures have been done [3]. An exergy analysis can identify the importance of such measures. Exergy efficiency will always consider the process [13]. An exergy analysis will provide a basis that can be used for comparison of today's practical value between technologies and comparison up against the theoretical value. An interesting suggestion by Sauar [14] is to tax the excess lost work, that is to say the destructed exergy. Questions have to be raised about reasonable values of lost work and the practical upper limit of the exergy efficiency.

Oliveira et al. [11] presented an exergy analysis of a Brazilian oil and gas processing platform which consisted of subsystems for separation, compression and pumping. They found that most exergy consuming processes were the petroleum heating and the gas compression process. The subsystem with the lowest exergy efficiency was the separation train. Voldsund et al. [1] carried out an exergy analysis of a North Sea oil and gas processing platform. It consisted of the production manifolds, the separation train, the recompression train, the reinjection train, the fuel gas system and the export system. The highest exergy destruction took place in the production manifolds and in the reinjection train. Nguyen et al. [15] did an overall analysis of the Norwegian oil and gas facilities. Their analysis showed that the production manifolds, the reinjection train, the recompression train and the separation train were the subsystems with most exergy destruction, in that order. It was shown that the results were very sensitive to the efficiencies of the compressors and pumps, and to the composition of the crude oil.

In this thesis a North Sea oil platform is analyzed by an exergy analysis. The platform produces heavy oil and heating is required in the separation train, a platform with this kind of process conditions has never previously been analyzed. The power generation system and the seawater and hot water distribution systems are also analyzed. A case study to identify the possibilities for utilizing exhaust gas in a combined cycle is also done.
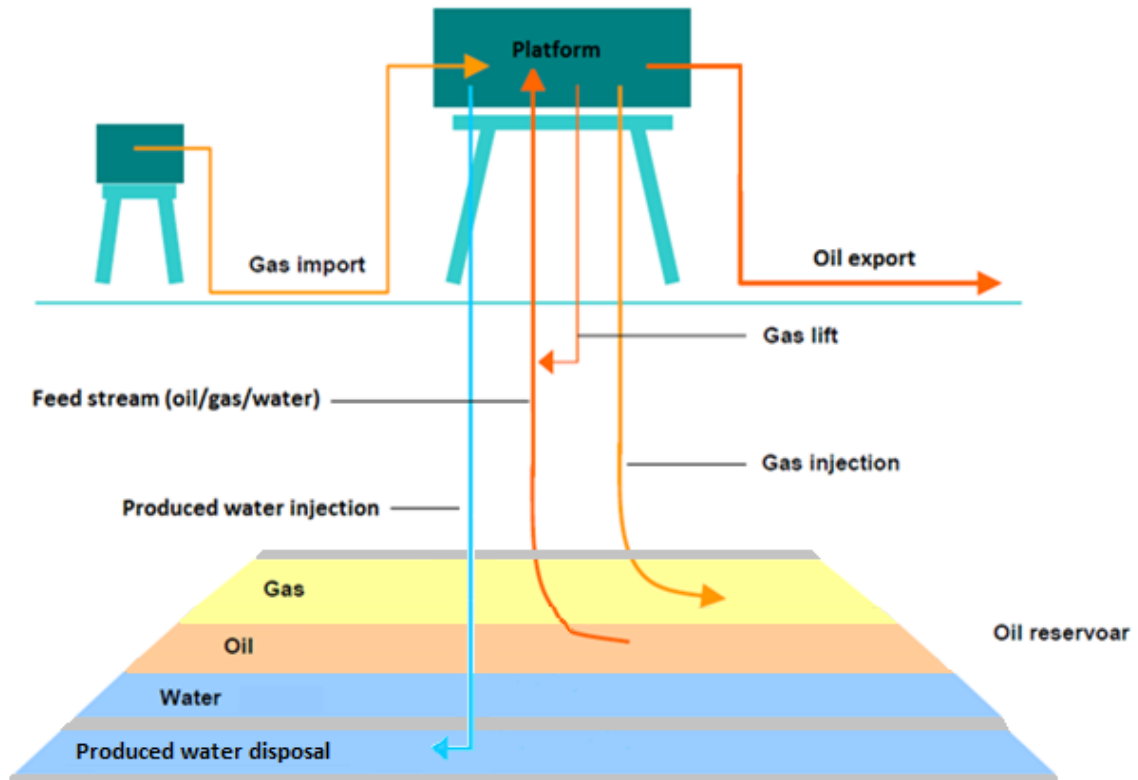
Figure 1.1 Schematic overview of the oil and gas processing process

A feed stream of oil, gas and water enters the platform together with gas import. After the oil and gas processing at the platform oil is exported, gas is injected back to the reservoir or used for lift and water is injected into another reservoir for disposal.

1.2   Report outline

This thesis is structured in the following way: The introduction clarifies the motivation for doing the analysis; it lays the base for the rest to follow. The second chapter is a brief theoretical presentation of the exergy concept and its efficiencies. The third chapter gives a system description and a process overview of the oil and gas processing and the power generation system at the platform. The methodology for simulation of the process flowsheet and the exergy analysis preformed in HYSYS [16] is discussed in the fourth chapter. The results are presented in the fifth chapter, together with an accompanying discussion in the sixth chapter. The seventh chapter provides concluding remarks.

Introduction

2   Theory

2.1   Exergy and anergy

To take into account that energy is found in very variable quality, the use of a universal standard expressing energy quality is needed. Energy can be divided into a part that could be used to produce work, and a part that cannot produce work. These two parts are called exergy and anergy, respectively. Quality of energy is synonymous with its capacity to cause change. The term exergy was coined by Zoran Rant in 1956 by using the Greek *ex* and *ergon* meaning "from work" [17]. Exergy can be defined in the following way:

"The maximum work which can be obtained from a given form of energy using the environmental parameters as the reference state" [18].

This is the background for why exergy is related to ideal work. There is a direct link between exergy and entropy production through the second law of thermodynamics, since the entropy production is proportional to exergy loss. The term exergy is also referred to as availability, available energy, exergic energy, utilizable energy, available useful work, maximum (or minimum) work, reversible work and ideal work [17]. Unlike energy, which is conserved, the exergy degrades. The degradation of exergy is equivalent to irreversibility losses, as a real process is not reversible. It is a goal to get the highest possible amount of exergy out of the energy, as this means more work available. This is not always easy; "We are bad energy engineers, because we have too much energy", Benjamin Franklin [10].

2.2   Environment and dead state

An ideal definition of the environment can be a very large medium in perfect thermodynamic equilibrium. The environment has no differences in pressure, temperature, chemical potential or kinetic and potential energy, and thus cannot produce any work from interactions between different parts of the environment. A system can be influenced by the environment through three mechanisms: thermal, mechanical and chemical interaction. The environment is therefore seen as a natural reference for pressure, temperature and chemical potential. This is not always true, since both the temperature and the concentrations in the environment can change, and e.g. the air and the ocean can have different temperature. It is important to notice that the process which is analyzed should not influence the environment.

A system emits its exergy if it is brought to equilibrium with the environment. There are two degrees of equilibrium; restricted and unrestricted. In the literature [18], these are often referred to as "environmental state" and "dead state", respectively. Environmental state requires that the pressure and temperature of the system and the surroundings will be similar; while in dead state there must be full thermodynamic equilibrium with the surroundings, which is mechanical, thermal and chemical equilibrium. Systems in dead state cannot produce any work in interaction with the environment. Figure 2.1 shows a substance going from an initial state, through environmental state, to dead state.
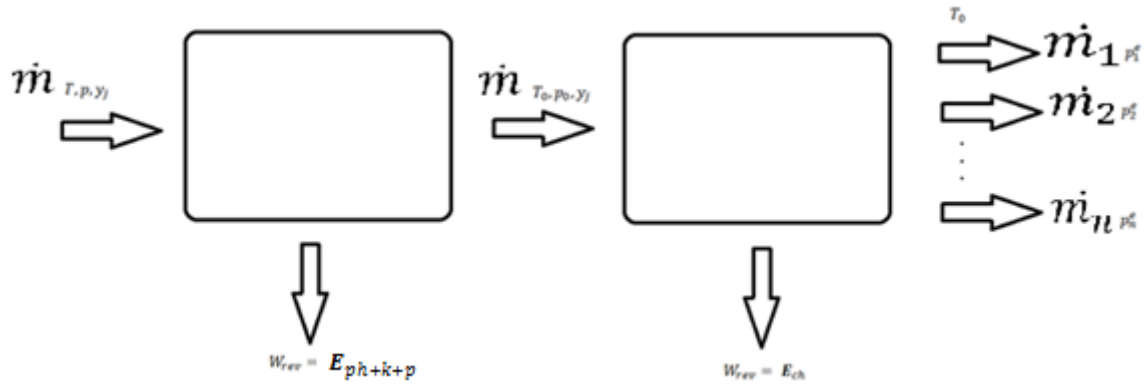
Figure 2.1 A substance going from an initial state, through environmental state, to dead state.

The horizontal arrows denote material streams, the vertical arrows denote streams of work and the boxes represent an irreversible process. Work produced in each transition is physical, kinetic and potential exergy, E_{ph+k+p}, and chemical exergy, E_{ch}, respectively. $\dot{m}$ denotes the mass flow and T, p and y_j denotes the temperature, the pressure and the mole fraction, respectively. The subscript 0 represents environmental state and the superscript e indicates that the property is in thermodynamic equilibrium with the environment.

2.3 Exergy balance

For an energy analysis, only the 1st law of thermodynamics must be taken into consideration, but for an exergy analysis both 1st and 2nd law of thermodynamics must be taken into account. Therefore the energy balance is a statement of the law of conservation of energy, and the exergy balance may be looked upon as a statement of the law of degradation of energy. Degradation of energy is equivalent to the irretrievable loss of exergy due to all real processes being irreversible.

An exergy balance, for an open system in steady state with constant mass flow rate, follows from the 1st and 2nd law of thermodynamics

$$0 \ = \ \sum_j \left(1 - \frac{T_0}{T_j}\right) Q_j - \dot{W}_{CV} + \sum_{in} \dot{m}_{in} \boldsymbol{e}_{f_{in}} - \sum_{ex} \dot{m}_{ex} \boldsymbol{e}_{f_{ex}} \ - \ \dot{E}_D \tag{1}$$

where the exergy destruction $\dot{E}_D \ = \ T_0 \dot{\sigma}_{CV}$, and $\dot{\sigma}_{CV}$ represent the entropy production rate of the control volume and T_0 is the environmental temperature. $\dot{Q}_{CV}$ denotes the net rate of energy transfer by heat across the boundary of the control volume, $\dot{W}_{CV}$ denotes the net rate of energy transfer by work across the boundary of the control volume. The subscript *in* and *ex* indicate inlet and exit, respectively. $\dot{m}$ denotes the mass flow, $\boldsymbol{e}_f$ is the specific flow exergy, $\dot{Q}_j$ represents the time rate of heat transfer at the location on the boundary where the instantaneous temperature is T_j [19]. A more detailed derivation can be seen in Appendix B.

2.4 Exergy associated with a steady stream of matter

"Exergy of a steady stream of matter is equal to the maximum amount of work obtainable when the stream is brought from its initial state to the dead state by processes during which the system may only react with the environment" [18].

In absence of nuclear effects, magnetism, electricity and surface tension, exergy can be divided into:

$$\dot{E} = \dot{E}_k + \dot{E}_p + \dot{E}_{ph} + \dot{E}_{ch} \tag{2}$$

where $\dot{E}_k$, $\dot{E}_p$, $\dot{E}_{ph}$ and $\dot{E}_{ch}$ is kinetic exergy, potential exergy, physical exergy and chemical exergy, respectively [18].

Kinetic and potential energies of a stream of a substance are ordered forms of energy, and thereby convertible to work. When evaluated with the environmental state as reference, they are equal to kinetic and potential exergy, respectively [18].

$$\dot{E}_k = \dot{m}\frac{V^2}{2} \tag{3}$$

$$\dot{E}_p = \dot{m}gz \tag{4}$$

where V, g and z denote velocity, acceleration of gravity and elevation, respectively.

The exergy of the disordered forms of energy has two components; physical exergy and chemical exergy [18].

"Physical exergy is equal to the maximum amount of work obtainable when the stream of substance is brought from its initial state to the environmental state defined by P_0 and T_0, physical processes involving only thermal interaction with the environment" [18].

$$\dot{E}_{ph} = \dot{m}\big((h - h_0) - T_0(s - s_0)\big) \tag{5}$$

where h and s denotes specific enthalpy and specific entropy, respectively. The subscript 0 indicates a reference state that is in equilibrium with the environment. The physical exergy can be divided into a component resulting from temperature difference between the stream and the environment, called temperature based component, and a component resulting from pressure difference between the stream and the environment, called pressure based component. This division can be considered as two hypothetical, reversible processes. First an isobaric process taking place at the initial pressure, followed by an isothermal process corresponding to the environmental temperature.

$$\dot{E}_{ph}^{Temperature} = \big(h - h_{T_0,p}\big) - T_0\big(s - s_{T_0,p}\big) \tag{6}$$

$$\dot{E}_{ph}^{Pressure} = \big(h_{T_0,p} - h_0\big) - T_0\big(s_{T_0,p} - s_0\big) \; , \tag{7}$$

where the subscripts T_0, p indicates a state with environmental temperature and actual pressure, respectively.

Exergy transport related to physical exergy, kinetic exergy and potential exergy accompanying to mass flow and flow work is thereby given as follows;

$$e_f^{ph+k+p} = (h - h_0) - T_0(s - s_0) + \frac{V^2}{2} + gz \tag{8}$$

where e_f^{ph+k+p} denotes the specific physical, kinetic and potential flow exergy.

The specific thermomechanical flow exergy consists of contributions from kinetic, potential and physical exergy. "Chemical exergy is equal to the maximum amount of work obtainable when the substance under consideration is brought from the environmental state to the dead state by processes involving heat transfer and exchange of substance only with the environment" [18]. The chemical exergy is the exergy which is released between the environmental state and the dead state. It consists of mixing and separation exergy and chemical reaction exergy.

If one assume that a combustion reaction is complete, it could look like this on general form
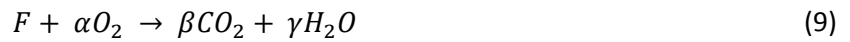
$$F + \alpha O_2 \rightarrow \beta CO_2 + \gamma H_2 O \tag{9}$$

where F denotes fuel, and the three constants α, β and γ represent the molar flow rate of the accompanying substance per molar flow rate of the fuel. The combustion reaction is illustrated in Figure 2.2.
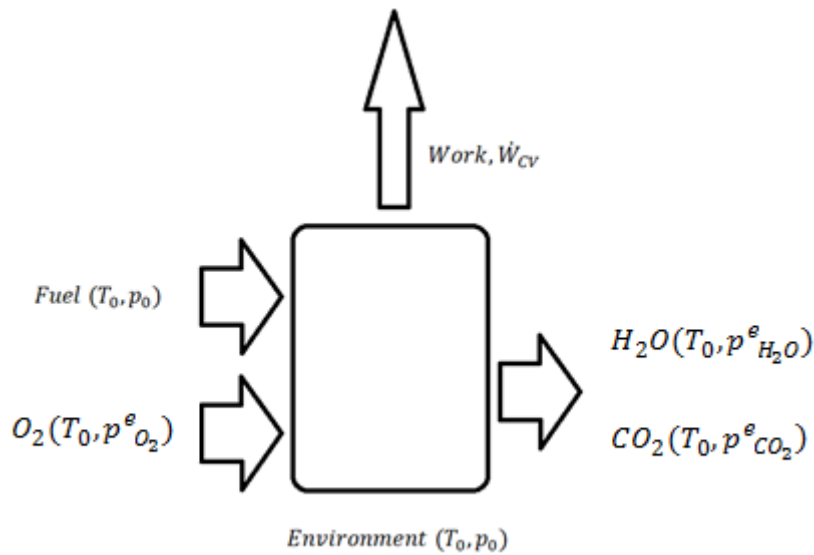
Figure 2.2: Chemical exergy in complete combustion.

The horizontal arrows denote material streams and the vertical arrow is a stream of work. The box represents a complete combustion process.

By combining the 1st and 2nd law of thermodynamics for this complete combustion, and realizing that maximum work is achieved when $\dot{\sigma}_{CV} = 0$, the chemical exergy becomes:

$$\bar{e}^{ch} = \left[(\bar{h}_F + \alpha \bar{h}_{O_2}) - (\beta \bar{h}_{CO_2} + \gamma \bar{h}_{H_2O}) \right] - T_0 \left[(\bar{s}_F + \alpha \bar{s}_{O_2}) - (\beta \bar{s}_{CO_2} + \gamma \bar{s}_{H_2O}) \right] \tag{10}$$

where the bar indicates that the property is on molar basis [19].

If no reactions occur, there is no change in the chemical composition of the streams crossing the control volume. If in addition no exchanges of substance occur with the environment, the chemical compounds of the exergy will cancel out in the exergy balance. The chemical exergy is simply:

$$e^{ch} = [h_{env.} - h_{dead}] - T_0[s_{env.} - s_{dead}]$$ (11)

where the subscripts $env.$ and $dead$ denote environmental state and dead state, respectively [20]. Another way to express the chemical exergy is to do a division between the molar chemical exergy of the components when they are pure and the molar chemical exergy of mixing effects.

$$\bar{e}^{ch} = \sum_i y_i \bar{e}_i + \left(\overline{h_0} - \sum_i y_i \bar{h}_{i,0} - T_0 \left(\overline{s_0} - \sum_i y_i \bar{s}_{i,0} \right) \right)$$ (12)

where $\bar{e}^{ch}$ is the specific chemical exergy, $y_i \bar{e}_i$ is the molar chemical exergy of chemical component i when it is pure and $\left(\overline{h_0} - \sum_i y_i \bar{h}_{i,0} - T_0 \left(\overline{s_0} - \sum_i y_i \bar{s}_{i,0} \right) \right)$ account for mixing effects. y_i denotes the mole fraction of component i. $\bar{h}_{i,0}$ and $\bar{s}_{i,0}$ are the molar enthalpy and molar entropy of pure i at p_0 and T_0, respectively. $\overline{h_0}$ and $\overline{s_0}$ are the molar enthalpy and entropy for the mixed stream at p_0 and T_0. It is worth noting that this way of calculating the chemical exergy can lead to a chemical exergy below zero for a single stream, since not all chemical exergy is included. However when calculating the difference between outlet and inlet of a process the change in chemical exergy becomes positive.

According to Rivero et. al [21] the standard chemical exergy of each pseudo component can be calculated with the following expression:

$$e_i^{ch} = LHV_i \beta_i + \sum_j z_j e_j^{ch} \quad ,$$ (13)

where LHV_i is the lower heating value of the pseudo component, z_j and e_j^{ch} are the mass fraction and the standard chemical exergy value of metal j. The β_i is the chemical exergy correction factor and for a specific component it is defined as follows [21]:

$$\beta = 1.0401 + 0.1728 \frac{z_{H_2}}{z_C} + 0.0432 \frac{z_{O_2}}{z_C} + 0.2169 \frac{z_S}{z_C} \left(1 - 2.0628 \frac{z_{H_2}}{z_C} \right) + 0.0428 \frac{z_{N_2}}{z_C}$$ (14)

The lower heating value for a specific component is determined based on the following [22]:

$$LHV = \frac{1}{0.429923} (16\,840 + 76.60\,API - 1.230\,API^2 + 0.008974\,API^3)\ [kJ/kg]$$ (15)

where API is the American Petroleum Institute gravity and measures how heavy the component is compared to water. The API of water is 10. It is defined in the following way:

$$API = \frac{141.5}{SG} - 131.5$$ (16)

where SG is the specific gravity. For a specific component it is defined as follows:

$$SG = \frac{\rho}{\rho_{H_2O}}$$ (17)

where ρ and ρ_{H_2O} are the density of the component and water, respectively [23].

The chemical exergy of the metals are given in Table 2.1

Table 2.1 Chemical exergy of metals in the crude oil [18]

Metal	Chemical exergy [kJ/kg]
Nickel	4 305.91
Vanadium	14 249.15

The total specific flow exergy becomes:

$$e_f = e_f^{ph+k+p} + e^{ch} \tag{18}$$

A more detailed derivation can be seen in Appendix B.

2.5 Exergy efficiency

The exergy efficiency compares the real process with the ideal process, or reversible process. The entropy production is always positive, which provides that the exergy leaving the process is smaller than the exergy entering. The question to be answered in an exergy analysis is how the exergy losses can be limited. Based on only absolute values of exergy destruction, it may be difficult to determine whether the destructed exergy in the process is disproportionately high. Exergy efficiency gives a better impression of whether the destruction should be reduced or if it is within acceptable ranges.

One of the goals of the exergy efficiency is to express the exergy rate of change in the system. In current practice, it is possible for individual interpretations of exergy performance. Exergy efficiency may generally be divided into two categories; «input-output» efficiency and «consumed-produced»-efficiency. In some sources the categories are referred to as universal and functional efficiencies, respectively [24].

"Input-output"- efficiency is also referred to as total or overall efficiency. It is appropriate to use when the major part of the output can be considered as "useful".

$$\psi_{"i-o",1} = \frac{\sum Exergy\ out}{\sum Exergy\ in} \tag{19}$$

There are also different variants of the "input-output"-efficiency. One option is that streams that go directly to the environment, such as often for cooling water, are subtracted from the rest of the exergy.

$$\psi_{"i-o",2} = 1 - \frac{\sum Exergy\ destroyed + \sum Exergy\ lost}{\sum Exergy\ in} \tag{20}$$

Another variant ,suggested by Rian and Ertesvåg [25], takes the overall chemical exergy increase and the physical exergy in the output streams, divided by the physical exergy in the inlet streams and the chemical exergy of the inlet streams used as fuel. For an oil and gas processing platform, the chemical exergy in the fuel is replaced with the exergy in the heat and work added to the system.

$$\psi_{"i-o",3} = \frac{\sum Physical\ exergy\ out + Change\ in\ chemical\ exergy}{\sum Physical\ exergy\ in + Exergy\ in\ with\ work\ and\ heat} \tag{21}$$

The "input-output"-efficiencies may be misleading as they may not show the effects of reducing the inefficiencies and of incorporating improvement strategies [26].

"Consumed-produced"-efficiency is often referred to as second law, task or utilitarian efficiency. There exist an unknown number of versions, but only the most common is mentioned here. It is worth noting that Eqs. (22) - (25) are not interpretations of the originals, but the actual definitions given by the authors referred to in [27]

$$\psi_{"c-p",1} = \frac{Useful\ exergy\ output}{Useful\ exergy\ input} \tag{22}$$

$$\psi_{"c-p",2} = \frac{Exergy\ of\ useful\ product}{Feeding\ exergy} \tag{23}$$

$$\psi_{"c-p",3} = \frac{Desired\ output}{Necessary\ input} \tag{24}$$

$$\psi_{"c-p",4} = \frac{Exergy\ of\ products}{Exergy\ of\ fuel} \tag{25}$$

As one can see, there is also room for different interpretations among these definitions [27] which can lead to confusion and mixing, or that some definitions may look similar or actually are similar.

The most used exergetic efficiency is maybe (24). It has the following advantages:

- Applicable to a wide range of thermal plants, both open and closed cycle as well as process components
- Gives a reasonable assessment of the performance of dual purpose plants
- The efficiency defect (see (31)) can be expressed as a linear function of component efficiency defects, giving an indication of the impact of each component to the efficiency of the total process [18]

Voldsund et al. [28] suggest some exergy based indicators for oil and gas processing platforms. One is the specific exergy consumption.

$$SEC = \frac{Exergy\ in\ with\ work\ and\ heat}{Exergy\ exported} \tag{26}$$

Another is the specific exergy destruction.

$$SED = \frac{Exergy\ destructed}{Exergy\ exported} \tag{27}$$

Other performance parameters are presented by Maragone et al. [2] and Riveiro et al. [21].

2.6 Parameters related to exergy used in this report

The definitions and important quantities in an exergy analysis, used further in this report, are defined as follows:

- Product exergy, E_P, represents the desired result expressed in terms of exergy. The desired result is the difference in the exergy of the material streams in and out of the process.
- Utilized exergy, E_U, represents the resources in terms of exergy used to provide the product exergy. This is electrical power and heating with a hot water distribution system.
- Exergy loss, E_L, represents thermodynamic inefficiencies of a system associated with the transfer of exergy with energy and material streams to the surroundings
- Exergy destruction, E_D, represents thermodynamic inefficiencies of a system associated with the irreversibilities within the system boundaries

$$E_D = E_U - E_P - E_L \qquad (28)$$

The exergy can be lost in two different ways; internal and external losses. Internal losses, often called destruction, are caused by the irreversibilities in the process, e. g. due to mixing, chemical reactions, heat transfer, unrestricted expansion etc. The external losses are a cause of exergy content in discharged streams and heat losses; this may be cooling water or exhaust gasses.

Some parameters that are assumed useful for an exergy analysis in the oil and gas processing industry:

- The specific power consumption is defined as consumed power per oil produced

$$SPC = \frac{E_U}{\dot{V}_{export}} \qquad (29)$$

where $\dot{V}_{export}$ is the volume flow rate of oil for export in [Sm³/h].

- The exergy efficiency is defined as:

$$\varepsilon = \frac{E_P}{E_U} \qquad (30)$$

The exergetic efficiency in Eq. (30) can under certain interpretations, of course, be equivalent to earlier discussed efficiencies, see Section 2.5. The symbol ε is used to avoid confusion with the different earlier discussed efficiencies. The reason why the "input-output"- efficiency is not used is that the chemical exergy of the streams with hydrocarbons will completely dominate, and improvement on physical and chemical exergy destruction will just lead to small changes in the exergy efficiency. In the literature these streams or flows are referred to as "ballast flows" [24]. That means exergy flows that are fed to the process, but not directly involved in the intended conversion. Uncertainties of the chemical exergy will also lead to a high level of uncertainties for the exergetic efficiency.

- The efficiency defect of a subsystem, i, as the fraction of the input exergy to the total system. This parameter shows the different subsystems contribution to reduction in exergy efficiency [13].

$$\delta_i = \frac{E_{D_i}}{E_U}$$

(31)

- The f-value quantifies the importance of each set of equipment or sub-process. It is defined as the relation between the exergy consumed in the module and in the whole plant.

$$f_i = \frac{E_{U_i}}{E_U}$$

(32)

In a case with an oil and gas platform, the exergy input is typical work and exergy input with utility streams such as hot water. The relation between the f-value and the total exergetic efficiency of the whole process can be expressed as the following [11], as long as all E_{U_i}'s are larger than zero.

$$\varepsilon_{total} = \sum_i \varepsilon_i f_i$$

(33)

where $\varepsilon_i = E_{P_i} / E_{U_i}$.

- The relative irreversibility of each set of equipment or sub-process is defined as the fraction of the exergy destruction of the total system. This parameter shows the contribution to the total exergy destruction.

$$\theta_i = \frac{E_{D_i}}{E_D}$$

(34)

2.7 Avoidable and intrinsic exergy destruction

The exergy destruction itself gives the theoretical potential for improvement in performance, but it says nothing about the practical potential of improvement in performance. The practical potential for improvement in a given component depends on the minimum irreversibility rate possible within limitations, such as economical, technological and physical. This exergy destruction rate is called intrinsic irreversibility rate. The difference between the actual and the intrinsic irreversibility rate is the avoidable irreversibility rate [18].

$$E_D = E_{D_{intrinsic}} + E_{D_{avoidable}}$$

(35)

The intrinsic irreversibility rate of a special type of equipment can be given some indications by comparing it to irreversibility rates of the same kind of equipment on other plants or by comparing to state of the art technologies. Svalheim and King [7] studied oil and gas facilities by comparing the energy consumption with an estimate of possible energy savings with best available technologies. Tsatsaronis and Park [29] discussed the possibility of investigating the exergy destruction by comparing it to state-of-the-art technologies.

2.8   Power generation

Power generation on the oil and gas processing platform is mostly done by gas turbines. In a gas turbine the atmospheric air (A) is compressed, and pressurized air (B) enters into a combustor. Gas with high temperature (C) enters a gas turbine and exhaust gases (D) with relative high temperature leaves the gas turbine. The compressor is driven by the gas turbine which also generates net power output via direct shaft power or electricity generation in a generator. The exhaust air (D) may be utilized for steam generation which can be used in a steam cycle to produce electricity, or it can be utilized for heating of water.

When a gas turbine power cycle and a steam turbine power cycle are connected in one plant it is called a combined cycle, because the heat discharged form one cycle is used as input energy to the other cycle. The heat from the exhaust air from the gas turbine goes through a heat recovery steam generator, which produces steam at high pressure and temperature levels. It typically consists of three heat transfer sections: economizer, evaporator and superheater. The steam is utilized in a steam turbine before it is condensed, and then pumped again through the heat recovery steam generator. This is seldom done on offshore platforms today, but it exists in a few examples. A schematic overview is presented in Figure 2.3.
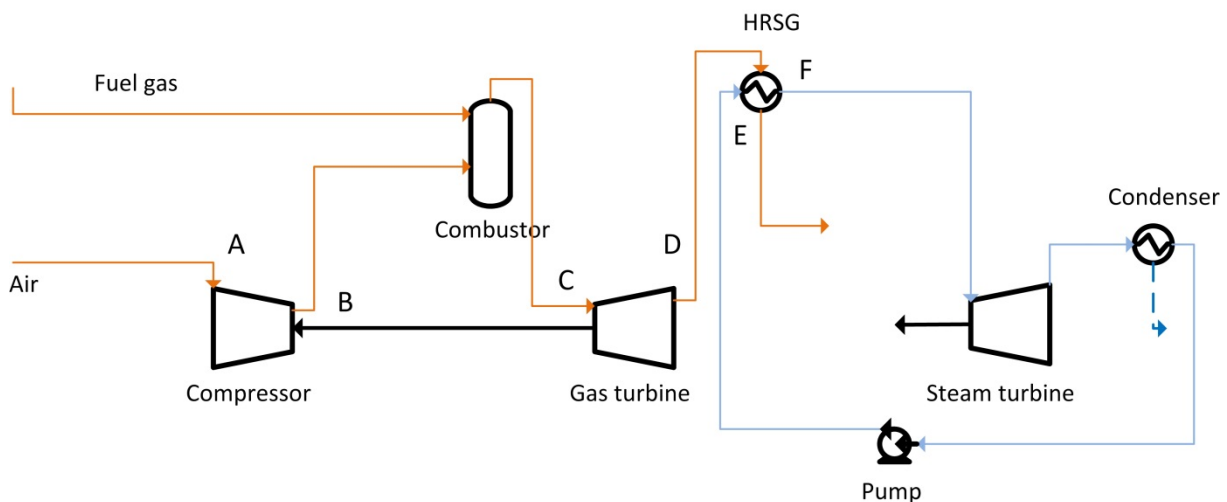
Figure 2.3 Schematic overview of a combined cycle

The thermal efficiency of a power cycle is defined as the ratio between the net useful output of power and heat, and the lower heating value of the fuel input.

$$\eta_{th} = \frac{\dot{W}_{net}}{\dot{m}\ LHV_{fuel}}\ , \tag{36}$$

where $\dot{W}_{net}$ is the net useful output and $\dot{m}$ and LHV_{fuel} are the mass flow rate and the lower heating value of the fuel, respectively.

Another important parameter is the pressure ratio of the air compressor in the power turbine unit. It is defined as the ratio between the outlet pressure and the inlet pressure of the compressor.

$$r = \frac{p_{out}}{p_{in}}\ , \tag{37}$$

where p_{out} and p_{in} are the outlet pressure and the inlet pressure of the compressor, respectively.

A parameter that is frequently used to quantify the amounts of air and fuel in combustion is the air-fuel ratio.

$$AF = \frac{m_{air}}{m_{fuel}} \ , \tag{38}$$

where m_{air} and m_{fuel} are the mass of air and fuel, respectively.

The minimum amount of air that supplies sufficient oxygen for complete combustion is called the theoretical amount of air and denoted λ_{stoich} . The amount of air actually supplied is often expressed in terms of the percent of theoretical air and simply denoted λ.

The temperature that would be achieved in the product in the limit of adiabatic operation of the reactor is called the adiabatic flame temperature. Assuming that the combustion air and the combustion products each form ideal gas mixtures, the energy rate balance reduces to:

$$\sum_P n_{ex}\bar{h}_{ex} = \sum_R n_{in}\bar{h}_{in} \ , \tag{39}$$

where n denotes mole. The subscripts P and R represent product and reactant, respectively.

For streams modeled as ideal gas, the enthalpy can be divided in the following way:

$$\bar{h} = \bar{h}_f^0 + \left[\bar{h}(T) - \bar{h}(T_{ref})\right] \ , \tag{40}$$

where $\bar{h}_f^0$ is the enthalpy of formation and the term $\left[\bar{h}(T) - \bar{h}(T_{ref})\right]$ accounts for the change in enthalpy from the temperature T_{ref} to the temperature T. Determination of the adiabatic flame temperature requires an iterative process.

Theory

3   System description and process overview

3.1   A general system description and process overview

An oil and gas platform consists of many subsystems; among other a power generation system which serves an oil and gas processing plant. The focus is first upon the oil and gas processing plant. In all simplicity the process in the processing plant aims to separate the crude oil into oil, gas and water. An overview of a typical process plant is given in the figure below.
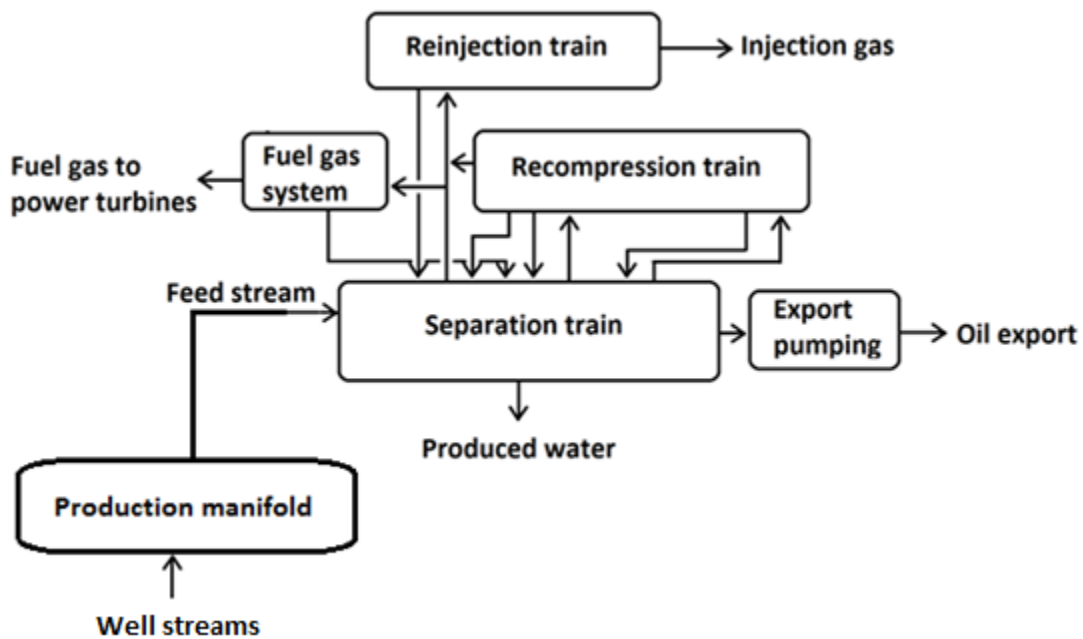
Figure 3.1 Schematic overview of mass streams at the oil and gas processing platform

Black lines indicate mass streams.

The feed stream comes from a production manifold and goes to a separation train. By the use of gravitational separators and an electrostatic coalescer, the water and gas are separated from the crude oil. The separation train on this platform consists of a high pressure degasser, one three-phase test separator, two stages with three-phase separators and an electrostatic coalescer. The number of stages and the stage pressure depends on flowing tubing pressure, GOR and required vapor pressure of the export crude product [30]. For each separator the pressure is reduced so that more gas is released from the oil. To reach required specifications of basic sediment content, water content and vapor pressure, the separation process is performed in several stages. Oil from the separation train enters the export pumping section where it is cooled and pressurized. Water from the separation process undergoes a treatment process before it is injected to the reservoir.

Heaters are served by a hot water distribution system which utilizes waste heat. There are two heat exchangers; one oil/oil-heat exchanger between the separation train and the export pumping, and one oil/water-heat exchanger within the separation train.

17

The gas from the separation stages is sent to the recompression train. The train consists of three stages, each with a cooler, a scrubber and a compressor. The cooler ensures a low temperature inlet for the compressor which gives an efficient compression. A scrubber is a two-phase separator which removes small amounts of condensed liquid. This protects the compressor and allows a more optimal compression.

After the recompression train the gas enters a reinjection train. In the reinjection train the gas is compressed up to injection well pressure for use in gas injection and gas lift. The train consists of two stages, each with cooler, scrubber and compressor, in the same way as for the recompression train. An import gas stream also enters the reinjection train. This gas has its own compression stage before it is mixed with the compressed gas after the second recompression stage.

The platform also consists of a power generation system and systems serving the oil and gas processing plant with cooling and heating water.
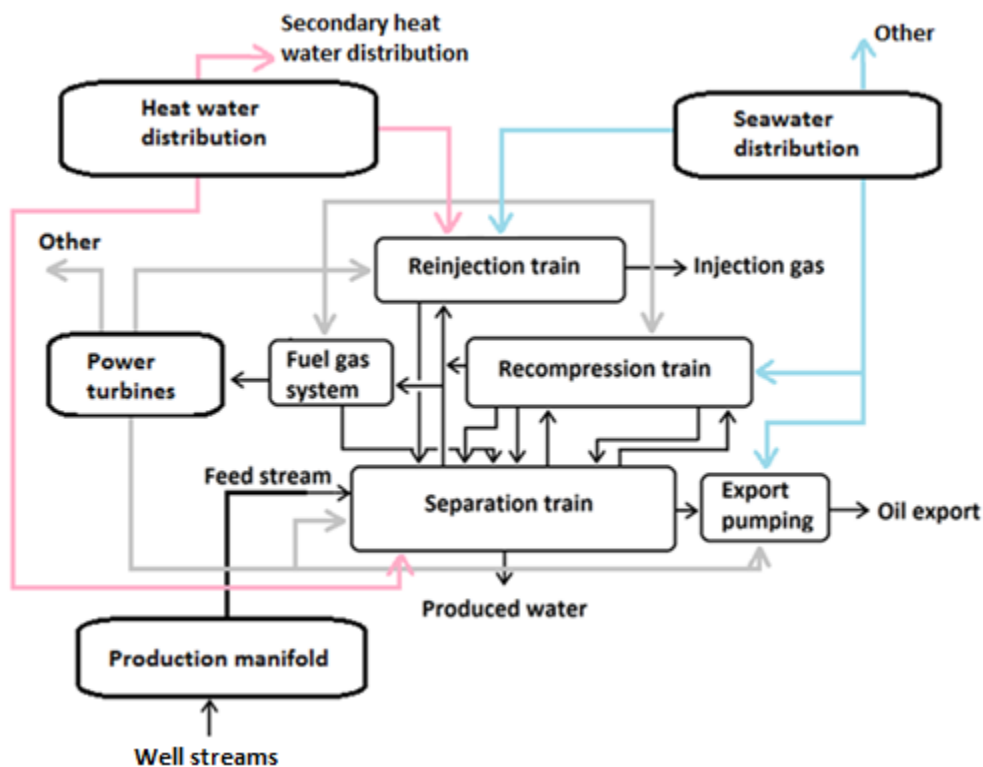
Figure 3.2 Schematic overview of energy steams at the oil and gas processing platform

Black, grey, pink and blue lines indicate mass, power, heating and cooling, respectively.

The power generation system consists of three gas turbines, two which generate electrical power and one that generates shaft power. The power goes to compressors, pumps and to other consumers. The fuel in the gas turbines is provided by the fuel gas system and comes originally from the well streams.

The seawater distribution system pumps seawater through the coolers in the recompression train, the reinjection train, the export pumping system and other to other consumers. The oil and gas

processing platform also has a hot water distribution system which distributes hot fresh water to the heaters in the separation train and the reinjection train. In addition, the hot water distribution system serves a secondary hot water distribution system, which goes to consumers outside the oil and gas processing plant. Heat from the power turbine exhaust is also utilized.

3.2   A more detailed system description

3.2.1   Oil and gas processing plant

Heavy crude oil enters as a feed stream from the wells. It is distributed in three different manifolds. In the manifold a selection of the wells are set into production. Depending on conditions, like pressure and temperature, streams which should be throttled down to high and low pressure (approximately 48 bar and 8 bar) go to the high and low pressure manifolds, respectively. There are also a test manifold and a separator, which are used to test the composition and quality of the wells. This test separator is normally only in use for analysis and detailed flow measurements or it can be used to reach the absolute maximum capacity. The pressure of the test manifold stream is 60.4 bar/ 97.4 bar (2010/ 2012). In the production manifold, the pressure of the HP, LP and test streams is reduced, parameters of the inlet streams to the separation train are presented in Table 3.1. The total incoming flow from the wells is approximately 1 665 Sm^3/h/ 1 724 Sm^3/h. An import gas stream enters the process in the reinjection train. This is gas from a 50 km long pipeline from a nearby gas center, and the total incoming flow with the gas import is approximately 160 000 Sm^3/h/ 0 Sm^3/h.

Table 3.1 Inlet conditions of the feed streams into the separation train

Feed streams into separation train	Pressure [bar]	Temperature [°C]	mol% gas	Flow [Sm^3/h]
2010				
HP	46.86	60.66	0.73	1168
LP	7.85	66.66	0.43	355
Test	13.76	60.09	0.83	141
2012				
HP	47.50	59.14	0.74	890
LP	7.52	68.63	0.12	801
Test	8.43	21.38	1.00	33

3.2.1.1   Separation train and export system

From the high pressure manifold, just referred to as the HP manifold, the oil enters a two-phase degasser. In the degasser the oil is given an extra degassing stage, which is important due to the oils high viscosity. This reduces the rate of gas to the 1st and 2nd stage compressors and thereby reduces compression work. The gas is sent to the first stage in the reinjection process, while the oil phase goes to the first separator in the separation train. Fluid from the LP manifold goes directly to the first separator. The pressure is reduced in several stages to allow a controlled separation of volatile components. A large pressure reduction in a single separator will cause flash vaporization and result in instability and safety hazards [31]. The separators are equipped with inlet cyclones to increase gas separation and prevent foaming. The three-phase separators are bigger and heavier than two-phase separators, but removal of water earlier in the process allows reduction of downstream equipment

size and heating duty. The oil droplets in the water are larger in size, which makes them easier to remove in the produced water injection system [30], see Section 3.2.1.5. An emulsion breaker is used to prevent the oil to form stable emulsions. The platform is also designed with downhole injection ports for chemical injection of emulsion breakers to each individual well.

The gas phase from the test separator goes, just like the gas from the HP degasser, to the first stage in the reinjection train. The two other streams go to the first separator.

The streams out from the first separator are distributed the following way; water enters the water treatment, gas goes to the second stage in the recompression train and the oil continues further against the second separator in the separation train. Heat is supplied after the first stage separator because sufficient separation of the crude is not achieved at low temperature,. The oil phase is divided into two streams. One for heat exchange in an oil/oil-exchanger with the oil from the coalescer which going to export, with a duty of 8 980 kW/ 7 878 kW, while the other part exchange heat with the water from the coalescer and the second separator in an oil/water-exchanger, with a duty of 234 kW/ 5 480 kW. UA-values, temperatures, pressures and flow rates are shown in Table 3.2. Pressure loss for the heat exchangers, and also heaters and coolers, are presented in Table 3.7. After the heating, the two streams are coupled together and additionally heated in an oil heater. From the second separator the gas, oil and water goes to the first stage in the recompression train, the electrostatic coalescer and water treatment, respectively. A pump is included on the water stream leaving the 2nd separator and the coalescer. The power of the pump is 2 kW/ 71 kW and the pressure has increased by 9.8 bar/ 8.6 bar.

The goal for a coalescer is final removal of water. In reality the platform has two electrostatic coalescers in parallel, but they are stowed in the model. The principle of the coalescer is that internal electrodes form an electric field to break surface bonds between conductive water and isolating oil in an oil-water emulsion. The coalescer is a two-phase separator that separates oil and water. It also has a little gas volume due to separation of eventual entrained gas. The coalescer sends the water phase for water treatment, the gas back to the second separator and the finished oil via a booster pump and an export pump to export. Between the two pumps the oil is cooled due to high separation train operating temperatures. The adiabatic efficiency of the pumps is presented in Table 3.6. The rate of oil export is 1 093 Sm^3/h/ 751 Sm^3/h at a pressure of 99 bar/ 92 bar and the oil goes through a 212 km long pipeline to an onshore terminal. The separation train and export system are shown in Figure 3.3, a larger version can be seen in Appendix K
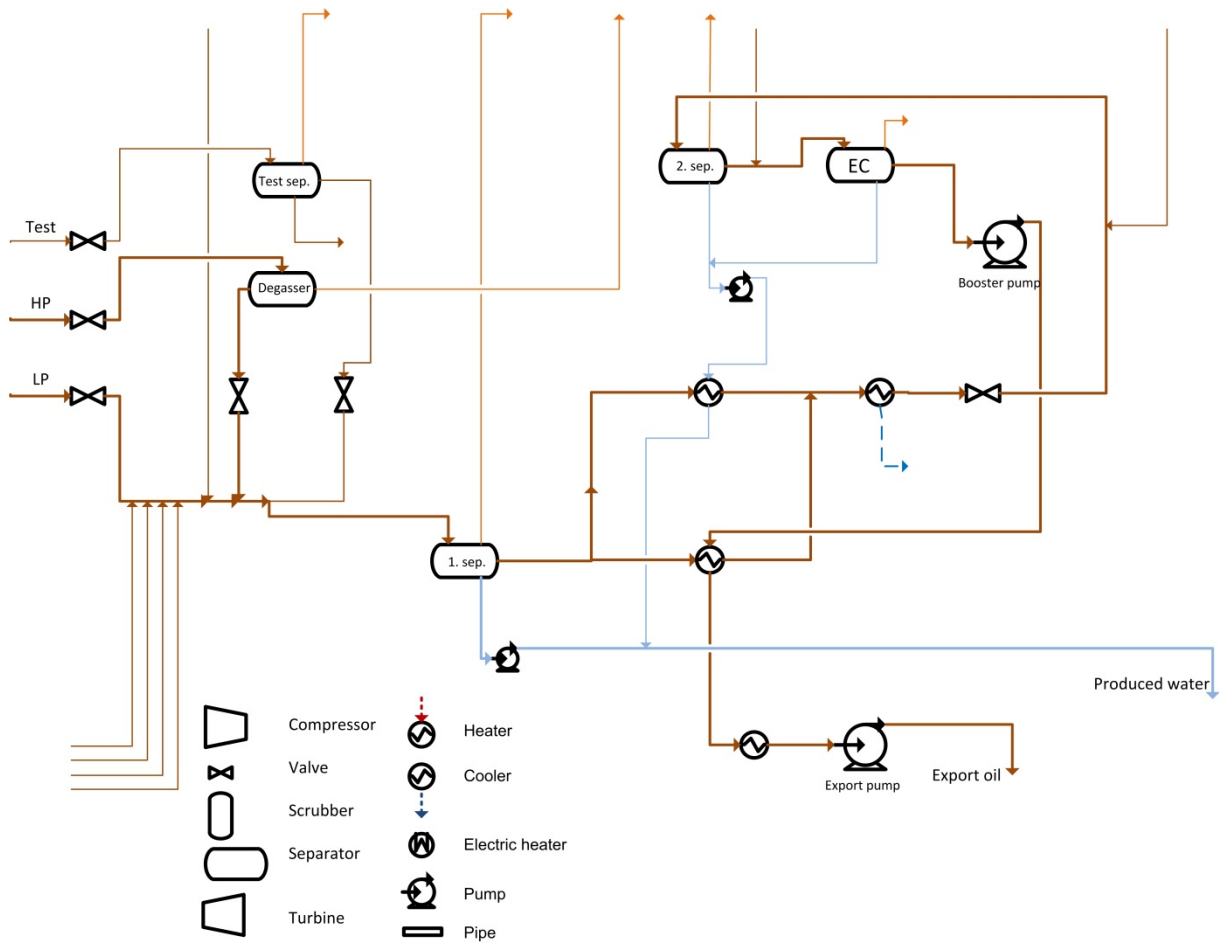
Figure 3.3 Schematic overview of the separation train and export system

Table 3.2 UA and maximum temperature, pressure and flow rate for the heat exchangers at two different dates

The design value is found in the heat exchangers datasheet.

	2010	2012	2010	2012	Design value
Model/Tagname	HB-20-0001		HB-20-0002		Alfa Laval M30-FD
UA [kJ/°Ch]	1.80E+07	1.09E+07	1.85E+06	1.85E+06	1.85E+06
Maximum temperature [°C]	97	101	97	101	180
Maximum pressure [barG]	12	13	13	11	25
Maximum flow rate [kg/s]	284	196	143	127	497

3.2.1.2 Recompression train

One stage in the recompression train consists of a cooler, a scrubber and a compressor, in that order. The separated gas from the separation train may contain small liquid droplets which can erode the fast rotating blades in the compressor. A scrubber removes these small fractions of liquid from the gas. After the first scrubber the gas enters the accompanying compressor and the oil enters the coalescer. After the compression, the stream enters the second scrubber, which distributes the gas and oil phase to the corresponding compressor and back to the second separator, respectively. In this stage the stream from the compressor also proceeds to the next scrubber. At the third scrubber

the oil is sent the whole way back to the first separator, and the gas is driven into the accompanying compressor. To prevent compressor surging, an anti-surge control system recirculates a part of the stream out of the compressors. The gas from the discharge side flows back to the suction side, via the cooler and the scrubber to prevent overheating [31]. In the 1st, 2nd and 3rd recompression stages, approximately 2 500 Sm^3/h/ 3 300 Sm^3/h, 30 500 Sm^3/h/ 6 500 Sm^3/h and 16 800 Sm^3/h/ 6 900 Sm^3/h are recirculated, respectively. The corresponding recirculation ratio is shown in Table 3.3. During the recompression train the pressure is increased from around 7.2 bar/ 6.9 bar to approximately 45.7 bar/ 46.6 bar. Centrifugal compressors, which are smaller and lighter than reciprocating compressors, are used. They have higher capacities and power and are more compatible with common offshore gas turbines and electric motors. The recompression train is shown in Figure 3.4, a larger version can be seen in Appendix K.
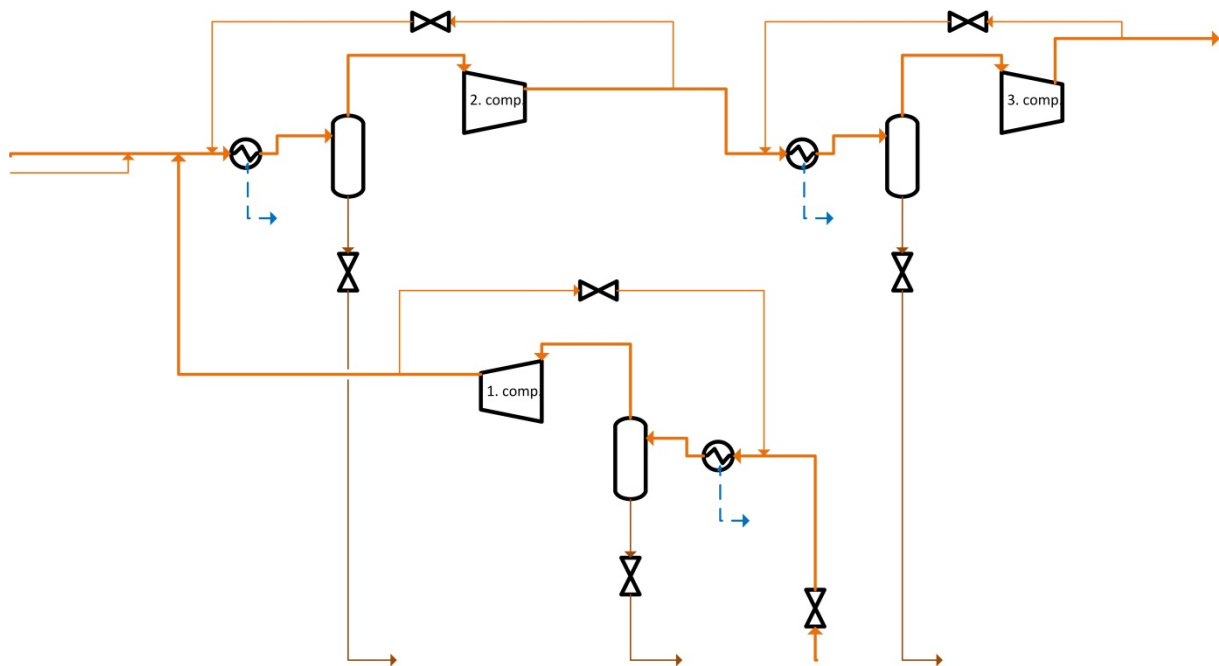
Figure 3.4 Schematic overview of the recompression train

3.2.1.3   Reinjection train

After the compression in the third stage in the recompression train, the stream enters the reinjection train. One stage in this train consists of a cooler, a scrubber and a compressor, just like in the recompression train. The first scrubber sends the oil back to the first separator, and the gas phase is divided between the corresponding compressor and the fuel gas system. After the compression, one part is returned to the first stage in the reinjection train and the other part is aiming further to the second stage in the reinjection train. The same procedure happens in the second scrubber, oil is sent back to the first separator and the gas enters the accompanying compressor. After the compression in the second stage the stream is distributed between gas lift, gas injection and the remaining part is returned back in front of the second stage in the reinjection train. The injected gas and gas lift have a pressure of 184.4 bar/ 170.8 bar and a total flow rate of 383 000 Sm^3/h/ 266 000 Sm^3/h. Gas injection is the primary drive mechanism and gives a better recovery than water injection. Since not enough gas is produced at the platform at all times it can be imported. The plan is to produce the injected gas in a later phase of the field development. The import gas is divided between the fuel gas

scrubber, the second stage in the reinjection train and an import gas stage consisting of a cooler, a scrubber and a compressor. The gas flow from the second scrubber go through an import gas heater, and a fraction can then be sent to the fuel gas system. The fuel gas is combusted in power turbines and in pilot flames in the flare system. From the import gas scrubber the oil and gas goes back to the first separator and the accompanying compressor, respectively. After the compression stages in the reinjection train, the gas is distributed between gaslift and gas injection. Also in the compressors in the reinjection train there is anti-surge control system, but it is only used in the import gas compression stage [32]. The reinjection train increases the pressure from the outlet pressure of the recompression train at roughly 46 bar to the well injection pressure at 184.4 bar/ 170.8 bar. The goal of the reinjection is to keep the reservoir pressure close to the initial pressure. The adiabatic efficiencies of the compressors are shown in Table 3.6. The reinjection train is shown in Figure 3.5, a larger version can be seen in Appendix K.
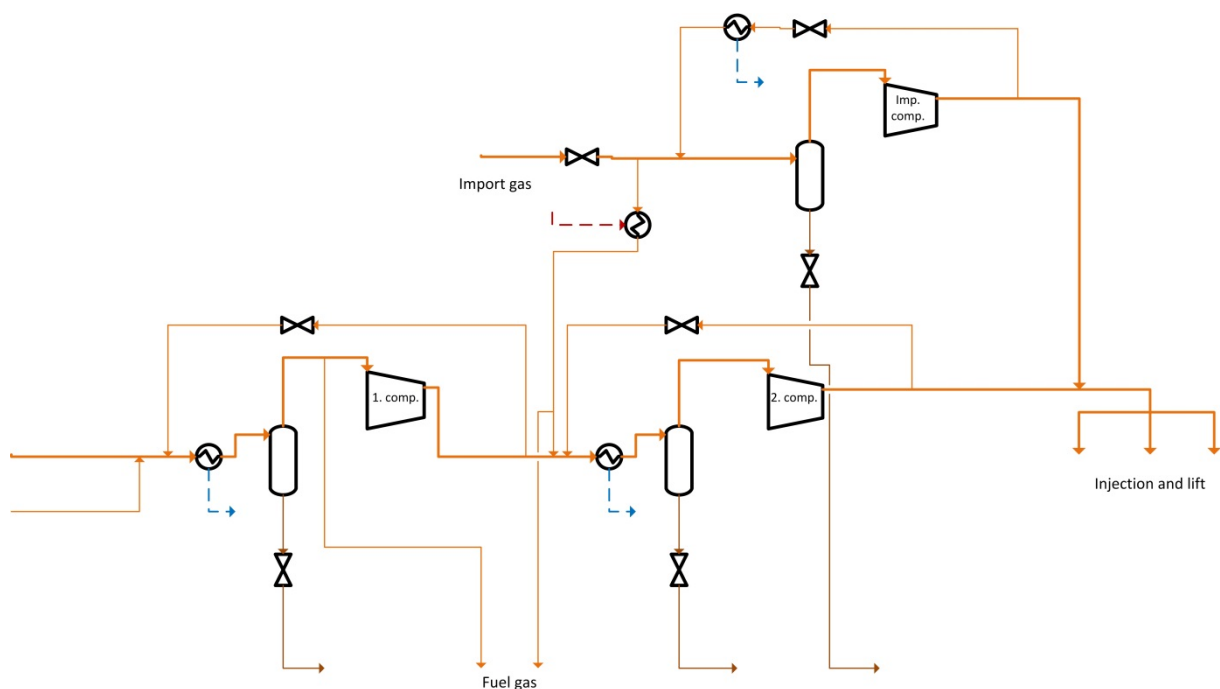
Figure 3.5 Schematic overview of the reinjection train

Table 3.3 Recirculation rates for the compressors

The recirculation rate is given in volume percent of the flow rate through the specific compressor

	Recirculation rate [%]	
Compressor	2010	2012
KA-23-0001	40	48
KA-23-0002	30	7
KA-23-0003	19	8
KA-23-0004	0	0
KA-23-0005	0	0
KA-23-0006	23	-

More details about the temperature and pressure in the different sub-processes are presented in Table 3.4 and Table 3.5.

Table 3.4 Temperature in different sub-processes

Description	Tag	Temperature [°C]	
		2010	2012
Well fluids from several producing wells	Wells	50.45 / 73.20 (LP / HP)	50.81 / 72.04 (LP / HP)
Mixed streams after production manifolds	1010 & 1020	60.66 / 66.16 (Low / High)	59.30 / 68.22 (Low / High)
Oil after separation train	2030	96.58	100.56
Oil pumped for export	1450	76.40	81.30
Treated gas before injection/lift	2560 (2010) and 2550 (2012)	74.96	86.00
Produced water before injection	4058a	61.78	74.35
Produced water after treatment	4058b	61.87	75.10
Fuel gas	2428	60.92	51.55
Gas import	2600	4.39	-

Table 3.5 Pressure in different sub-processes

Description	Tag	Pressure [bar]	
		2010	2012
Well fluids from several producing wells	Wells	13.04 / 110.50 (LP / HP)	11.05 / 99.80 (LP / HP)
Mixed streams after production manifolds	1010 & 1020	7.22 / 46.04 (Low /High)	6.90 / 46.96 (Low / High)
Oil after separation train	2030	2.75	2.61
Oil pumped for export	1450	99.12	92.05
Treated gas before injection/lift	2560 (2010) and 2550 (2012)	184.40	170.75
Produced water before injection	4058a	7.22	9.76
Produced water after treatment	4058b	2.32	57.70
Fuel gas	2428	38.88	38.30
Gas import	2600	109.96	-

3.2.1.4   Fuel gas system

The fuel gas system provides gas to the power turbines. The fuel gas is drained from the gas stream just before entering the 1st compressor in the reinjection train. It is also possible to let a part of the import gas enter the fuel gas system, but this is seen as a backup solution. The drained gas goes to a scrubber where the final removal of liquid happens. The amount of fuel gas is 9 656 Sm^3/h/ 9 179 Sm^3/h. Before the fuel gas is ready to be used in power turbines it is heated up to 61 °C/ 52 °C and has a pressure of 38.9 bar/ 38.8 bar. The fuel gas system is shown in Figure 3.6, a larger version can be seen in Appendix K.
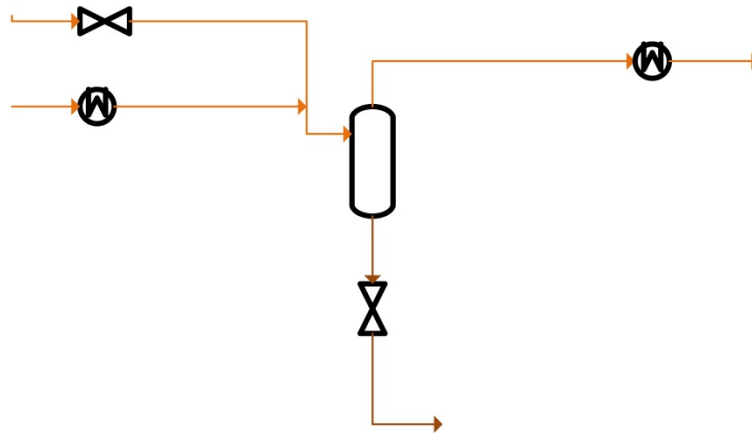
Figure 3.6 Schematic overview of the fuel gas system

3.2.1.5 Produced water injection system

Treatment of produced water is achieved by using a hydro cyclone and a degasser tank. Oil and water are separated by gravitational forces and flotation in the degasser tank. Flotation is degradation of oil-water emulsions by using fuel gas. After treatment the water, with a flow rate of 8 Sm^3/h/ 305 Sm^3/h, is injected to the reservoir and delivers produced water to the same formation as the drill cuttings. The pressure of the produced water is 2.3 bar/ 57.7 bar. Alternatively water is sent back to the sea if the injection system is out of order. The water injection uptime was reported to be 95 % in 2005. The produced water injection system is shown in Figure 3.7, a larger version can be seen in Appendix K.

Hydrocyclone/Degassing
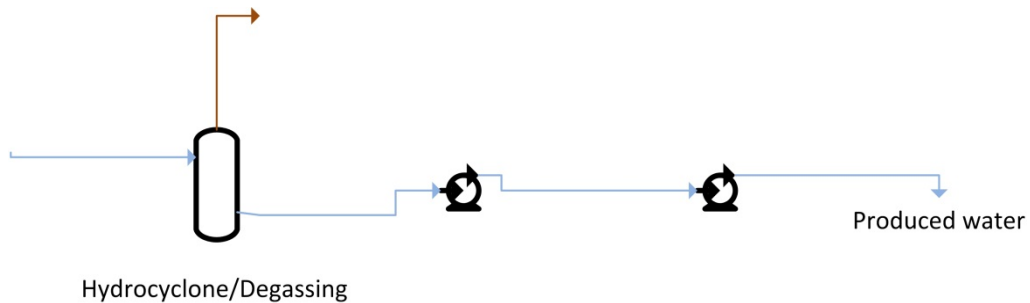
Produced water

Figure 3.7 Schematic overview of the produced water injection system

Table 3.6 Adiabatic efficiency of compressors and pumps

	Adiabatic efficiency [%]		
	2010	2012	Source
Compressor:			
KA-23-0001	61	66	Calculated
KA-23-0002	74	73	Calculated
KA-23-0003	65	66	Calculated
KA-23-0004	81	78	Calculated
KA-23-0005	71	66	Calculated
KA-23-0006	68	-	Calculated
Pumps:			
PA-21-0001	76	76	Performance curves
PA-21-0002	74	74	Performance curves
PG-20-0001A/B/C/D	75	75	Default value
PG-20-0001E/F	75	75	Default value
PA-50-0001A/B	77	80	Performance curves
PA-41-0001A/B/C	81	80	Performance curves
PA-4058-1	75	75	Default value
PA-4058-2	75	75	Default value

Table 3.7 Pressure loss in heaters, coolers and heat exchangers

	Pressure loss [bar]					
Component	2010		2012		Datasheet	
	Hot side	Cold side	Hot side	Cold side	Hot side	Cold side
HA-22-0001	1	1	-	-	1	1
HA-23-0003	0.68	1	0.65	1	0.8	1
HA-23-0004	1.28	1	1.54	1	0.7	1
HA-23-0005	1.24	1	1.52	1	0.5	1
HA-23-0006	1	1	-	-	1	1
HB-20-0001	1.5	1.5	1.5	1.5	1.5	1.5
HB-20-0002	1.5	1.5	1.5	1.5	1.5	1.5
HB-20-0003A/B/C	1	1.5	1	1.5	1	1.5
HB-21-0001	3.14	1	0.12	1	0.8	1
HB-23-0001	1.51	1	1.34	1	0.35	1
HB-23-0002	1.29	1	1.11	1	0.8	1

3.2.2 Power generation system and distribution systems

The processes on the platform may use three forms of energy; heat and cooling for processing of oil and gas, mechanical power to drive compressors and pumps and electricity to drive compressors, pumps, electrical heaters and living quarters.

3.2.2.1 Seawater distribution system

The seawater distribution system delivers seawater to the consumers at the platform. The seawater is primarily both used as cooling water and in the drilling system. Since the platform utilizes seawater injection for reservoir pressure maintenance, the incremental cost to utilize this water for process cooling is considerably reduced. 2 201 Sm^3/h/ 2 400 Sm^3/h of seawater is pumped up from an intake 50 meters below the sea level. The distribution pressure is 11.4 bar and 692 Sm^3/h/ 694 Sm^3/h of the seawater goes to the coolers in the oil and gas processing process. The seawater distribution system is shown in Figure 3.8, a larger version can be seen in Appendix K.
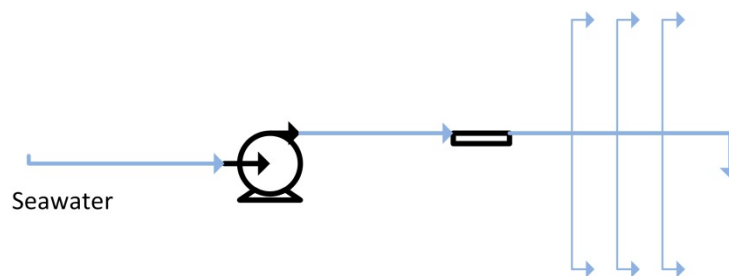
Seawater

Figure 3.8 Schematic overview of the seawater distribution system

3.2.2.2 Hot water distribution system

The water distribution system consists of pure fresh water, only added corrosion inhibitor. The system utilizes waste heat from the exhaust of the three power turbines. The hot water distribution system is used in the heater before the second stage separator to make the separation easier. If import gas is used in the second compression stage in the reinjection train, the gas is heated in the import gas heater which is served by the hot water distribution system. In addition the hot water is used in a secondary hot water distribution system which serves HVAC and the fresh water generator. The distribution pressure is 24.9 bar and the temperature is 122 °C/ 126 °C. The hot water distribution system is shown in Figure 3.9, a larger version can be seen in Appendix K.

Exhaust gas

To hot water consumers

Secondary hot water

From hot water consumers
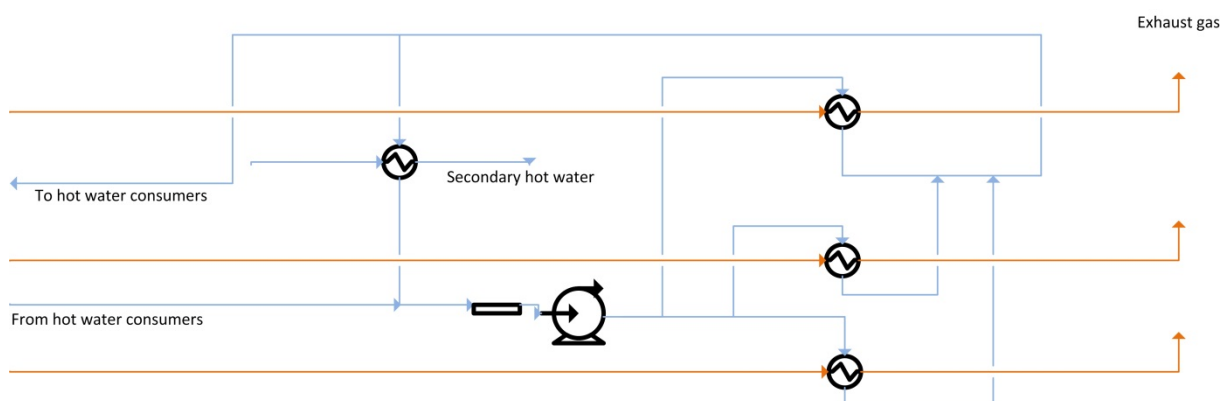
Figure 3.9 Schematic overview of the hot water distribution system

3.2.2.3 Turbine system

All mechanical and electrical power consumed at the oil and gas processing platform originate from the platform's power generation system, which consists of three gas turbines. Each turbine has a nominal capacity of 25 MW. Table 3.8 shows data for the real turbines. The data is based on engineering manuals and the simulated turbines try to fit these data as good as possible. A mechanical drive turbine serves shaft power to the second and third compressor in the recompression train, and to the first and second compressor in the reinjection train. This is a LM2500+ Dry Low Emissions power turbine. The other compressors in the oil and gas processing plant use electrical power from the two remaining gas turbines. One is a LM2500+ Dry Low Emission high speed power turbine that runs on fuel gas, and the other is a LM2500+ Standard Annular Combustor high speed power turbine that can run on both diesel and fuel gas. As long as the electric load is under 20 MW, only one of the turbines is in action. The air compressors have a pressure ratio of 23 and a mass based air fuel ratio of approximately 44/ 43. The combustion gives a stoichiometric lambda, λ_{stoich} ,of approximately 10.57 and a corresponding mass based air fuel ratio, AF , of about 16.28. This gives a percent of theoretical air, λ, at roughly 2.70/ 2.64, which is quite normal for this kind of gas turbines. The temperature just after the combustion is 1 350 °C, somewhat lower than the adiabatic flame temperature of the combustion, which is calculated to circa 1 522 °C. The thermal efficiency of the gas turbines varies between 31 % and 41 %. This and more details of the gas turbines are presented in Table 3.9. GG is an abbreviation for gas generator.
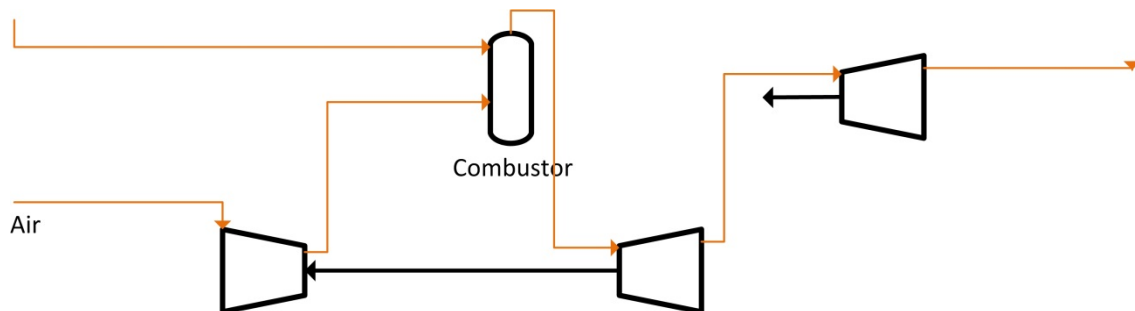
Figure 3.10 Schematic overview of a turbine unit

Table 3.8 Data for the real gas turbines at the power generation system based on engineering manuals

Turbine	CT-23-0001	CT-80-0001A	CT-80-0001B
Unit	LM2500+ HSPT DLE	LM2500+ /PGT SAC, Aeroderivative	LM2500+ /PGT DLE, Aeroderivative
Application	Mechanical Drive	Generator Drive	Generator Drive
Fuel pressure required	38-42	33-38	35-40
Air compressor:			
Stages	17	17	17
Pressure ratio	23	23	23
Turbine:			
Stages	2+2	2	2

Table 3.9 Data for the simulated gas turbines at the power generation system

	2010		2012	
Turbine	CT-23-0001	CT-80-0001B	CT-23-0001	CT-80-0001A
LHV [kW]	65 382	34 482	62 641	33 036
Net power output [kW]	26 807	13 507	25 683	10 102
Thermal efficiency [%]	41	39	41	31
AF [kg/kg]	44	44	43	43
Pressure ratio	23	23	23	23
TIT GG Turbine [°C]	1 350	1 350	1 350	1 350
TIT Power Turbine [°C]	929	923	937	937
Adiabatic efficiency GG Compressor [%]	75	75	75	75
Adiabatic efficiency GG Turbine [%]	90	90	90	90
Adiabatic efficiency Power Turbine [%]	94	91	94	70

Table 3.10 Adiabatic efficiency of compressors and turbines

	Adiabatic efficiency [%]		
	2010	2012	Source
GG Compressor-3	75	75	Default value
GG Turbine-1	90	90	Assumed
GG Turbine-3	90	90	Assumed
Power Turbine-1	94	94	Calculated
Power Turbine-3	91	70	Calculated

4   Methodology

4.1   Simulation of the process flowsheet

The processes of the oil and gas platform were simulated using Aspen HYSYS [16]. A model of the oil and gas processing at the platform has been developed by the oil company. This model has been modified and extended. The Peng Robinson property package was used, which is the recommended property package for oil and gas applications [33]. Thermodynamic properties of all mass and energy streams were calculated with the Peng Robinson equation of state (PR EOS). The HYSYS version of the PR EOS is given in Appendix C. HYSYS uses the COSTALD (corresponding states liquid density) method as a default for all property systems for mixtures/streams with a pseudo critical temperature below unity. The COSTALD method calculates better liquid densities than the equation of state [33]. Elevation differences were neglected, but a table with the elevation of the real components is shown in Appendix E. The error in mass balance, due to Recycle-components, is negligible. Heavy oil fractions were simulated by the use of pseudo components. They are made-up components that represent oil fractions that can consist of a number of different real components. For more details and properties of the pseudo components, see Appendix D. Composition of oil, gas and water fractions were set as predicted for 2009 by the oil company and is shown in **Error! Reference source not found.**

4.1.1   Input data

The measured values are obtained from the oil company's own live tracking system. The relevant measurements to read of are found from piping and instrument diagrams. Two different dates are evaluated; 2010-10-29 and 2012-10-29, both at 12:00 o'clock.

Approximately uncertainties for different type of measurements for another oil and gas processing platform in the North Sea are given in Table 4.1. [34].

Table 4.1 Uncertainty of measurements for temperature, pressure, flow rates and electric current

Type	Uncertainty
Temperature	1 °C
Pressure	1 %
Oil export flow rate	0.3 %
Fuel gas flow rate	1.8 %
Other flow rate	10 %
Electric current	2 %

The uncertainties in the measured values are based on the oil company's own requirements for accuracy on process measurements, the requirements from The Norwegian Petroleum Directorate and The Climate and Pollution Agency for fiscal metering, and discussions with the operators of the platform.

The main process of an oil and gas processing platform usually takes approximately 15-30 minutes, but if the process is not in a stationary state there will be some lagging effects. It is also worth noting

that the measurements of temperature and pressure represent a snapshot, but the measurements of flow rates often are average over a short period of time. Also the frequency of measurements varies. A normal production day was selected based on pressure, temperature and flow rates of inlet and outlet material streams of the platform. The measured values in and out of the process are investigated over a period of 24 hours for both dates. For the date in 2010 the deviation within 24 hours is under 0.4 % for temperatures, 1.0 % for pressures and 1.8 % for flow rates. The exceptions are the measurements related to the test manifold, the pressure out of one of the oil export pumps and the water injection flow rate. The date in 2012 has a deviation below 2.4 % for temperatures, 7.0 % for pressures and 6.1 % for flow rates. The exceptions are the pressure out of one of the water injection pumps and the water injection flow rate. More details can be seen in Appendix I.

Most of the measured values of pressure are given in gauge pressure and the input values in HYSYS are in absolute pressure. The atmospheric pressure difference between gauge and absolute pressure is approximated to one bar, instead of one atm, to make the manually read of of the measured values easier.

Measured values which are not used direct as input are compared with the values simulated to check the validity of the produced flowsheet. The comparison can be seen in Appendix J.

Where measurements are not available other sources have to be applied. Documentation of the process equipment, in datasheets given by the contractors, gives information about the process variables. The values given are not automatically representative for the real process, but the order of magnitude should be reasonable. Pump efficiencies are set based on the pumps performance curves provided by the contractors. The efficiencies are given as function of flow rates and rotational speed, and are based on tests with similar fluid to the fluid in question. Also the so called engineering manuals give useful information, mostly on typical temperatures and pressures of the fluid in the seawater distribution system and the hot water distribution system. When no form of documentation is found, values are assumed based on discussions with people with experience or set to the default value in HYSYS. Some input values are calculated based on two or three measured values. All these input values are listed in Appendix G.

The number of digits of the input value in the appendix varies a lot, much depending on source, but in the simulation the input values of temperature, pressure and flow have two decimals.

4.1.2   Facilitating Components

Different facilitating components are used to make the implementation of the HYSYS process flowsheet easier. The Set-component is used to set a variable of the target stream to a function of the corresponding variable of source stream, e.g. set the pressure of the target stream equal to the pressure of the source stream. A Set-component is shown in Figure 4.1.
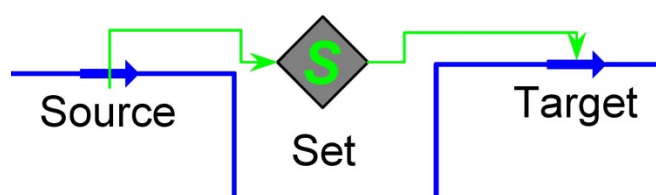
Figure 4.1 A Set-component linked to a source stream and a target stream

The Adjust-component is used to set a variable of the target stream to a specified value by adjust a variable of the adjusted stream. The target value can be a user supplied value, another object or a spreadsheet cell. An Adjust-component is shown in Figure 4.2.
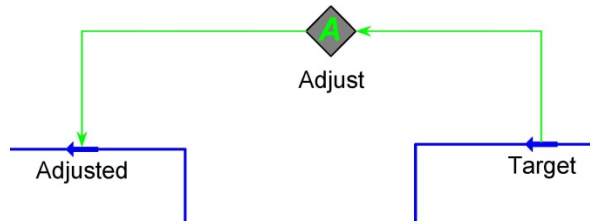
Figure 4.2 An Adjust-component linked to an adjusted stream and a target stream

The Recycle-component is used to help the simulation to converge. It has settings for how much the different variables are allowed to change through the component. A Recycle-component is shown in Figure 4.3.
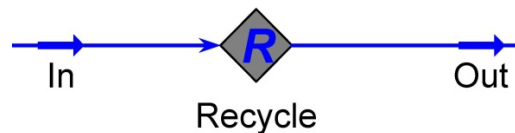
Figure 4.3 A Recycle-component linked to an in stream and an out stream

The Cutter-component is used for a transition, e.g. change of fluid package. This is necessary if an operation should be done on a stream where important parameters of the fluid package are unknown. A Cutter-component is shown in Figure 4.4.
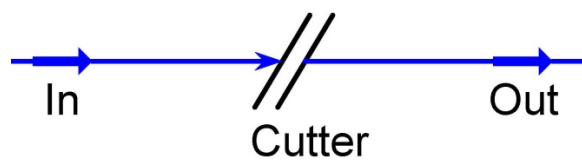
Figure 4.4 A Cutter-component linked to an in stream and an out stream

In this simulation the sensitivities of all Recycle-components is set to 0.02, except for the sensitivity of the enthalpy in RCY-6, where it is set to 0.06. The tolerance of the Adjust-components is shown in Table 4.2. ## indicates the number of the well and # indicates the number of the compressor.

Table 4.2 Tolerance of the Adjust-components

Adjust	Tolerance	Unit
ADJ-##-Oil	1	m^3/d
ADJ-##-Gas	1	Sm^3/d
ADJ-##-Water	1	m^3/d

ADJ-KA-23-000#	10	Sm^3/d
ADJ-Temp	0.1	°C

4.1.3   Process components

All separators are simulated without pressure loss and the only user specified value based on measurements is the pressure of the inlet stream. A separator is shown in Figure 4.5.
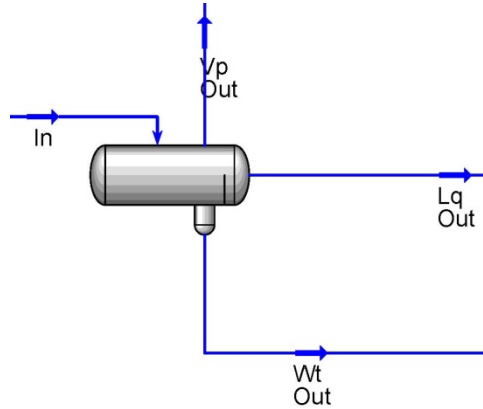
Figure 4.5 A separator with an inlet stream, a vapor stream, a liquid stream and a water stream

All scrubbers are simulated without pressure loss. Pressure and temperature of the inlet stream are specified for all scrubbers, except the import gas scrubber, VG-23-0006, where no variables are specified. A scrubber is shown in Figure 4.6.
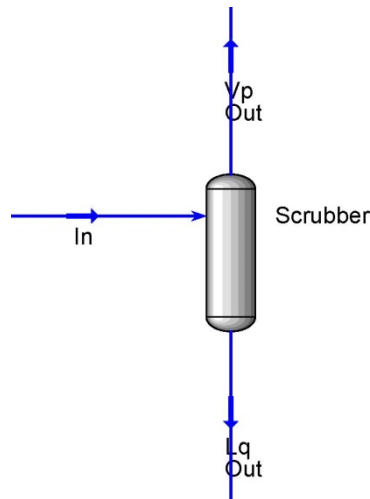
Figure 4.6 A scrubber with an inlet stream, a vapor stream and a liquid stream

All mixers set the outlet pressure equal to the lowest inlet pressure. A mixer is shown in Figure 4.7.
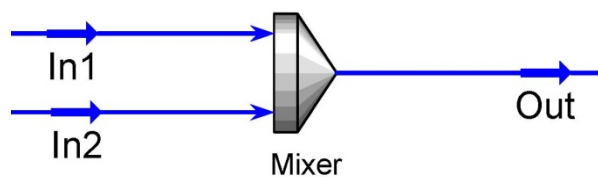
Figure 4.7 A mixer with two inlet streams and one outlet stream

The important parameter of a tee is the splits of the flow ratios. Most split flow ratios are not specified, but based on specified flow of the corresponding streams. For the tees PROD_DIV and FUEL2 the split flow ratio is specified based on the engineering manuals of the platform. The split flow ratio of FUEL1 is manually adjusted to fit the measured flow out of the superheater FE-45-0002A/B. For TEE-Turbine the split ratio is based on the flows to CT-23-0001 and CT-80-0001A in 2012. Due to lack of information the split flow ratios in the water distribution system is assumed to be 50/50 for all tees. A tee is shown in Figure 4.8.
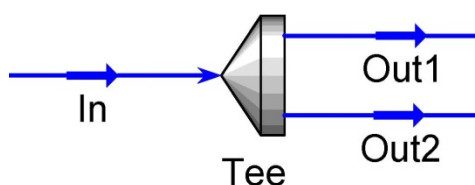
Figure 4.8 A tee with one inlet stream and two outlet streams

The valves can be divided into five categories; valves at the liquid stream out of the scrubbers, valves at the recycle stream of the compressors, valves related to separators, valves in the manifolds and other valves. The pressures after the valves at the liquid streams out of the scrubbers VG-23-0002/6, are set equal to the pressure of the inlet stream of the first separator, VA-20-0001. The valve at the liquid stream out of the scrubber VG-23-0001 is assumed to have no pressure drop, and the valve related to VG-23-0002 is assumed to have an outlet pressure of 5 bar. The valves related to the recycle stream of the compressors have an outlet pressure equal to the lowest pressure at the inlet of the related mixer, see Figure 4.17. The exception is the valve related to the import gas compressor where the pressure is set in a way that the pressure at the inlet of the scrubber is equal to the measured value. The valves related to the separators decrease the pressure down to the specified pressure of the upcoming separator. The valves in the wells have specified values for both inlet and outlet pressure, and the valves in the manifolds reduces the pressure down to the inlet pressure of the corresponding separator. The valve PV-45-0103 decreases the pressure of the fuel gas stream down to the specified inlet pressure of the fuel gas scrubber, VG-45-0001. A valve is shown in Figure 4.9.
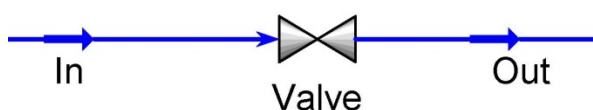
Figure 4.9 A valve with an inlet stream and an outlet stream

All compressors have specified outlet pressure and temperature. The inlet condition is calculated based on the inlet conditions of the corresponding scrubber. The exception is the import gas compressor which has measured values for inlet pressure and temperature. A compressor is shown in Figure 4.10.
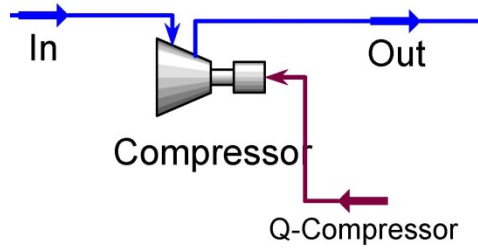
Figure 4.10 A compressor with an inlet and an outlet stream and a power stream

The coolers have no specified values. The related heaters has specified pressure drop from the components datasheet. The heater is just for calculation purpose. A cooler with its related heater is shown in Figure 4.11.
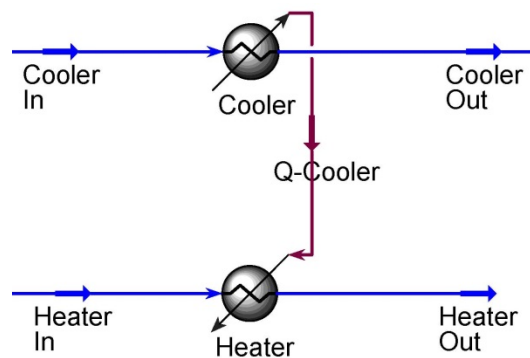
Figure 4.11 A cooler with an inlet and an outlet stream

It is connected to a heater for calculation purpose.

The heaters have specified pressure drop from the components datasheet, the exception is the electrical superheater FE-45-0002A/B where both inlet and outlet pressure are specified. The cooler is just for calculation purpose. A heater with its related cooler is shown in Figure 4.12.
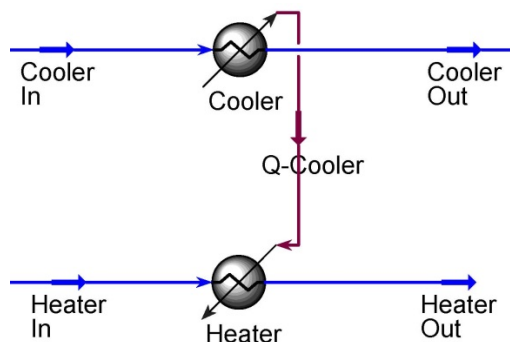
Figure 4.12 A heater with an inlet and an outlet stream

It is connected to a cooler for calculation purpose.

The heat exchangers have specified pressure drop, both on shell side and tube side. The oil/water heat exchanger, HB-20-0002, has also specified UA-value form datasheet, called UA service value. A heat exchanger is shown in Figure 4.13.
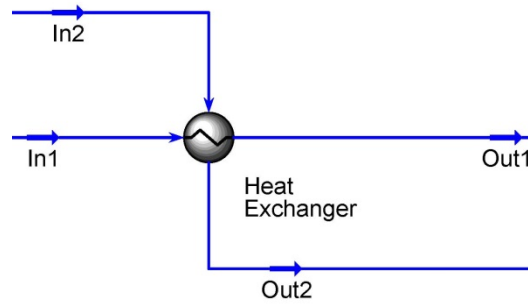
Figure 4.13 A heat exchanger

The heat exchanger has one inlet and one outlet stream at the tube side, and one inlet and one outlet stream at the shell side.

Nearly all pumps have a specified adiabatic efficiency; this is found in the pumps performance curves. The exception is PG-20-0001A/B/C/D, PG-20-0001E and the pumps in the produced water injection, which uses the default value of 75 % adiabatic efficiency. The dummy pump, which only is included for simulation purposes in order to secure no vapor phase out of the coalescer, has a specified adiabatic efficiency of 100% and a specified duty that is as low as possible. A pump is shown in Figure 4.14.
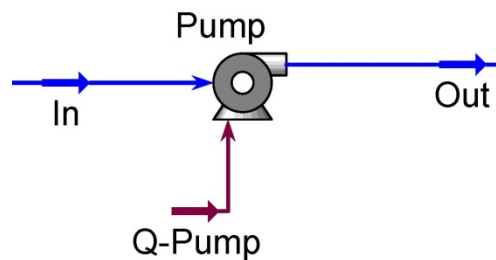
Figure 4.14 A pump with an inlet and outlet stream and a power stream

The pipes are used to simulate the pressure loss in the long pipes in the seawater and hot water distribution. Both the inlet and the outlet stream have specified/calculated pressures, so the only specification of the pipes is an assumed geometry. A pipe is shown in Figure 4.15.
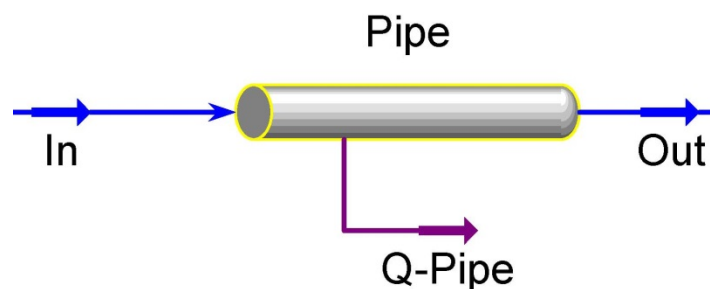
Figure 4.15 A pipe with an inlet and an outlet stream and a heat stream

The turbines GG Compressor and GG Turbine have assumed adiabatic efficiencies of 75 % and 90 %, respectively. The temperature of the surroundings is assumed to be the measured value of the surrounding air for CT-80-0001A. The GG Compressor has a pressure ratio of 23 according to user manuals. The temperature after the combustion is assumed to be 1350 °C and is achieved by

adjusting the mass flow of air. The power out of the Power Turbine is specified based on measurements for the generator drive turbines and for the mechanical drive turbine the thermal efficiency is assumed to be 41 %. Generator efficiency is neglected. Since the reaction stoichiometry is not known, the reactor type "Gibbs Reactions Only" is chosen. The Gibbs reactor is assumed to have no pressure drop; thereby the outlet pressure is equal to the air inlet pressure. A figure of the turbine unit can be seen in Section 3.2.2.3 or in Appendix K.

4.1.4   Process units

The measured values for oil, gas and water flow rates were given in m^3/h, Sm^3/h and m^3/h, respectively. For each well the temperature and pressure of the oil, gas and water feed stream were set, and the molar flow rate were adjusted to fit with measured values for volumetric flow rate. The "measured" values of volumetric flow are only calculated values and the uncertainty is considered high. The way to manage this was to tune the flow rate to fit the flow rates out of the process, since these flow rates are measured with a better precision. A solution, where the adjust-component of the feed streams of oil, gas and water was linked to a spreadsheet cell, was made. The ratio between the linked target value and the calculated flow rate from the measurements was tuned until the simulated volumetric flow rate out of the process became equal to the measured volumetric flow rate out of the process. Since the volumetric flow rate out of the process is dependent of the temperature and pressure, the ratio between the linked target value and the calculated flow rate from measurements had to be further tuned when pressures, temperatures and efficiencies were set throughout the process. Table 4.3 shows the ratio between measured and simulated flow rates of gas, water and oil outlet and inlet of the oil and gas processing platform. Figure 4.16 shows a well unit, a larger version can be seen in Appendix K.

Table 4.3 Ratio between measured flow rates and simulated flow rates of gas, water and oil outlet and inlet of the oil and gas processing platform

	Measured / Simulated, outlet		Measured / Simulated, inlet	
	2010	2012	2010	2012
Gas Flow Rates	1.010	1.008	1.25	1.15
Water Flow Rates	1.028	0.974	0.03	0.72
Oil Flow Rates	1.007	0.991	0.79	1.10
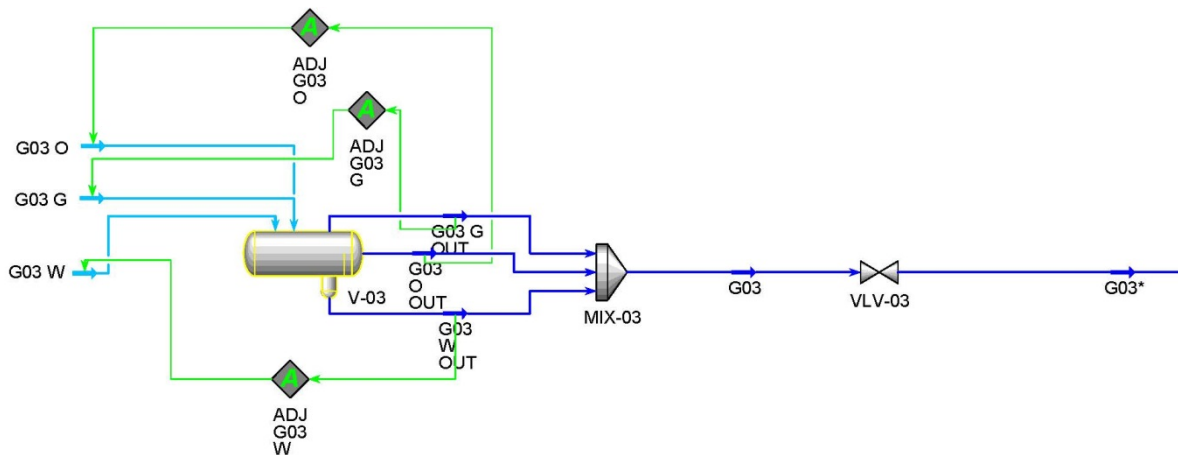
Figure 4.16 Schematic overview of a well unit

For the compression stages, Adjust-components are used to set the flow rate through the compressor by adjusting the recirculation flow rate. The Set-components set the pressure of the recycle stream after the throttling. As an example, the 3rd compression stage in the recompression train is shown in Figure 4.17, a larger version can be seen in Appendix K.
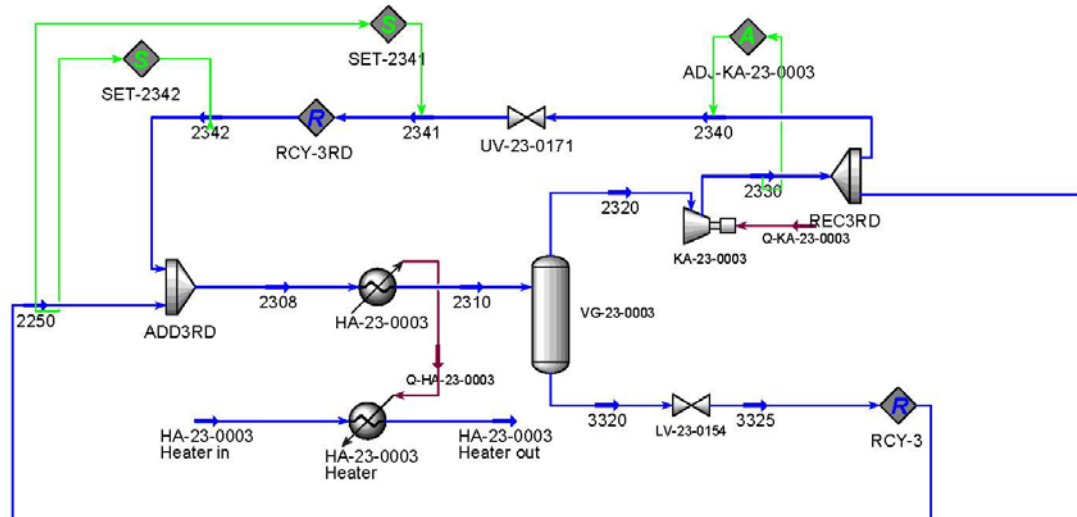
Figure 4.17 Schematic overview of a gas compression stage

The power turbines are modeled by a reactor where the combustion of fuel gas and compressed air takes place, a compressor to compress the air, a turbine to supply the compressor with shaft work and another turbine to produce the net power output. An Adjust-component sets the temperature out of the combustion, which means the TIT of the first turbine, by adjusting the flow rate of air into the compressor. A cutter changes the fluid package from the fluid package used in the simulation of the oil and gas processing to a fluid package which makes HYSYS able to simulate the combustion, before the fuel enters the combustion. The change in mass flow rates due to the cutter is presented in Table 4.4. A figure of the turbine unit can be seen in Figure 4.18 and a larger version is available in Appendix K.

Table 4.4 Changes in mass flow rates due to the cutter

	Mass flow [kg/h]	
Cutter	In	Out
2010		
Fuel Gas CT-23-0001-Cutter	5 076	4 992
Fuel Gas CT-80-0001B-Cutter	2 677	2 633
2012		
Fuel Gas CT-23-0001-Cutter	4 842	4 765
Fuel Gas CT-80-0001A-Cutter	2 554	2 513
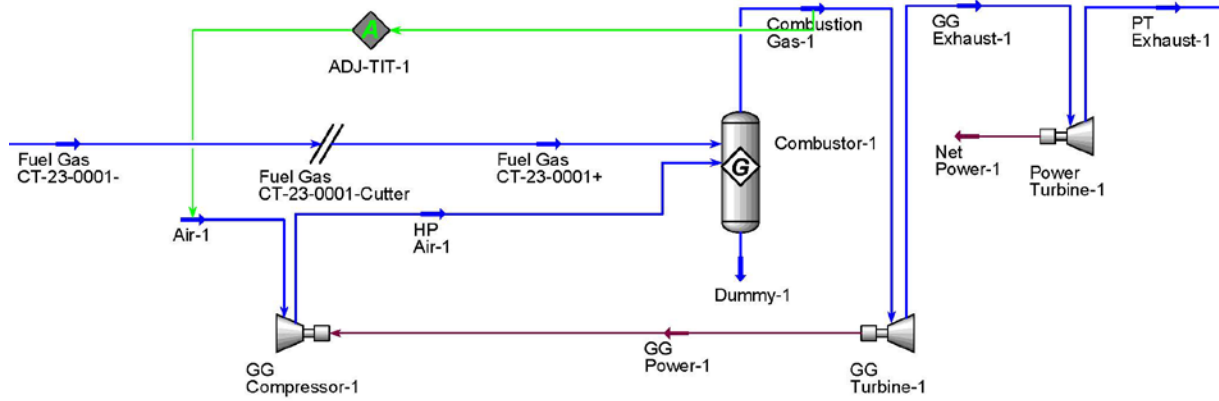
Figure 4.18 Schematic overview of a gas turbine unit

The fuel is modeled by the following components and mole fractions:

Table 4.5 Components and mole fractions of the fuel

Component	Mole fraction
CO_2	0.012967102
CH_4	0.864927367
C_2H_6	0.076566101
C_3H_8	0.027601713
C_4H_{10}	0.007040184
C_5H_{12}	0.001314781
H_2O	0.000906046
N_2	0.008676707

The air is modeled by the following components and mole fractions [35]:

Table 4.6 Components and mole fractions of the air

Component	Mole fraction
CO_2	0.000300
H_2O	0.010110
N_2	0.772886
O_2	0.207396
Ar	0.009308

The produced water treatment is modeled in a simplified way. Due to the "perfect" separation, pure water enters the produced water treatment, so the only purpose of the produced water treatment simulation is to get an opinion on what the power consumption and the exergy destruction could be. In reality there is an oil/water separation with gravitational forces and flotation in a degasser tank. With low production flow rate of produced water, the produced water pumps would start and stop at regular intervals and the hydro cyclone would not work as optimal. Long residence time (10-20 minutes) in the degasser would secure a satisfactory treatment before the produced water is injected. In the HYSYS simulation, the whole produced water treatment is just modeled as a tank with specified pressures for the inlet and outlet streams.

A study to identify the possibilities for integrating a steam turbine in a combined cycle with a power turbine is figured out. The steam cycle is simulated with a heat exchanger, an expander, a cooler and a pump, as presented in Figure 4.19. A larger version can be seen in Appendix K. Assumptions are based on a master thesis on offshore combined cycles [5].
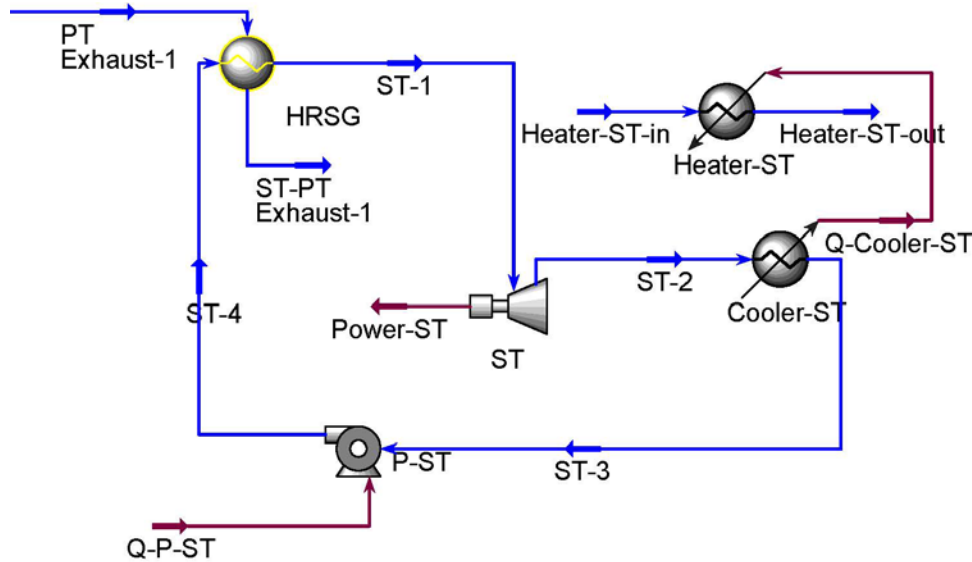
Figure 4.19 A steam turbine unit used in combined cycle

4.2 Exergy analysis

4.2.1 Exergy calculations

The destructed exergy in each process and in each component was found from the exergy balance, see Eq. (1). Contribution from kinetic and potential energy was neglected, except according to the coalescer where the potential energy was taken into account by including a dummy pump (on stream 3120a, see Appendix K). The exergy lost with the cooling water is regarded as destructed exergy, E_D, since the cooling water is mixed irreversibly with the sea. No other streams are considered as exergy loss and because of that the exergy loss, E_L, is equal to zero. The product exergy, E_P, is the exergy difference between process material streams entering and leaving the system. The utilized exergy, E_U, is the power supplied to the system. For the whole process E_D, E_P and E_U are regarded as the exergy destruction, product exergy and utilized exergy, respectively, for all streams entering and leaving the whole process. For the sub-processes E_D, E_P and E_U are regarded as the exergy destruction, product exergy and utilized exergy, respectively, for all streams entering and leaving the relevant sub-process. The sub-processes in the oil and gas processing are LP (low pressure) manifold, HP (high pressure) manifold, test manifold, separation train, recompression train, reinjection train, export system and fuel gas system, see Section 3.2.1. The power and heat distribution system consists of the sub-processes turbine system A, B and C, seawater distribution system and hot water distribution system, see Section 3.2.2.

The standard liquid density is given in the simulation basis and in a "crude oil assay", both given by the oil company. The metal content of the pseudo components is determined by comparison of

parameters for the heavy oil fractions in the "crude oil assay" and given in the simulation basis. When the relation between the pseudo components and the heavy oil fractions was recognized, the metal content was found in the "crude oil assay". Table 4.7 gives the pseudo components and their corresponding real components.

Table 4.7 Pseudo components and their corresponding real components

Pseudo component	Corresponding real component
Pseudo -01	Lt. Naphta
Pseudo -02	Hvy Naphta
Pseudo -03	Kerosene
Pseudo -04	Diesel
Pseudo -05	Vucuum Gas Oil
Pseudo -06	Vacuum Residue

To determine the chemical exergy of the pseudo components we need their specific gravity. The specific gravity can be calculated based on the "crude oil assay" or on values in the simulation basis calculated by HYSYS. Both alternatives where performed. The differences in chemical exergy varied between 0.1 % and 0.8 %, except for Lt. Naphta where the difference was approximately 3.2 %. The chemical exergy based on the "crude oil assay" is used in further calculations. The content in the pseudo components according to the "crude oil assay" given by the oil company can be seen in Appendix D.

To find the absolute value of the chemical exergy of a material stream, values for chemical exergy from [18] were used. They are presented in Appendix D. The chemical exergy is given in Table 4.8 [18]. The calculated is based on the method presented in Section 2.4.

Table 4.8 Chemical exergy of the pseudo components

Pseudo component	Chemical exergy [kJ/kg]
Pseudo -01	48 566
Pseudo -02	46 413
Pseudo -03	45 597
Pseudo -04	44 958
Pseudo -05	44 222
Pseudo -06	42 867
Pseudo -07	47 752

No data was found on the pseudo component Pseudo -07, so data for an equivalent pseudo component for another oil and gas processing platform is applied.

The chemical exergy is calculated according to Eq. (13). The chemical exergy used to calculate the chemical exergy difference between the inlet and outlet state of a sub-process or component is a relative chemical exergy, computed down to a reference state with pure substances at ambient temperature and pressure, see Eq. (12). This is seen as a more accurate way to compute the change in chemical exergy, compared to use the absolute value of the chemical exergy, since it is not so sensitive for small errors in mass balance.

For compressors, pumps and turbines there are only material streams of matter and energy streams of work included. The exergy balance, Eq. (1), reduces to

$$\dot{E}_D = \sum_{in} \dot{m}_{in} \boldsymbol{e}_{f_{in}} - \sum_{ex} \dot{m}_{ex} \boldsymbol{e}_{f_{ex}} - \dot{W}_{CV} \tag{41}$$

where work added is negative according to the sign convention. For scrubbers, three phase separators, mixers, tees, valves, heaters, coolers and heat exchangers there are no energy streams of work included. The destructed exergy in the separators are due to the separation. In reality the phase change takes some time and gravitational forces will separate the phase better. This is neglected in the HYSYS model. The retention time varies in reality between 6 minutes and up to 22 minutes for the different separators, according to the oil and gas processing manuals for this oil and gas processing platform. The temperature based component and the pressure based component of the physical exergy were calculated according to Eqs. (6) and (7).

The exergetic efficiency, exergy defect and f-value for the different sub-processes are computed in accordance with Eqs. (30), (31) and (32), respectively. In Eq. (30) the product exergy and the utilized exergy correspond to the current sub-process, and in Eq. (31) and Eq. (32)the utilized exergy and the exergy input to total process applies to the whole oil and gas processing at the platform.

4.2.2   User variables

All the exergy calculations are done by using user variables in HYSYS. The user variables were programmed with Visual Basic. User variables that set the ambient temperature and pressure for all material streams were made. The ambient pressure and temperature were set to 1 atm and 8 °C, respectively. This temperature is the average temperature for the North Sea throughout the year [13]. For a material stream user variables were made to calculate the physical exergy, the temperature based component of the physical exergy, the pressure based component of the physical exergy, the absolute chemical exergy and the relative chemical exergy. User variables that take into account the change in fluid package throughout the process were also made, allowing using user variables in the turbine units. For each type of process components, including compressors, pumps, turbines, valves, mixers, tees, heaters, coolers, heat exchangers, separators, scrubbers, reactors and pipes , user variables were made to calculate the destructed exergy, physical exergy, pressure based component of the physical exergy, temperature based component of the physical exergy and chemical exergy. A user variable was made for the Recycle-component to calculate its exergy destruction. Flowsheet user variables that "activate" the user variables for all material streams and components in all flowsheets were made. To demonstrate the principle, some of the most important user variables are shown in Appendix L. The user variables for calculating the physical exergy and the relative chemical exergy of material streams and set ambient pressure and temperature, were developed in cooperation with Mari Voldsund in connection with the specialization project [36]; all other user variables are made for this particular thesis.

4.2.3   Control volumes and system boundaries

The valves at the liquid stream out of the scrubbers, and the valves at the recycle stream of the compressor decrease the pressure down to the pressure of the rest of the streams that it is going to mix with. This is done to charge the "imperfect" process of e.g. a compressor that needs anti-surge recycle. Due to this much exergy destruction is in the valve, relative to the subsequent mixer. The pipes are assumed to have no irreversibilities, so the exergy destruction is added to the

corresponding components. The exception is in the hot water distribution system and the seawater distribution system, where the long pipelines are simulated by a pipe component with pressure loss.

The exergy destruction in coolers and heaters that are served by the seawater distribution system and the hot water system, are charged the process that is cooled or heated and not the distribution system. The secondary hot water system is regarded as a part of the hot water system. The export system starts after the coalescer and includes the oil/oil heat exchanger.

4.2.4   Cases

Different cases are studied:

-One case is the exergy analysis of the oil and gas processing platform at 2010-10-29 at 12:00 o'clock.

-Another case is the exergy analysis of the oil and gas processing platform two years later, at 2012-10-29 at 12:00 o'clock. Also a comparison between these two production days is done.

-A comparison with an exergy analysis on another oil and gas processing platform done by Voldsund et al. [1] is performed.

-A case where the possibility of an integration of a combined cycle is carried out. The goal is to see if a steam turbine, which utilizes the exhaust gas from the turbines, can replace a generator turbine or two and thereby reduce the exergy destruction. Two ideas are tested; the first attempt is to let the exhaust air from the mechanical drive gas turbine supply the steam cycle and shut down the two turbines left, the other attempt is to drive one of the generator drive gas turbines at part load and utilize the exhaust air form this turbine together with the mechanical drive turbine in the steam cycle.

5 Results

5.1 Results for oil and gas processing plant

5.1.1 Exergy flows entering and leaving the process

The exergy entering and leaving the process are given in Table 5.1 and Table 5.2. The physical and chemical exergy are calculated according to (5) and (13), respectively. We see that approximately 50 MW/ 37 MW (2010/ 2012) of physical exergy enters the oil and gas processing at the platform in the well streams. Much of this exergy is caused by the high pressure in the well streams. More than 29 MW/ 26 MW enters the process through process units like pumps, compressors and heaters. Due to high pressure in the injection streams (184.4 bar/ 170.8 bar), the exergy out of the process is dominated by this.

Table 5.1 Physical exergy, chemical exergy, power and mass flow entering and leaving the process (2010)

Exergy streams	Physical Exergy [kW]	Chemical Exergy [kW]	Power [kW]	Mass flow [ton/h]
In				
HP well	24 627	10 317 156		825
LP well	3 134	3 677 455		303
Test well	3 463	1 121 581		90
Import gas	18 978	1 739 338		127
Power			28 870	
Total in	50 201	16 855 530	28 870	1 344
Out				
Oil export	6 880	12 558 309		1 022
Fuel gas	874	106 114		8
Gas injection	48 219	3 954 492		289
Gaslift LP	2 880	236 231		17
Gaslift Test	0	9		0
Produced water	43	375		8
Total out	58 897	16 855 530	0	1 344

Table 5.2 Physical exergy, chemical exergy, power and mass flow entering and leaving the process (2012)

Exergy streams	Physical Exergy [kW]	Chemical Exergy [kW]	Power [kW]	Mass flow [ton/h]
In				
HP well	25 838	6 371 816		530
LP well	9 133	5 044 495		689
Test well	1 585	149 969		11
Power			26 209	
Total in	36 556	11 566 281	26 209	1 230
Out				
Oil export	5 022	8 520 728		705
Fuel gas	869	98 039		7
Gas injection	32 257	2 671 359		195
Gaslift LP	2 945	243 857		18
Gaslift HP	213	17 675		1
Produced water	3 119	14 624		304
Total out	44 425	11 566 281	0	1 230

The exergy rates and performance parameters of the oil and gas processing are summarized in Table 5.3. Product exergy, E_P, is the difference in the exergy of the material streams in and out of the process. The utilized exergy, E_U, represents the resources in terms of exergy used to provide the product exergy. This is electrical power and heating with the hot water distribution system. The exergetic efficiency is the ratio between the product exergy and the utilized exergy.

Table 5.3 Exergy rates and performance parameters of the oil and gas processing

Parameter	2010	2012
Utilized exergy (Eu) [MW]	30.7	27.8
Destructed exergy (Ed) [MW]	21.4	19.3
Product exergy (Ep) [MW]	9.3	8.5
SPC [kWh/Sm^3]	28.1	35.3
Exergetic efficiency	0.303	0.303

5.1.2   Exergy destruction in each sub-process

Table 5.4 gives the power consumption and destructed exergy for each sub-process in the oil and gas processing at the platform. The power consumption is physical exergy in with electrical power, shaft power and hot water and also includes heat transferred with heat exchangers from other sub-processes. Both the power consumption and the exergy destruction for the whole process are dominated by the reinjection train, which consumes over 15 MW/ 13 MW power and destructs more than half of it. Other sub-processes with high power consumption and exergy destruction are the recompression train, the separation train and the export system.

The chemical exergy increase and the increase in temperature based and pressure based exergy that corresponds to each sub-process is given in Table 5.5 and Table 5.6. All inlet and outlet process streams are taken into account. The increases are the output of exergy minus the input of exergy. We see that in sections without mixing or separation the chemical exergy increase is zero. Increased chemical exergy is due to separation and a reduction is caused by mixing of streams. The separation train increases the chemical exergy and the gas compression parts, recompression and reinjection trains, reduce the chemical exergy. This is due to more separation than mixing in the separation train, and more mixing than separation in the gas compression parts. In total the chemical exergy increases with approximately 18 kW/ 50 kW during the oil and gas processing at the platform. We see that the pressure based exergy increase much through the reinjection and recompression train, caused by the compression stages. It is also worth noting the temperature based exergy increase in the separation train, affected by the need for heating the heavy crude oil.

Table 5.4 Power consumption and exergy destruction of the sub-processes

	Power consumption [kW]		Destructed exergy [kW]	
	2010	2012	2010	2012
LP manifold	0	0	1 052	2 814
HP manifold	0	0	3 537	3 069
Test manifold	0	0	1 174	820
Separation	4 736	5 505	2 439	2 123
Recompression	9 488	9 359	5 714	4 398
Reinjection	15 003	13 277	5 635	4 940
Export System	4 312	2 720	1 686	895
Fuel Gas System	188	151	199	173
Produced Water Injection	0	629	1	109

Table 5.5 Chemical, temperature based and pressure based exergy increase in the sub-processes (2010)

Sub-process	Chemical exergy increase [kW]	Temperature based exergy increase [kW]	Pressure based exergy increase [kW]
LP manifold	-2	-62	-987
HP manifold	-20	-242	-3 275
Test manifold	0	-69	-1 105
Separation	65	3 964	-1 744
Recompression	-19	320	2 875
Reinjection	-5	697	10 242
Export System	0	-2 465	3 091
Fuel Gas System	0	18	-28
Produced Water Injection	0	0	-1

Table 5.6 Chemical, temperature based and pressure based exergy increase in the sub-processes (2012)

Sub-process	Chemical exergy increase [kW]	Temperature based exergy increase [kW]	Pressure based exergy increase [kW]
LP manifold	-3	-132	-2 679
HP manifold	-2	-287	-2 780
Test manifold	0	-36	-784
Separation	39	3 653	1 103
Recompression	-9	305	4 048
Reinjection	24	309	6 829
Export System	0	-1 729	1 978
Fuel Gas System	0	12	-34
Produced Water Injection	0	49	471

Table 5.7 and Table 5.8 shows the increase in chemical, temperature based and pressure based exergy for oil and gas in the sub-processes. The increase is calculated based on all process streams entering the sub-process and the oil or gas leaving the relevant sub-process. The increases are the output of exergy minus the input of exergy. Since there is a high change in mass during the sub-processes, due to separation of oil, gas and water, the exergy increase is given per mass. The chemical exergy increase is dominated by the separation train and the recompression train. Due to a very low rate of produced water in 2010 compared to 2012, the change in chemical exergy in the separation train is much lower in 2010 than in 2012. This applies to both oil and gas. Temperature based exergy increase is not vital, but it is worth noting that the temperature based exergy increases (due to heating and compression) in all sub-processes, except the export system. The increase in pressure based exergy is dominated by compression of gas in the separation train, the recompression train and the reinjection train.

Table 5.7 Chemical, temperature based and pressure based exergy increase in the sub-processes in the oil and gas processing (2010)

Sub-process	Chemical exergy increase [kJ/kg]	Temperature based exergy increase [kJ/kg]	Pressure based exergy increase [kJ/kg]
Separation, oil	-494	12	-66
Separation, gas	3 745	8	321
Recompression, gas	1 970	21	187
Reinjection, gas	101	8	89
Export System, oil	0	-9	11
Fuel Gas System, gas	3	9	-14

Table 5.8 Chemical, temperature based and pressure based exergy increase in the sub-processes in the oil and gas processing (2012)

Sub-process	Chemical exergy increase [kJ/kg]	Temperature based exergy increase [kJ/kg]	Pressure based exergy increase [kJ/kg]
Separation, oil	9 681	10	-73
Separation, gas	14 458	4	302
Recompression, gas	2 408	18	221
Reinjection, gas	158	5	113
Export System, oil	0	-9	10
Fuel Gas System, gas	4	6	-16

Table 5.9 and Table 5.10 give the relative irreversibility, the efficiency defect, the exergetic efficiency and the f-value for each sub-process and the whole oil and gas processing at the platform, calculated according to Eqs. (34), (31), (30) and (32). The efficiency defect is also illustrated in Figure 5.1 and Figure 5.2, together with the exergetic efficiency of the whole oil and gas processing at the platform. This is a dimensionless exergy balance in the form of a pie chart and it is worth noting that the efficiency defects and the exergetic efficiency are summed to one. The destructed exergy distribution for each sub-process distributed on type of process unit is presented in Figure 5.3 and Figure 5.4.

Table 5.9 Relative irreversibility, efficiency defect, exergetic efficiency and f-value of the sub-processes (2010)

	Relative irreversibility	Efficiency defect	Exergetic efficiency	f-value
LP manifold	0.049	0.034	-	0.000
HP manifold	0.165	0.115	-	0.000
Test manifold	0.055	0.038	-	0.000
Separation	0.114	0.079	-	0.140
Recompression	0.267	0.186	-	0.281
Reinjection	0.263	0.183	-	0.445
Export System	0.079	0.055	-	0.128
Fuel Gas System	0.009	0.006	-	0.006
Produced Water Injection	0.000	0.000	-	0.000
Total process	1.000	0.697	0.303	1.000

Table 5.10 Relative irreversibility, efficiency defect, exergetic efficiency and f-value of the sub-processes (2012)

	Relative irreversibility	Efficiency defect	Exergetic efficiency	f-value
LP manifold	0.145	0.101	-	0.000
HP manifold	0.159	0.111	-	0.000
Test manifold	0.042	0.030	-	0.000
Separation	0.110	0.076	-	0.058
Recompression	0.227	0.158	-	0.337
Reinjection	0.255	0.178	-	0.478
Export System	0.046	0.032	-	0.098
Fuel Gas System	0.009	0.006	-	0.005
Produced Water Injection	0.006	0.004	-	0.023
Total process	1.000	0.697	0.303	1.000

Table 5.10 Relative irreversibility, efficiency defect, exergetic efficiency and f-value of the sub-processes (2012)
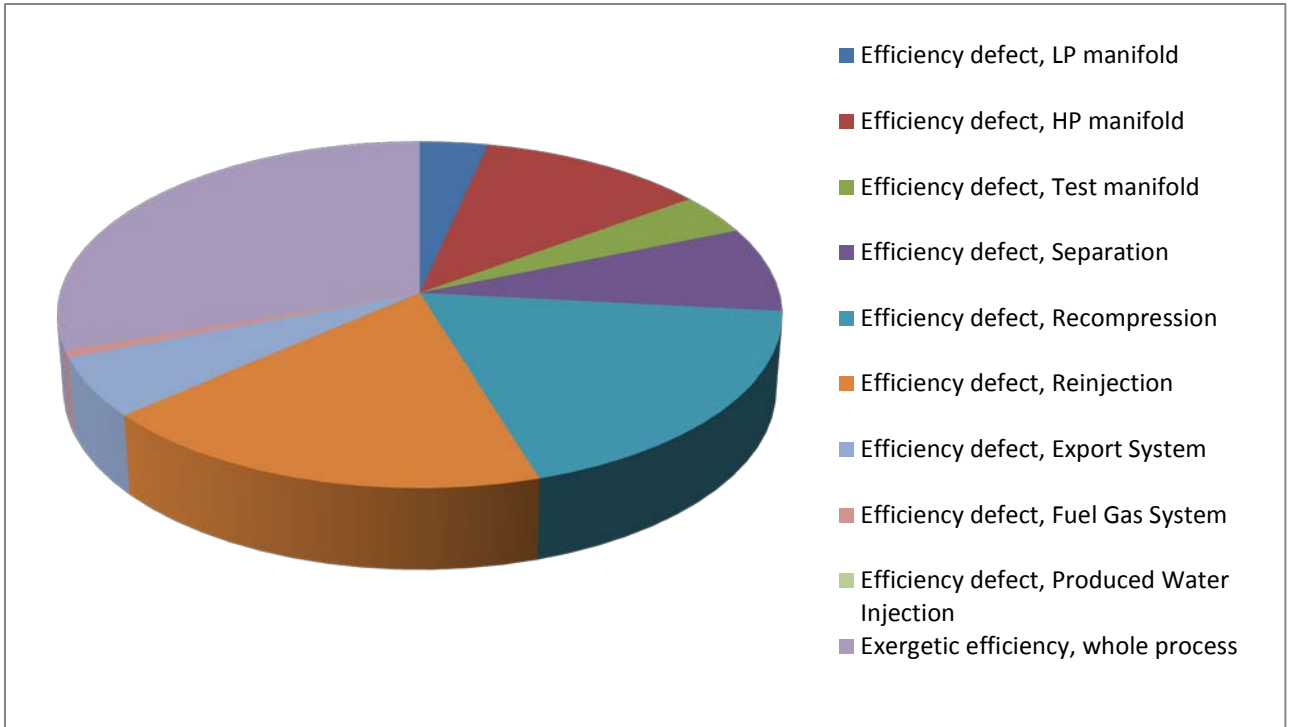
Figure 5.1 Efficiency defect for the sub-processes together with the exergetic efficiency of the whole oil and gas processing process (2010)
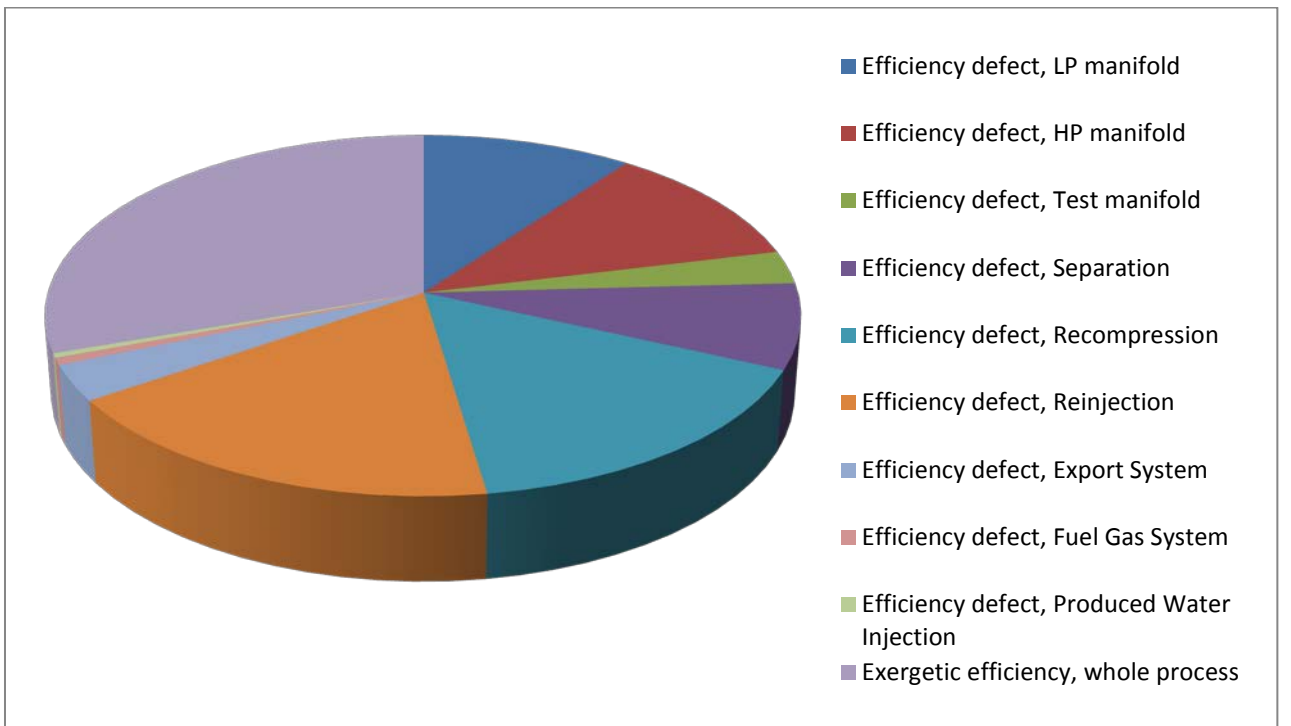
Figure 5.2 Efficiency defect for the sub-processes together with the exergetic efficiency of the whole oil and gas processing process (2012)
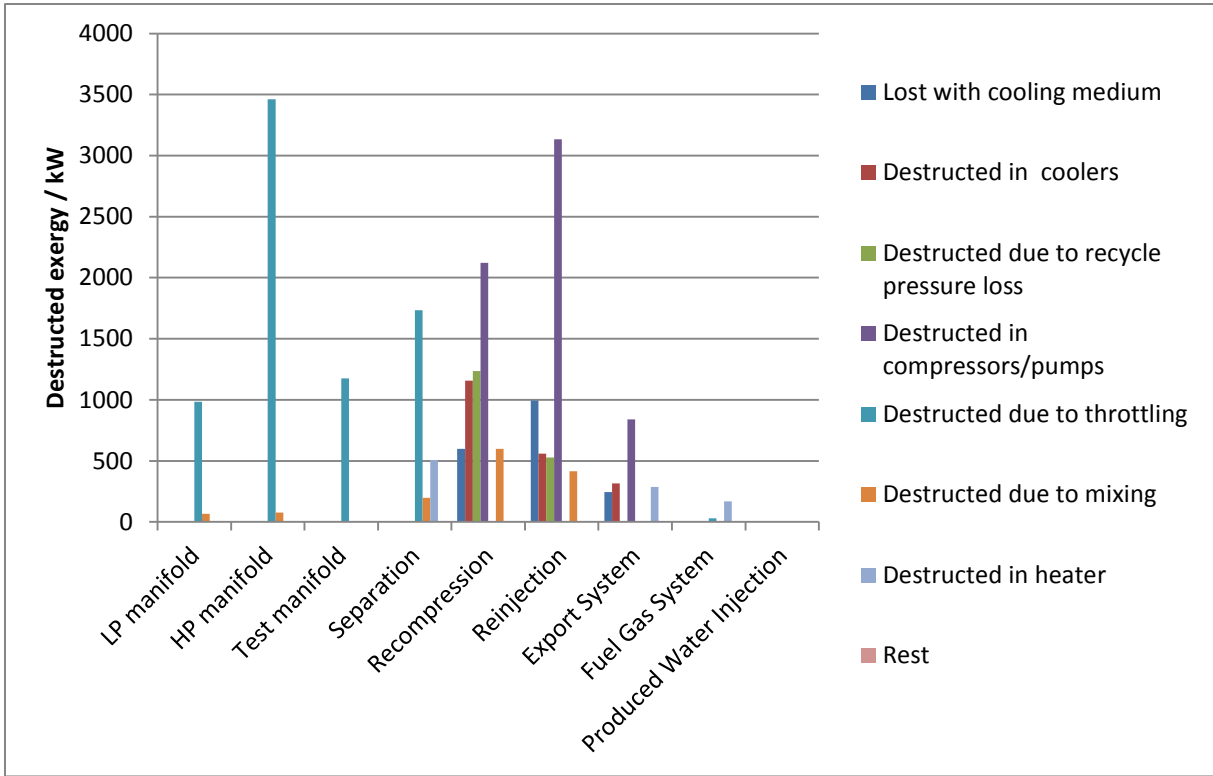
Figure 5.3 Exergy destruction in the sub-processes in the oil and gas processing process (2010)
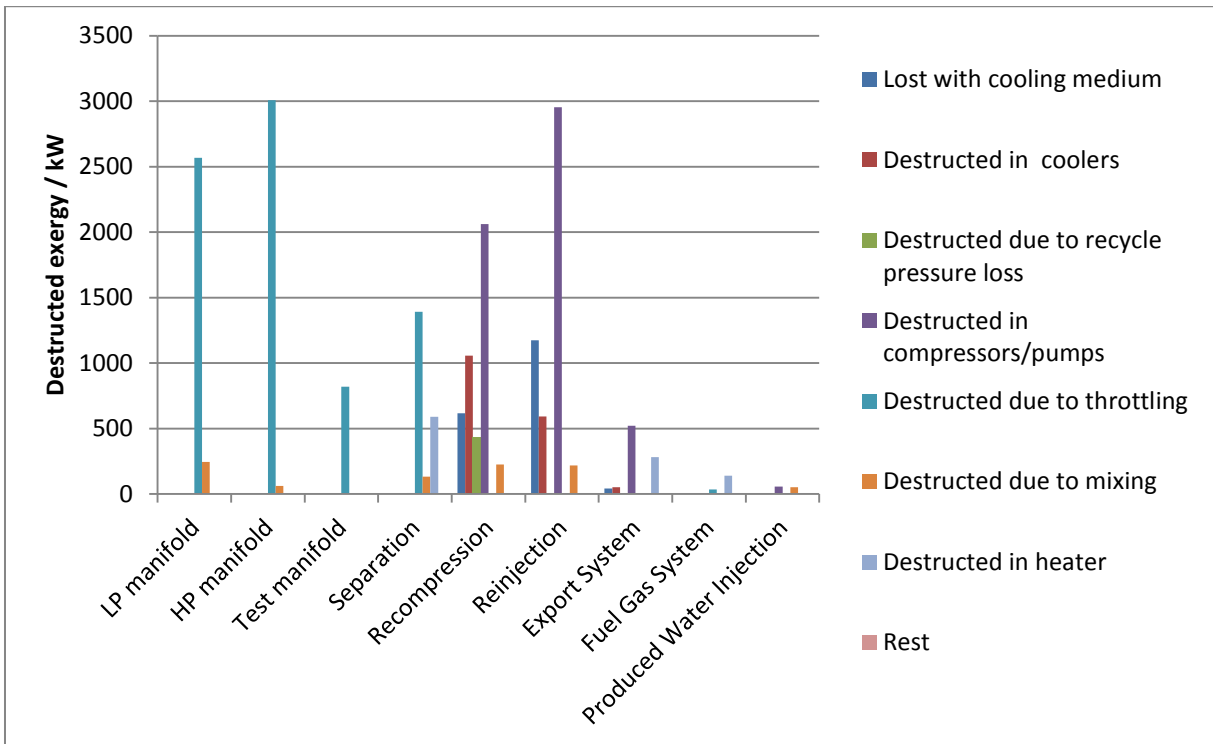
Figure 5.4 Exergy destruction in the sub-processes in the oil and gas processing process (2012)

In the production manifold, where the pressures of the well streams are reduced, nearly all exergy destruction is caused by throttling with an exergy destruction of 5 763 kW/ 6 703 kW.

Destructed exergy related to throttling and heating is the largest part of the exergy destruction in the separation train. Heating is done via heat exchange with the hot water distribution system and the export stream of oil and produced water. The efficiency defect of the separation train is around 0.079/ 0.076. The separation is done in several stages with reducing pressure, thus 1 734 kW/ 1 392 kW of exergy is destructed due to throttling. From Table 5.5 and Table 5.6 we see that the chemical exergy is increased by 65 kW/ 39 kW during the separation train.

In the recompression train the pressure is increased with around 38.5 bar/ 39.7 bar. From Table 5.4 and Figure 5.3 and Figure 5.4 we see that of the 9 MW/ 9 MW power consumed, 6 MW/ 4 MW is destructed and the destruction does mainly take place in the compressors and accompanying coolers. Table 5.9 and Table 5.10 show that this gives the recompression train one of the highest efficiency defects of all the sub-processes with a value of 0.186/ 0.158. Small rates of exergy are destructed in mixing, separation, pump work and recycle pressure loss due to anti-surge. Note that the exergy destruction in the compressors, coolers and separators are higher than necessary because of the increased flow due to off-design conditions for the compressors that require anti-surge flows.

The pressure is increased from the outlet pressure of the recompression train to the well injection pressure at 184.4 bar/ 170.8 bar. The reinjection train is a sub-process with one of the largest efficiency defect at 0.183/ 0.178, and because of that it plays an important role in the exergy analysis. Exergy is destructed in much the same ways that for the recompression train. The exceptions are that there are no pumps in the reinjection train, but a heater is included, which uses the hot water distribution system. The pumps give only a small contribution to the exergy destruction.

In the export system sub-process power is applied in the booster pump and the export pump, hence exergy is destructed here due to an adiabatic efficiency of around 75 %. The other contributor to exergy destruction is cooling, both from heat exchanging with the separation train and from cooling with cooling water.

The fuel gas system and the produced water injection system have negligible exergy destruction, one thing to notice is the exergy destruction due to electrical heating in the superheater in the fuel gas system which destructs 169 kW/ 139 kW.

To sum up, the highest contributions to exergy destruction are due to throttling in production manifolds, irreversibilities in coolers and losses with cooling medium and inefficiencies in compressors.

The power and heat exergy that is consumed in each sub-process is presented in Figure 5.5 and Figure 5.6.
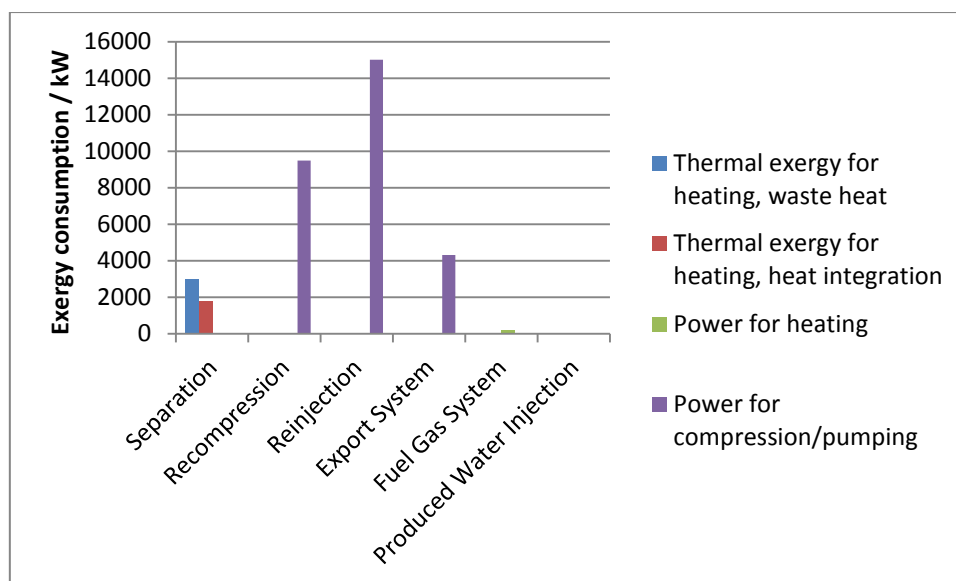
Figure 5.5 Exergy consumption in the sub-processes (2010)
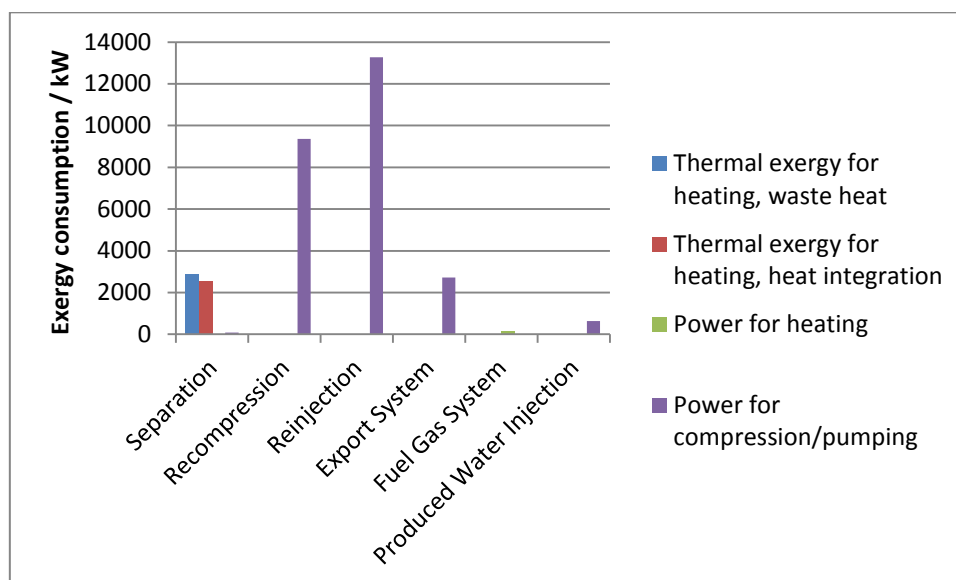
Figure 5.6 Exergy consumption in the sub-processes (2012)

Power is mainly used for compression in the recompression and reinjection train and in the export system. In the separation train the required crude oil heating is done with exergy from heat integration with other product streams and waste heat from the power turbines. Power used for heating and pumping in the fuel gas system and in the produced water injection is almost negligible to the other power consumption.

Figure 5.7 and Figure 5.8 show the inlet and outlet temperature based exergy and pressure based exergy of the process streams of each sub-process. The figures illustrates if the temperature is high or low, if the pressure is high or low and if there is a temperature or pressure increase or decrease during the sub-process. The main thing to notice is the high increase of pressure based exergy

through the recompression and reinjection process. It is also interesting to see the pressure based exergy destruction in the LP, HP and test manifolds due to throttling of the feed streams.
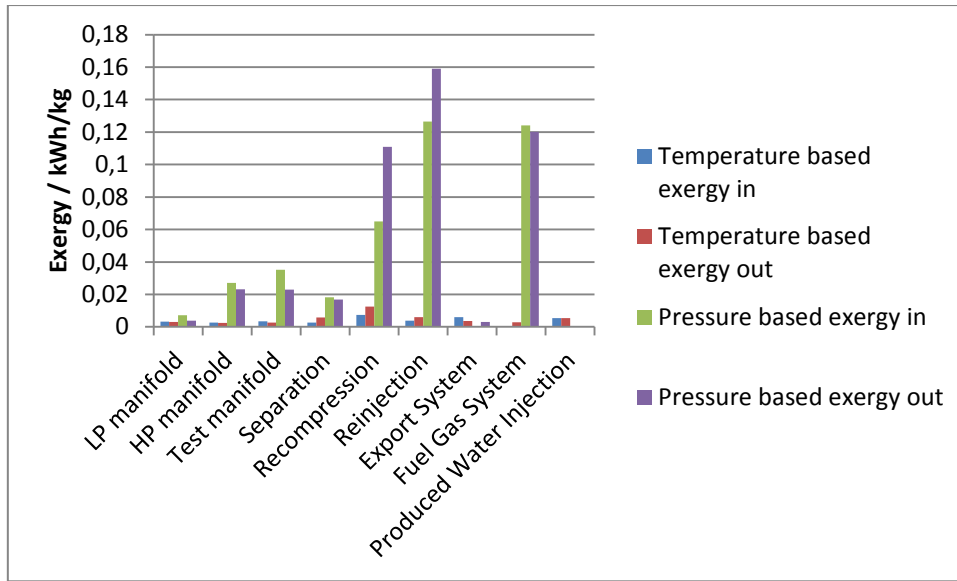
Figure 5.7 Specific exergy content in the material streams entering and leaving the sub-processes (2010)
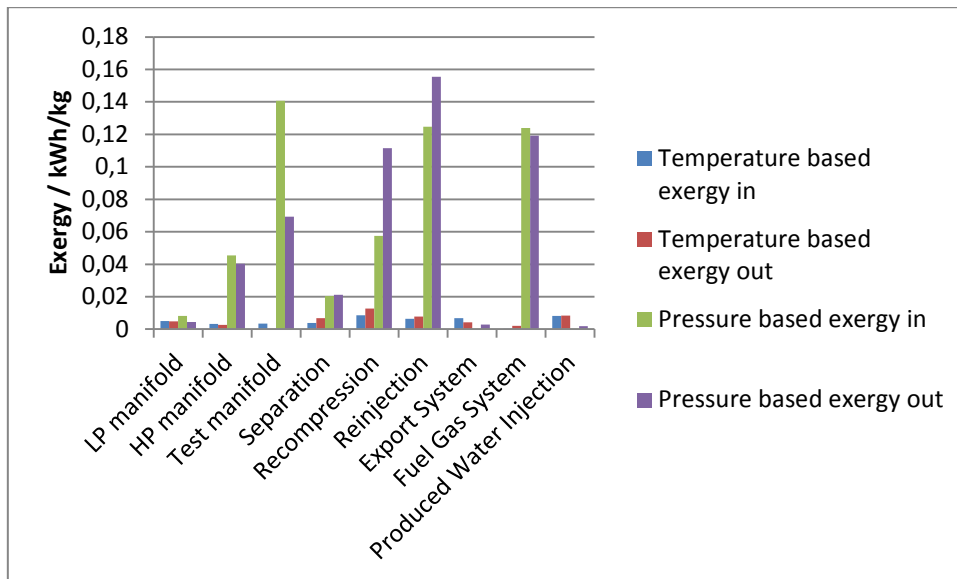
Figure 5.8 Specific exergy content in the material streams entering and leaving the sub-processes (2012)

Figure 5.9 and Figure 5.10 show the exergy in for heating and compression/pumping and the change in pressure based and temperature based exergy in each sub-process. This is a way to illustrate the input of power to a sub-process and the corresponding response as expressed by change in exergy. We see, of course, that the exergy input is higher than the exergy change. The main increase in temperature based exergy takes place in the separation train, and the exergy in for compression/pumping and the change in pressure based exergy is dominated by the recompression train and the reinjection train.
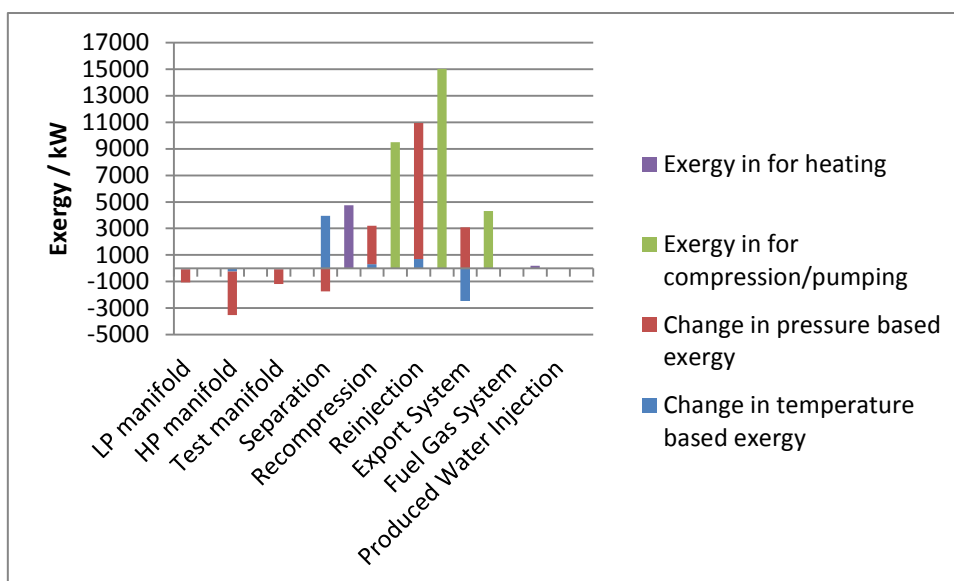
Figure 5.9 Exergy in for heating and exergy in for compression/pumping for the sub-processes together with the change in pressure based exergy and change in temperature based exergy (2010)
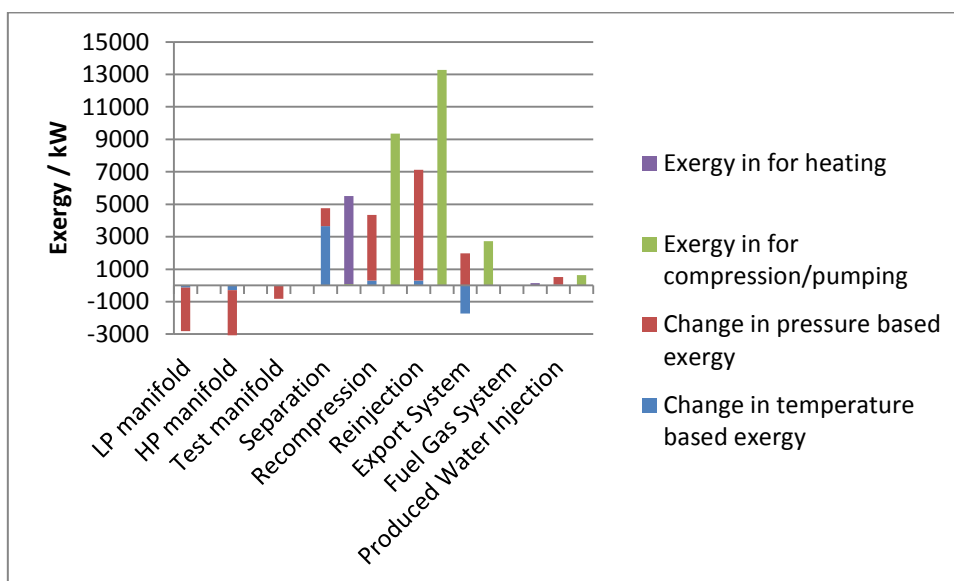
Figure 5.10 Exergy in for heating and exergy in for compression/pumping for the sub-processes together with the change in pressure based exergy and change in temperature based exergy (2012)

5.2   Results for power generation system and distribution systems

5.2.1   Exergy destruction in power generation system and distribution systems

The gas turbines, the hot water distribution system and the seawater distribution system are the auxiliary system for the process plant and also for other processes at the platform. The destructed exergy in the sub-processes is presented in Figure 5.11 and Figure 5.12. The turbine systems have a high rate of destructed exergy in the combustion reactor with 16.8 MW/ 17.1 MW destructed exergy just in turbine C. A major part is also destructed in the compression of the inlet combustion air. The

hot water distribution system has exergy destruction due to the heat exchange with the exhaust gas from the turbine systems, and due to pressure loss in the long pipelines needed for distribution of the heated water. The exergy destruction in the seawater distribution is negligible.
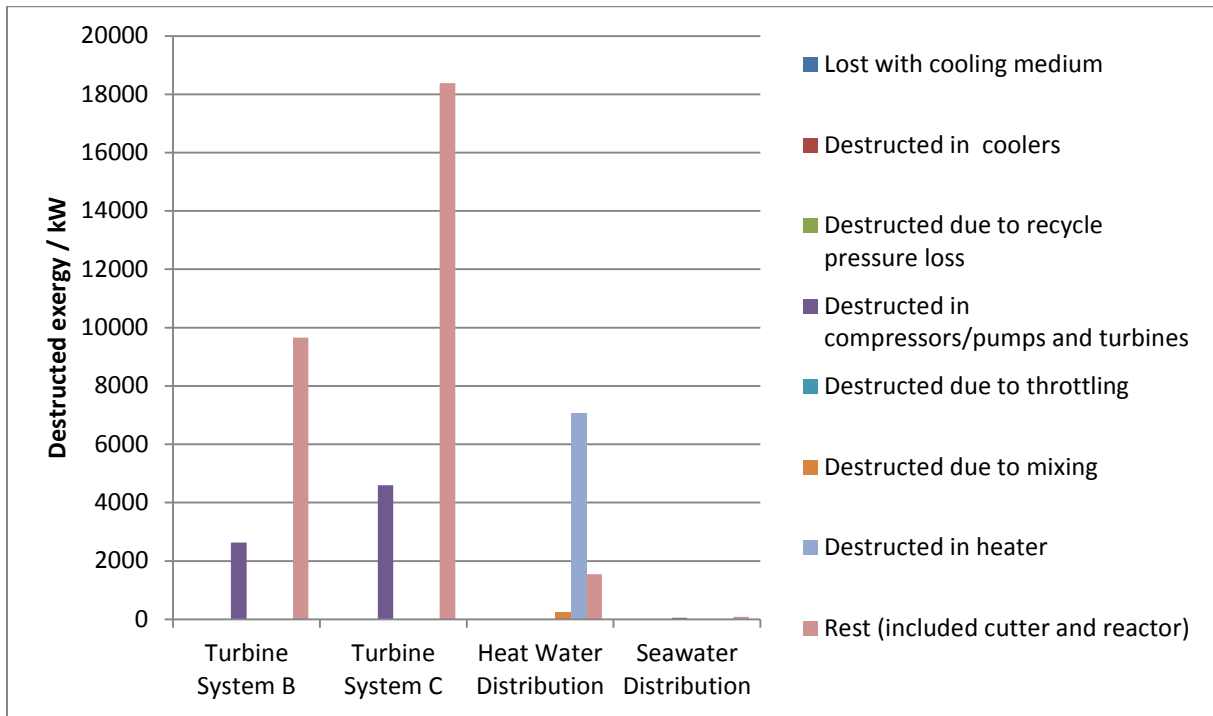
Figure 5.11 Exergy destruction in the sub-processes in the power generation system and distribution systems (2010)
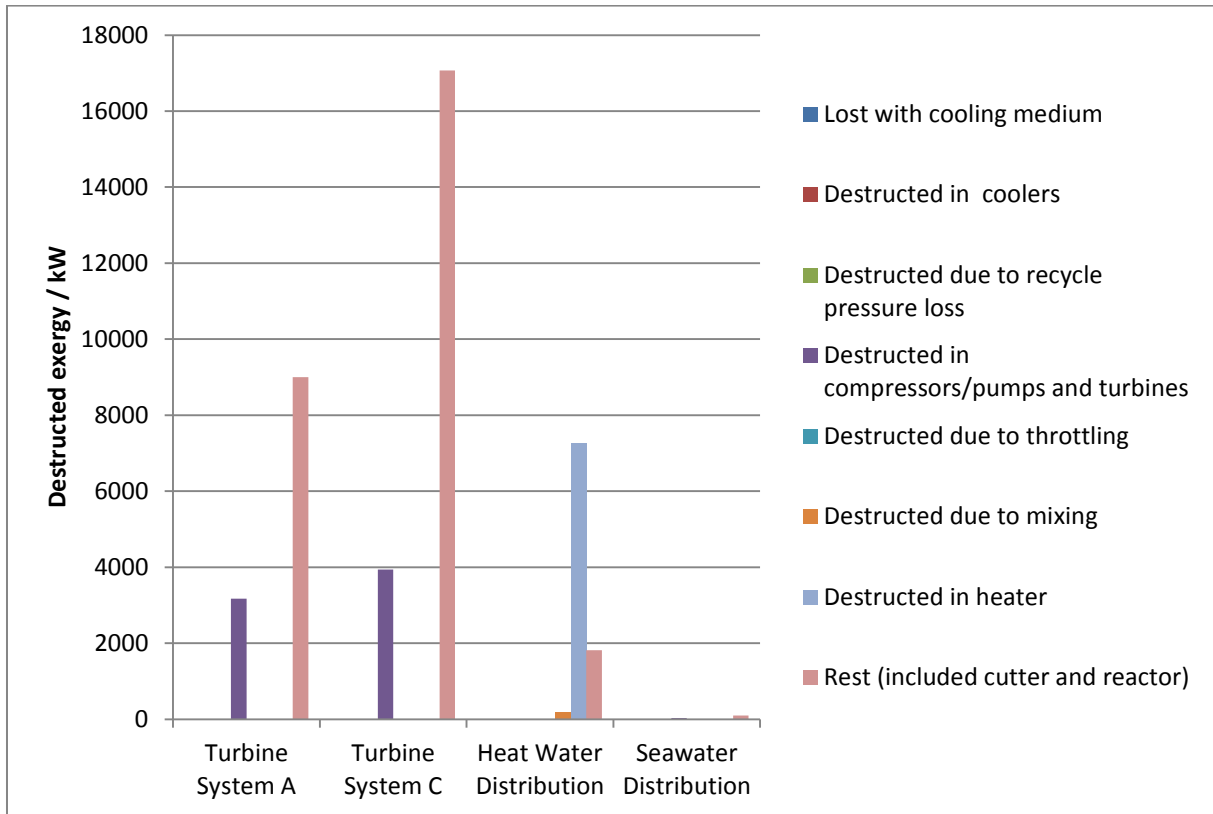
Figure 5.12 Exergy destruction in the sub-processes in the power generation system and distribution systems (2012)

Figure 5.13 and Figure 5.14 show the efficiency defect for the sub-processes and the exergetic efficiency for the whole auxiliary system, calculated according to Eqs. (30) and (31). We see that the efficiency defect of the seawater distribution is negligible compared to the turbine system and the hot water distribution. Turbine System C has the largest efficiency defect with the value of 0.357/ 0.400 and the exergetic efficiency of the whole process is 0.292/ 0.189.
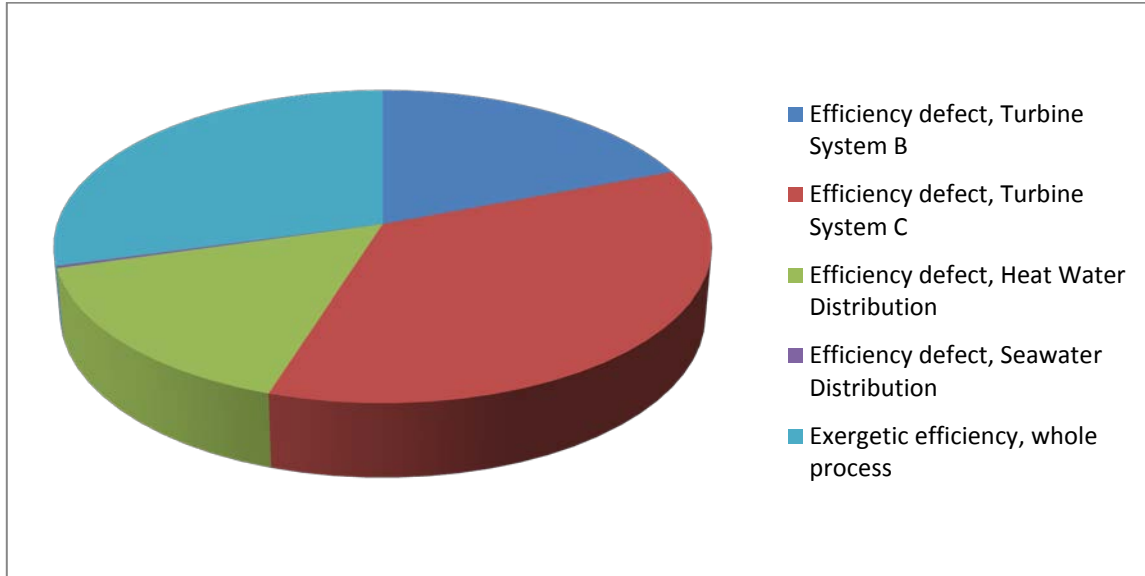
Figure 5.13 Efficiency defect for the sub-processes together with the exergetic efficiency of the whole power generation system and distribution systems (2010)
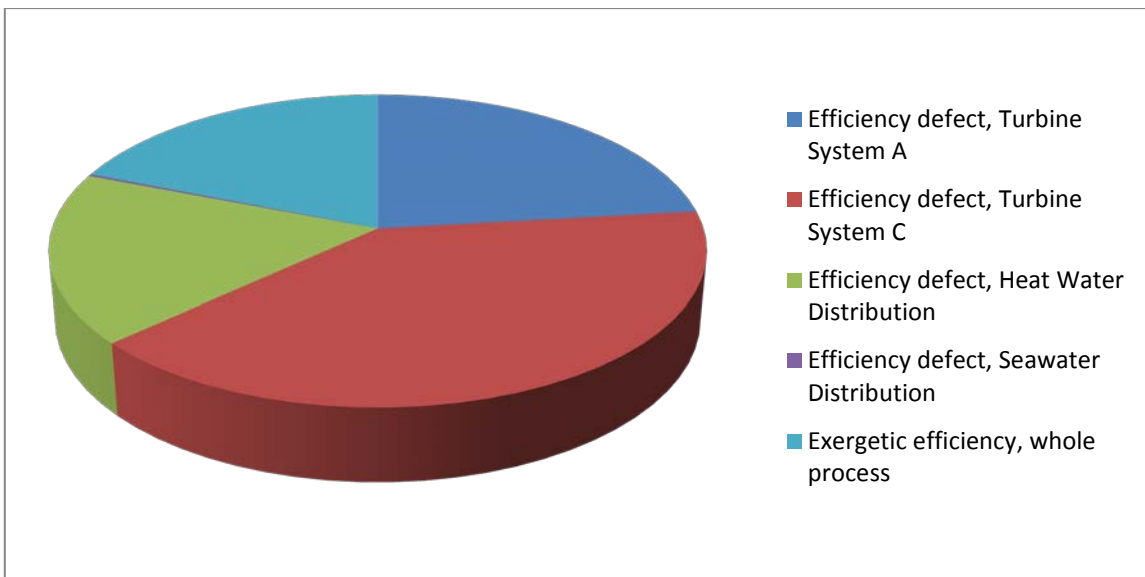
Figure 5.14 Efficiency defect for the sub-processes together with the exergetic efficiency of the whole power generation system and distribution systems (2012)

5.2.2 Exergy destruction in the turbine systems

The exergy in with fuel and combustion air and the net power output is shown in Table 5.11 and Table 5.12, together with the ratio between them. The inlet exergy is circa 104 MW/ 100 MW and the net power output is approximately 40 MW/ 36 MW. The ratio between exergy out and exergy in lies between 0.39 and 0.36.

Table 5.11 Inlet and outlet exergy of the turbine systems and the ratio between them (2010)

	Turbine System B	Turbine System C
Exergy in with fuel gas [kW]	34 480	65 378
Exergy in with air [kW]	1 568	2 937
Exergy out with power [kW]	13 507	26 807
Exergy out / Exergy in	0.375	0.392

Table 5.12 Inlet and outlet exergy of the turbine systems and the ratio between them (2012)

	Turbine System A	Turbine System C
Exergy in with fuel gas [kW]	32 898	62 378
Exergy in with air [kW]	1 537	2 915
Exergy out with power [kW]	10 102	25 683
Exergy out / Exergy in	0.293	0.393

The exergy destruction in the turbine systems is presented in Figure 5.15 and Figure 5.16. The exergy destruction is dominated by the reactor with a rate of destructed exergy of approximately 8 MW for Turbine System B and 16 MW for Turbine System C in 2010, and 8 MW for Turbine System A and 16 MW for Turbine System C in 2012.
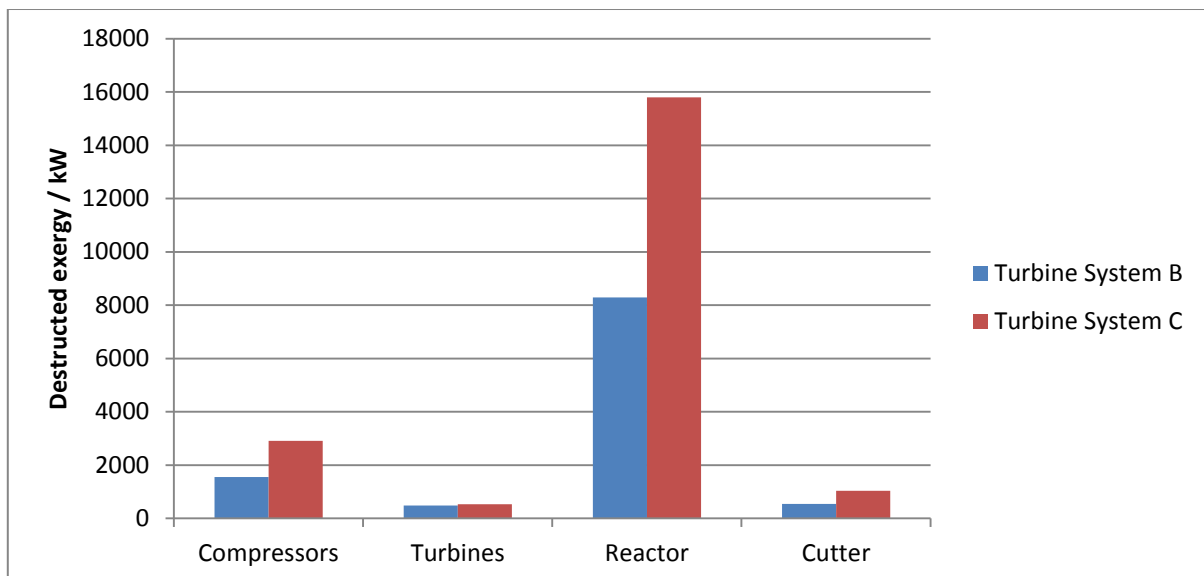
Figure 5.15 Exergy destruction in the turbine systems distributed on compressors, turbines, reactor and cutter (2010)
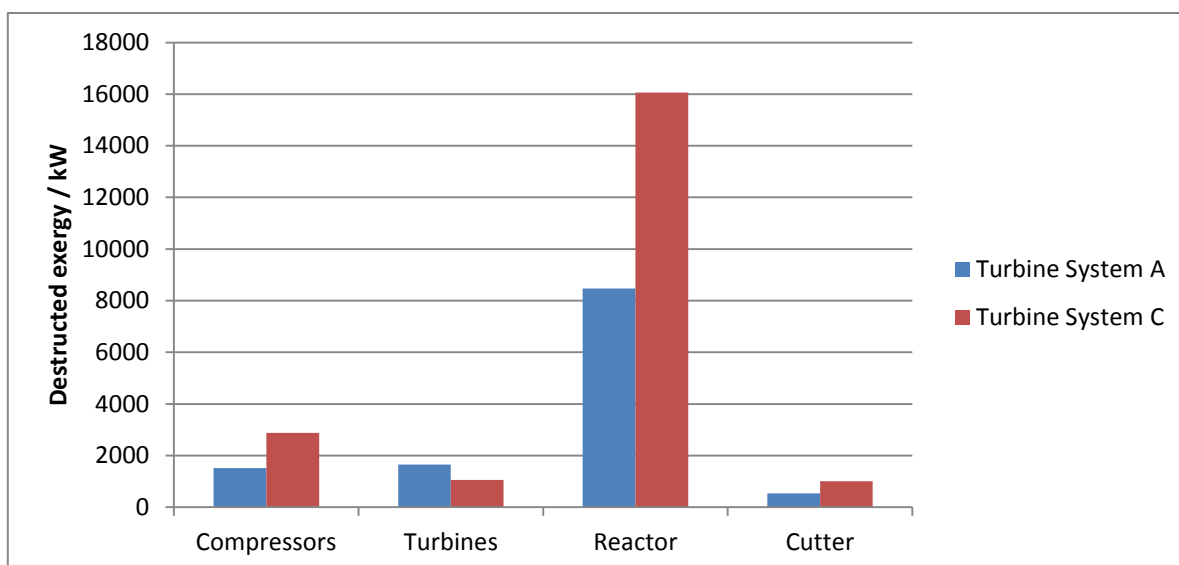
Figure 5.16 Exergy destruction in the turbine systems distributed on compressors, turbines, reactor and cutter (2012)

5.2.3 Combined cycle

5.2.3.1 *Steam cycle only supplied by mechanical drive turbine*

The exergy destruction in the steam cycle of the combined cycle is shown in Figure 5.17. The exergy destruction is dominated by the heat exchanger, which simulates the heat recovery steam generator, with an amount of 3.9 MW/ 3.7 MW.
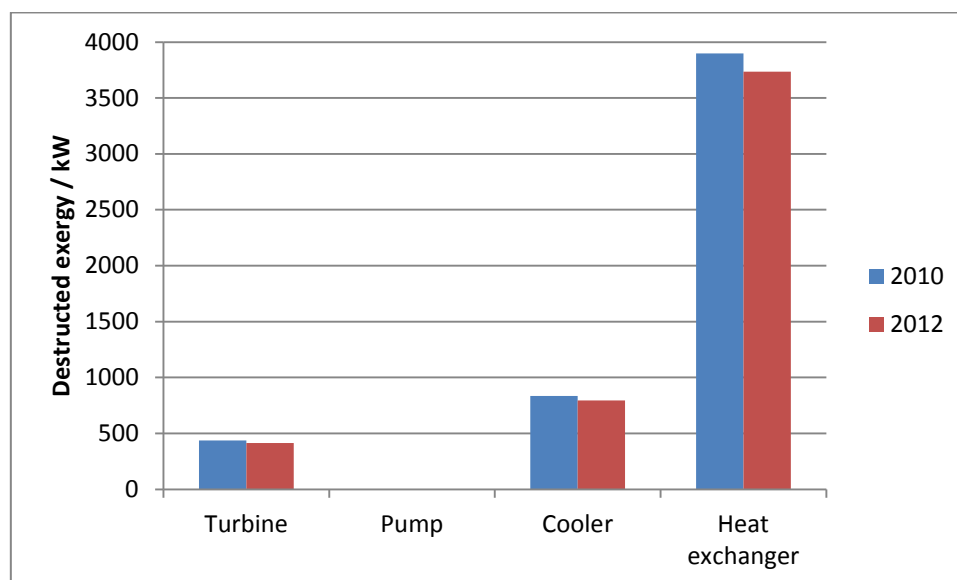
Figure 5.17 Destructed exergy in the steam cycle of the combined cycle distributed on turbine, pump, cooler and heat exchanger

The steam turbine's net power output is 9.3 MW/ 8.8 MW and the thermal efficiency of the combined cycle is 0.55/ 0.55. This and more performance details of the combined cycle are presented in Table 5.13.

Table 5.13 Gas turbine net power, steam turbine net power, LHV fuel and thermal efficiency of the combined cycle

	2010	2012
Gas turbine net power [MW]	26.8	25.7
Steam turbine net power [MW]	9.3	8.8
LHV fuel [MW]	65.4	62.6
Thermal efficiency	0.55	0.55

5.2.3.2   *Steam cycle also supplied by generator drive turbine at part load*

The destructed exergy in the combined cycle and in the hot water distribution system is presented in Table 5.14.

Table 5.14 Destructed exergy in the combined cycle and the hot water distribution system

	Destructed exergy [kW]	
	2010	2012
Generator drive system	5 295	3 059
Mechanical drive system	22 914	22 086
Steam turbine system	5 475	4 832
Hot water distribution system	4 645	4 293

The steam turbine's net power output is 7.6 MW/ 6.7 MW and the thermal efficiency of the combined cycle is 0.50/ 0.50. More details of the combined cycle are presented in Table 5.15.

Table 5.15 Gas turbine net power, steam turbine net power, LHV fuel and thermal efficiency of the combined cycle

	2010	2012
Gas turbines net power [MW]	32.8	29.2
Steam turbine net power [MW]	7.6	6.7
LHV fuel [MW]	80.3	71.3
Thermal efficiency	0.50	0.50

6   Discussion

6.1   Exergy losses, performance and improvement possibilities

6.1.1   Oil and gas processing plant

6.1.1.1   Wells and production manifolds

As showed in Appendix F, the pressure in the well streams are throttled from pressures as high as 110.5 bar and down to approximately 47 bar for the HP manifold and 8 bar for the LP manifold. The exergy destruction due to throttling in the manifolds is 5.6 MW/ 6.4 MW (2010/ 2012) and indicates a potential for improvement. The exergy destruction due to throttling is 1 734 kW/ 1 392 kW and 30 kW/ 35 kW in the separation train and fuel gas system, respectively. Due to this the exergy destruction related to valves should be evaluated. The pressure reductions have the possibility to be utilized in ejectors and expanders. Multiphase ejectors are able to use the exergy in high pressure wells to enhance recovery and flow rates in depleted wells .Technology for expanders based on multiphase flow is under development [1] and expansion of gas is a mature technology. Voldsund et al. [1] suggest that attention should be drawn to the concept of separator turbines. If some of this exergy destruction is recovered in expanders, the decrease in temperature compared to throttling must be taken into consideration. To see the influence on the temperature some well streams in the simulation were equipped with turbines instead of valves. The temperature drop increased by approximately 10 °C, so additional heating in the separation train is viewed as necessary. This potential is more relevant on platforms where the temperature of the crude oil is not a critical factor for the separation, or even better, on platforms where cooling is needed in the separation train. Voldsund et al. [1] suggest that it might be interesting to assess the concept of separation turbines to production of power in the study of another oil and gas processing platform.

6.1.1.2   Separation

Some of the separators have zero or close to zero exergy destruction. Since the kinetic and potential energy is neglected, or taken into consideration in other ways, the only function of the separator, if the streams already consists of different phases, is to let the phases go in different directions. The separation has occurred due to other processes upstream where the exergy destruction took place, e.g. in a mixer or cooler. Hence, in those separators, the exergy destruction becomes zero since there is no pressure loss. It is worth noting that as the physical exergy becomes lower during the separation, the chemical exergy increases because the different streams out of the separator is purer than into the separator. Of course, in total, exergy is destructed or at best zero.

From Table 5.5 and Table 5.6 we see that the chemical exergy increases in the separation train due to separation. The scrubbing is of high relative importance for the overall separation process. The chemical exergy increase in the recompression train and the reinjection train where -19 kW/ -9 kW and -5 kW/ 24 kW, respectively. It is worth noting that the chemical exergy increases in the reinjection train in the 2010 case, while it decreases in the 2012 case. This is much due to gas import in the 2010 case, which destructs exergy in the mixing process with the process streams.

To maximize the pressure into the separation train reduces the exergy destruction in the production manifolds and the power consumption and exergy destruction in the recompression train. Another

oil and gas processing platform [37] has a pressure of the reservoir fluids into the separation train at approximately 120 bar.

6.1.1.3   Compression

More than 27.9 %/ 28.8 % of the total exergy destruction in the oil and gas processing is related to compression and pumping, and both the efficiency defect and the f-value have high values at the reinjection train, with 0.183/ 0.178 and 0.445/ 0.478, respectively. This indicates that the gas compression is of importance regarding the exergy analysis. In the total gas compression section, consisting of the recompression train and the reinjection train, the pressure is increased significantly and it is the place where most power is supplied.

The exergy destruction in the compression trains is mainly due to compression, cooling and anti-surge recycle. In the compressors some power is transformed into thermal energy due to adiabatic efficiencies lower than 100 %, see Table 3.6. The adiabatic efficiencies are considered as fairly high and the improvement is only possible up to a certain level with present technology. Much of the exergy destruction in the compressors must therefore be regarded as intrinsic, see Section 2.7. The compression in the recompression train consists of three stages and the compression in the reinjection train has two stages; more stages would give a compression nearer reversible. To improve the exergy efficiency and lower the power consumption, focus upon the gas compression is of importance. At another North Sea oil platform Voldsund et al. [20] propose that the effect of introducing a number of extra steps should be examined. This could likely be taken into consideration at this platform too [38], but the adiabatic efficiencies of the compressors are in general higher than for Voldsund et al. [13]. The coolers are needed to ensure a low inlet temperature for the compressors, and there is not much sensible that can be done to reduce the exergy destruction. Some of the compressors are designed for a larger volume than the current volume of gas. To deal with this an anti-surging control system recycles gas around the gas compressors [39]. The recycle pressure loss, due to anti-surging, has a perceptible effect on the exergy destruction. Recirculation leads to increased exergy destruction in the accompanying coolers and scrubbers, since the gas has to be recirculated also through these components to not get overheated. The recirculation rates correspond to a volume flow of roughly 96 000 Sm^3/h/ 17 000 Sm^3/h.

A case where the anti-surge recycle were eliminated was studied in [36]. The drawback of compressors running off-design resulted in an extra exergy destruction of 1.2 MW, which is equivalent to a 4.3 % increase in the total exergy destruction of the oil and gas processing platform. We see that the anti-surge recycle of the compressors have a direct impact of the exergy destruction and thereby the exergetic efficiency.

6.1.2   Power generation system and distribution systems

6.1.2.1   Hot water distribution system

The hot water distribution system utilizes waste heat via three waste heat recovery units. This is seen as a good solution in terms of exergy destruction. There is a possibility for improvement concerning the electrical heated superheater. Its duty can easily be covered by e.g. the export cooler. The heater HB-20-0003 raises the temperature from 78 °C/ 86 °C to 98 °C/ 102 °C with a duty of 11.5 MW/ 10.9 MW heat. There is no cooling demand at this temperature level and at this amount of heat, so the hot water distribution system is seen as the best solution. The use of thermal exergy and power in

the different sub-systems is presented in Figure 5.5 and Figure 5.6. The compromise between heat recovery through waste heat recovery units and heat recovery steam generators is discussed in Section 6.1.2.4.

6.1.2.2   Seawater distribution system

The exergy losses related to the coolers are charged the corresponding oil and gas processing sub-system. This is done in order to compare the study with other studies not including the distribution systems. It is a theoretic potential to exploit the exergy in the cooling water before it is dumped back into the sea. The temperatures after the cooling of the oil and gas processing process is only 45 °C, this is too low to utilize otherwise than with direct heat exchange. Since there are no heaters with an outlet temperature below this temperature, the discharged cooling water is considered as worthless.

6.1.2.3   Turbine system

The ratio between the exergy output and the exergy input of the turbines can be seen in Table 5.11 and Table 5.12. The ratio for both gas turbines is 0.39/ 0.36. Another power generation system on an offshore platform was simulated by Widarena [40]. The power generation system has an efficiency of 0.3 with a desired exergy output of 32 MW. The destructed exergy was distributed between compressors, turbines and reactors with 3 %, 13 % and 84 %, respectively. Our power generation system has an output of 40.3 MW/ 35.8 MW. If the exergy destruction in the Cutter-component is included in the reactor, the destructed exergy between compressors, turbines and reactors are 14 %/ 13 %, 3 %/ 8 % and 82 %/ 79 %. Although the AF ratio for our power generation system is smaller, a higher part of the exergy destruction takes place in the compressors. This has to do with a lower adiabatic efficiency and a higher pressure ratio of the compressors than in Widarenas simulation. However, the exergy destruction in the compressors and turbines are small relative to the exergy destruction in the reactor. It is important to focus on a well-functioning combustion.

6.1.2.4   Combined cycle

Nowadays the offshore oil and gas processing sector is developing towards a more energy demanding production. More gas production, more mature fields, more subsea operation and more activities further north are contributing to a higher energy demand. Together with higher taxes for emissions, this may result in an increased interest in offshore combined cycle plants. Kloster [8], [9] argued that replacement of gas turbines by combined cycles at offshore platforms would be the most energy efficient initiative.

It is clear that a combined cycle increases both the thermal efficiency and the exergetic efficiency of the plant, especially in a case where the alternative is another gas turbine unit. Many other factors must be taken into account. Offshore combined cycles have other requirements which in many ways are different to an onshore combined cycle plant. Important requirements are availability/reliability, high power to weight ratio, size and area requirements, hostile requirements offshore and easy maintenance and repair [5]. Offshore combined cycles are often divided into three so called lift skids; gas turbine skid, steam turbine skid and heat recovery steam generator skid. A skid includes all relevant equipment. The weight of a 15-20 MW steam turbine skid is approximately the same as for a 20 MW gas turbine skid, which has the weight of about 150-175 tons [5]. The weight of the heat recovery steam generator skid designed for a LM2500+ gas turbine is approximately 125 tons [8]. The area occupied by a gas turbine skid is much the same as for a steam turbine skid. The heat recovery steam generator skid is often placed on top of the gas turbine skid, and therefore no additional

footprint is needed. This is done on Oseberg D, Eldfisk and Snorre B with a single pressure heat recovery steam generator with vertical gas flow. Gas turbine power, steam turbine power and thermal efficiency of the combined cycle at these platforms are presented in Table 6.1.

Table 6.1 Gas turbine power, steam turbine power and thermal efficiency of combined cycle at Oseberg D, Eldfisk and Snorre B [5]

	Oseberg D	Eldfisk	Snorre B
Gas turbine power	2x25.9 MW (LM2500+, 88 % load)	2x12.2 MW (LM1600) 1x14.4 MW (LM2500)	2x30 MW (LM2500+)
Steam turbine power	15.8 MW at 88 % load (19 MW at 100 % load) 15.3 MW (11.65 MW steam extraction)	10.3 MW	17.3 MW 15.2 MW (8.0 MW steam extraction)
Thermal efficiency plant	47 % (88 % load) 50 % (100% load)	ca. 50 %	ca. 50%

The gas turbine of our platform, a LM2500+ HSPT DLE with mechanical drive and 26.8 MW/ 25.7 MW net power output, is comparable with the gas turbines on Oseberg D, Eldfisk and Snorre B, which is used in combined cycles.

During the recent three years the maximum effects of electrical power produced form turbine A and B have been 14.3 MW and 14.0 MW, respectively. The total electrical power productions from both turbines have never exceeded 14.3 MW, so a power demand which pass this would seem unlikely. There is a decreasing trend in the power production from when the measurements started in 2007 and to the present. The steam turbine should not be designed to cover more than 14.3 MW.

The first attempt is to cover the electricity demand by utilizing the exhaust air from the mechanical drive gas turbine in a steam turbine and shut down the two other gas turbines. If we compare the net power output from the steam turbine, see Table 5.13, with the electricity demand of 13.5 MW/ 10.1 MW, it is clear that the net power output from the simulated steam turbine is not enough to cover the electricity demand. If we compare the exergy destruction in the simulated steam turbine with the exergy destruction in the existing gas turbines, it is clear that the exergy destruction is decreased dramatically with an amount of approximately 7.1 MW/ 7.8 MW. Since the savings in destructed exergy is so significant, some additional heating of the steam may advantageously be made, allowing the steam turbine to cover the electricity demand.

A related problem is the demand of 4.6 MW/ 4.8 MW thermal exergy for heating which was covered by heat exchange with the exhaust gas from all gas turbines. The heat exchangers have a total duty of 17.2 MW/ 18.0 MW heat. After the heat recovery steam generator the exhaust gas has a temperature of only 170 °C and far from enough heat to cover the demand. The thermal efficiency of the existing power generation system, if we include the waste heat recovery units, is 58 %/ 56 %. This is higher than the thermal efficiencies for the combined cycle presented in Table 5.13 and does not cover the need for heating in the separation train.

Another attempt is to shut down only one of the generator drive gas turbines and utilize the exhaust air from the two other gas turbines in a heat recovery steam generator. In other words; the generator drive gas turbine is used as top load. To use multiple gas turbines on one single heat recovery steam generator is commonly used offshore to save weight [5]. The power output from the generator drive gas turbine is reduced with 7.5 MW/ 6.6 MW according to Table 5.15. The steam turbine net power is approximately equal to this reduction, so the electricity demand is covered. The fuel gas consumption is reduced with 1 881 Sm^3/h/ 2 351 Sm^3/h, this corresponds to a 20 %/ 26 % reduction. The adiabatic efficiency of the generator drive gas turbine is 92.7 %/ 92.4 %. According to Table 5.14, the exergy destruction in the generator drive gas turbine is reduced with 7.0 MW/ 9.7 MW. Now, the temperature of the exhaust air is 310 °C and the amount of exhaust air is somewhat higher due to the use of two turbines. Via waste heat recovery units this covers the heating of the water in the hot water distribution system. Since the temperature of the exhaust air is reduced compared to the original case, the exergy destruction in the hot water distribution system reduces dramatically with 4.2 MW/ 4.8 MW. The steam turbine destructs 5.5 MW/ 4.8 MW of exergy, but in total the exergy destruction is reduced with 5.8 MW/ 10.0 MW. The high difference between 2010 and 2012 is affected by the increase in adiabatic efficiency for the generator drive gas turbine in 2012. The thermal efficiency in the power generation system, when including the heat exchange with the hot water distribution system, is 72%/ 76 %. In addition to the reduction in exergy destruction, the cost for emissions and fuel would be reduced.

Advantages and disadvantages are many, but the idea of utilizing parts of the exhaust air in a combined cycle should be further investigated, even though today's solution is satisfying.

6.2   Validity of the simulated process flowsheet

The validity of the simulation results is dependent on the conformity with reality. Therefore it is important to compare the simulated process flowsheet with measurements done at the oil and gas processing platform.

The process units are placed on different height levels, with a total height difference of about 45 m, which is neglected in the simulation. This can lead to that some process units have been assigned a too high or too low exergy destruction, since the measured values take the height difference into account. Physical exergy transferred into potential exergy will look like exergy destruction in the simulation, and in the opposite way. The difference in measured and simulated pressure out of the electrostatic coalescer is 1.22 bar/ 1.20 bar, which corresponds to a 31 %/ 31 % higher measured pressure than simulated. For the pressure out of the first separator the deviation was 19 % in 2012, while there are no measured values for 2010. The pressure of the liquid stream out the first scrubber is increased by a dummy pump to prevent gas phase out from the electrostatic coalescer. This is the only consideration done concerning potential exergy. The separation train has a relatively low efficiency defect and the accuracy of the pressures is not critical for the overall result. Comparison between simulated and measured value and the actual elevation of the process units can be seen in Appendix J and Appendix E, respectively.

Referring to Appendix J, there is a noticeable difference between the simulated and the measured temperature downstream the throttling in the manifolds. As we can see, this results in a difference between the simulated and measured temperature in the crude oil streams from the manifolds and

into the separation train. This is especially significantly in the 2010 case. Investigations have been done to clarify the reason. One reason is that it was assumed that the composition of the phases in the well streams were constant over time and equal for all wells. The same assumption was made by Voldsund et al. [1] in an exergy analysis of another oil and gas processing platform in the North Sea. To test the impact of this assumption, a description from a nearby oil reservoir was used. The influence on the result was mostly within calculated uncertainties. In this simulation a case where the measured temperatures in each well were reached by the use of pipe segments with heat loss/supply were performed. The resulting temperature in the crude oil streams from the manifolds and into the separation train did not approach the measured value appreciably. The updating of the description by the use of Adjust-components has also a certain tolerance and can contribute to deviations. The uncertainty in the measured value must also be taken into account. It could be predicted to be approximately 1 °C [34]. According to [41] there could also be a perceptible difference between the calculations in the simulated valve and the actual behavior of a real valve. The water in the simulation is fresh water, while it in fact should be sea water. This difference can change the heat capacity up to 20 % [41].

According to Table 3.2, the UA values for the heat exchanger HB-20-0001 are quite higher than the design value. The main reason is assumed to be that the temperatures of the inlet and outlet streams of the heat exchanger simulated are different from the actual values. No measurements of these temperatures are done, so it is associated some uncertainty with this assumption. As presented in Table 3.7, almost all heaters, coolers and heat exchangers simulated have a higher pressure loss than the design value from the datasheet. This is due to, as earlier mentioned, the assumption of pipes with no irreversibilities and no change in elevation during the process, so the exergy destruction is added to the corresponding components.

From Table 4.3 we see the ratio between measured and simulated flow rates inlet and outlet of the oil and gas processing platform. The inlet flow is tuned to get a match between the measured and simulated outlet streams of oil, gas and water. This is assumed to be a good solution, but the ratio between the measured and simulated inlet streams are maybe too far from unity. Questions can be raised about the accuracy of the calculated flow "measurements". A part of the reason, since the oil and gas processing process is not in a complete stationary state, can be the time it takes from crude oil enters to oil, gas and water leave the platform. Especially the produced water pumps start and stop at regular intervals if the flow rate of produced water is low, which could affect the water ratio; this applies most in the 2010 case. The possibility of better measurements of the inlet flow rates should be studied. The fuel gas flow rate is quite accurately measured, but the distribution of fuel gas between the gas turbines is more uncertain. As mentioned in Section 4.1.3 the split ratio is based on calculated flow "measurements" in 2012, and the deviation between the measured and simulated flow rate through the mechanical drive turbine is shown in Appendix J. The simulated value is somewhat higher than the measured value, but it is assumed that the total flow rate of fuel gas and the ratios between the calculated flow rates are more accurate than the measurements of flow rates in the turbine system.

A weakness of the simulation of the two different dates, by two years in between, is the use of the same composition of the oil given by the oil company in 2009. To get a more accurate simulation, compositions closer to the actual date should be used. Then it could be possible to see the impact of

the composition of the oil on the exergy destruction in the sub-processes and equipment by comparing dates with almost the same rates of production.

The exergy analysis conducted in this thesis does not take into account the evaluation of interactions and cost flows in components and sub-processes, as it does not consider their mutual dependencies. There are measures that interfere with each other, like utilizing the high pressure in the production manifolds in turbines, and operating the separation at the highest pressure possible. Another example is the use of combined cycle to generate power and the use of waste heat recovery units for heating. Operating the separation at high pressure reduces the exergy destruction in the production manifolds and the exergy destruction and power consumption in the gas compression, but may not lead to better exergetic efficiency in the separation train. This shows the importance of investigating collaborations and dependencies between sub-processes for improving the overall process at the platform. Nor are the exergy losses concerning emissions of pollutants taken into account.

6.3 Comparison between 2010, 2012 and another oil and gas processing platform

An exergy analysis was performed on another North Sea oil and gas platform by Voldsund et al. in 2012 [13]. The oil and gas processing at this platform started about 20 years ago, hereby referred to as the Old-platform, while the processing at the platform in this report began less than 10 years ago, referred to as the New-platform. The Old-platform and the New-platform are built up roughly the same way. There is no gaslift, heating in the separation train and import of gas at the Old-platform. The recompression train consists on both platforms of a three stages compression with anti-surge recycling. In the reinjection train the Old-platform has three parallel trains with two stages compression. From the Old-platform oil is pumped to a nearby platform and gas is injected into the reservoir. Water injection is used, but the injection water originates from another platform. A detailed system description of the Old-platform can be seen in [13].

Table 6.2 shows the temperature and pressure for mass streams at the Old-platform. The exergy exported, power exergy consumption and heat exergy consumption are presented in Table 6.3, while the exergy destruction in the sub-processes can be seen in Figure 6.1. It is important to notice that the power exergy consumption just includes electrical power and shaft power. The exergy exported includes both physical exergy and chemical exergy.

Table 6.2 Temperature and pressure of the mass streams at the Old-platform

Description	Temperature [°C]	Pressure [bar]
Well fluids from several producing wells	79 - 87	80 - 170
Mixed streams after production manifolds	74	70
Oil after separation train	55	2.8
Oil pumped for export	50	32
Treated gas before injection/lift	78	236

Table 6.3 Exergy exported, power exergy consumption and heat exergy consumption for the New-platform in 2010 and 2012 and the Old-platform

	2010	2012	Old-platform
Exergy exported [MW]	12 600	8 500	1 400
Power exergy consumption [MW]	29	26	24
Heat exergy consumption [MW]	5	5	0
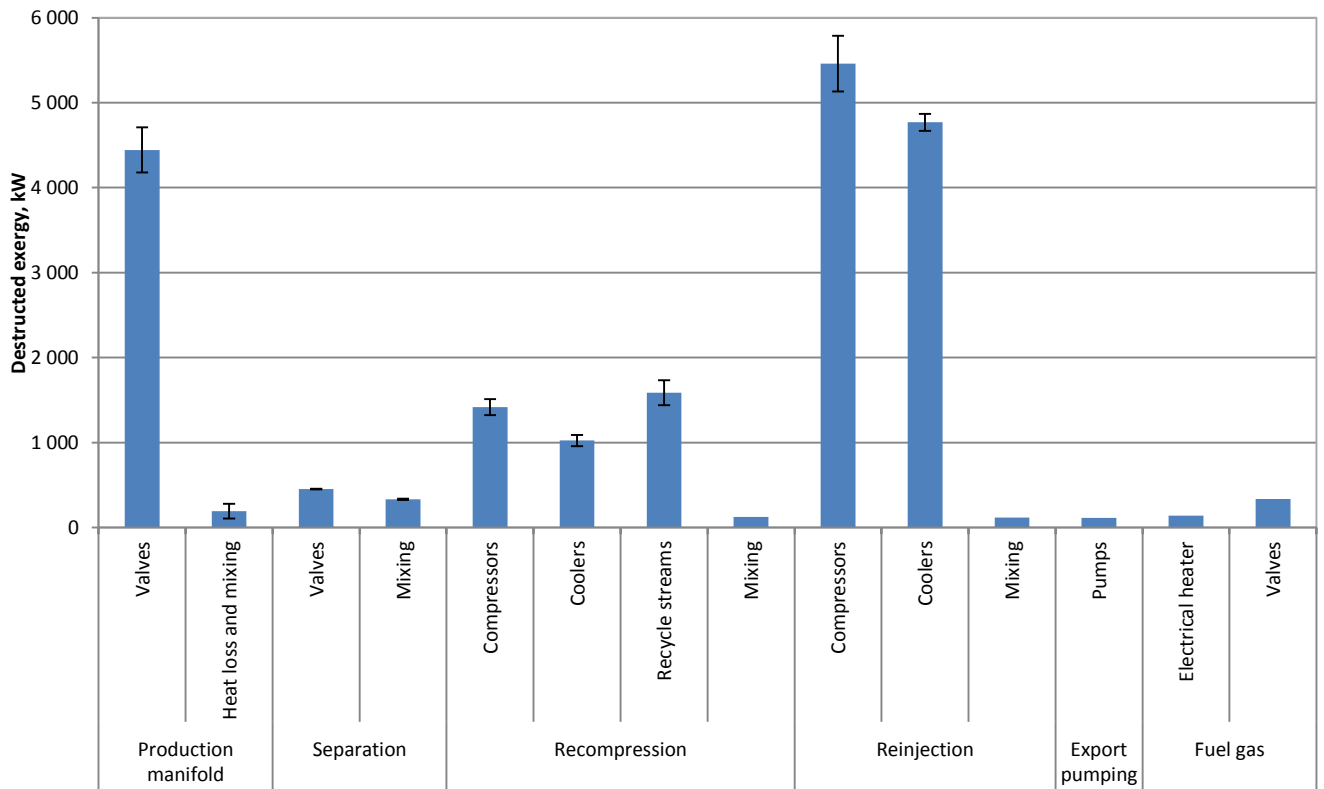
Figure 6.1 The major contributes to exergy destruction distributed on type of process unit in the different sub-processes of the oil and gas processing at the Old-platform [1]

By comparing to Table 3.4 and Table 3.5 we see that the well fluids in general have a higher temperature and pressure than the 2010 case and the 2012 case. This also applies to the mixed streams after the production manifold. The New-platform produces oil with high viscosity. Heating is required in the separation train to enhance separation and avoid problems with emulsions, although the separation train inlet temperature is not much lower than for the Old-platform. This results in a higher temperature of the oil after the separation train for the New-platform. The temperature and pressure of the oil pumped for export, and the treated gas before injection or lift lies much in the same range for the New-platform and the Old-platform, with the exception of the pressure of the exported oil which is 99 bar/ 92 bar at the New-platform.

Figure 6.2 compares the efficiency defect of the sub-processes at the New-platform and the Old-platform. It also contains the exergetic efficiency of the whole oil and gas processing platforms.
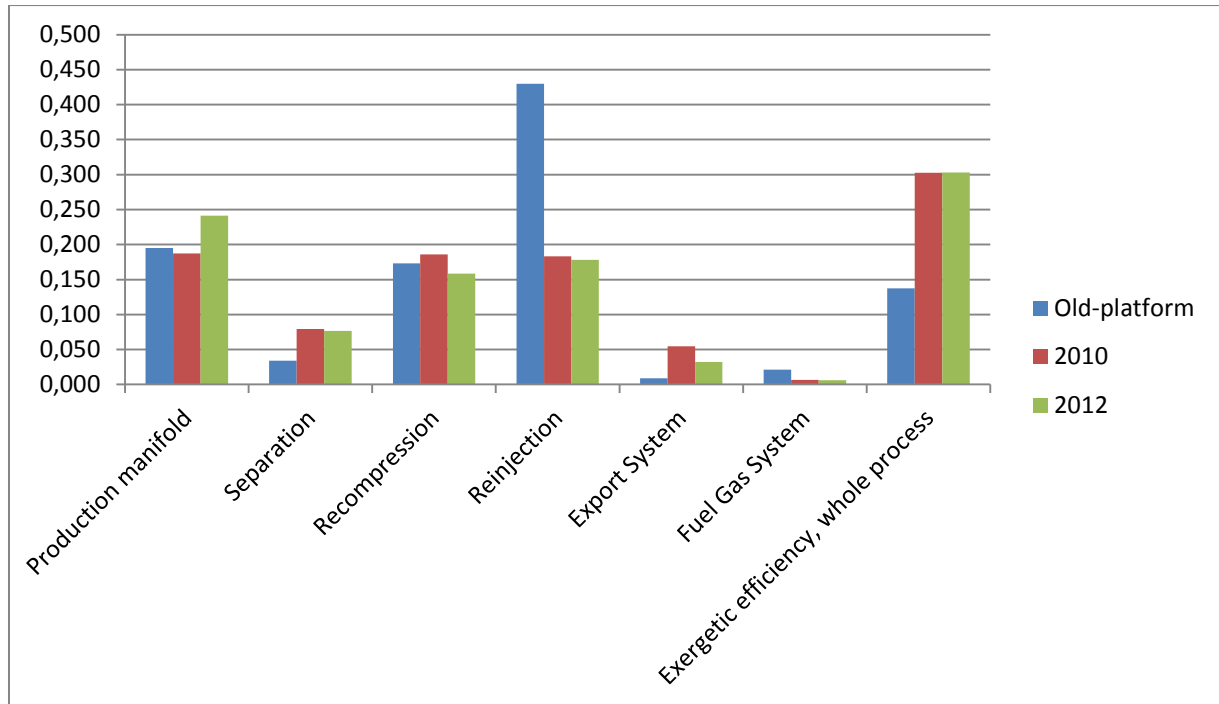
Figure 6.2 Efficiency defect of the sub-processes together with the exergetic efficiency of the whole oil and gas processing process at the Old-platform and the New-platform in 2010 and 2012

Important parameters for the New-platform and the Old-platform are presented in Table 6.4. Exergetic efficiency and f-value of the sub-processes at the Old-platform are shown in Table 6.5.

Table 6.4 Parameters of the New-platform in 2010 and 2012 and the Old-platform

Parameter	2010	2012	Old-platform
Exergetic efficiency	0.303	0.303	0.131
GOR	336	338	2 800
SPC [kWh/Sm^3]	28	35	179
Adiabatic efficiencies of compressors [%]	61 - 81	66 - 78	47 - 69
Oil export [Sm^3/h]	1 093	787	133
Injection gas and gaslift [10^3 Sm^3/h]	383	266	369
Produced water [Sm^3/h]	8	300	67
Exergy destruction / oil export [kJ/kg]	75	99	690
Exergy destruction / gas injection [kJ/kg]	252	325	240
SEC	0.003	0.004	0.017
SED	0.002	0.002	0.015
$\psi_{"i-o",3}$	0.729	0.698	0.717

Table 6.5 f-value of the sub-processes at the Old-platform

	f-value
Production manifold	0
Separation train	4,9E-06
Recompression train	0.197
Reinjection train	0.783
Fuel gas system	0.007
Export system	0.013
Total process	1

6.3.1.1 Comparison between the New-platform in 2010 and 2012

The most important differences in the conditions in 2010 and 2012 can be summarized as follows:

- No gas import in 2012
- Nearly no water injection in 2010
- More exported oil and injection gas and gaslift in 2010 than in 2012
- Lower recycle rates at 2nd and 3rd compression stage in the recompression train in 2012 than in 2010
- Generator turbine B used in 2012 and generator turbine A used in 2010

From Table 6.4 we see that the exergetic efficiency is equal, however the specific power consumption is lowest in 2010. In spite of the higher production rates of oil and gas in 2010, the GOR is almost the same. When it comes to the efficiency defect Figure 6.2 illustrates the differences. The production manifold is the only sub-process with higher efficiency defect in 2012 than in 2010. The reason is throttling from a higher pressure in 2012 than in 2010. The exergy destruction per oil exported and per gas injected is better in 2010. Probably because of the gas import in 2010, it has low exergy destruction and contributes to the gas injection.

6.3.1.2 Performance parameters

Table 6.4 shows that the exergetic efficiencies for the New- and Old-platform are 0.30/ 0.30 and 0.13, respectively. The specific power consumption is 28 kWh/Sm^3/ 35 kWh/Sm^3 for the New-platform and 179 kWh/Sm^3 for the Old-platform. It is clear, when comparing the performance of oil and gas processing process on platforms, that more than one performance parameter must be taken into account. The parameters chosen here have their strengths and weaknesses. The inlet conditions of the feed stream entering the process, with respect to temperature, pressure and composition, are of importance. These conditions set the guidelines for how much oil, gas and water that are produced. Specific power consumption would seem favorable for a platform producing much oil relative to gas. The exergetic efficiency will benefit from favorable conditions of the oil, like low viscosity, since then not so much heating is required in the separation train.

The Old-platform has a GOR of 2800, which is quite high. All the gas is injected and is responsible for a major part of the power consumption and exergy destruction. This will impact performance parameters like specific power consumption, exergy destruction/oil export, SEC and SED in a negative direction. From Table 6.4 we see that the New-platform has better values on all these performance parameters. The "input-output"-efficiency based on (21) is 0.73/ 0.70 and 0.72 for the New- and Old-

platform, respectively. This parameter takes all streams entering and leaving the process into account, so the platforms are not "charged" for the gas injection.

6.3.1.3 Compression and cooling

The compressors at the New-platform have in general better adiabatic efficiencies than the Old-platform. This can at least explain much of the difference when it comes to exergetic efficiency and exergy destruction in the recompression train where the design of the two platforms is much the same. One difference to notice is that the recycle rate to prevent surging is quite high for the compressors in the recompression train at the Old-platform. The recycle ration for the 1st, 2nd and 3rd recompression stages are 92 %, 69 % and 72 % for the Old-platform, respectively. According to [13] this has led to almost constant flow rates, even if the amount of oil in the separation train has decreased, and the recycle pressure loss contributes to the highest exergy destruction in the recompression train. The reinjection train at the Old-platform should have advantages due to no anti-surge is required unlike the New-platform. In spite of this the efficiency defect in the reinjection train is significantly larger for the Old-platform than for the New-platform. The platforms have nearly equal rates of injection gas and gaslift and the exergy destruction per oil export is in the same range. However the adiabatic efficiencies of the compressors at the New-platform lie significantly higher than the adiabatic efficiencies at the Old-platform, which lie in the range of 54-69 %. In addition it is worth noticing that the reinjection train at the Old-platform consists of six compressors, as opposed to the New-platform which only has three compressors in the reinjection train. The adiabatic efficiencies for the compressors are improved at the New-platform compared to the Old-platform. This might be due to technological development and wear and tear. The differences in adiabatic efficiencies for the compressors have considerable influence on the exergy destruction. Low efficiencies in the compressors give unfavorable temperatures, which in turn causes a higher demand for cooling. Referring to Figure 6.1, the compressors and coolers in the reinjection train at the Old-platform contributes for the highest exergy destruction at the whole platform. As much as nearly 50 % of the exergy destruction for the Old-platform happens in the reinjection train and the f-value is 0.783. This is in contrast to the New-platform where the reinjection train contributes for 26 %/ 26 % of the total exergy destruction. The high GOR for the Old-platform gives a relatively high significance to the exergy destruction in the compression sections, like it also gives an impact on the specific power consumption, since more gas has to be compressed relative to the amount of oil produced.

6.3.1.4 Export system

There is a large difference in the rate of oil produced at the two platforms. Taking the ratio between the oil exports for the two platforms we get 8.2/ 5.6. Taking the ratio between the efficiency defects of the export system we get the value 6.1/ 3.6, showing that there is a link between the rate of oil exported and the magnitude of the exergy defect for the export pumping system. This of course has something to do with that the exergy destruction takes place in the pumps and coolers in the export section, and is strongly dependent of the mass flow of oil to export.

6.3.1.5 Fuel gas system

The fuel gas system at the New-platform contributes less than 1.0 % of the total exergy destruction. The relative irreversibility of the fuel gas system at the Old-platform is approximately 2.5 %. The explanation is based on the design of the fuel gas system. As described in Section 3.2.1.4, the fuel gas at the New-platform is tapped by after the second scrubber in the reinjection train, while at the Old-platform the fuel gas is tapped by after the first separator in the separation train. Due to this the fuel

gas at the Old-platform needs more treatment before it is ready to be used in power turbines and pilot flame at the flare. Thereby more power is consumed and more exergy destructed in the fuel gas system.

7 Conclusion

An exergy analysis has been performed on a North Sea oil platform for two real production days with two years in between. The overall oil and gas processing process utilizes 33.6 MW/ 31.6 MW (2010/ 2012) exergy and destructs 21.3 MW/ 19.3 MW. The specific power consumption was 28 kWh/Sm^3/ 35 kWh/Sm^3, while exergetic efficiency was 0.30/ 0.30. The highest losses were related to the gas compression. The high f-value $\left(E_{U_i}/E_U\right)$ illustrates the importance of the recompression train and the reinjection train concerning exergy destruction. It was shown that the highest exergy destruction took place in processes that increased (compressors/pumps) or decreased (throttling) the pressure of the material streams, like in the production manifolds (5 800 kW/ 6 700kW), the separation train (2 400 kW/ 2 100 kW), the recompression train (5 700 kW/ 4 400 kW) and in the reinjection train (5 500 kW/ 4 900 kW). The latter three sub-processes also have the highest power consumptions.

The temperature based exergy increases most in the separation train (4 000 kW/ 3 700 kW), since heating is required to separate the heavy oil. The highest increase in pressure based exergy happens in the reinjection train (10 200 kW/ 6 800 kW) due to compression of gas to lift and injection.

Nearly all power is used for compression and pumping, and major parts of the thermal exergy for heating come from internal heat integration. The oil and gas processing process is served by the power generation system and distribution systems. Its highest exergy destruction is related to the turbine system and specially the combustion reactors. The mechanical drive turbine system has an efficiency defect of 0.36/ 0.40. The hot water distribution system has the highest exergy destruction related to the heat exchangers which destructed 7 000 kW/ 7 300 kW. The hot water distribution system, which utilizes waste heat, is considered as a good solution. Therefore as much as practically possible concerning the heat deficits should be covered by that, or even better by internal heat integration.

The possibility of utilizing a part of the exhaust from the gas turbines for a combined cycle was investigated. The best solution found will reduce the exergy destruction with 5.8 MW/ 10.0 MW and results in a thermal efficiency of the power generation system of 0.72/ 0.76. Other measures to decrease the exergy destruction are proposed. The suggestions discussed can be categorized in; updating existing process units, modifying the configuration of the process and developing new process units. All suggestions have to be evaluated as a tradeoff between capital cost and operating cost. On offshore installations the demand for a simple and compact process also matters significantly.

When comparing the performance of different oil and gas processing processes, it is clear that more than just a performance parameter or two must be taken into account. The more different the conditions and processes are, the more difficult it is to compare performance parameters. As important as the value of a performance parameter itself, is the reasons why the value is what it is.

It has been shown that an exergy analysis is a good method to detect, locate and quantify the theoretical potential for savings. Parameters such as destructed exergy and exergetic efficiency give useful information in addition to other more regular measures of performance.

Conclusion

References

[1]   M. Voldsund, I. S. Ertesvåg, W. He and S. Kjelstrup, "Exergy Analysis of the Oil and Gas Processing a Real Production Day on a North Sea Oil Platform," *Atricle in press,* pp. 1-12, 2013.

[2]   M. Margarone, S. Magi, G. Gorla, S. Biffi, P. Siboni, G. Valenti, M. Romano, A. Giuffrida, E. Negri and E. Macchi, "Revamping, Energy Efficiency, and Exergy Analysis of an Existing Upstream Gas Treatment Facility," *Journal of Energy Resources Technology,* vol. 133, pp. 012001-1-012001-9, 2011.

[3]   J. Hansen and B. Rasen, Fakta 2012, Oslo: Norsk petroleumsvirksomhet, 2012.

[4]   European Commission, "Climate Action," 2012. [Online]. Available: http://ec.europa.eu/clima/policies/package/index_en.htm/. [Accessed 9 September 2012].

[5]   Ø. Flatebø, Off-design Simulations of Offshore Combined Cycles, Master Thesis, Trondheim: Norwegian University of Science and Technology, Department of Energy and Process Engineering, 2012.

[6]   S. M. Svalheim, "Environmental Regulations and Measures on the Norwegian Continental Shelf," *Society of Petroleum Engineers, Paper SPE 73982, http://www.onepetro.org/mslib/app/Preview.do?paperNumber=00073982&societyCode=SPE,* pp. 1-10, 2002.

[7]   S. M. Svalheim and D. C. King, "Life of Field Energy Performance," *Society of Petroleum Engineers, Paper SPE 83993, http://www.onepetro.org/mslib/app/Preview.do?paperNumber=00083993&societyCode=SPE,* pp. 1-10, 2003.

[8]   P. Kloster, "Energy optimization on offshore installations with emphasis on offshore and combined cycle plants," *Society of Petroleum Engineers, Paper SPE 56964, http://www.onepetro.org/mslib/app/Preview.do?paperNumber=00056964&societyCode=SPE,* pp. 1-9, 1999.

[9]   P. Kloster, "Reduction of emissions to air through energy optimisation on offshore installations," *Society of Petroleum Engineers, Paper SPE 61651, http://www.onepetro.org/mslib/app/Preview.do?paperNumber=00061651&societyCode=SPE,* pp. 1-7, 2000.

[10]   C.-J. Winter, "Energy efficiency, no: It's exergy efficiency!," *International Journal of Hydrogen Energy,* vol. 32, pp. 4109-4111, 2007.

[11]   S. Oliveira Jr. and M. van Hombeeck, "Exergy analysis of petroleum separation process in offshore platforms," *Energy Convers Manage,* vol. 38, pp. 1577-1584, 1997.

References

[12]   I. S. Ertesvåg, "SINTEF Energy," 2004. [Online]. Available:
         http://www.energy.sintef.no/publ/xergi/98/1/art-2.htm. [Accessed 29 January 2013].

[13]   M. Voldsund, W. He, A. Røsjorde, I. S. Ertesvåg and S. Kjelstrup, "Evaluation of the Oil and Gas
         Processing at a Real Production day on a North Sea Platform Using Exergy Analysis," *The 26th
         International Conference on Efficiency, Cost, Optimization, Simulation and Envonmental Impact of
         Energy Systems,* 2012.

[14]   E. Sauar, Energy efficient process design by equipartion of forces, Dr. Techn. thesis no. 1998:77,
         Trondheim: Norwegian University of Science and Technology Department of Physical Chemistry,
         1998.

[15]   T.-V. Nguyen, L. Pierobon, B. Elmegaard, F. Haglind, P. Breuhaus and M. Voldsund, "Exergetic
         assesment of energy systems on North Sea oil and gas platforms," *Article in press,* pp. 1-14, 2013.

[16]   Aspen Technology Inc., "Aspen HYSYS, Sorftware package Ver. 7.1," Aspen Technology Inc., 2009.

[17]   Wikipedia, "Wikipedia," 2013. [Online]. Available: http://en.wikipedia.org/wiki/Exergy. [Accessed
         23 May 2013].

[18]   T. J. Kotas, The Exergy Method of Thermal Plant Analysis, Malabar, Florida: Krieger Publishing
         Company, 1995.

[19]   M. J. Moran and H. N. Shapiro, Fundamentals of Engineering Thermodynamics, USA: John Wiley &
         Sons, 2008.

[20]   M. Voldsund, I. S. Ertesvåg, A. Røsjorde, W. He and S. Kjelstrup, "Exergy analysis of the Oil and Gas
         Separation Process on a North Sea Oil Platform," *The 26th International Conference on Efficiency,
         Cost, Optimization, Simulation and Environmental Impact of Energy Systems,* 2010.

[21]   R. Riveiro, C. Rendon and L. Monroy, "The Exergy of Crude Oil Mixtures and Petroleum Fractions:
         Calculation and Application," *Int.J. Applied Thermodynamics,* vol. 2, pp. 115-123, 1999.

[22]   J. B. Maxwell, Data book on hydrocarbons: application to process engineering, California:
         University of California, 1950.

[23]   Wikipedia, "Wikipedia," 2013. [Online]. Available: http://en.wikipedia.org/wiki/API_gravity.
         [Accessed 3 May 2013].

[24]   T. Delft, "Deltf University of Technology," 2012. [Online]. Available:
         http://www.3me.tudelft.nl/fileadmin/Faculteit/3mE/Over_de_faculteit/Afdelingen/
         Process_and_Energy_PE/Energy_Technology/research/software/cycletempo/publications/remaini
         ng/doc/Value_diagrams_and_exergy_efficiencies.pdf/. [Accessed 20 November 2012].

[25]   N. Lior and N. Zhang, "Energy, exergy, and second law performance criteria," *Energy,* vol. 32, no. 4,
         pp. 281-296, 2007.

References

[26]   G. Tsatsaronis, "Definitions and nomenclature in exergy and exergoeconomics," *Energy,* vol. 32, no. 4, pp. 249-253, 2007.

[27]   D. Marmolejo-Correa and T. Gundersen, "A comparison of exergt efficiency definitions with focus on low temperature processes," *Energy,* vol. 44, pp. 477-489, 2012.

[28]   M. Voldsund, T.-V. Nguyen, B. Elmegaard, I. S. Ertesvåg, A. Røsjorde, W. He and S. Kjelstrup, "Performance indicators for evaluation on North Sea oil and gas platforms," *The 26th International Conference of Efficiency, Cost, Optimalization, Simulation and Environmental Impact of Energy Systems,* 2013.

[29]   G. Tsatsaronis and M. Park, "Onavoidalble and unavoidable exergy destructions and investment costs in thermal systems," *Energy Conversion and Management,* vol. 43, no. 9-12, pp. 1259-1270, 2002.

[30]   M. Bothnamley and J. M. Campbell, "Offshore processing options for oil platforms," *Society of Petroleum Engineers, Paper SPE 90325, http://www.onepetro.org/mslib/app/Preview.do?paperNumber=00090325&societyCode=SPE,* 2004.

[31]   H. Devold, Oil and gas production handbook, An introduction to oil and gas production, Oslo: ABB Oil and Gas, 2010.

[32]   E-mail correspondance with Solvik O., Interviewee, *E-mail correspondance.* [Interview]. 11 February 2013.

[33]   Aspen Technology Inc., Aspen Hysys 7.2 Documentation. Simulation Basis., Aspen Technology Inc., 2010.

[34]   E-mail correspondance with Voldsund M., Interviewee, *E-mail correspondance.* [Interview]. 22 February 2012.

[35]   E-mail correspondance with Voldsund M., Interviewee, *E-mail correspondance.* [Interview]. 9 March 2013.

[36]   K. Jøssang, Evaluation of a North Sea oil platform using exergy analysis, specialization project, Trondheim: Nowegian University of Science and Technology, Department of Energy and Process Engineering, 2012.

[37]   M. Voldsund, T.-V. Nguyen, B. Elmegaard, I. S. Etresvåg, A. Røsjorde, K. Jøssang and S. Kjelstrup, "Comparative study of the sources of exergy destruction on four North Sea oil and gas platforms," *The 26th International Conference on Efficiency, Cost, Optimalization, Simulation and Environmental Impact of Energy Systems,* 2013.

[38]   A. Zvolinschi, E. Johannessen and S. Kjelstrup, "The second-law optimal operation of a paper drying machine," *Chemical Engineering Science,* vol. 61, pp. 3653-3662, 2006.

References

[39]   R. H. Gabrielsen and J. Grue, Norwegian Energy Policy in Context of the Global Energy Situation, Oslo: Det Norske Vitenskaps Akademi, 2012.

[40]   T. Widarena, Quantitative efficiency assesment of oil and gas processing platform, master thesis, Trondheim: Norwegan University of Science and Technology, Department of Chemical Engineering, 2010.

[41]   E-mail correspondance with Røsjorde A., Interviewee, *E-mail correspondance.* [Interview]. 11 February 2013.

[42]   D. B. Robinson, D. Peng and S. Y.-K. Chung, "The developing of the Peng Robinson Equation and its application to phase equilibrium in a system containing methanol," *Fluid Phase Equilibria,* vol. 24, pp. 25-41, 1985.

[43]   Simbasis, "ebookbrowse.com," 2010. [Online]. Available: http://ebookbrowse.com/pages-from-simbasis-appendix-a-property-packages-pdf-d14896027. [Accessed 17 November 2012].

[44]   E-mail correspondance with Solvik O., Interviewee, *E-mail correspondance.* [Interview]. 8 May 2013.

[45]   E. D. Encyclopedia, "Enggcyclopedia," 2013. [Online]. Available: http://www.enggcyclopedia.com/wp-content/uploads/2011/12/combined-cycle-power-plant.png. [Accessed 29 April 2013].

Appendices

Appendix

A. Laws, definitions and formulas which are expected known

1st and 2nd law of thermodynamics:

1st law of thermodynamics, open system (energy balance) is

$$\frac{dE_{CV}}{dt} = \dot{Q}_{CV} - \dot{W}_{CV} + \sum_{in} \dot{m}_{in}\left(h_{in} + \frac{V_{in}^2}{2} + gz_{in}\right) - \sum_{ex} \dot{m}_{ex}\left(h_{ex} + \frac{V_{ex}^2}{2} + gz_{ex}\right) \tag{A.1}$$

where E_{CV} denotes the energy of the control volume at time t, $\dot{Q}_{CV}$ denotes the net rate of energy transfer by heat across the boundary of the control volume, $\dot{W}_{CV}$ denotes the net rate of energy transfer by work across the boundary of the control volume. The subscript *in* and *ex* indicates inlet and exit, respectively. $\dot{m}$ denotes the mass flow rate and h denotes the enthalpy. V, g and z denotes velocity, acceleration of gravity and elevation, respectively.

2nd law of thermodynamics, open system (entropy balance)

$$\frac{dS_{CV}}{dt} = \sum_{j} \frac{\dot{Q}_j}{T_j} + \sum_{in} \dot{m}_{in}s_{in} - \sum_{ex} \dot{m}_{ex}s_{ex} + \dot{\sigma}_{CV} \tag{A. 2}$$

where S_{CV} denotes the entropy of the control volume, $\dot{Q}_j$ represents the time rate of heat transfer at the location on the boundary where the instantaneous temperature is T_j. s denotes the specific entropy and $\dot{\sigma}_{CV}$ represents the entropy production rate of the control volume.

Definitions of enthalpy and entropy:

$$H \equiv U + pV \tag{A.3}$$

where H and U denote enthalpy and internal energy, respectively. Pressure is denoted by p, and V represents the volume.

$$dS \equiv \left(\frac{\delta Q}{T}\right)_{int.rev.} \tag{A. 4}$$

where the subscript $int.rev.$ indicates that the process is internal reversible.

The Tds-equations:

1st Tds-equation

$$Tds = du + pdv \tag{A.5}$$

where u and v denote specific internal energy and volume, respectively.

2nd Tds-equation:

$$Tds = dh - vdp \tag{A.6}$$

[19]

Appendix

B. Derivation of exergy equations

Derivation of specific exergy:

For an open system in a steady state, with constant mass flow rate and seen as an internal reversible process and thereby no entropy production, the 1st and 2nd law of thermodynamics reduces to the following

$$\frac{\dot{Q}_{CV}}{\dot{m}} = T_0(s_0 - s) \tag{B.1}$$

$$\frac{\dot{W}_{CV}}{\dot{m}} = \frac{\dot{Q}_{CV}}{\dot{m}} - (h_0 - h) + \frac{V^2}{2} + gz \tag{B.2}$$

where the subscript 0 indicates a reference state that is in equilibrium with the environment.

Since exergy can be defined as the net maximum theoretical work output from a system, before it reaches equilibrium with the surroundings, the following equations occur for the specific exergy

$$e = T_0(s_0 - s) - (h_0 - h) + \frac{V^2}{2} + gz = (u - u_0) + p_0(v - v_o) - T_0(s - s_0) + \frac{V^2}{2} + gz \tag{B.3}$$

where e denotes the specific exergy transfer accompanying to mass flow.

Exergy transport accompanying to mass flow and flow work is given by

$$\begin{aligned} e_f &= e + (pv - p_0v) = (e - u_0) + p_0(v - v_o) - T_0(s - s_0) + (pv - p_0v) \\ &= \left(u + \frac{V^2}{2} + gz - u_0\right) + p_0(v - v_o) - T_0(s - s_0) + (pv - p_0v) \\ &= (h - h_0) - T_0(s - s_0) + \frac{V^2}{2} + gz \end{aligned} \tag{B.4}$$

where e_f denotes the specific flow exergy.

Derivation of an exergy balance:

An exergy balance, for an open system in a steady state with constant mass flow rate and no chemical reactions, follows from the 1st and 2nd law of thermodynamics

$$0 = \left[\dot{Q}_{CV} - \dot{W}_{CV} + \sum_{in} \dot{m}_{in}\left(h_{in} + \frac{V_{in}^2}{2} + gz_{in}\right) - \sum_{ex} \dot{m}_{ex}\left(h_{ex} + \frac{V_{ex}^2}{2} + gz_{ex}\right)\right] \tag{B.5}$$

$$- T_0\left[\sum_j \frac{\dot{Q}_j}{T_j} + \sum_{in} \dot{m}_{in}s_{in} - \sum_{ex} \dot{m}_{ex}s_{ex} + \dot{\sigma}_{CV}\right]$$

$$\begin{aligned} &= \sum_j \left(1 - \frac{T_0}{T_j}\right)Q_j - \dot{W}_{CV} \\ &+ \sum_{in} \dot{m}_{in}\left(h_{in} - T_0s_{in} + \frac{V_{in}^2}{2} + gz_{in}\right) \\ &- \sum_{ex} \dot{m}_{ex}\left(h_{ex} - T_0s_{ex} + \frac{V_{ex}^2}{2} + gz_{ex}\right) - \dot{E}_D \end{aligned} \tag{B.6}$$

where $\dot{E}_D = T_0\dot{\sigma}_{CV}$

With one inlet and one outlet mass flow rate with $\dot{m}_{in} = \dot{m}_{ex} = \dot{m}$, the equation simplifies to

$$0 = \sum_j \left(1 - \frac{T_0}{T_j}\right) \dot{Q}_j - \dot{W}_{CV} + \dot{m}\left(e_{f_{in}} - e_{f_{ex}}\right) - \dot{E}_D \qquad (B.7)$$

Derivation of chemical exergy:

If one assumes that the combustion reaction is complete, it could look like this

$$F + \alpha O_2 \rightarrow \beta CO_2 + \gamma H_2O \qquad (B.8)$$

where F denotes fuel, and the three constants α, β and γ represent the molar flow rate of the accompanying substance per molar flow rate of the fuel.
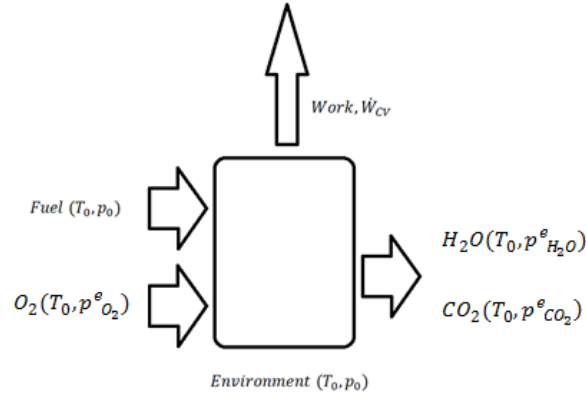
Figure B.1 Chemical exergy in complete combustion

The horizontal arrows denote material streams and the vertical arrow is a stream of work. The box represents a complete combustion process.

The 1st and 2nd law of thermodynamics for this complete combustion is as follows

$$\frac{\dot{W}_{CV}}{\dot{n}_F} = \frac{\dot{Q}_{CV}}{\dot{n}_F} + \left(\bar{h}_F + \alpha\bar{h}_{O_2}\right) - \left(\beta\bar{h}_{CO_2} + \gamma\bar{h}_{H_2O}\right) \qquad (B.9)$$

$$0 = \frac{\dot{Q}_{CV}}{\dot{n}_F T_0} + \left(\bar{s}_F + \alpha\bar{s}_{O_2}\right) - \left(\beta\bar{s}_{CO_2} + \gamma\bar{s}_{H_2O}\right) + \frac{\dot{\sigma}_{CV}}{\dot{n}_F} \qquad (B.10)$$

where $\dot{n}_F$ denotes the molar flow rate of fuel and the substances are at the conditions presented in Figure B.1.

By combining these one get:

$$\frac{\dot{W}_{CV}}{\dot{n}_F} = \left[\left(\bar{h}_F + \alpha\bar{h}_{O_2}\right) - \left(\beta\bar{h}_{CO_2} + \gamma\bar{h}_{H_2O}\right)\right] - T_0\left[\left(\bar{s}_F + \alpha\bar{s}_{O_2}\right) - \left(\beta\bar{s}_{CO_2} + \gamma\bar{s}_{H_2O}\right)\right]$$
$$- T_0 \frac{\dot{\sigma}_{CV}}{\dot{n}_F} \qquad (B.11)$$

Maximum work is achieved when $\dot{\sigma}_{CV} = 0$, thereby the chemical exergy becomes:

$$\bar{e}^{ch} = \left[\left(\bar{h}_F + \alpha\bar{h}_{O_2}\right) - \left(\beta\bar{h}_{CO_2} + \gamma\bar{h}_{H_2O}\right)\right] - T_0\left[\left(\bar{s}_F + \alpha\bar{s}_{O_2}\right) - \left(\beta\bar{s}_{CO_2} + \gamma\bar{s}_{H_2O}\right)\right] \qquad (B.12)$$

where $\bar{e}^{ch}$ represents the chemical exergy on molar basis [19].

C.   The Peng Robinson equation of state

The equation was developed in 1976 and its main goal was to be useful for all calculations on fluid properties in processes including natural gas. For oil, gas and petrochemical applications, the Peng Robinson Equation of State (PR EOS) is generally recommended property package for HYSYS simulations. The recommended limits for temperature and pressure are greater than -271 °C and lower than 1000 bar.

The PR package in HYSYS contains enhanced binary interaction parameters for all library hydrocarbon-hydrocarbon pairs, as well as for most hydrocarbon-nonhydrocarbon binaries. For non-library or hydrocarbon pseudo components, HC-HC interaction parameters will be generated automatically by HYSYS.

Formulation used in HYSYS for the PR EOS:

$$P = \frac{RT}{V-b} - \frac{a}{V(V+b)+b(V-b)} \tag{C.1}$$

$$Z^3 - (1-B)Z^2 + (A - 2B - 3B^2)Z - (AB - B^2 - B^3) = 0 \tag{C.2}$$

Explanation of the symbols regarding Eqs. (C.1) and (C.2) are listed below:

$$b = \sum_{i=1}^{N} x_i b_i \tag{C.3}$$

$$b_i = 0.077796 \frac{RT_{ci}}{P_{ci}} \tag{C.4}$$

$$a = \sum_{i=1}^{N}\sum_{j=1}^{N} x_i x_j (a_i a_j)^{0.5}(1 - k_{ij}) \tag{C.5}$$

$$a_i = a_{ci}\alpha_i \tag{C.6}$$

$$a_{ci} = 0.457235 \frac{(RT_{ci})^2}{p_{ci}} \tag{C.7}$$

$$\alpha_i^{0.5} = 1 + m_i(1 - T_{ri}^{0.5}) \tag{C.8}$$

$$m_i = 0.37464 + 1.54226\omega_i - 0.26992\omega_i^2 \tag{C.9}$$

When an acentric factor > 0.49 is present, HYSYS uses the following corrected form:

$$m_i = 0.379642 + (1.48503 - (0.164423 - 1.016666\omega_i)\omega_i)\omega_i \tag{C.10}$$

$$A = \frac{aP}{(RT)^2} \tag{C.11}$$

$$B = \frac{bP}{RT} \tag{C.12}$$

Here ω_i denotes the acentric factor, Z the compressibility factor, R universal gas constant, V molar volume, x_i mole fraction, k_{ij} interaction parameter and T_{ci} and P_{ci} critical temperature and pressure, respectively. These equations match the original Peng Robinson Equation of State [42].

The enthalpy and entropy calculations are performed rigorously by HYSYS using the following exact thermodynamic relations:

$$\frac{H - H^{ID}}{RT} = Z - 1 + \frac{1}{RT} \int_{\infty}^{V} \left[T \left(\frac{\partial P}{\partial T} \right)_V - P \right] dV \tag{C.13}$$

$$\frac{S - S_0^{ID}}{RT} = \ln Z - \ln \frac{P}{P^0} + \int_{\infty}^{V} \left[\frac{1}{R} \left(\frac{\partial P}{\partial T} \right)_V - \frac{1}{V} \right] dV \tag{C.14}$$

For the PR EOS the following enthalpy and entropy departure functions can be derived:

$$\frac{H - H^{ID}}{RT} = Z - 1 - \frac{1}{2^{1.5} bRT} \left[a - T \frac{da}{dt} \right] ln \left(\frac{V + (2^{0.5} + 1)b}{V + (2^{0.5} - 1)b} \right) \tag{C.15}$$

$$\frac{S - S_0^{ID}}{RT} = \ln(Z - B) - \ln \frac{P}{P^0} - \frac{A}{2^{1.5} bRT} \left[\frac{T}{a} \frac{da}{dt} \right] \ln \left(\frac{V + (2^{0.5} + 1)b}{V + (2^{0.5} - 1)b} \right) \tag{C.16}$$

The ideal gas (indicated by superscript ID) enthalpy basis used in HYSYS is equal to the ideal gas enthalpy of formation at 25 °C amd 1 atm. The subscript 0 indicates a reference state. [43]

Appendix

D.   Input data related to chemical exergy calculations

Table D.1 Composition of oil, gas and water as predicted for 2009 by the oil company

	Oil	Gas	Water
Nitrogen	0.0027	0.0082	0.0000
CO_2	0.0006	0.0137	0.0000
Methane	0.1602	0.8615	0.0000
Ethane	0.0113	0.0783	0.0000
Propane	0.0028	0.0305	0.0000
i-Butane	0.0058	0.0026	0.0000
n-Butane	0.0016	0.0040	0.0000
i-Pentane	0.0037	0.0005	0.0000
n-Pentane	0.0010	0.0004	0.0000
Pseudo -01	0.0546	0.0000	0.0000
Pseudo -02	0.0827	0.0000	0.0000
Pseudo -03	0.1392	0.0000	0.0000
Pseudo -04	0.2357	0.0000	0.0000
Pseudo -05	0.2027	0.0000	0.0000
Pseudo -06	0.0953	0.0000	0.0000
Pseudo -07	0.0000	0.0002	0.0000
H_2O	0.0000	0.0000	1.0000

Table D.2 Molecular weight, boiling temperature and standard liquid density of the pseudo components in the feed stream in the HYSYS simulation basis

Component	Molecular weight [kg/kmol]	Boiling temperature [°C]	Standard liquid density [kg/m^3]
Pseudo -01	98.78	85.76	754.33
Pseudo -02	141.22	173.90	816.60
Pseudo -03	185.79	240.50	861.05
Pseudo -04	241.09	314.54	902.54
Pseudo -05	404.51	487.06	955.27
Pseudo -06	906.97	552.83	1 007.46
Pseudo -07	81.00	73.00	721.23

Table D.3 Content in the pseudo components given by the oil company

Pseudo component	Carbon, wt-%	Hydrogen, wt-%	Nitrogen, wt-%	Sulphur, wt-%	Nickel, wt-%	Vanadium, wt-%	Sum, wt-%
Pseudo -01	84.07	15.93	-	-	-	-	100.00000
Pseudo -02	86.16	13.84	-	0.0054	-	-	100.00540
Pseudo -03	86.92	13.02	0.00009	0.0646	-	-	100.00470
Pseudo -04	87.36	12.23	0.00600	0.3681	-	-	99.96410
Pseudo -05	86.90	11.93	0.15004	0.8588	0.00001	0.00001	99.83886
Pseudo -06	-	-	0.75658	1.5348	0.00189	0.00591	2.29918

Table D.4 Chemical exergy of components [18]

Component	Chemical exergy [kJ/kg]
CO_2	457.63
Methane	52 142.07
Ethane	50 028.77
Propane	49 055.26
i-Butane	48 498.55
n-Butane	48 498.55
i-Pentane	48 171.06
n-Pentane	48 171.06
H_2O	173.19
Nitrogen	25.70
Oxygen	124.06
Argon	292.63

E.   Elevation

Table E.1 Elevation of important components at the platform

The elevation is not taken into account in the simulation.

Component	Elevation [m]	Component	Elevation [m]
HB-23-0001	540.300	VA-20-0010	515.700
VG-23-0001	538.000	VA-13-0001	522.825
KA-23-0001	536.500	VA-20-0001	515.480
		VA-20-0002	515.480
HB-23-0002	531.590	VJ-20-0001	506.215
VG-23-0002	528.770		
KA-23-0002	539.725	HB-20-0001	506.000
		HB-20-0002	506.000
HA-23-0003	533.400	HB-20-0003	523.500
VG-23-0003	528.790	HB-21-0001	506.000
KA-23-0003	539.725	HA-22-0001	529.500
HA-23-0004	533.400	PA-21-0001	500.000
VG-23-0004	528.840	PA-21-0002	500.000
KA-23-0004	539.725	PG-20-0001	500.000
HA-23-0005	533.400	VG-45-0001	529.140
VG-23-0005	528.940	FE-45-0002	533.000
KA-23-0005	539.725		
		PA-50-0001	500.000
HA-23-0006	533.400	PA-41-0001	545.000
VG-23-0006	529.090	HW-41-0001	545.000
KA-23-0006	538.865		
		CT-23-0001	536.500
		CT-80-0001A	532.000
		CT-80-0001B	532.000

Appendix

Appendix

F.   Measured values

Table F.1 Table F.2 Measured values used in the simulation of 2010-10-29 and 2012-10-29

Values used as input in the simulation are marked with orange background, values used comparison with simulation are marked with white background and values used to calculate input values for simulation are marked with yellow background.

Component	Tag	Description	Unit	Measured value, 2010-10-29, at 12:00	Measured value, 2012-10-29, at 12:00
Compressors					
KA-23-0001					
	TIC-23-0101:X.Value	1 tr væskeutskiller inn	°C	30.50	27.32
	TZT-23-0116:Y	1 tr gasskompressor ut	°C	164.74	152.09
	PZT-23-0113:Y	1 tr kompressor inn	barg	0.24	0.26
	PZT-23-0117:Y	1 tr gasskompressor ut	barg	6.14	5.73
	FT-23-0111-S:Y	1 tr kompressor flowrate	Sm^3/h	6262.25	6909.83
KA-23-0002					
	TIC-23-0131:X.Value	2 tr komp væskeutskiller inn	°C	28.28	25.60
	TZT-23-0146:Y	2 tr kompr gass ut	°C	122.97	125.25
	PZT-23-0143:Y	2 tr kompressor inn	barg	4.84	4.61
	PZT-23-0147:Y	2 tr kompressor ut	barg	16.45	16.42
	FT-23-0141-S:Y	2 tr kompressor flowrate	Sm^3/h	100703.06	95895.94
KA-23-0003					
	TIC-23-0161:X.Value	3 tr væskeutskiller inn	°C	26.50	26.797842
	TZT-23-0176:Y	3 tr kompr gass ut	°C	125.08	126.017784
	PZT-23-0173:Y	3 tr kompr gass inn	barg	15.77	15.649688
	PZT-23-0177:Y	3 tr kompr gass ut	barg	44.69	45.577827
	FT-23-0171-S:Y	3 tr kompressor flowrate	Sm^3/h	86638.38	90560.55469
KA-23-0004					
	TIC-23-0191:X.Value	4 tr komp væskeutskiller inn	°C	27.00	24.02
	TZT-23-0206:Y	4 tr kompr gass ut	°C	91.90	87.89
	PZT-23-0203:Y	4 tr kompr gass inn	barg	43.41	44.04
	PZT-23-0207:Y	4 tr kompr gass ut	barg	93.32	92.39
	FT-23-0201-S:Y	4 tr kompressor flowrate	Sm^3/h	244478.25	275685.00

Appendix

Component	Tag	Description	Unit	Measured value, 2010-10-29, at 12:00	Measured value, 2012-10-29, at 12:00
KA-23-0005					
	TIC-23-0221:X.Value	5 tr komp væskeutskiller inn	°C	30.00	28.06
	TZT-23-0236:Y	5 tr komprs gass ut	°C	91.57	86.00
	PZT-23-0233:Y	5 tr kompr gass inn	barg	92.08	90.87
	PZT-23-0237:Y	5 tr kompr gass ut	barg	183.88	169.75
	FT-23-0231-S:Y	5 tr kompressor flowrate	Sm^3/h	262401.78	291854.78
KA-23-0006					
	TIC-23-0251:X.Value	Impgass væskeutskiller inn	°C	*29.00*	*-*
	TT-23-0262:Y	Impgasskompr inn	°C	*9.00*	*-*
	TZT-23-0266:Y	Impgasskompr ut	°C	52.47	*-*
	PZT-23-0263:Y	Impgasskompr inn	barg	*107.74*	*-*
	PZT-23-0267:Y	Impgasskompr ut	barg	183.37	*-*
	FT-23-0261-S:Y	Importgasskompressor flowrate	Sm^3/h	*200000.00*	*-*
Separators					
VA-13-0001					
	PZT-13-0915:Y	Testseparator	barg	11.90	7.03
	TT-13-0916:Y	Test sep gassutløp	°C	*50.80*	*39.65*
VA-20-0010					
	PZT-20-0101:Y	HT avgasser	barg	45.04	45.96
VA-20-0001					
	PZT-20-0123:Y	1 t separator	barg	6.22	5.90
	TT-20-0121:Y	1 tr sep innløp	°C	*65.08*	*65.67*
VA-20-0002					
	PZT-20-0143:Y	2 t separator	barg	1.75	1.61
	TZT-20-0141:Y	2 t separator inn	°C	96.58	*100.52*

Appendix

Component	Tag	Description	Unit	Measured value, 2010-10-29, at 12:00	Measured value, 2012-10-29, at 12:00
Heaters, coolers and heat exchangers					
HB-20-0003					
	TIC-20-0138:X.Value	Olje varmer	°C	98.00	102.10
HB-21-0001					
	TT-20-0108:Y	Innløp til oljeeksp kjøler	°C	80.80	*21.17*
	TIC-21-0113:X.Value	Oljeeksp kjøling	°C	74.00	79.17
Pumps					
PA-21-0001					
	PT-21-0101:Y	Oljeeksp innløp B.pmp A	barg	2.95	*2.88*
	PT-21-0103:Y	Oljeeksp innløp B.pmp B	barg	2.97	*2.96*
	PT-21-0131:Y	Oljeeksp innløp B.pmp C	barg	3.07	*2.82*
	PZT-21-0102:Y	Oljetrykkøkningspumpe A ut	barg	11.48	11.60
	PZT-21-0104:Y	Oljetrykkøkningspumpe B ut	barg	11.49	11.57
	PZT-21-0132:Y	Oljetrykkøkningspumpe C ut	barg	3.08	*2.79*
	FIC-21-0105:X.Value	Oljeeksp B.pmp min strømning	Sm³/h	*1125.58*	*783.40*
PA-21-0002					
	PT-21-0107:Y	Oljeeksp innløp H.pmp A	barg	8.12	*10.18*
	PT-21-0109:Y	Oljeeksp innløp H.pmp B	barg	8.42	9.97
	PT-21-0111:Y	Oljeeksp innløp H.pmp C	barg	8.29	*10.17*
	PT-21-0106:Y	Oljeeksp innløp H.pmp	barg	8.46	*10.20*
	PZT-21-0108:Y	Oljeeksportpumpe A ut	barg	98.12	*10.07*
	PZT-21-0110:Y	Oljeeksportpumpe B ut	barg	8.18	91.05
	PZT-21-0112:Y	Oljeeksportpumpe C ut	barg	98.12	*10.20*
	PIC-21-0127:YR	Oljeeksp trykk	barg	96.86	*89.58*
	FIC-21-0117:X.Value	Oljeeksp utløp H.pmp A	Sm³/h	*524.54*	*0.55*
	FIC-21-0118:X.Value	Oljeeksp utløp H.pmp B	Sm³/h	*0.61*	*720.64*
	FIC-21-0119:X.Value	Oljeeksp utløp H.pmp C	Sm³/h	*508.78*	*1.05*

Appendix

Component	Tag	Description	Unit	Measured value, 2010-10-29, at 12:00	Measured value, 2012-10-29, at 12:00
PG-20-0001					
	PT-20-0271:Y	2 tr prod vann pump.A innløp	barg	3.38	3.22
	PZT-20-0272:Y	Sek prod vannpumpe A ut	barg	12.53	10.37
	PT-20-0273:Y	2 tr vann pmp.B innløp	barg	3.41	_3.28_
	PZT-20-0274:Y	Sek prod vannpumpe B ut	barg	3.46	_3.32_
	PT-20-0275:Y	E/S A prod vann pmp C innløp	barg	3.2	3.16
	PZT-20-0276:Y	Sek prod vannpumpe C ut	barg	12.48	10.06
	PT-20-0277:Y	2 tr prod vann pmp.D innløp	barg	3.21	3.10
	PZT-20-0278:Y	Sek prod vannpumpe D ut	barg	12.51	10.34
	PT-20-0122:Y	1 tr prod vann pmp.E innløp	barg	3.76	_7.55_
	PZT-20-0124:Y	Prim prod vannpumpe E ut	barg	3.81	_10.14_
	PT-20-0132:Y	1 tr prod vann pmp.F innløp	barg	4.01	_7.61_
	PZT-20-0134:Y	Prim prod vannpumpe F ut	barg	3.98	_7.56_
Fuel gas system					
VG-45-0001					
	TZT-45-0132A:Y	Supervarmer inn	°C	23.13	19.14
	TZT-45-0132B:Y	Supervarmer ut	°C	60.92	51.55
	PT-45-0103:Y	Brenngass væskeutsk.innløp	barg	38.00	37.50
	FYI-45-0201:Y	Brenngassmålest	Sm^3/h	9649.30	9218.74
	FYI-43-0201:Y	Fakkelgassmålest	Sm^3/h	_0.00_	_0.00_
Gas import					
	FYI-22-0250:Y	Gassimportmålest	Sm^3/h	159103.58	_0.00_
	PZT-22-0102:Y	Målest gass linje A nedstr	barg	109.18	-
	PZT-22-0104:Y	Målest gass linje B nedstr	barg	108.74	-
	TT-22-0106:Y	Målest gass linje nedstr	°C	4.39	-

Component	Tag	Description	Unit	Measured value, 2010-10-29, at 12:00	Measured value, 2012-10-29, at 12:00
Gas injection					
	PZT-23-0317:Y	Gassinjeksjons manifold	barg	*183.98*	*169.93*
	FYI_13 9480:Value	Gassløftrate total	Sm^3/h	21666.62	23883.80
	FYI_13 9481:Value	Gassrate injeksjon	Sm^3/h	362682.75	243955.59
	FYI_13 9465:Value	Total gassløftrate HP prod manifold	Sm^3/h	0.00	1614.16
	FYI_13 9475:Value	Total gassløftrate LP prod manifold	Sm^3/h	21665.76	22269.64
Oil export					
	FI_22-0201:Value	Eksport råolje rate	m^3/h	1147.24	779.75
Water injection					
	FYI_13 9482:Value	Vanninjeksjonsrate Utsira	NA	7.90	291.79
	FYI_13 9483:Value	Vanninjeksjonsrate Heimdal	NA	*0*	*0*
	PZT-29-0101:Y	Vanninj trykkøknpumpe A inn	barg	1.85	2.51
	PZT-29-0111:Y	Vanninj hovedpumpe A inn	barg	1.49	19.14
	PZT-29-0115:Y	Vanninj hovedpumpe A ut	barg	1.28	57.66
	PZT-29-0121:Y	Vanninj trykkøknpumpe B inn	barg	1.97	2.59
	PZT-29-0131:Y	Vanninj hovedpumpe B inn	barg	1.56	19.11
	PZT-29-0135:Y	Vanninj hovedpumpe B ut	barg	1.36	57.74
Manifolds					
	PT-13-0903:Y	Test manifold	barg	12.76	7.78
	PT-20-0930:Y	HT produksjons fordelingsrør	barg	45.86	46.55
	PT-20-0940:Y	LT manifold	barg	6.85	6.52
	TT-13-0904:Y	Test manifold	°C	*56.76*	*40.91*
	TT-20-0932:Y	HT produksjons fordelingsrør	°C	*62.49*	*59.59*
	TT-20-0942:Y	LT manifold	°C	*68.43*	*68.90*

Appendix

Component	Tag	Description	Unit	Measured value, 2010-10-29, at 12:00	Measured value, 2012-10-29, at 12:00
Wells:					
	PZT-13-0029:Y	#01 Brønnhode olje	barg	59.39	18.97
	PZT-13-0304:Y	#02 Brønnhode olje	barg	84.76	70.08
	PZT-13-0054:Y	#03 Brønnhode olje	barg	13.61	67.49
	PZT-13-0079:Y	#04 Brønnhode olje	barg	*0.00*	*0.00*
	PZT-13-0104:Y	#05 Brønnhode olje	barg	5.32	47.77
	PZT-13-0129:Y	#06 Brønnhode olje	barg	94.90	11.33
	PZT-13-0154:Y	#07 Brønnhode olje	barg	*0.00*	10.05
	PZT-13-0179:Y	#08 Brønnhode olje	barg	92.88	92.77
	PZT-13-0204:Y	#09 Brønnhode olje	barg	91.08	67.10
	PZT-13-0679:Y	#10 Brønnhode olje	barg	94.63	35.21
	PZT-13-0229:Y	#11 Brønnhode olje	barg	36.89	*0*
	PZT-13-0254:Y	#12 Brønnhode olje	barg	89.24	90.47
	PZT-13-0454:Y	#13 Brønnhode olje	barg	12.04	74.46
	PZT-13-0704:Y	#15 Brønnhode olje	barg	64.40	79.65
	PZT-13-0329:Y	#16 Brønnhode olje	barg	76.04	92.57
	PZT-13-0354:Y	#17 Brønnhode plje	barg	109.51	*0.00*
	PZT-13-0379:Y	#18 Brønnhode olje	barg	104.41	69.60
	PZT-13-0279:Y	#19 Brønnhode olje	barg	82.68	45.65
	PZT-13-0404:Y	#21 Brønnhode olje	barg	95.41	39.15
	PZT-13-0429:Y	#22 Brønnhode olje	barg	69.17	84.20
	PZT-13-0479:Y	#25 Brønnhode olje	barg	86.44	87.80
	PZT-13-0504:Y	#26 Brønnhode olje	barg	93.07	96.24
	PZT-13-0529:Y	#27 Brønnhode olje	barg	79.81	75.59
	PZT-13-0554:Y	#28 Brønnhode olje	barg	93.45	65.89
	PZT-13-0579:Y	#29 Brønnhode olje	barg	*0.00*	*0.00*
	PZT-13-0779:Y	#30 Brønnhode olje	barg	93.01	98.80
	PZT-13-0754:Y	#34 Brønnhode olje	barg	47.39	48.84
	PZT-13-0604:Y	#35 Brønnhode olje	barg	95.57	96.43
	PZT-13-0804:Y	#38 Brønnhode olje	barg	*0.00*	12.93
	PZT-13-0629:Y	#39 Brønnhode olje	barg	21.50	17.07
	PZT-13-0654:Y	#40 Brønnhode olje	barg	87.52	93.34

Component	Tag	Description	Unit	Measured value, 2010-10-29, at 12:00	Measured value, 2012-10-29, at 12:00
	PZT-13-0037:Y	#01 Strupevntil olje nedstrøms	barg	13.76	6.64
	PZT-13-0312:Y	#02 Strupevntil olje nedstrøms	barg	46.08	46.84
	PZT-13-0062:Y	#03 Strupevntil olje nedstrøms	barg	8.20	47.15
	PZT-13-0087:Y	#04 Strupevntil olje nedstrøms	barg	*0.00*	*0.00*
	PZT-13-0112:Y	#05 Strupevntil olje nedstrøms	barg	47.458	8.26
	PZT-13-0137:Y	#06 Strupevntil olje nedstrøms	barg	45.95	*0.00*
	PZT-13-0162:Y	#07 Strupevntil olje nedstrøms	barg	0.00	7.45
	PZT-13-0187:Y	#08 Strupevntil olje nedstrøms	barg	45.98	46.69
	PZT-13-0212:Y	#09 Strupevntil olje nedstrøms	barG	45.97	46.66
	PZT-13-0687:Y	#10 Strupevntil olje nedstrøms	barG	46.08	7.05
	PZT-13-0237:Y	#11 Strupevntil olje nedstrøms	barg	36.41	6.11
	PZT-13-0262:Y	#12 Strupevntil olje nedstrøms	barg	7.08	46.64
	PZT-13-0462:Y	#13 Strupeventil olje nedstrøms	barg	8.36	74.57
	PZT-13-0712:Y	#15 Strupevntil olje nedstrøms	barg	46.77	47.32
	PZT-13-0337:Y	#16 Strupeventil olje nedstrøms	barg	46.41	46.88
	PZT-13-0362:Y	#17 Strupeventil olje nedstrøms	barg	46.23	37.85
	PZT-13-0387:Y	#18 Strupeventil olje nedstrøms	barg	46.00	46.73
	PZT-13-0287:Y	#19 Strupevntil olje nedstrøms	barg	45.89	45.37
	PZT-13-0412:Y	#21 Strupeventil olje nedstrøms	barg	45.92	7.80
	PZT-13-0437:Y	#22 Strupevntil olje nedstrøms	barg	6.85	46.52
	PZT-13-0487:Y	#25 Strupevntil olje nedstrøms	barg	45.88	6.76
	PZT-13-0512:Y	#26 Strupeventil olje nedstrøms	barg	45.90	46.61
	PZT-13-0537:Y	#27 Strupeventil olje nedstrøms	barg	45.82	46.50
	PZT-13-0562:Y	#28 Strupeventil olje nedstrøms	barg	46.02	46.62
	PZT-13-0587:Y	#29 Strupeventil olje nedstrøms	barg	17.81	0.01
	PZT-13-0787:Y	#30 Strupevntil olje nedstrøms	barg	46.19	46.84

Component	Tag	Description	Unit	Measured value, 2010-10-29, at 12:00	Measured value, 2012-10-29, at 12:00
	PZT-13-0762:Y	#34 Strupevntil olje nedstrøms	barg	7.05	6.82
	PZT-13-0612:Y	#35 Strupeventil olje nedstrøms	barg	46.05	7.43
	PZT-13-0812:Y	#38 Strupevntil olje nedstrøms	barg	*0.00*	8.07
	PZT-13-0637:Y	#39 Strupevntil olje nedstrøms	barg	7.22	7.03
	PZT-13-0662:Y	#40 Strupevntil olje nedstrøms	barg	45.98	46.70
	TT-13-0034:Y	#01 Strupeventil oppstrøms	°C	68.37	67.63
	TT-13-0309:Y	#02 Strupeventil oppstrøms	°C	64.51	63.74
	TT-13-0059:Y	#03 Strupeventil oppstrøms	°C	71.11	65.03
	TT-13-0084:Y	#04 Strupeventil oppstrøms	°C	*-20.00*	*-20.00*
	TT-13-0109:Y	#05 Strupeventil oppstrøms	°C	10.94	70.80
	TT-13-0134:Y	#06 Strupeventil oppstrøms	°C	66.07	*-20.00*
	TT-13-0159:Y	#07 Strupeventil oppstrøms	°C	*-20.00*	71.95
	TT-13-0184:Y	#08 Strupeventil oppstrøms	°C	58.03	59.90
	TT-13-0209:Y	#09 Strupeventil oppstrømns	°C	60.59	56.30
	TT-13-0684:Y	#10 Strupeventil oppstrøms	°C	62.39	70.38
	TT-13-0234:Y	#11 Strupeventil oppstrøms	°C	11.09	7.21
	TT-13-0259:Y	#12 Strupeventil oppstrøms	°C	61.73	60.73
	TT-13-0459:Y	#13 Strupeventil oppstrøms	°C	70.88	7.96
	TT-13-0709:Y	#15 Strupeventil oppstrøms	°C	71.80	69.37
	TT-13-0334:Y	#16 Strupeventil oppstrøms	°C	66.75	62.75
	TT-13-0359:Y	#17 Strupeventil oppstrøms	°C	51.73	*-20.00*
	TT-13-0384:Y	#18 Strupeventil oppstrøms	°C	57.86	62.02
	TT-13-0284:Y	#19 Strupeventil oppstrøms	°C	61.90	7.86
	TT-13-0409:Y	#21 Strupeventil oppstrøms	°C	50.45	72.04
	TT-13-0434:Y	#22 Strupeventil oppstrøms	°C	55.99	53.13
	TT-13-0484:Y	#25 Strupeventil oppstrøms	°C	58.52	58.91

Appendix

Component	Tag	Description	Unit	Measured value, 2010-10-29, at 12:00	Measured value, 2012-10-29, at 12:00
	TT-13-0509:Y	#26 Strupeventil oppstrøms	°C	60.91	61.24
	TT-13-0534:Y	#27 Strupeventil oppstrøms	°C	57.03	55.02
	TT-13-0559:Y	#28 Strupeventil oppstrøms	°C	60.94	53.82
	TT-13-0584:Y	#29 Strupeventil oppstrøms	°C	-20.00	-20.00
	TT-13-0784:Y	#30 Strupeventil oppstrøms	°C	64.19	62.10
	TT-13-0759:Y	#34 Strupeventil oppstrøms	°C	57.15	50.81
	TT-13-0609:Y	#35 Strupeventil oppstrøms	°C	67.76	60.48
	TT-13-0634:Y	#39 Strupeventil oppstrøms	°C	71.82	68.95
	TT-13-0659:Y	#40 Strupeventil oppstrøms	°C	64.42	64.27
	TT-13-0036:Y	#01 Strupeventil nedstrøms	°C	64.90	67.05
	TT-13-0311:Y	#02 Strupeventil nedstrøms	°C	61.52	61.19
	TT-13-0061:Y	#03 Strupeventil nedstrøms	°C	70.54	63.11
	TT-13-0086:Y	#04 Strupeventil nedstrøms	°C	-20.00	25.23
	TT-13-0111:Y	#05 Strupeventil nedstrøms	°C	11.97	66.44
	TT-13-0136:Y	#06 Strupeventil nedstrøms	°C	62.67	9.06
	TT-13-0161:Y	#07 Strupeventil nedstrøms	°C	-20.00	71.56
	TT-13-0186:Y	#08 Strupeventil nedstrøms	°C	53.93	53.38
	TT-13-0211:Y	#09 Strupeventil nedstrøms	°C	58.62	57.15
	TT-13-0686:Y	#10 Strupeventil nedstrøms	°C	58.54	67.62
	TT-13-0236:Y	#11 Strupeventil nedstrøms	°C	11.90	7.47
	TT-13-0261:Y	#12 Strupeventil nedstrøms	°C	53.04	54.82
	TT-13-0461:Y	#13 Strupeventil nedstrøms	°C	70.56	8.78
	TT-13-0711:Y	#15 Strupeventil nedstrøms	°C	70.70	66.04
	TT-13-0336:Y	#16 Strupeventil nedstrøms	°C	64.70	56.13
	TT-13-0361:Y	#17 Strupeventil nedstrøms	°C	43.43	8.34
	TT-13-0386:Y	#18 Strupeventil nedstrøms	°C	51.61	61.05

Appendix

Component	Tag	Description	Unit	Measured value, 2010-10-29, at 12:00	Measured value, 2012-10-29, at 12:00
	TT-13-0286:Y	#19 Strupeventil nedstrøms	°C	*59.87*	*8.55*
	TT-13-0411:Y	#21 Strupeventil nedstrøms	°C	*47.02*	*69.11*
	TT-13-0436:Y	#22 Strupeventil nedstrøms	°C	*52.03*	*49.98*
	TT-13-0486:Y	#25 Strupeventil nedstrøms	°C	*56.72*	*47.79*
	TT-13-0511:Y	#26 Strupeventil nedstrøms	°C	*57.76*	*54.93*
	TT-13-0536:Y	#27 Strupeventil nedstrøms	°C	*55.45*	*52.87*
	TT-13-0561:Y	#28 Strupeventil nedstrøms	°C	*57.09*	*52.76*
	TT-13-0586:Y	#29 Strupeventil nedstrøms	°C	*-20.00*	*25.12*
	TT-13-0786:Y	#30 Strupeventil nedstrøms	°C	*61.48*	*54.35*
	TT-13-0761:Y	#34 Strupeventil nedstrøms	°C	*54.94*	*47.09*
	TT-13-0611:Y	#35 Strupeventil nedstrøms	°C	*63.73*	*41.94*
	TT-13-0811:Y	#38 Strupeventil nedstrøms	°C	*0.00*	*71.84*
	TT-13-0636:Y	#39 Strupeventil nedstrøms	°C	*70.78*	*67.80*
	TT-13-0661:Y	#40 Strupeventil nedstrøms	°C	*62.15*	*58.94*
	FYI-13-9010:Y	#01 kalkulert Oljerate	Sm^3/h	91.81	6.04
	FYI-13-9020:Y	#02 kalkulert Oljerate	Sm^3/h	43.69	17.07
	FYI-13-9030:Y	#03 kalkulert Oljerate	Sm^3/h	183.26	81.56
	FYI-13-9040:Y	#04 kalkulert Oljerate	Sm^3/h	*0.00*	*0.00*
	FYI-13-9050:Y	#05 kalkulert Oljerate	Sm^3/h	*0.00*	103.43
	FYI-13-9060:Y	#06 kalkulert Oljerate	Sm^3/h	17.49	*0.00*
	FYI-13-9070:Y	#07 kalkulert Oljerate	Sm^3/h	*0.00*	25.58
	FYI-13-9080:Y	#08 kalkulert Oljerate	Sm^3/h	17.56	19.48
	FYI-13-9090:Y	#09 kalkulert Oljerate	Sm^3/h	11.49	10.80
	FYI-13-9100:Y	#10 kalkulert Oljerate	Sm^3/h	20.03	47.92
	FYI-13-9110:Y	#11 kalkulert Oljerate	Sm^3/h	*0.00*	*0.00*
	FYI-13-9120:Y	#12 kalkulert Oljerate	Sm^3/h	24.28	11.55
	FYI-13-9130:Y	#13 kalkulert Oljerate	Sm^3/h	105.37	0.00
	FYI-13-9150:Y	#15 kalkulert Oljerate	Sm^3/h	133.09	71.30
	FYI-13-9160:Y	#16 kalkulert Oljerate	Sm^3/h	106.90	39.46
	FYI-13-9170:Y	#17 kalkulert Oljerate	Sm^3/h	7.41	*0.00*
	FYI-13-9180:Y	#18 kalkulert Oljerate	Sm^3/h	13.49	11.02
	FYI-13-9190:Y	#19 kalkulert Oljerate	Sm^3/h	33.02	0.00
	FYI-13-9210:Y	#21 kalkulert Oljerate	Sm^3/h	7.81	52.23

Component	Tag	Description	Unit	Measured value, 2010-10-29, at 12:00	Measured value, 2012-10-29, at 12:00
	FYI-13-9220:Y	#22 kalkulert Oljerate	Sm3/h	14.28	9.47
	FYI-13-9230:Y	#23 kalkulert Oljerate	Sm3/h	0.00	0.00
	FYI-13-9250:Y	#25 kalkulert Oljerate	Sm3/h	22.91	5.18
	FYI-13-9260:Y	#26 kalkulert Oljerate	Sm3/h	20.60	21.60
	FYI-13-9270:Y	#27 kalkulert Oljerate	Sm3/h	14.40	7.29
	FYI-13-9280:Y	#28 kalkulert Oljerate	Sm3/h	41.93	8.29
	FYI-13-9290:Y	#29 kalkulert Oljerate	Sm3/h	0.00	0.00
	FYI-13-9300:Y	#30 kalkulert Oljerate	Sm3/h	19.17	15.09
	FYI_13_9300:Y	#30 kalkulert Oljerate	Sm3/h	19.17	15.09
	FYI-13-9340:Y	#34 kalkulert Oljerate	Sm3/h	14.15	6.84
	FYI-13-9350:Y	#35 kalkulert Oljerate	Sm3/h	48.19	0.39
	FYI_13_9380:Y	#38 kalkulert Oljerate	Sm3/h	0.00	0.00
	FYI-13-9380:Y	#38 kalkulert Oljerate	Sm3/h	0.00	68.11
	FYI-13-9390:Y	#39 kalkulert Oljerate	Sm3/h	43.17	42.42
	FYI-13-9400:Y	#40 kalkulert Oljerate	Sm3/h	27.01	16.18
	FYI-13-9011:Y	#01 kalkulert Gassrate	Sm^3/h	22083.03	84.51
	FYI-13-9021:Y	#02 kalkulert Gassrate	Sm^3/h	18059.70	9628.15
	FYI-13-9031:Y	#03 kalkulert Gassrate	Sm^3/h	2877.24	31842.20
	FYI-13-9041:Y	#04 kalkulert Gassrate	Sm^3/h	0.00	0.00
	FYI-13-9051:Y	#05 kalkulert Gassrate	Sm^3/h	0.00	17710.10
	FYI-13-9061:Y	#06 kalkulert Gassrate	Sm^3/h	6840.43	0.00
	FYI-13-9071:Y	#07 kalkulert Gassrate	Sm^3/h	0.00	401.55
	FYI-13-9081:Y	#08 klakulert Gassrate	Sm^3/h	7287.65	11571.48
	FYI-13-9091:Y	#09 kalkulert Gassrate	Sm^3/h	3972.76	3506.96
	FYI-13-9101:Y	#10 kalkulert Gassrate	Sm^3/h	7346.34	3200.13
	FYI-13-9111:Y	#11 kalkulert Gassrate	Sm^3/h	0.00	0.00
	FYI-13-9121:Y	#12 kalkulert Gassrate	Sm^3/h	9144.03	12115.10
	FYI-13-9131:Y	#13 kalkulert Gassrate	Sm^3/h	1654.38	0.00
	FYI-13-9151:Y	#15 kalkulert Gassrate	Sm^3/h	30522.05	32096.67
	FYI-13-9161:Y	#16 kalkulert Gassrate	Sm^3/h	30508.40	24790.40
	FYI-13-9171:Y	#17 kalkulert Gassrate	Sm^3/h	3880.53	0.00
	FYI-13-9181:Y	#18 kalkulert Gassrate	Sm^3/h	6845.84	2897.55
	FYI-13-9191:Y	#19 kalkulert Gassrate	Sm^3/h	7221.44	0.00
	FYI-13-9211:Y	#21 kalkulert Gassrate	Sm^3/h	2716.48	16113.67
	FYI-13-9221:Y	#22 kalkulert Gassrate	Sm^3/h	390.82	3678.15
	FYI-13-9231:Y	#23 kalkulert Gassrate	Sm^3/h	0.00	0.00
	FYI-13-9251:Y	#25 kalkulert Gassrate	Sm^3/h	4434.49	3896.95
	FYI-13-9261:Y	#26 kalkulert Gassrate	Sm^3/h	6591.50	12303.65
	FYI-13-9271:Y	#27 kalkulert Gassrate	Sm^3/h	3714.10	2983.41
	FYI-13-9281:Y	#28 kalkulert Gassrate	Sm^3/h	15509.77	6356.37
	FYI-13-9291:Y	#29 kalkulert Gassrate	Sm^3/h	0.00	0.00
	FYI-13-9301:Y	#30 kalkulert Gassrate	Sm^3/h	6151.27	9697.36

Component	Tag	Description	Unit	Measured value, 2010-10-29, at 12:00	Measured value, 2012-10-29, at 12:00
	FYI_13_9301:Y	#30 kalkulert Gassrate	Sm^3/h	6151.27	9697.36
	FYI-13-9341:Y	#34 kalkulert Gassrate	Sm^3/h	209.42	100.60
	FYI-13-9351:Y	#35 kalkulert Gassrate	Sm^3/h	18615.67	11523.10
	FYI_13_9381:Y	#38 kalkulert Gassrate	Sm^3/h	*0.00*	*0.00*
	FYI-13-9381:Y	#38 kalkulert Gassrate	Sm^3/h	*0.00*	1068.71
	FYI-13-9391:Y	#39 kalkulert Gassrate	Sm^3/h	677.75	665.92
	FYI-13-9401	#40 kalkulert Gassrate	Sm^3/h	6399.58	8862.79
	FYI-13-9012:Y	#01 kalkulert Vannrate	Sm^3/h	27.42	35.60
	FYI-13-9022:Y	#02 kalkulert Vannrate	Sm^3/h	9.59	10.98
	FYI-13-9032:Y	#03 kalkulert Vannrate	Sm^3/h	29.83	10.99
	FYI-13-9042:Y	#04 kalkulert Vannrate	Sm^3/h	*0.00*	*0.00*
	FYI-13-9052:Y	#05 kalkulert Vannrate	Sm^3/h	*0.00*	24.13
	FYI-13-9062:Y	#06 kalkulert Vannrate	Sm^3/h	4.10	*0.00*
	FYI-13-9072:Y	#07 kalkulert Vannrate	Sm^3/h	*0.00*	115.65
	FYI-13-9082:Y	#08 kalkulert Vannrate	Sm^3/h	0.54	0.40
	FYI-13-9092:Y	#09 kalkulert Vannrate	Sm^3/h	0.01	0.01
	FYI-13-9102:Y	#10 kalkulert Vannrate	Sm^3/h	0.83	13.52
	FYI-13-9112:Y	#11 kalkulert Vannrate	Sm^3/h	*0.00*	*0.00*
	FYI-13-9122:Y	#12 kalkulert Vannrate	Sm^3/h	2.41	2.28
	FYI-13-9132:Y	#13 kalkulert Vannrate	Sm^3/h	89.76	*0.00*
	FYI-13-9152:Y	#15 kalkulert Vannrate	Sm^3/h	18.15	7.92
	FYI-13-9162:Y	#16 kalkulert Vannrate	Sm^3/h	5.63	0.40
	FYI-13-9172:Y	#17 kalkulert Vannrate	Sm^3/h	0.01	*0.00*
	FYI-13-9182:Y	#18 kalkulert Vannrate	Sm^3/h	0.01	4.95
	FYI-13-9192:Y	#19 kalkulert Vannrate	Sm^3/h	0.33	0.00
	FYI-13-9212:Y	#21 kalkulert Vannrate	Sm^3/h	*0.00*	69.23
	FYI-13-9222:Y	#22 kalkulert Vannrate	Sm^3/h	0.60	0.71
	FYI-13-9232:Y	#23 kalkulert Vannrate	Sm^3/h	*0.00*	*0.00*
	FYI-13-9252:Y	#25 kalkulert Vannrate	Sm^3/h	3.42	0.71
	FYI-13-9262:Y	#26 kalkulert Vannrate	Sm^3/h	0.42	0.22
	FYI-13-9272:Y	#27 kalkulett Vannrate	Sm^3/h	0.45	0.15
	FYI-13-9282:Y	#28 kalkulert Vannrate	Sm^3/h	2.21	0.92
	FYI-13-9292:Y	#29 kalkulert Vannrate	Sm^3/h	*0.00*	*0.00*
	FYI-13-9302:Y	#30 kalkulert Vannrate	Sm^3/h	4.21	0.79
	FYI_13_9302:Y	#30 kalkulert Vannrate	Sm^3/h	4.21	0.79
	FYI-13-9342:Y	#34 kalkulert Vannrate	Sm^3/h	0.44	0.68
	FYI-139352:Y	#35 kalkulert Vannrate	Sm^3/h	3.08	0.01
	FYI_13_9382	#38 kalkulert Vannrate	Sm^3/h	*0.00*	*0.00*
	FYI-13-9382:Y	#38 kalkulert Vannrate	Sm^3/h	*0.00*	102.11
	FYI-13-9392:Y	#39 kalkulert Vannrate	Sm^3/h	54.94	27.12
	FYI-13-9402:Y	#40 kalkulert Vannrate	Sm^3/h	1.42	0.85

Appendix

Component	Tag	Description	Unit	Measured value, 2010-10-29, at 12:00	Measured value, 2012-10-29, at 12:00
Turbines Fuel gas metering					
	PI-45-0202:Y	Brenngassmålest	Bar	*38.88*	*38.45*
	TI-45-0203:Y	Brenngassmålest	°C	*60.00*	*51.71*
CT-23-0001					
	FT-23-0699:Y	BRENNGASS TILFØRSEL	Sm^3/h	*4276.94*	*4362.21*
	FT-23-0699_STDMD:Y	Core kalkulert gassflow ST	Sm^3/h	-	**6174.45**
	PIT-23-0705:Y	BRENNGASS TILFØRSEL	barg	*37.09*	*34.05*
	TIC-41-0146B:X.Value	Varmvæske eksoskjel C utløp	°C	129.98	119.86
CT-80-0001A					
	FT-80-1112_STDM:Y	Core kalkulert gassflow ST	Sm^3/h	-	**3256.36**
	PI-80-1110A:Y	Brenngass før avstengningsventil	bar	*2.10*	*38.24*
	TIC-41-0126B:X.Value	Varmvæske eksoskjel A utløp	°C	*94.03*	132.51
	TT-80-1111:Y	Brenngass før avstengningsventil	°C	*13.27*	*50.55*
	TT-80-1400:Y	Gassturbinhus omgivelsesluft	°C	*10.44*	6.64
	PI-80-1033A:Y	Komp Inn Trykk PS3_A	bar	-	*13.51*
	EG-80-0001AZPA:Value	Effektmaaling	NA	*179.76*	10102.45
CT-80-0001B					
	PI-80-2110A:Y	Brenngass før avstengningsventil	bar	*38.59*	*1.83*
	TIC-41-0136B:X.Value	Varmvæske eksoskjel B utløp	°C	119.00	*95.92*
	TT-80-2111:Y	Brenngass før avstengningsventil	°C	*59.41*	*9.27*
	TT-80-2400:Y	Gasstrubinhus omgivelsesluft	°C	11.28	*6.41*
	FT-80-2112_STDM:Y	Core kalkulert gassflow ST	Sm^3/h	-	*0.00*
	EG-80-0001BZPA:Value	Effektmaaling	NA	13506.93	*0.00*

Appendix

Component	Tag	Description	Unit	Measured value, 2010-10-29, at 12:00	Measured value, 2012-10-29, at 12:00
Hot water distribution					
	FT-41-0128:Y	Varmvæske eksoskjel A utløp	m^3/h	*53.96*	235.53
	FT-41-0138:Y	Varmvæske eksoskjel B utløp	m^3/h	248.19	*72.62*
	FT-41-0148:Y	Varmvæske eksoskjel C utløp	m^3/h	262.76	248.56
	TT-41-0127:Y	Varmvæske eksoskjel A utløp	°C	94.02	132.47
	TT-41-0137:Y	Varmvæske eksoskjel B utløp	°C	118.93	95.79
	TT-41-0147:Y	Varmvæske eksoskjel C utløp	°C	130.11	120.04
	TT-41-0103:Y	Varmvæske distrubusjon	C	*91.71*	*88.64*
	TT-41-0122:Y	Varmvæske sirk pumper utløp	C	96.98	99.23
	TT-41-0156:Y	Varmvæske returlinje	C	*95.65*	*98.71*
	TT-50-0102:Y	Sjøvann/varmevæske dumpkjøler	C	10.83	9.83
	FT-41-0121:Y	Varmvæske sirk pumper utløp	m3/h	508.15	504.13
	PT-41-0106:Y	Varmev primærpumpe C innløp	barG	15.31	16.01
	PT-41-0111:Y	Varmev primærpumpe B innløp	barG	15.33	15.90
	PT-41-0116:Y	Varmev primærpumpe A innløp	barG	15.25	16.00
	TIC-41-0101X.Value	Varmevæske prim/sek kontroll	C	86.39	84.55
	TIC-41-0104X:Value	Varmevæske HVAC kontroll	C	84.28	78.05
Seawater distribution:					
	FT-50-0111:Y	Sjøvann distribusjon	m3/h	2201.32	2399.76
	PT-50-0108:Y	Sjøvann løftepumpe A utløp	barg	11.45	11.80
	PT-50-0113:Y	Sjøvann løftepumpe B utløp	barg	11.76	7.71
	FT-50-0131:Y	Sjøvann ess.pumpe	m3/h	*0.79*	*0.60*

G. Other input values

Table G.1 Other input values used in the simulation

Description	Unit	Value, 2010	Value, 2012	Source
Air-1 temperature	°C	11.28	6.64	Measured at Main generator B (2010) and Main generator A (2012)
Combustion Gas-1 temperature	°C	1350.00	1350.00	Assumed
Combustion Gas-2 temperature	°C	-	1350.00	Assumed
Combustion Gas-3 temperature	°C	1350.00	-	Assumed
GG Compressor-1 adiabatic efficiency	%	75.00	75.00	Default value
GG Compressor-1 pressure ratio	-	23.00	23.00	Datasheet
GG Compressor-2 pressure ratio	-	-	23.00	Datasheet
GG Compressor-3 adiabatic efficiency	%	75.00	75.00	Default value
GG Compressor-3 pressure ratio	-	23.00	-	Datasheet
GG Turbine-1 adiabatic efficiency	%	90.00	90.00	Assumed
GG Turbine-3 adiabatic efficiency	%	90.00	90.00	Assumed
HA-22-0001 pressure loss cold side	bar	1.00	-	Datasheet
HA-22-0001 pressure loss hot side	bar	1.00	-	Datasheet
HA-23-0003 pressure loss cold side	bar	1.00	1.00	Datasheet
HA-23-0004 pressure loss cold side	bar	1.00	1.00	Datasheet
HA-23-0005 pressure loss cold side	bar	1.00	1.00	Datasheet
HA-23-0006 pressure loss cold side	bar	1.00	-	Datasheet
HA-23-0006 pressure loss hot side	bar	1.00	-	Datasheet
HB-20-0001 pressure loss cold side	bar	1.50	1.50	Datasheet
HB-20-0001 pressure loss hot side	bar	1.50	1.50	Datasheet
HB-20-0002 pressure loss cold side	bar	1.50	1.50	Datasheet
HB-20-0002 pressure loss hot side	bar	1.50	1.50	Datasheet
HB-20-0002 UA	kJ/°C h	1846000	1846000	Datasheet
HB-20-0003A/B/C pressure loss cold side	bar	1.50	1.50	Datasheet
HB-20-0003A/B/C pressure loss hot side	bar	1.00	1.00	Datasheet
HB-21-0001 pressure loss cold side	bar	1.00	1.00	Datasheet
HB-23-0001 pressure loss cold side	bar	1.00	1.00	Datasheet
HB-23-0002 pressure loss cold side	bar	1.00	1.00	Datasheet
HW-41-0001A flow water	m^3/h	-	245.28	Scaled based on flow through pump and the three heat exchangers
HW-41-0001B flow water	m^3/h	246.83	-	Scaled based on flow through pump and the three heat exchangers
HW-41-0001C flow water	m^3/h	261.32	258.85	Scaled based on flow through pump and the three heat exchangers
IMP_DIV split ratio	-	1/0	-	[44]
Description	Unit	Value, 2010	Value, 2012	Source

Appendix

PA-21-0001 adiabatic efficiency	%	76.00	76.00	Performance curves
PA-21-0001 pressure intlet	barg	2.96	2.80	Root of pressure of pump a times b (2010) and root of pressure of pump b times c (2012)
PA-21-0001 pressure outlet	barg	11.48	11.59	Root of pressure of pump a times b (2010) and root of pressure of pump b times c (2012)
PA-21-0002 adiabatic efficiency	%	74.00	74.00	Performance curves
PA-21-0002 pressure inlet	barg	8.20	-	Root of pressure of pump a times c
PA-21-0002 pressure outlet	barg	98.12	-	Root of pressure of pump a times c
PA-4058-1 adiabatic efficiency	%	75.00	75.00	Default value
PA-4058-1 pressure inlet	barg	1.91	2.55	Root of pressure of pump a times b
PA-4058-2 adiabatic efficiency	%	75.00	75.00	Default value
PA-4058-2 pressure inlet	barg	1.52	19.13	Root of pressure of pump a times b
PA-4058-2 pressure outlet	barg	1.32	57.70	Root of pressure of pump a times b
PA-41-0001 pressure inlet	barg	15.30	15.97	3rd root of pressure of pump a times b times c
PA-41-0001 pressure outlet	barg	24.90	24.90	Engineering manual
PA-41-0001A/B/C adiabatic efficiency	%	81.00	80.00	Performance curves
PA-50-0001A/B adiabatic efficiency	%	77.00	80.00	Performance curves
PA-50-0001A/B pressure inlet	bar	4.91	4.91	Calculated based on engineering manual
PA-50-0001A/B pressure outlet	barg	11.60	9.54	Root of pressure of pump a times b
PA-50-0001A/B tempearture outlet	°C	10.00	10.00	Engineering manual
PG-20-0001 pressure outlet	barg	12.51	10.26	3rd root of pressure of pump a times c times d
PG-20-0001A/B/C/D adiabatic efficiency	%	75.00	75.00	Default value
PG-20-0001E/F adiabatic efficiency	%	75.00	75.00	Default value
PIPE-SEAWATER pressure outlet	barg	10.40	10.40	Engineering manual
TEE-HM-3 split ratio	-	0.5/0.5	0.5/0.5	Assumed
TEE-HM-4 split ratio	-	0.5/0.5	-	Assumed

H. Input values of case with combined cycle

Table H.1 Input values used in the simulation of the case with combined cycle supplied by mechanical drive turbine

Description	Unit	Value, 2010	Value, 2012	Source
Pressure loss, both sides, HRSG	bar	0.022	0.022	Assumed
Outlet exhaust temperature, HRSG	°C	170	170	Assumed
Outlet steam temperature, HRSG	°C	470	470	Assumed
Inlet pressure steam turbine, ST	bar	24	24	Assumed
Outlet pressure steam turbine, ST	bar	0.08	0.08	Assumed
Adiabatic efficiency steam turbine, ST	-	0.95	0.95	Assumed
Pressure loss condenser, Cooler ST	bar	0	0	Assumed
Outlet temperature, Cooler ST	°C	40	40	Assumed
Adiabatic efficiency pump, P-ST	-	0.9	0.9	Assumed
Pressure loss, Heater-ST	bar	1	1	Assumed
Inlet temperature, Heater-ST	°C	10	10	Engineering manual
Outlet temperature, Heater-ST	°C	45	45	Engineering manual

Table H.2 Input values used in the simulations of the case with combined cycle also supplied by generator drive turbine

Description	Unit	Value, 2010	Value, 2012	Source
Inlet flow generator drive turbine	Sm^3/h	1450	832	Assumed
Power output generator drive turbine	kW	6000	3500	Assumed
Pressure loss, both sides, HRSG	bar	0.022	0.022	Assumed
Outlet exhaust temperature, HRSG	°C	310	310	Assumed
Outlet steam temperature, HRSG	°C	470	470	Assumed
Inlet pressure steam turbine, ST	bar	24	24	Assumed
Outlet pressure steam turbine, ST	bar	0.08	0.08	Assumed
Adiabatic efficiency steam turbine, ST	-	0.95	0.95	Assumed
Pressure loss condenser, Cooler ST	bar	0	0	Assumed
Outlet temperature, Cooler ST	°C	40	40	Assumed
Adiabatic efficiency pump, P-ST	-	0.9	0.9	Assumed
Pressure loss, Heater-ST	bar	1	1	Assumed
Inlet temperature, Heater-ST	°C	10	10	Engineering manual
Outlet temperature, Heater-ST	°C	45	45	Engineering manual
Split ratio of exhaust gas after HRSG	-	0.62/0.38	0.40/0.60	Assumed

Appendix

I.   Normal production day

Table I. 1 Deviation in important inlet and outlet conditions during 2010-10-29

Tag	Description	Unit	Measured value, 2010-10-29, at 12:00	Deviation, maximum point	Deviation, minimum point
PZT-22-0102:Y	Målest gass linje A nedstr	barg	109.18	0.003 %	-0.008 %
PZT-22-0104:Y	Målest gass linje B nedstr	barg	108.74	0.001 %	-0.002 %
PZT-23-0317:Y	Gassinjeksjons manifold	barg	183.98	0.021 %	-0.013 %
PZT-29-0115:Y	Vanninj hovedpumpe A ut	barg	1.28	0.564 %	-0.402 %
PZT-29-0135:Y	Vanninj hovedpumpe B ut	barg	1.36	0.172 %	-0.120 %
PT-13-0903:Y	Test manifold	barg	12.76	23.501 %	-35.762 %
PT-20-0930:Y	HT produksjons fordelingsrør	barg	45.86	0.004 %	-0.019 %
PT-20-0940:Y	LT manifold	barg	6.85	0.106 %	-0.361 %
PZT-21-0108:Y	Oljeeksportpumpe A ut	barg	98.12	0.539 %	-12.175 %
PZT-21-0112:Y	Oljeeksportpumpe C ut	barg	98.12	0.425 %	-0.967 %
TT-13-0904:Y	Test manifold	°C	56.76	13.777 %	-22.957 %
TT-20-0932:Y	HT produksjons fordelingsrør	°C	62.49	0.064 %	-0.125 %
TT-20-0942:Y	LT manifold	°C	68.43	0.381 %	-0.645 %
TT-22-0106:Y	Målest gass linje nedstr	°C	4.39	0.198 %	-0.128 %
TZT-45-0132B:Y	Supervarmer ut	°C	60.92	0.213 %	-0.307 %
TIC-21-0113:X.Value	Oljeeksp kjøling	°C	74.00	0.000 %	0.000 %
FYI_13 9480:Value	Gassløftrate total	Sm^3/h	21666.62	0.286 %	-0.408 %
FYI_13 9481:Value	Gassrate injeksjon	Sm^3/h	362682.75	0.428 %	-1.788 %
FYI-22-0250:Y	Gassimportmålest	Sm^3/h	159103.58	0.386 %	-0.607 %
FYI-45-0201:Y	Brenngassmålest	Sm^3/h	9649.30	0.023 %	-0.123 %
FI_22 0201:Value	Eksport råolje rate	m^3/h	1147.24	0.422 %	-0.573 %
FYI_13 9482:Value	Vanninjeksjonsrate Utsira	NA	7.90	16.565 %	-21.762 %

Table I.2 Deviation in important inlet and outlet conditions during 2012-10-29

Tag	Description	Unit	Measured value, 2012-10-29, at 12:00	Deviation, maximum point	Deviation, minimum point
PZT-23-0317:Y	Gassinjeksjons manifold	barg	169.93	1.114 %	-0.724 %
PZT-29-0115:Y	Vanninj hovedpumpe A ut	barg	57.66	4.012 %	-45.979 %
PZT-29-0135:Y	Vanninj hovedpumpe B ut	barg	57.75	3.992 %	-3.242 %
PT-13-0903:Y	Test manifold	barg	7.78	1.876 %	-7.032 %
PT-20-0930:Y	HT produksjons fordelingsrør	barg	46.55	0.515 %	-0.211 %
PT-20-0940:Y	LT manifold	barg	6.52	2.186 %	-2.553 %
PZT-21-0110:Y	Oljeeksportpumpe B ut	barg	91.05	6.843 %	-3.986 %
TT-13-0904:Y	Test manifold	°C	40.91	0.594 %	-2.097 %
TT-20-0932:Y	HT produksjons fordelingsrør	°C	59.59	0.459 %	-0.185 %
TT-20-0942:Y	LT manifold	°C	68.90	0.227 %	-0.125 %
TZT-45-0132B:Y	Supervarmer ut	°C	51.55	2.413 %	-0.148 %
TIC-21-0113:X.Value	Oljeeksp kjøling	°C	79.17	1.044 %	-0.883 %
FYI_13 9480:Value	Gassløftrate total	Sm^3/h	23883.80	4.590 %	-4.129 %
FYI_13 9481:Value	Gassrate injeksjon	Sm^3/h	243955.59	2.051 %	-2.772 %
FYI-45-0201:Y	Brenngassmålest	Sm^3/h	9218.74	3.125 %	-0.544 %
FI_22 0201:Value	Eksport råolje rate	Sm^3/h	779.75	6.118 %	-2.138 %
FYI_13 9482:Value	Vanninjeksjonsrate Utsira	NA	291.79	9.417 %	-11.554 %

J.   Comparison between measured values and simulated values

Table J.1 Comparison between measured values and simulated values 2010-10-29

Component	Tag	Description	Unit	Measured value 10.29.2010 at 12:00	Simulated value
KA-23-0006					
	FT-23-0261-S:Y	Importgasskompressor flowrate	Sm^3/h	200000.00	159628.54
	TT-23-0262:Y	Impgasskompr inn	°C	9.00	8.93
	PZT-23-0263:Y	Impgasskompr inn	barg	107.74	107.70
VA-13-0001					
	TT-13-0916:Y	Test sep gassutløp	°C	50.80	59.73
VA-20-0001					
	TT-20-0121:Y	1 tr sep innløp	°C	65.08	61.72
PA-21-0001					
	FIC-21-0105:X.Value	Oljeeksp B.pmp min strømning	Sm^3/h	1125.58	1092.54
PA-21-0002					
	FIC-21-0117:X.Value	Oljeeksp utløp H.pmp A	Sm^3/h	524.54	1092.54
	FIC-21-0118:X.Value	Oljeeksp utløp H.pmp B	Sm^3/h	0.61	
	FIC-21-0119:X.Value	Oljeeksp utløp H.pmp C	Sm^3/h	508.78	
Gas injection:					
	PZT-23-0317:Y	Gassinjeksjons manifold	barg	183.98	183.40
Manifolds:					
	TT-13-0904:Y	Test manifold	°C	56.76	60.09
	TT-20-0932:Y	HT produksjons fordelingsrør	°C	62.49	60.66
	TT-20-0942:Y	LT manifold	°C	68.43	66.66
Wells:					
	TT-13-0036:Y	#01 Strupeventil nedstrøms	°C	64.90	60.47
	TT-13-0311:Y	#02 Strupeventil nedstrøms	°C	61.52	54.38
	TT-13-0061:Y	#03 Strupeventil nedstrøms	°C	70.54	70.72
	TT-13-0086:Y	#04 Strupeventil nedstrøms	°C	-20	-
	TT-13-0111:Y	#05 Strupeventil nedstrøms	°C	11.97	-
	TT-13-0136:Y	#06 Strupeventil nedstrøms	°C	62.67	51.31
	TT-13-0161:Y	#07 Strupeventil nedstrøms	°C	-20.00	-
	TT-13-0186:Y	#08 Strupeventil nedstrøms	°C	53.93	50.35
	TT-13-0211:Y	#09 Strupeventil nedstrøms	°C	58.62	57.26
	TT-13-0686:Y	#10 Strupeventil nedstrøms	°C	58.54	61.36

Component	Tag	Description	Unit	Measured value 10.29.2010 at 12:00	Simulated value
	TT-13-0236:Y	#11 Strupeventil nedstrøms	°C	11.90	-
	TT-13-0261:Y	#12 Strupeventil nedstrøms	°C	53.04	44.97
	TT-13-0461:Y	#13 Strupeventil nedstrøms	°C	70.56	70.61
	TT-13-0711:Y	#15 Strupeventil nedstrøms	°C	70.70	72.12
	TT-13-0336:Y	#16 Strupeventil nedstrøms	°C	64.70	64.58
	TT-13-0361:Y	#17 Strupeventil nedstrøms	°C	43.43	42.28
	TT-13-0386:Y	#18 Strupeventil nedstrøms	°C	51.61	51.54
	TT-13-0286:Y	#19 Strupeventil nedstrøms	°C	59.87	59.77
	TT-13-0411:Y	#21 Strupeventil nedstrøms	°C	47.02	46.04
	TT-13-0436:Y	#22 Strupeventil nedstrøms	°C	52.03	54.55
	TT-13-0486:Y	#25 Strupeventil nedstrøms	°C	56.72	56.33
	TT-13-0511:Y	#26 Strupeventil nedstrøms	°C	57.76	61.82
	TT-13-0536:Y	#27 Strupeventil nedstrøms	°C	55.45	56.31
	TT-13-0561:Y	#28 Strupeventil nedstrøms	°C	57.09	57.10
	TT-13-0586:Y	#29 Strupeventil nedstrøms	°C	-20.00	-
	TT-13-0786:Y	#30 Strupeventil nedstrøms	°C	61.48	59.53
	TT-13-0761:Y	#34 Strupeventil nedstrøms	°C	54.94	61.66
	TT-13-0611:Y	#35 Strupeventil nedstrøms	°C	63.73	63.23
	TT-13-0811:Y	#38 Strupeventil nedstrøms	°C	0.00	-
	TT-13-0636:Y	#39 Strupeventil nedstrøms	°C	70.78	72.47
	TT-13-0661:Y	340 Strupeventil nedstrøms	°C	62.15	61.10

Turbines:

Fuel gas metering

	PI-45-0202:Y	Brenngassmålest	bar	38.88	38.88
	TI-45-0203:Y	Brenngassmålest	°C	60.00	60.92

CT-23-0001

	FT-23-0699:Y	BRENNGASS TILFØRSEL	Sm^3/h	4276.94	6321.98
	PIT-23-0705:Y	BRENNGASS TILFØRSEL	barg	37.09	37.88

CT-80-0001A

	PI-80-1110A:Y	Brenngass før avstengningsventil	bar	2.10	-
	TT-80-1111:Y	Brenngass før avstengningsventil	°C	13.27	-

CT-80-0001B

	PI-80-2110A:Y	Brenngass før avstengningsventil	Bar	38.59	38.88
	TT-80-2111:Y	Brenngass før avstengningsventil	°C	59.41	60.92

Hot water distribution:

	TT-41-0103:Y	Varmvæske distrubusjon	°C	91.71	122.05
	TT-41-0156:Y	Varmvæske returlinje	°C	95.65	96.88

Appendix

Component	Tag	Description	Unit	Measured value 10.29.2012 at 12:00	Simulated value
KA-23-0006					
	FT-23-0261-S:Y	Importgasskompressor flowrate	Sm^3/h	-	-
VA-13-0001					
	TT-13-0916:Y	Test sep gassutløp	°C	39.65	21.14
VA-20-0001					
	TT-20-0121:Y	1 tr sep innløp	°C	65.67	65.34
PA-21-0001					
	FIC-21-0105:X.Value	Oljeeksp B.pmp min strømning	Sm^3/h	783.40	751.40
PA-21-0002					
	FIC-21-0117:X.Value	Oljeeksp utløp H.pmp A	Sm^3/h	0.55	751.40
	FIC-21-0118:X.Value	Oljeeksp utløp H.pmp B	Sm^3/h	720.64	
	FIC-21-0119:X.Value	Oljeeksp utløp H.pmp C	Sm^3/h	1.05	
Gas injection:					
	PZT-23-0317:Y	Gassinjeksjons manifold	barg	169.93	169.75
Manifolds:					
	TT-13-0904:Y	Test manifold	°C	40.91	21.38
	TT-20-0932:Y	HT produksjons fordelingsrør	°C	59.59	59.14
	TT-20-0942:Y	LT manifold	°C	68.90	68.63
Wells:					
	TT-13-0036:Y	#01 Strupeventil nedstrøms	°C	67.05	67.82
	TT-13-0311:Y	#02 Strupeventil nedstrøms	°C	61.19	61.64
	TT-13-0061:Y	#03 Strupeventil nedstrøms	°C	63.11	62.94
	TT-13-0086:Y	#04 Strupeventil nedstrøms	°C	25.23	-
	TT-13-0111:Y	#05 Strupeventil nedstrøms	°C	66.44	66.08
	TT-13-0136:Y	#06 Strupeventil nedstrøms	°C	9.06	-
	TT-13-0161:Y	#07 Strupeventil nedstrøms	°C	71.56	71.97
	TT-13-0186:Y	#08 Strupeventil nedstrøms	°C	53.38	53.03
	TT-13-0211:Y	#09 Strupeventil nedstrøms	°C	57.15	54.28
	TT-13-0686:Y	#10 Strupeventil nedstrøms	°C	67.62	68.47
	TT-13-0236:Y	#11 Strupeventil nedstrøms	°C	7.47	-
	TT-13-0261:Y	#12 Strupeventil nedstrøms	°C	54.82	52.77
	TT-13-0461:Y	#13 Strupeventil nedstrøms	°C	8.78	-
	TT-13-0711:Y	#15 Strupeventil nedstrøms	°C	66.04	65.77
	TT-13-0336:Y	#16 Strupeventil nedstrøms	°C	56.13	55.72

Component	Tagname	Description	Unit	Measured value 10.29.2012 at 12:00	Simulated value
	TT-13-0361:Y	#17 Strupeventil nedstrøms	°C	8.34	-
	TT-13-0386:Y	#18 Strupeventil nedstrøms	°C	61.05	60.90
	TT-13-0286:Y	#19 Strupeventil nedstrøms	°C	8.55	-
	TT-13-0411:Y	#21 Strupeventil nedstrøms	°C	69.11	68.48
	TT-13-0436:Y	#22 Strupeventil nedstrøms	°C	49.98	49.03
	TT-13-0486:Y	#25 Strupeventil nedstrøms	°C	47.79	40.96
	TT-13-0511:Y	#26 Strupeventil nedstrøms	°C	54.93	54.08
	TT-13-0536:Y	#27 Strupeventil nedstrøms	°C	52.87	51.45
	TT-13-0561:Y	#28 Strupeventil nedstrøms	°C	52.76	50.38
	TT-13-0586:Y	#29 Strupeventil nedstrøms	°C	25.12	-
	TT-13-0786:Y	#30 Strupeventil nedstrøms	°C	54.35	54.41
	TT-13-0761:Y	#34 Strupeventil nedstrøms	°C	47.09	51.03
	TT-13-0611:Y	#35 Strupeventil nedstrøms	°C	41.94	21.38
	TT-13-0811:Y	#38 Strupeventil nedstrøms	°C	71.84	71.90
	TT-13-0636:Y	#39 Strupeventil nedstrøms	°C	67.80	68.86
	TT-13-0661:Y	#40 Strupeventil nedstrøms	°C	58.94	58.02

Turbines:

Fuel gas metering

Component	Tagname	Description	Unit	Measured value 10.29.2012 at 12:00	Simulated value
	PI-45-0202:Y	Brenngassmålest	bar	38.45	38.30
	TI-45-0203:Y	Brenngassmålest	°C	51.71	51.55

CT-23-0001

Component	Tagname	Description	Unit	Measured value 10.29.2012 at 12:00	Simulated value
	FT-23-0699:Y	BRENNGASS TILFØRSEL	Sm^3/h	4362.21	6009.68
	PIT-23-0705:Y	BRENNGASS TILFØRSEL	barg	34.05	37.30

CT-80-0001A

Component	Tagname	Description	Unit	Measured value 10.29.2012 at 12:00	Simulated value
	PI-80-1110A:Y	Brenngass før avstengningsventil	bar	38.24	38.30
	TT-80-1111:Y	Brenngass før avstengningsventil	°C	50.55	51.55

CT-80-0001B

Component	Tagname	Description	Unit	Measured value 10.29.2012 at 12:00	Simulated value
	PI-80-2110A:Y	Brenngass før avstengningsventil	bar	1.83	-
	TT-80-2111:Y	Brenngass før avstengningsventil	°C	9.27	-

Hot water distribution:

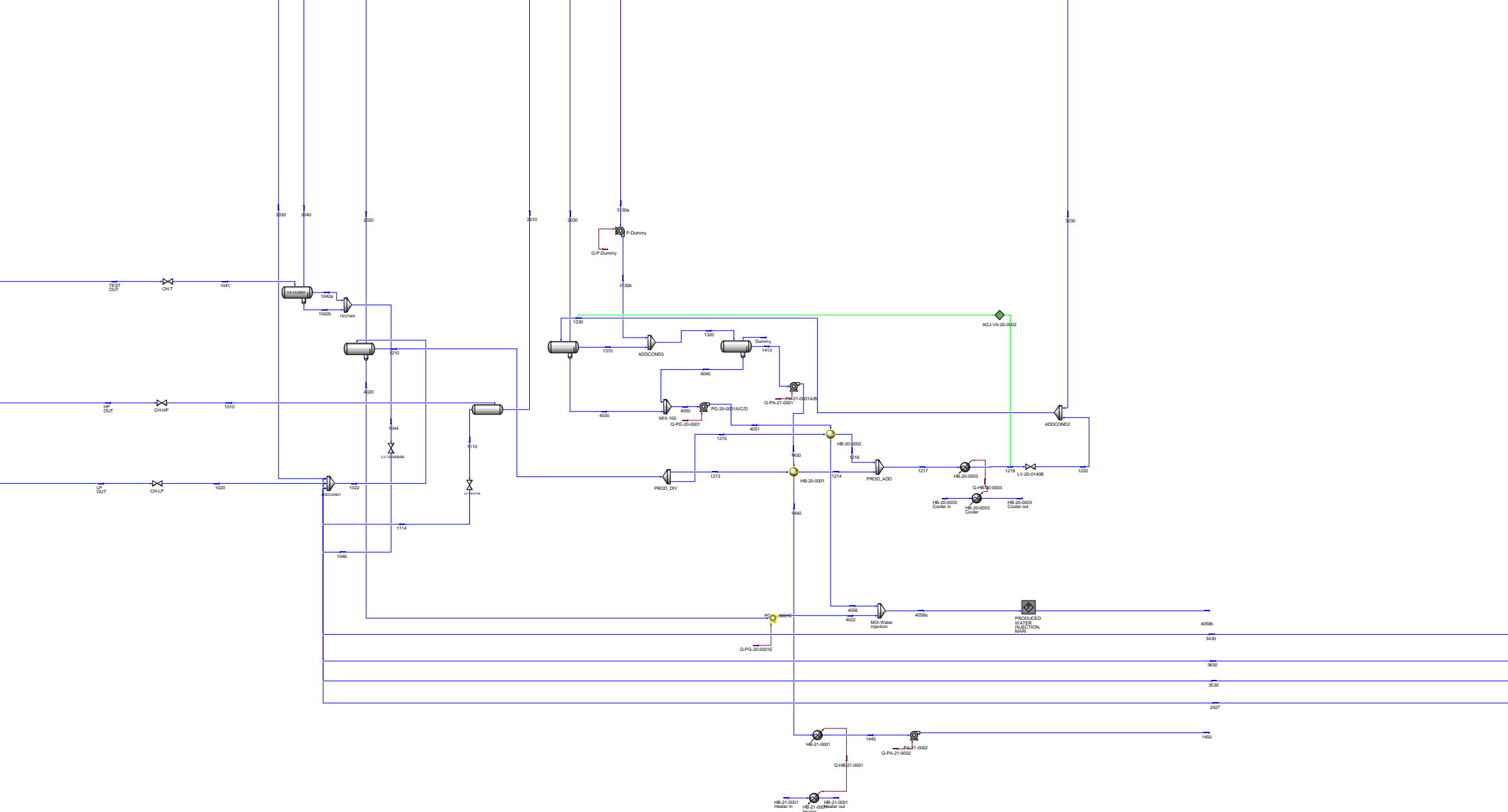| Component	Tagname	Description	Unit	Measured value 10.29.2012 at 12:00	Simulated value
	TT-41-0103:Y	Varmvæske distrubusjon	°C	88.64	126.10
	TT-41-0156:Y	Varmvæske returlinje	°C	98.71	96.88

K.   Simulated flowsheets

Figure K.1 Schematic overview of separation train and export system
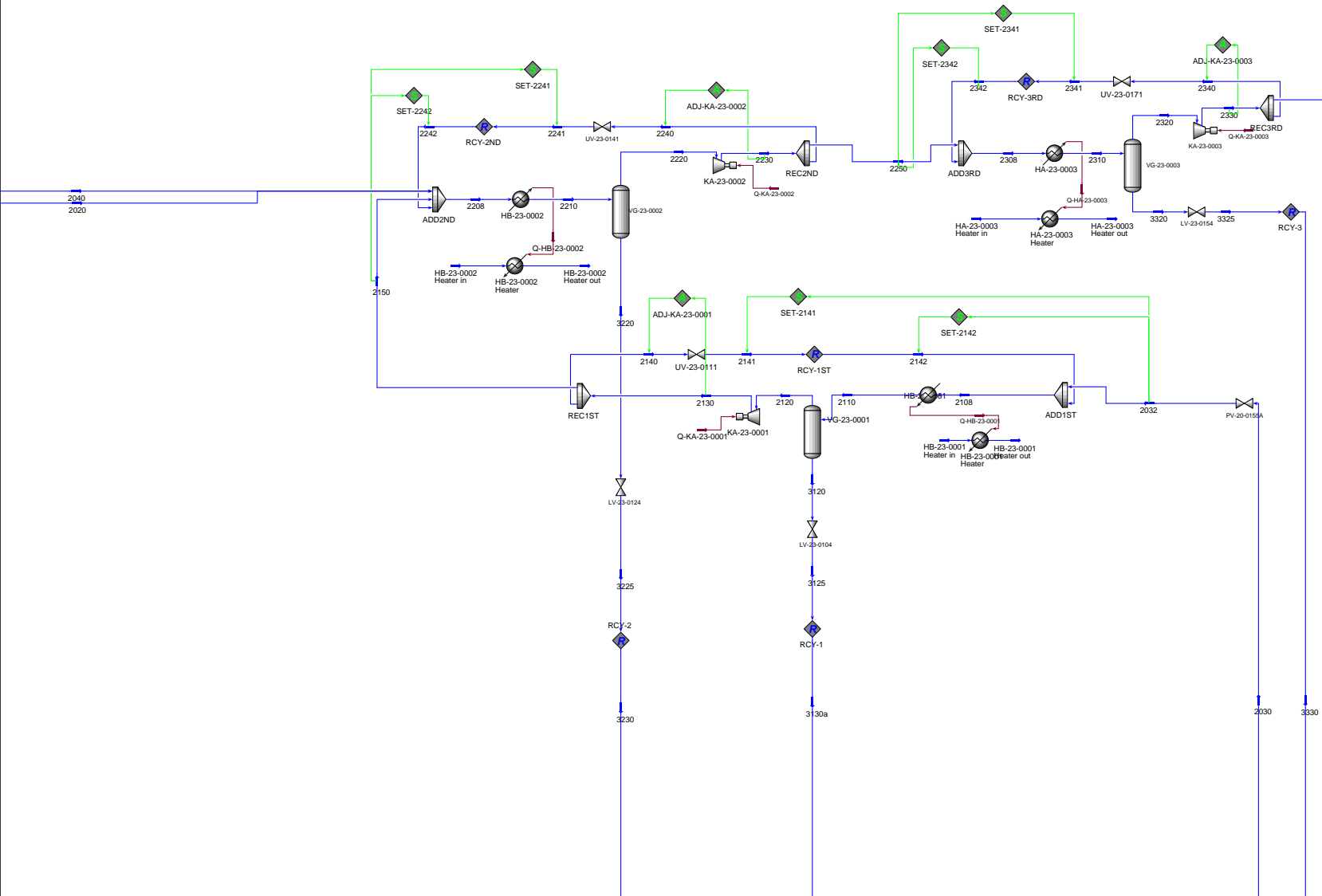
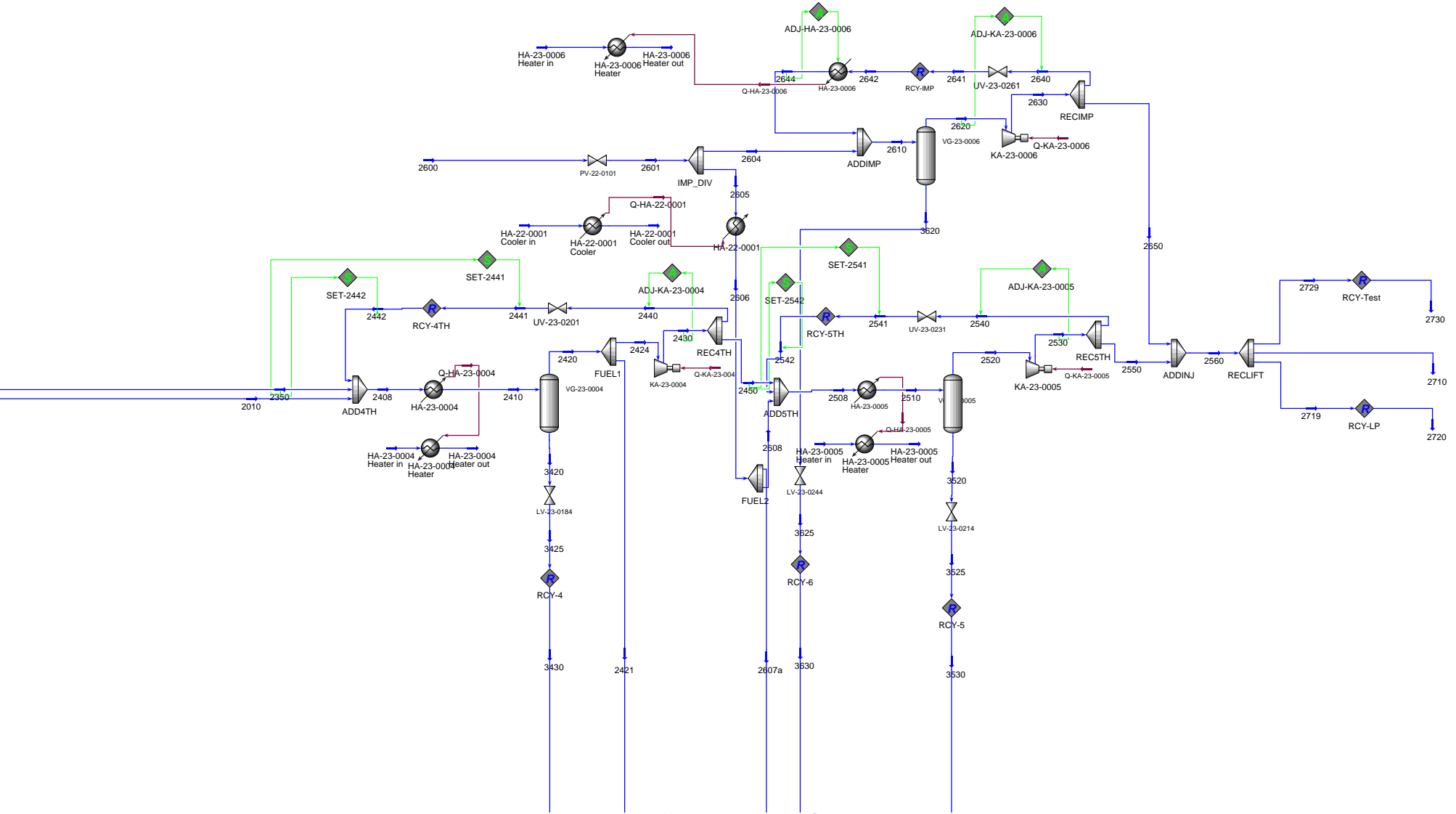**Figure K.2 Schematic overview of recompression train**
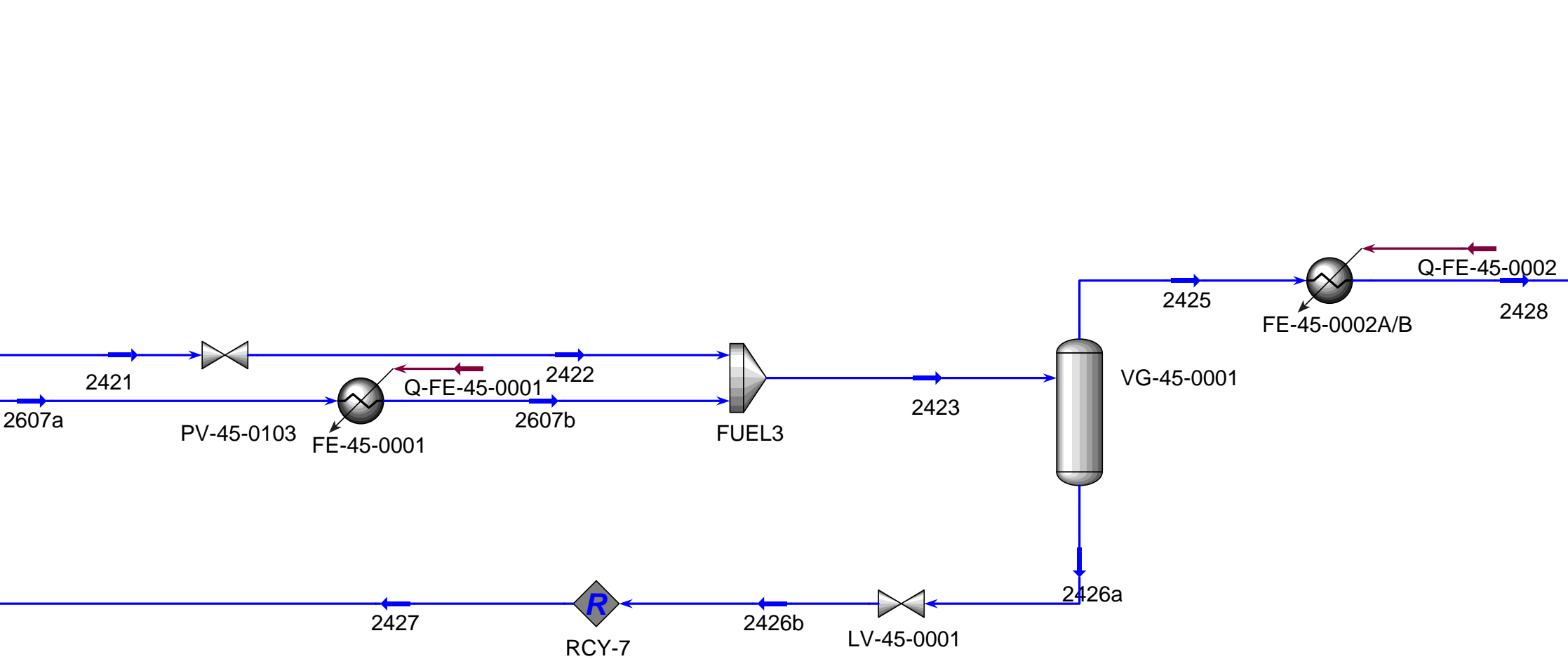
Figure K.3 Schematic overview of reinjection train
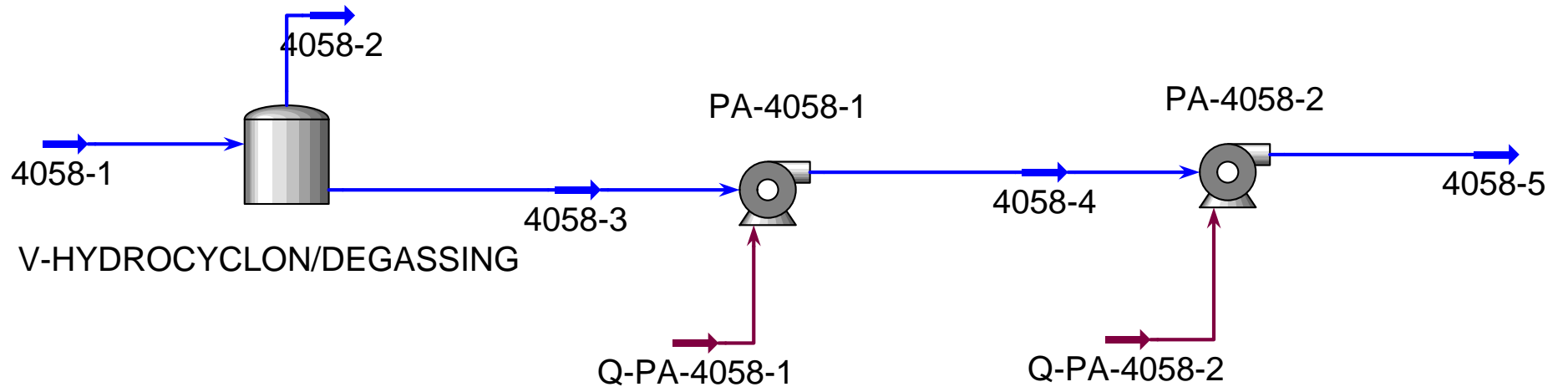
Figure K.4 Schematic overview of fuel gas system

4058-2

PA-4058-1

PA-4058-2

4058-1

V-HYDROCYCLON/DEGASSING

4058-3

4058-4

4058-5

Q-PA-4058-1

Q-PA-4058-2

Figure K.5 Schematic overview of produced water injection

S-4

PIPE-SEAWATER

S-1

PA-50-0001A/B　　S-2

S-3

TEE-S

Q-101

Q-PA-50-0001A/B
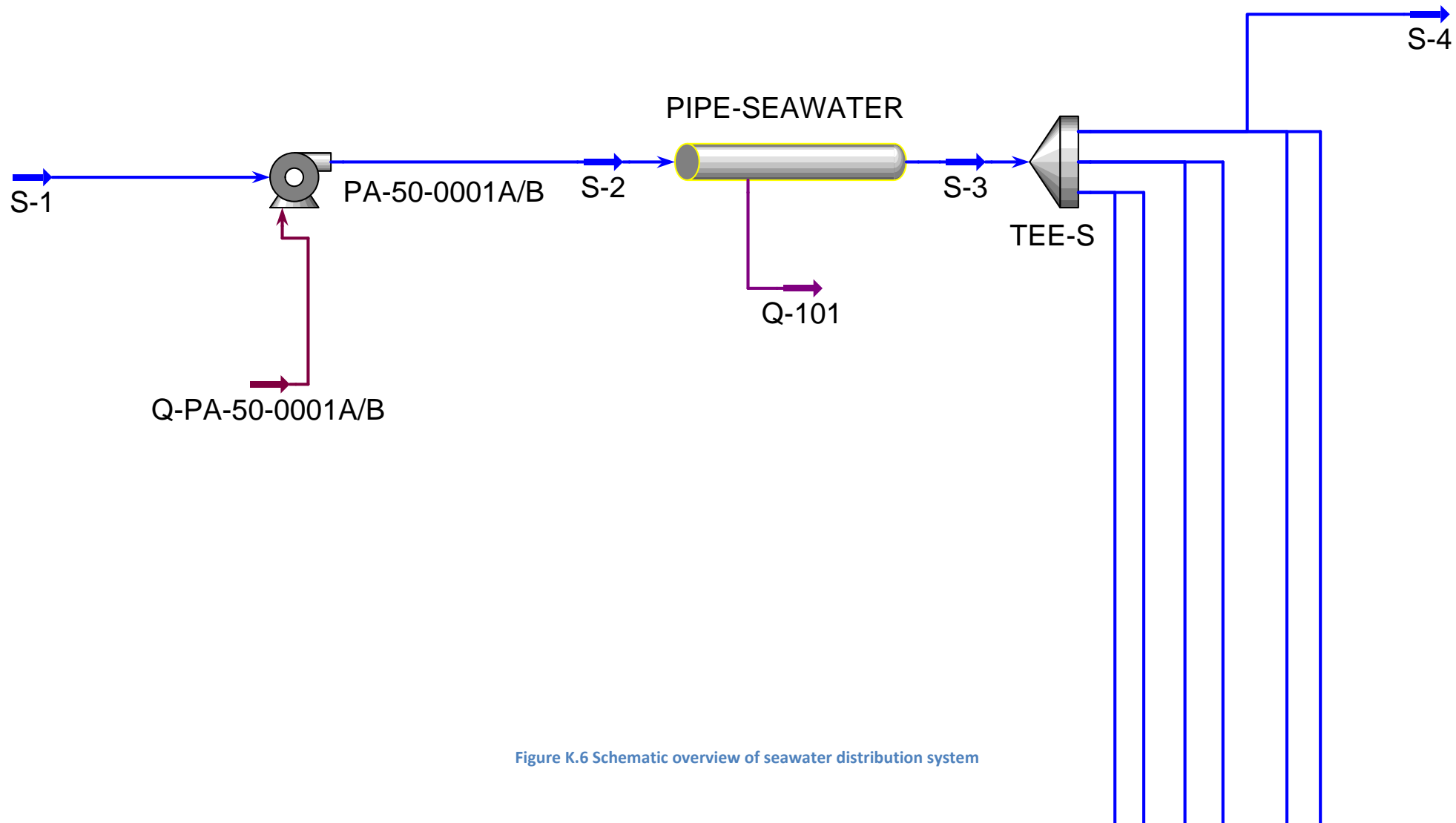
Figure K.6 Schematic overview of seawater distribution system
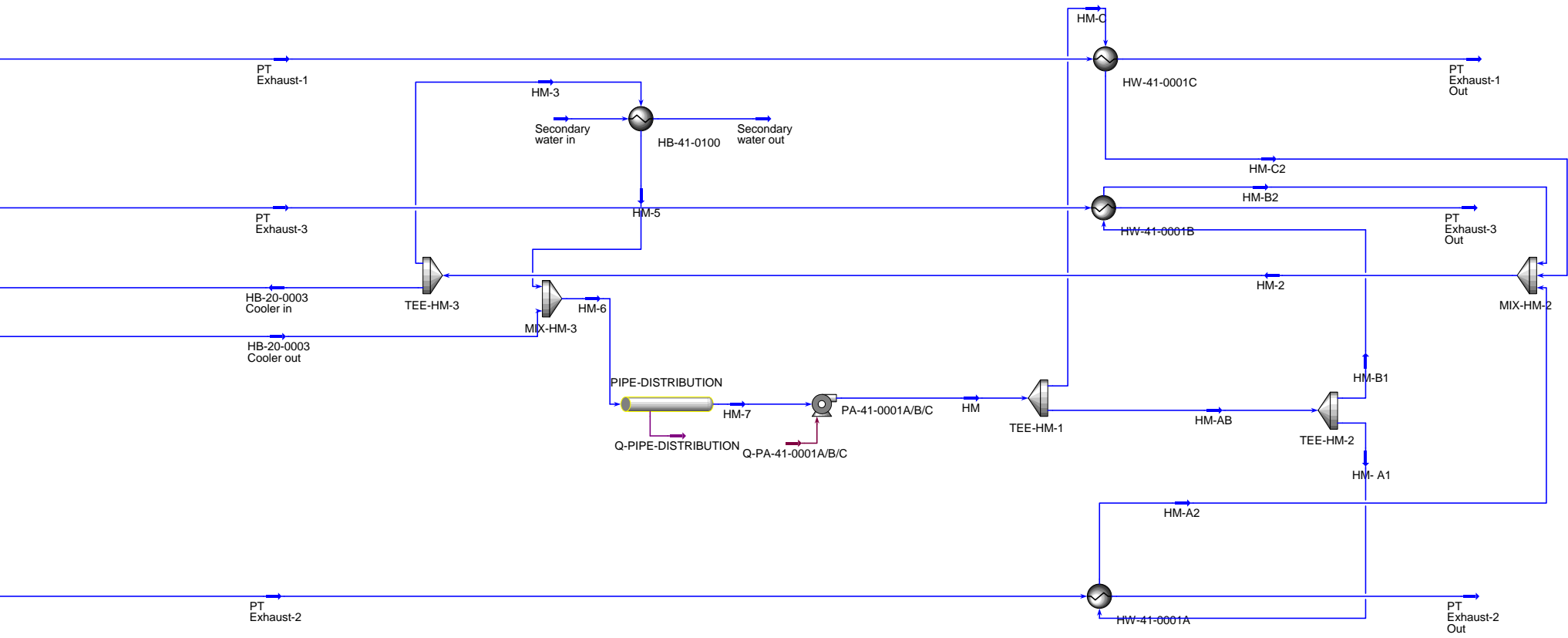
Figure K.7 Schematic overview of heat water distribution system

G03 O

ADJ
G03
O
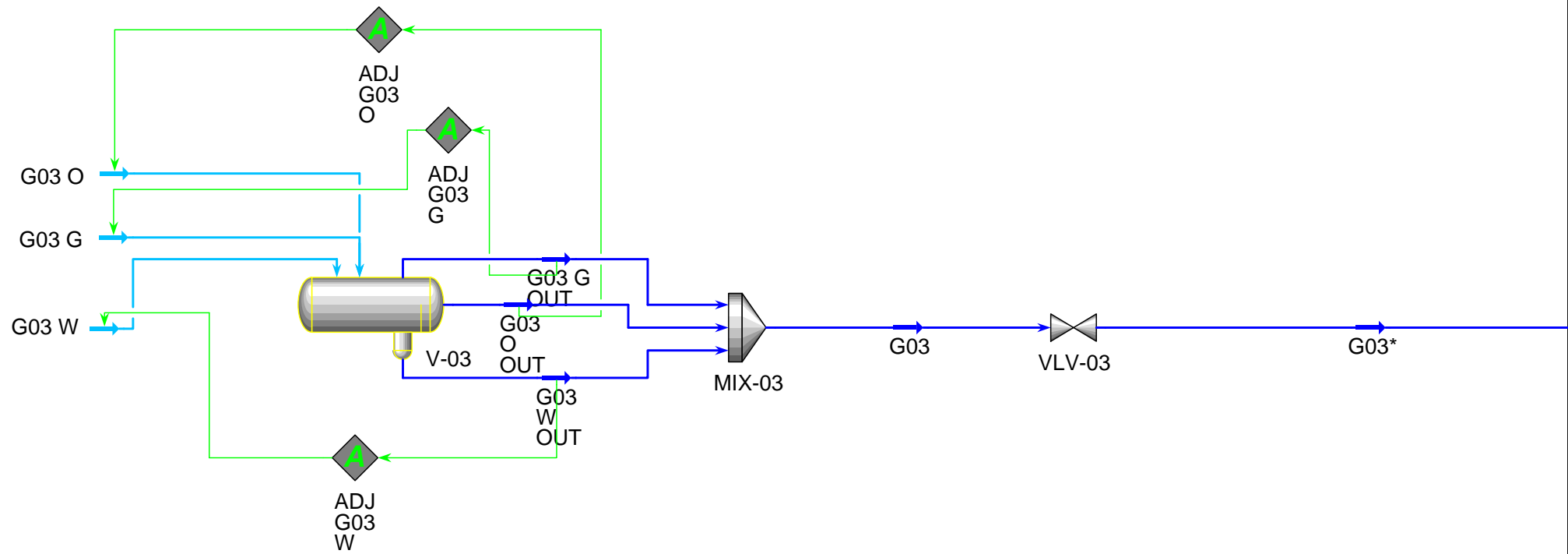
ADJ
G03
G

G03 G

G03 G
OUT

G03 W

V-03

G03
O
OUT

MIX-03

G03

VLV-03

G03*

G03
W
OUT

ADJ
G03
W

A

A

A

Figure K.8 Schematic overview of a well

ADJ-TIT-1

A

Combustion
Gas-1

GG
Exhaust-1

PT
Exhaust-1

Fuel Gas
CT-23-0001-

Fuel Gas
CT-23-0001-Cutter

Fuel Gas
CT-23-0001+

Combustor-1

G

Net
Power-1

Power
Turbine-1

Air-1

HP
Air-1

Dummy-1

GG
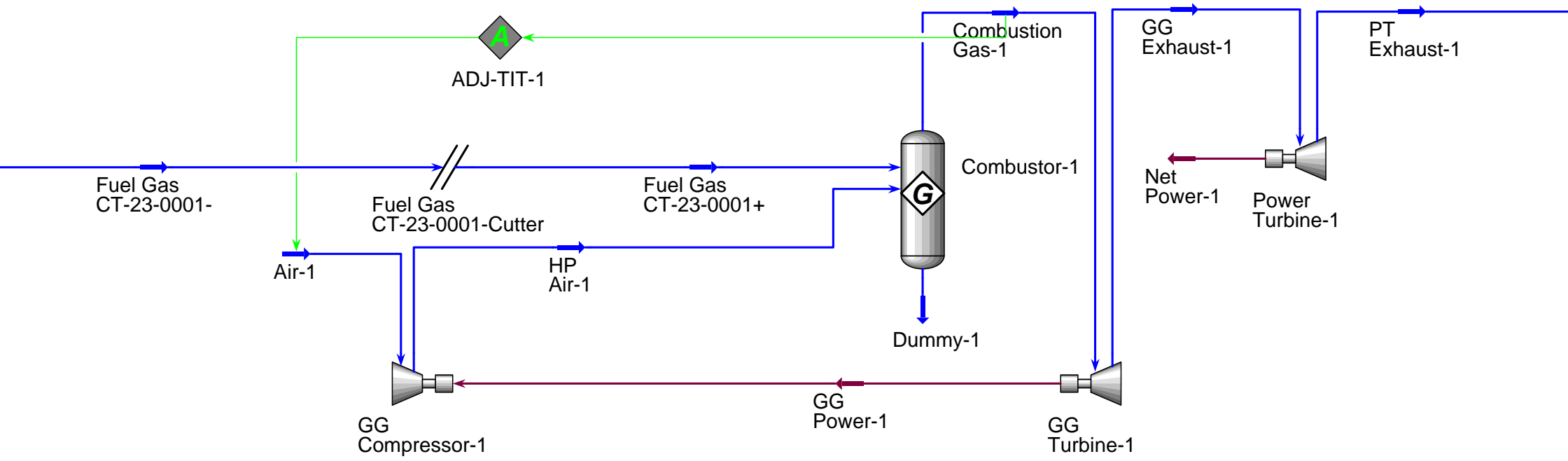Compressor-1

GG
Power-1

GG
Turbine-1

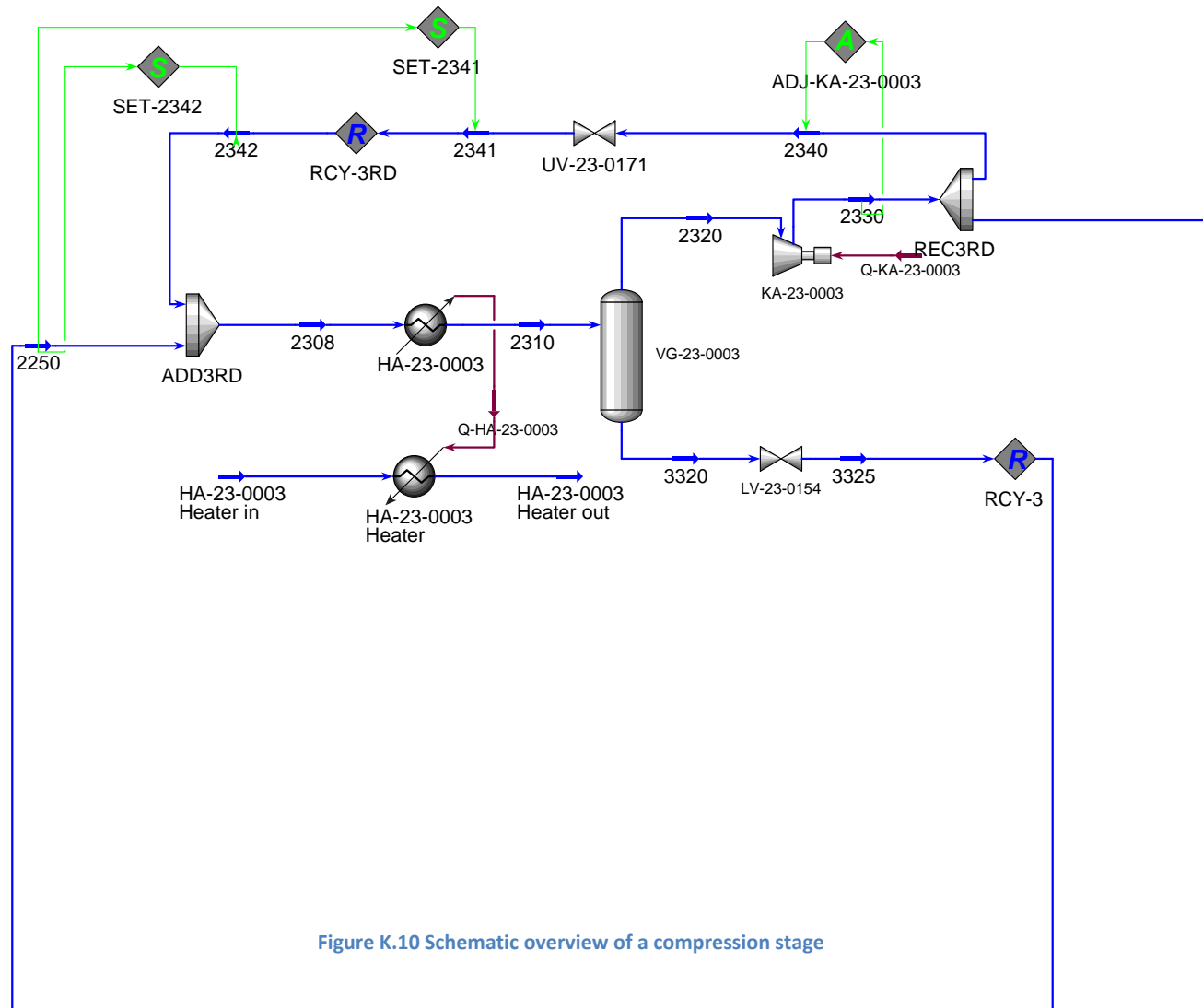Figure K.9 Schematic overview of a turbine unit

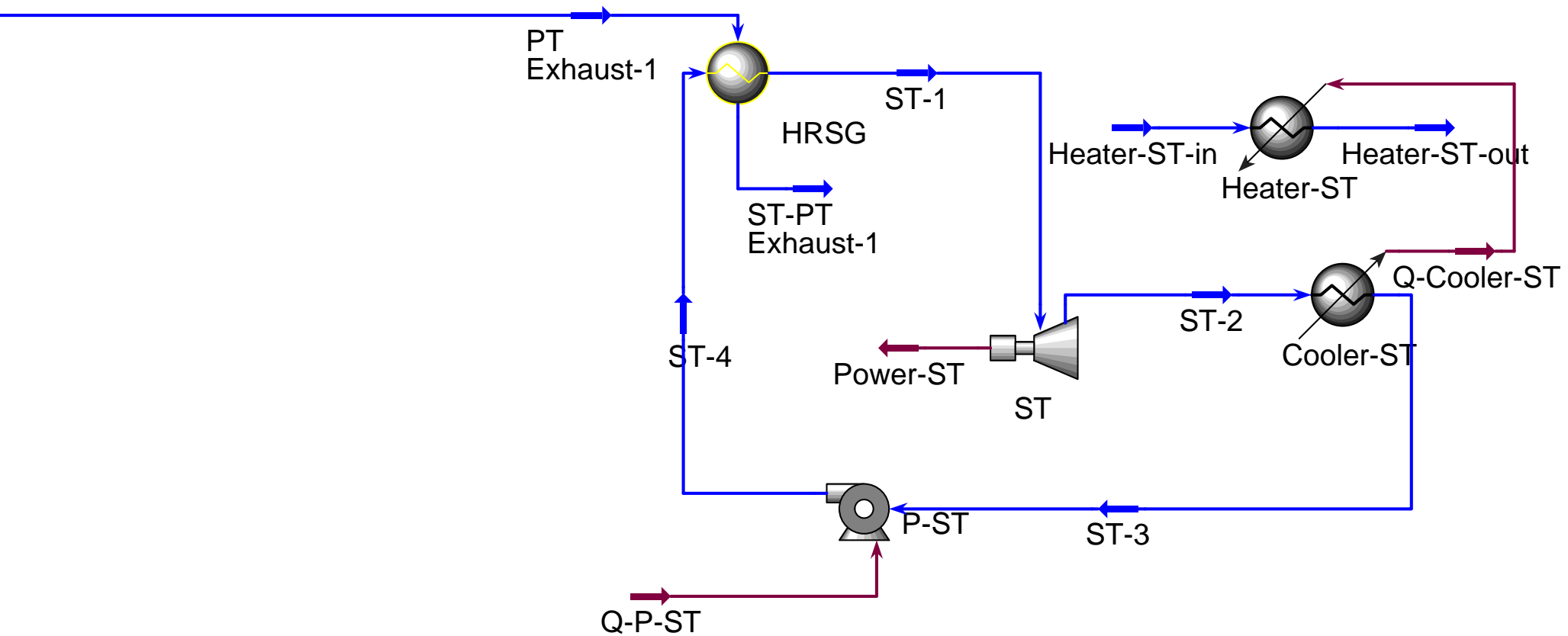Figure K.10 Schematic overview of a compression stage

Figure K.11 Schematic overview of a steam turbine unit used in combined cycle

L.   User variables

Physical exergy:

```
Sub VariableChanged()

On Error GoTo ErrorHandler


'Declare variables---------------------------------------------------------------

Dim MS As Streams

Dim ST As ProcessStream

Dim Exergy As Double

Dim T0,P0,H,S,H0,S0 As Double

Dim Stream As Fluid

Dim X As InternalVariableWrapper

Dim hyFlowsheet As Flowsheet

Dim hySubFlowsheets As Flowsheets

Dim hyFlowsheetInUse As Flowsheet

Dim j,k As Integer


'Procedure---------------------------------------------------------------------

Set hyFlowsheet = ActiveObject

Set hySubFlowsheets = hyFlowsheet.Flowsheets

Set hyFlowsheetInUse = hyFlowsheet


'Go through all flowsheets

For j = 0 To hySubFlowsheets.Count

    Set MS = hyFlowsheetInUse.MaterialStreams

            For Each ST In MS

        Set Stream = ST.DuplicateFluid

        Set X = ST.GetUserVariable("AmbTemp")

        T0 = X.Variable.GetValue()

        Set X = ST.GetUserVariable("AmbPres")
```

```
P0 = X.Variable.GetValue()

If (Stream.VapourFraction.IsKnown And Stream.Pressure.IsKnown And Stream.MolarFlow.IsKnown And T0<>-32767 And Stream.MolarFractions.IsKnown(0)) Then

    H = Stream.MolarEnthalpy.GetValue("kJ/kgmole")

    S = Stream.MolarEntropy.GetValue("kJ/kgmole-C")

    Stream.Temperature.SetValue(T0,"C")

    Stream.Pressure.SetValue(P0,"kPa")

    Stream.TPFlash()

    H0 = Stream.MolarEnthalpy.GetValue("kJ/kgmole")

    S0 = Stream.MolarEntropy.GetValue("kJ/kgmole-C")

                        Exergy = (H-H0-(T0 + 273.15)*(S-S0))*Stream.MolarFlow.GetValue("kgmole/h")

                        Set X = ST.GetUserVariable("Physical Exergy")

                        X.Variable.SetValue(Exergy,"kJ/h")


    Else

                        Set X = ST.GetUserVariable("Physical Exergy")

                        X.Variable.Erase()

    End If


        Next ST


        If j <> hySubFlowsheets.Count Then

                Set hyFlowsheetInUse = hySubFlowsheets(j)

        End If


Next j


ActiveVariableWrapper.Variable.SetValue(1)

ErrorHandler:

End Sub
```

Appendix

Chemical exergy, relative:

```
Sub VariableChanged()

On Error GoTo ErrorHandler


'Declare variables----------------------------------------------------------------

Dim MS As Streams

Dim St As ProcessStream

Dim T0,P0,H,S,H0,S0,Exergy,HPureSum,SPureSum,HPure,SPure As Double

Dim Stream,StreamPure As Fluid

Dim X As InternalVariableWrapper

Dim hyFlowsheet As Flowsheet

Dim hySubFlowsheets As Flowsheets

Dim hyFlowsheetInUse As Flowsheet

Dim j,k As Integer

Dim Comps As HYSYS.Components

Dim Comp As HYSYS.Component

Dim var,var2,MolFrac As Variant


'Procedure----------------------------------------------------------------

Set hyFlowsheet = ActiveObject

Set hySubFlowsheets = hyFlowsheet.Flowsheets

Set hyFlowsheetInUse = hyFlowsheet


'Go through all flowsheets

For j = 0 To hySubFlowsheets.Count

    Set MS = hyFlowsheetInUse.MaterialStreams

            For Each St In MS

        Set Stream = St.DuplicateFluid

        Set X = St.GetUserVariable("AmbTemp")

        T0 = X.Variable.GetValue("K")

        Set X = St.GetUserVariable("AmbPres")
```

P0 = X.Variable.GetValue("bar")

If (Stream.VapourFraction.IsKnown And Stream.Pressure.IsKnown And Stream.MolarFlow.IsKnown And T0<>-32767 And Stream.MolarFractions.IsKnown(0)) Then

Stream.Temperature.SetValue(T0,"K")

Stream.Pressure.SetValue(P0,"bar")

Stream.TPFlash()

H0 = Stream.MolarEnthalpy.GetValue("kJ/kgmole")

S0 = Stream.MolarEntropy.GetValue("kJ/kgmole-K")

HPureSum = 0

SPureSum = 0

Set StreamPure = St.DuplicateFluid

StreamPure.Temperature.SetValue(T0,"K")

StreamPure.Pressure.SetValue(P0,"bar")

MolFrac = StreamPure.MolarFractionsValue

MolFracPure = StreamPure.MolarFractionsValue

Set Comps = Stream.Components

For var2 = 0 To Comps.Count-1

MolFracPure(var2) = 0

Next var2

For var = 0 To Comps.Count-1

Set Comp = Comps.Item(var)

MolFracPure(var) = 1

StreamPure.MolarFractions.SetValues(MolFracPure)

StreamPure.TPFlash()

HPure = StreamPure.MolarEnthalpy.GetValue("kJ/kgmole")

SPure = StreamPure.MolarEntropy.GetValue("kJ/kgmole-K")

HPureSum = HPureSum + MolFrac(var)*HPure 'kJ/kmole

SPureSum = SPureSum + MolFrac(var)*SPure 'kJ/kmole-K

MolFracPure(var) = 0

```
        Next var


    Exergy = ( (H0-HPureSum) -T0*(S0-SPureSum) )*Stream.MolarFlow.GetValue("kgmole/s")

                Set X = St.GetUserVariable("Chemical Exergy")

                X.Variable.SetValue(Exergy,"kW")


    Else

                Set X = St.GetUserVariable("Chemical Exergy")

                X.Variable.Erase()
    End If


        Next St


        If j <> hySubFlowsheets.Count Then

                Set hyFlowsheetInUse = hySubFlowsheets(j)

        End If


Next j


ActiveVariableWrapper.Variable.SetValue(1)

ErrorHandler:

End Sub
```

Thermal exergy:

```
Sub VariableChanged()

On Error GoTo ErrorHandler


'Declare variables-------------------------------------------------------------

Dim MS As Streams

Dim ST As ProcessStream

Dim Exergy As Double

Dim T0,P0,H,S,HT0,ST0 As Double

Dim Stream As Fluid

Dim X As InternalVariableWrapper

Dim hyFlowsheet As Flowsheet

Dim hySubFlowsheets As Flowsheets

Dim hyFlowsheetInUse As Flowsheet

Dim j,k As Integer


'Procedure-------------------------------------------------------------------

Set hyFlowsheet = ActiveObject

Set hySubFlowsheets = hyFlowsheet.Flowsheets

Set hyFlowsheetInUse = hyFlowsheet


'Go through all flowsheets

For j = 0 To hySubFlowsheets.Count

    Set MS = hyFlowsheetInUse.MaterialStreams

            For Each ST In MS

        Set Stream = ST.DuplicateFluid

        Set X = ST.GetUserVariable("AmbTemp")

        T0 = X.Variable.GetValue()

        Set X = ST.GetUserVariable("AmbPres")

        P0 = X.Variable.GetValue()
```

Appendix

```vb
        If (Stream.VapourFraction.IsKnown And Stream.Pressure.IsKnown And Stream.MolarFlow.IsKnown And T0<>-32767 And Stream.MolarFractions.IsKnown(0)) Then

        H = Stream.MolarEnthalpy.GetValue("kJ/kgmole")

    S = Stream.MolarEntropy.GetValue("kJ/kgmole-C")

    Stream.Temperature.SetValue(T0,"C")

    Stream.TPFlash()

    HT0 = Stream.MolarEnthalpy.GetValue("kJ/kgmole")

    ST0 = Stream.MolarEntropy.GetValue("kJ/kgmole-C")

    Exergy = (H-HT0-(T0 + 273.15)*(S-ST0))*Stream.MolarFlow.GetValue("kgmole/h")


      Set X = ST.GetUserVariable("Thermal")

                        X.Variable.SetValue(Exergy,"kJ/h")

        Else


                        Set X = ST.GetUserVariable("Physical Exergy")

                        X.Variable.Erase()


        End If


            Next ST


            If j <> hySubFlowsheets.Count Then

                    Set hyFlowsheetInUse = hySubFlowsheets(j)

            End If


Next j


ActiveVariableWrapper.Variable.SetValue(1)

ErrorHandler:

End Sub
```

Mechanical exergy:

```
Sub VariableChanged()

On Error GoTo ErrorHandler


'Declare variables-----------------------------------------------------------------

Dim MS As Streams

Dim ST As ProcessStream

Dim Exergy As Double

Dim T0,P0,H0,S0,HT0,ST0 As Double

Dim Stream As Fluid

Dim X As InternalVariableWrapper

Dim hyFlowsheet As Flowsheet

Dim hySubFlowsheets As Flowsheets

Dim hyFlowsheetInUse As Flowsheet

Dim j,k As Integer


'Procedure----------------------------------------------------------------------------

Set hyFlowsheet = ActiveObject

Set hySubFlowsheets = hyFlowsheet.Flowsheets

Set hyFlowsheetInUse = hyFlowsheet


'Go through all flowsheets

For j = 0 To hySubFlowsheets.Count

    Set MS = hyFlowsheetInUse.MaterialStreams

            For Each ST In MS

        Set Stream = ST.DuplicateFluid

        Set X = ST.GetUserVariable("AmbTemp")

        T0 = X.Variable.GetValue()

        Set X = ST.GetUserVariable("AmbPres")

        P0 = X.Variable.GetValue()
```

Appendix

```
        If (Stream.VapourFraction.IsKnown And Stream.Pressure.IsKnown And Stream.MolarFlow.IsKnown And T0<>-
32767 And Stream.MolarFractions.IsKnown(0)) Then

      Stream.Temperature.SetValue(T0,"C")

     Stream.TPFlash()

       HT0 = Stream.MolarEnthalpy.GetValue("kJ/kgmole")

       ST0 = Stream.MolarEntropy.GetValue("kJ/kgmole-C")

       Stream.Pressure.SetValue(P0,"kPa")

                    Stream.TPFlash()

       H0 = Stream.MolarEnthalpy.GetValue("kJ/kgmole")

       S0 = Stream.MolarEntropy.GetValue("kJ/kgmole-C")

       Exergy = (HT0-H0-(T0 + 273.15)*(ST0-S0))*Stream.MolarFlow.GetValue("kgmole/h")

         Set X = ST.GetUserVariable("Mechanical")

                   X.Variable.SetValue(Exergy,"kJ/h")


      Else

                   Set X = ST.GetUserVariable("Mechanical")

                   X.Variable.Erase()

      End If


         Next ST


         If j <> hySubFlowsheets.Count Then

                Set hyFlowsheetInUse = hySubFlowsheets(j)

         End If


Next j


ActiveVariableWrapper.Variable.SetValue(1)

ErrorHandler:

End Sub
```

Chemical exergy, absolute, fluid package 1:

```
Sub VariableChanged()

Dim MS As Streams

Dim ST As ProcessStream

Dim X As InternalVariableWrapper

Dim hyFlowsheet As Flowsheet

Dim hySubFlowsheets As Flowsheets

Dim hyFlowsheetInUse As Flowsheet

Dim j,k As Integer

Dim chem1, chem2, c0, c1,c2,c3, c4, c5, c6, c7, c8, c9, c10,c11, c12, c13, c14, c15, c16,  h As Double

Dim m As Variant


'Procedure---------------------------------------------------------------------

Set hyFlowsheet = ActiveObject

Set hySubFlowsheets = hyFlowsheet.Flowsheets

Set hyFlowsheetInUse = hyFlowsheet


'Go through all flowsheets

For j = 0 To hySubFlowsheets.Count

    Set MS = hyFlowsheetInUse.MaterialStreams

            For Each ST In MS

            gg=ST.FluidPackage.Components.Count

If  (gg=17) Then

'std chemical exergy [kJ/kg]

        c0=25.70235203120060

        c1=457.62637884994700

        c2=52142.06879956250000

        c3=50028.76545483980000

        c4=49055.26439467110000

        c5=48498.55435549770000

        c6=48498.55435549770000
```

```
c7=48171.05726820070000

c8=48171.05726820070000

c9=48565.50221421180000

c10=46413.39477257570000

c11=45597.16819923210000

c12=44958.08717387720000

c13=44221.80913019920000

c14=42866.59657055740000

c15=47752.23011820570000

c16=173.1880432


'hour=3600sec

h=3600

m=ST.ComponentMassFlow.GetValues("kg/h")

'chemical exergy [kJ/h]

chem1=c0*m(0)+c1*m(1)+c2*m(2)+c3*m(3)+c4*m(4)+c5*m(5)+c6*m(6)+c7*m(7)+c8*m(8)+c9*m(9)+c10*m(10)
+c11*m(11)+c12*m(12)+c13*m(13)+c14*m(14)+c15*m(15)+c16*m(16)

'chemical exergy [kW]

chem2=chem1/h

                Set X = ST.GetUserVariable("Exergychem1")

                X.Variable.SetValue(chem2,"kW")

End If

        Next ST

        If j <> hySubFlowsheets.Count Then

                Set hyFlowsheetInUse = hySubFlowsheets(j)

        End If

Next j

ActiveVariableWrapper.Variable.SetValue(1)

ErrorHandler:

End Sub
```

Appendix

Chemical exergy, absolute, fluid package 3:

```
Sub VariableChanged()

Dim MS As Streams

Dim ST As ProcessStream

Dim X As InternalVariableWrapper

Dim hyFlowsheet As Flowsheet

Dim hySubFlowsheets As Flowsheets

Dim hyFlowsheetInUse As Flowsheet

Dim j,k As Integer

Dim chem1, chem2, c0, c1,c2,c3, c4, c5, c6, c7, c8, c9, c10,c11, c12, c13,  h As Double

Dim m As Variant


'Procedure-------------------------------------------------------------------

Set hyFlowsheet = ActiveObject

Set hySubFlowsheets = hyFlowsheet.Flowsheets

Set hyFlowsheetInUse = hyFlowsheet


'Go through all flowsheets

For j = 0 To hySubFlowsheets.Count

    Set MS = hyFlowsheetInUse.MaterialStreams

            For Each ST In MS

gg=ST.FluidPackage.Components.Count

If (gg=14) Then

'std chemical exergy [kJ/kg]

        c0=457.62637884994700000

        c1=52142.06879956250000000

        c2=50028.76545483980000000

        c3=49055.26439467110000000

        c4=48498.55435549770000000

        c5=48498.55435549770000000

        c6=48171.05726820070000000
```

```
c7=48171.05726820070000000

c8=173.18804319826700000

c9=25.70235203120060000

c10=0

c11=124.06250000000000000

c12=0

c13=292.63040590886500000


'hour=3600sec

h=3600

m=ST.ComponentMassFlow.GetValues("kg/h")

'chemical exergy [kJ/h]

chem1=c0*m(0)+c1*m(1)+c2*m(2)+c3*m(3)+c4*m(4)+c5*m(5)+c6*m(6)+c7*m(7)+c8*m(8)+c9*m(9)+c10*m(10)
+c11*m(11)+c12*m(12)+c13*m(13)

'chemical exergy [kW]

chem2=chem1/h

                Set X = ST.GetUserVariable("Exergychem3")

                X.Variable.SetValue(chem2,"kW")


End If

        Next ST

        If j <> hySubFlowsheets.Count Then

                Set hyFlowsheetInUse = hySubFlowsheets(j)

        End If

Next j


ActiveVariableWrapper.Variable.SetValue(1)

ErrorHandler:

End Sub
```

Appendix

Exergy set, fluid package 1:

'Give number to initiate calculation of physical exergy in material streams

```
Sub VariableChanged()

        On Error GoTo ErrorHandler

'Dimensioning

        Dim Stream As Fluid

        Dim Exergyset As RealVariable

        Set Exergyset=ActiveVariableWrapper.Variable

        Dim MS As Streams

        Dim ST As ProcessStream

        Dim X As InternalVariableWrapper

        Dim Exergycalc As Variant

        Dim T0,P0,H,S,H0,S0 As Double

        Dim phys, chem As Double


'For loop to calculate physical exergy for each process stream

        Set MS=ActiveObject.MaterialStreams

        For Each ST In MS

                Set Stream=ST.DuplicateFluid

                Set X=ST.GetUserVariable("AmbTemp")

                T0=X.Variable.GetValue()

                Set X=ST.GetUserVariable("AmbPres")

                P0=X.Variable.GetValue()

                If (Stream.VapourFraction.IsKnown And Stream.Pressure.IsKnown And Stream.MolarFlow.IsKnown And
T0<>-32767 And Stream.MolarFractions.IsKnown(0)) Then

                        H =  Stream.MolarEnthalpy.GetValue("kJ/kgmole")

                        S = Stream.MolarEntropy.GetValue("kJ/kgmole-C")

                        Stream.Temperature.SetValue(T0,"C")

                        Stream.Pressure.SetValue(P0, "kPa")

                        Stream.TPFlash()

                        H0 = Stream.MolarEnthalpy.GetValue("kJ/kgmole")
```

Appendix

```
S0 = Stream.MolarEntropy.GetValue("kJ/kgmole-C")

Exergycalc=((H-H0-(T0+273.15)*(S-S0))*Stream.MolarFlow.GetValue("kgmole/h"))



'setting the value for the uservariable

        Set X=ST.GetUserVariable("Exergy")

        X.Variable.SetValue(Exergycalc, "kJ/h")

    End If


Set X=ST.GetUserVariable("Exergy")

phys=X.Variable.GetValue()

Set X=ST.GetUserVariable("Exergychem1")

chem=X.Variable.GetValue()

Set X=ST.GetUserVariable("Exergytot")

X.Variable.SetValue(phys+chem)

Next ST


Exergyset.SetValue(1)

Errorhandler:

End Sub
```

Appendix

Exergy set, fluid package 3:

'Give number to initiate calculation of physical exergy in material streams

Sub VariableChanged()

On Error GoTo ErrorHandler

'Dimensioning

```
Dim Stream As Fluid

Dim Exergyset3 As RealVariable

Set Exergyset3=ActiveVariableWrapper.Variable

Dim MS As Streams

Dim ST As ProcessStream

Dim X As InternalVariableWrapper

Dim Exergycalc As Variant

Dim T0,P0,H,S,H0,S0 As Double

Dim phys, chem As Double
```

'For loop to calculate physical exergy for each process stream

```
Set MS=ActiveObject.MaterialStreams

For Each ST In MS

        Set Stream=ST.DuplicateFluid

        Set X=ST.GetUserVariable("AmbTemp")

        T0=X.Variable.GetValue()

        Set X=ST.GetUserVariable("AmbPres")

        P0=X.Variable.GetValue()

        If (Stream.VapourFraction.IsKnown And Stream.Pressure.IsKnown And Stream.MolarFlow.IsKnown And
T0<>-32767 And Stream.MolarFractions.IsKnown(0)) Then

                H =  Stream.MolarEnthalpy.GetValue("kJ/kgmole")

                S = Stream.MolarEntropy.GetValue("kJ/kgmole-C")

                Stream.Temperature.SetValue(T0,"C")

                Stream.Pressure.SetValue(P0, "kPa")

                Stream.TPFlash()

                H0 = Stream.MolarEnthalpy.GetValue("kJ/kgmole")
```

Appendix

```
S0 = Stream.MolarEntropy.GetValue("kJ/kgmole-C")

Exergycalc=((H-H0-(T0+273.15)*(S-S0))*Stream.MolarFlow.GetValue("kgmole/h"))



'setting the value for the uservariable

        Set X=ST.GetUserVariable("Exergy")

        X.Variable.SetValue(Exergycalc, "kJ/h")

    End If


Set X=ST.GetUserVariable("Exergy")

phys=X.Variable.GetValue()

Set X=ST.GetUserVariable("Exergychem3")

chem=X.Variable.GetValue()

Set X=ST.GetUserVariable("Exergytot3")

X.Variable.SetValue(phys+chem)

Next ST


Exergyset3.SetValue(1)

Errorhandler:

End Sub
```

Appendix

Physical exergy destruction, pump:

```
Sub VariableChanged()

On Error GoTo ErrorHandler


Dim Stream As Fluid

Dim PumpphysEx As RealVariable

Set PumpphysEx=ActiveVariableWrapper.Variable

Dim X As InternalVariableWrapper

Dim Feed As ProcessStream

Dim energy As Variant

Dim pump As PumpOp

Dim Physin, Physout,nergy As Double


Set pump=ActiveObject

nergy=pump.EnergyStream.HeatFlow

Set X=ActiveObject.FeedStream.GetUserVariable("Physical exergy")

Physin=X.Variable.GetValue()

Set X=ActiveObject.ProductStream.GetUserVariable("Physical exergy")

Physout=X.Variable.GetValue()

PumpphysEx.SetValue(Physout-Physin-nergy)


ErrorHandler:

End Sub
```

Physical exergy destruction, pump:

Chemical exergy destruction, pump:

```
Sub VariableChanged()

On Error GoTo ErrorHandler


Dim Stream As Fluid

Dim PumpchemEx As RealVariable

Set PumpchemEx=ActiveVariableWrapper.Variable

Dim X As InternalVariableWrapper

Dim Feed As ProcessStream

Dim energy As Variant

Dim pump As PumpOp

Dim Chemin, Chemout,nergy As Double


Set pump=ActiveObject

Set X=ActiveObject.FeedStream.GetUserVariable("Chemical Exergy")

Chemin=X.Variable.GetValue()

Set X=ActiveObject.ProductStream.GetUserVariable("Chemical Exergy")

Chemout=X.Variable.GetValue()

PumpchemEx.SetValue(Chemout-Chemin)


ErrorHandler:

End Sub
```

Appendix

Thermal exergy destruction, pump:

```
Sub VariableChanged()

On Error GoTo ErrorHandler


Dim Stream As Fluid

Dim PumptherEx As RealVariable

Set PumptherEx=ActiveVariableWrapper.Variable

Dim X As InternalVariableWrapper

Dim Feed As ProcessStream

Dim pump As PumpOp

Dim therin, therout As Double


Set X=ActiveObject.FeedStream.GetUserVariable("Thermal")

therin=X.Variable.GetValue()

Set X=ActiveObject.ProductStream.GetUserVariable("Thermal")

therout=X.Variable.GetValue()

PumptherEx.SetValue(therout-therin)


ErrorHandler:

End Sub
```

Mechanical exergy destruction, pump:

```
Sub VariableChanged()

On Error GoTo ErrorHandler


Dim Stream As Fluid

Dim PumpmechEx As RealVariable

Set PumpmechEx=ActiveVariableWrapper.Variable

Dim X As InternalVariableWrapper

Dim Feed As ProcessStream

Dim pump As PumpOp

Dim mechin, mechout As Double


Set X=ActiveObject.FeedStream.GetUserVariable("Mechanical")

mechin=X.Variable.GetValue()

Set X=ActiveObject.ProductStream.GetUserVariable("Mechanical")

mechout=X.Variable.GetValue()

PumpmechEx.SetValue(mechout-mechin)


ErrorHandler:

End Sub
```

Total exergy destruction, pump:

```
Sub VariableChanged()

On Error GoTo ErrorHandler:


Dim Pumptot As RealVariable

Set Pumptot=ActiveVariableWrapper.Variable

Dim X As InternalVariableWrapper

Dim phys,chem As Double


Set X=ActiveObject.GetUserVariable("PumpphysEx")

phys=X.Variable.GetValue()

Set X=ACtiveObject.GetUserVariable("PumpchemEx")

chem=X.Variable.GetValue()

Pumptot.SetValue(phys+chem)


ErrorHandler:

End Sub
```

Total exergy destruction, pump:

M. ECOS paper

The results in this thesis are used in a paper for the 26th international conference on efficiency, cost, optimization, simulation and environmental impact of energy systems, July 16-19, 2013, Guilin, China

M. ECOS paper

Comparative study of the sources of exergy destruction on four North Sea oil and gas platforms

Mari Voldsund[a], Tuong-Van Nguyen[b], Brian Elmegaard[c], Ivar Ståle Ertesvåg[d], Audun Røsjorde[e], Knut Jøssang[f] and Signe Kjelstrup[g]

[a] *Department of Chemistry, Norwegian University of Science and Technology, Høgskoleringen 5, 7491 Trondheim, Norway, mari.voldsund@ntnu.no*
[b] *Section of Thermal Energy, Department of Mechanical Engineering, Technical University of Denmark, Nils Koppels Allé, 2800 Kongens Lyngby, Denmark, tungu@mek.dtu.dk, CA*
[c] *Section of Thermal Energy, Department of Mechanical Engineering, Technical University of Denmark, Nils Koppels Allé, 2800 Kongens Lyngby, Denmark, be@mek.dtu.dk*
[d] *Department of Energy and Process Engineering, Norwegian University of Science and Technology, Kolbjørn Hejes vei 1b. 7491 Trondheim, Norway, ivar.s.ertesvag@ntnu.no*
[e] *Statoil ASA, Martin Linges vei 33, 1364 Fornebu, Norway, audr@statoil.com*
[f] *Department of Energy and Process Engineering, Norwegian University of Science and Technology, Kolbjørn Hejes vei 1b. 7491 Trondheim, Norway, knutjos@stud.ntnu.no*
[g] *Department of Chemistry, Norwegian University of Science and Technology, Høgskoleringen 5, 7491 Trondheim, Norway, signe.kjelstrup@ntnu.no*

Abstract:

In this paper, the oil and gas processing systems on four North Sea offshore platforms are reported and discussed. Sources of exergy destruction are identified and the findings for the different platforms are compared. Different platforms have different working conditions, such as reservoir temperatures and pressures, gas- and water-to-oil ratios in the feed, crude oil properties, product specifications and recovery strategies. These differences imply that some platforms naturally need less power for oil and gas processing than others. Reservoir properties and composition also vary over the lifetime of an oil field, and to maintain the efficiency of an offshore platform is therefore challenging. In practice, variations in the process feed result in the use of control strategies such as anti-surge recycling, which cause additional power consumption and exergy destruction. For all four platforms, more than 27% of the total exergy destruction takes place in the gas treatment section while at least 16% occurs in the production manifold systems. The exact potential for energy savings and for enhancing system performances differ across offshore platforms. However, the results indicate that the largest potential for improvement lie (i) in gas compression systems where large amounts of gas are often compressed and might be recycled to prevent surge, and (ii) in production manifolds where well-streams are depressurised and mixed before being sent to the separation system.

Keywords:
Exergy destruction, oil and gas processing, energy-intensive techniques, thermodynamic efficiency

1. Introduction

Oil and gas processing on North Sea offshore platforms consume substantial amounts of power and have a significant environmental impact, being responsible for about 26% of the total CO_2 emissions of Norway in 2011 [1]. Onsite processes on offshore facilities suffer from significant performance losses over the lifetime of the installation, as a consequence of substantial variations of the reservoir properties (e.g. pressure and temperature) and of the production flow rates and composition changes (e.g. gas- and water-to-oil ratios, crude oil properties). These off-design conditions lead to the use of control strategies such as anti-surge recycling, and thus to greater power consumption and larger exergy destruction. Moreover, as the oil production decreases with

1

time, energy-intensive techniques such as gas and water injection are employed to enhance oil recovery from the reservoir. It is therefore challenging to maintain a high performance of the overall system over time, while optimising the oil and gas production.

Svalheim and King [2,3] stressed the large power demand of the gas compression and water injection processes over the lifespan of the oilfield. Their studies also emphasised the benefits that resulted from applying best practices in energy management (e.g. gas turbine operation near design load, reduction of flaring and venting practices, and integration of waste heat recovery). Similarly, Kloster [4,5] argued that these measures could and did contribute to significant energy savings and a reduction of the CO_2-emissions of the Norwegian oil and gas installations. A mapping of the thermodynamic inefficiencies is useful, as it indicates rooms for improvements in a rational manner. Such information can be obtained by carrying out an exergetic analysis, which is based on both the 1st and 2nd laws of thermodynamics. The exergy of a system is defined as the maximum theoretical ability to do work in interaction with the environment, and is, unlike energy, not conserved in real processes [6,7]. An exergy accounting reveals the locations and extents of thermodynamic irreversibilities present in a given system and these irreversibilities account for a greater fuel use throughout successive processes [8].

Oliveira and Van Hombeeck [9] conducted an exergy analysis of a Brazilian oil platform which included the separation, compression and pumping modules but not the production manifolds. Their work showed that the least exergy-efficient subsystem was the oil and gas separation, while the most exergy-consuming ones were the petroleum heating and the gas compression processes. Voldsund et al. [10] carried out an exergy analysis of a Norwegian oil platform and considered the production manifold, the separation and recompression processes, the fuel gas subsystem and the oil pumping and gas reinjection trains. Their study demonstrated that the largest exergy destruction took place in the production manifold and in the gas reinjection systems. There was no considerable petroleum heating operations on this platform, since the feed temperature was high enough for separation of the specific oil by pressure reduction only: there was therefore no exergy destruction due to heating operations. Nguyen et al. [11] conducted a generic analysis of Norwegian oil and gas facilities. Their work suggested that the production manifold and gas compression trains were generally the most exergy-destructive parts, followed by the recompression and separation modules. It was also shown that these results were particularly sensitive to the compressor and pump efficiencies, as well as to the petroleum composition.

The similitudes and discrepancies in the results of these studies suggest that differences in the design setup and in the field conditions may affect the locations and extents of the thermodynamic irreversibilities of the overall system. The literature appears to contain no systematic comparison of the sources of exergy destruction for oil and gas platforms. Therefore, in this work, the platform analysed by Voldsund et al. [10] is compared with three other North Sea offshore platforms, which have not been studied in this manner before. The work was carried out in three main steps:

- simulation and investigation of the platforms;
- exergy accounting and analysis;
- comparison of the four platforms, based on the outcomes from the two previous steps.

The present paper is part of two larger projects dealing with modelling and analysis of oil and gas producing platforms. It builds on previous works conducted by the same authors and is structured as follows. *Section 2* describes the methodology followed in this work, with a strong emphasis on the system description and on the similarities and differences between the four cases. *Section 3* presents a comparison of the results obtained for each platform. Explanations and discussions are detailed in *Section 4* and are followed by concluding remarks in *Section 5*.

2. Methodology

2.1. System description

The structural designs of the oil and gas processing at the four platforms are similar. Meanwhile, different reservoir fluid characteristics and reservoir properties as well as different requirements for the products, have led to dissimilar temperatures, pressures and flow rates throughout the process, and different demands for compression, heating, cooling and dehydration.

In Section 2.1.1 we give a generalised overview of the oil and gas processing system for the studied platforms, in Section 2.1.2 we present key information on the platforms, to indicate the main differences between them, and in Section 2.1.3 we list process data that are important to explain the varying results for the platforms. The appendix contains detailed process flowsheets for the four platforms, see Figs. A.1 – A.4.

2.1.1. A generalised overview of the processing system

A generalised overview of the oil and gas processing at the four platforms is shown schematically in Fig. 1. Well fluids from several producing wells (1) enter one or more production manifolds where pressure is reduced and streams from the different wells are mixed. The mixed streams (2) are sent to a separation train where oil, gas and water are separated in several stages by reducing pressure. Heating may be required in the separation process.

Oil or condensate (3) is sent to the main oil/condensate treatment section where it is pumped for further export (4). Produced gas is compressed in a recompression train to match the pressure of the stream entering the separation train (2). This compression is done in several stages, each stage with a cooler, a scrubber and a compressor. Condensate from the recompression train is sent back to the separation train, while compressed gas is sent to the gas treatment section.

The produced gas is treated differently on the four platforms, with different demands for compression and dehydration, depending on the properties of the gas and on whether the product (5) is to be exported or used for enhanced oil recovery (injection or gas lift). On one of the platforms additional gas is imported (10) and compressed in this section. Condensate from the gas treatment is either recycled to the separation train or pumped, dehydrated and exported (6) in a separate condensate treatment section. Fuel gas is taken from one of the streams with produced gas, treated in a fuel gas system and sent (9) to the power turbines, and for two of the platforms also to the flares for pilot flames.

Produced water is treated and either discharged to the sea (7) or injected into another reservoir (8). Seawater (11) may be compressed for injection into the reservoir for enhanced recovery (12).

2.1.2. Key information on the studied platforms

The studied platforms are labelled Platform A, B, C and D, and main characteristics for each of them are given below:

- Platform A has been in production for approximately 20 years and is characterised by a high gas-to-oil ratio. Oil is pumped to a nearby platform while gas is injected into the reservoir for pressure maintenance. Water injection is also used as a recovery technique, but the injection water is produced at another platform, and is therefore not taken into consideration in this analysis. Produced water is discharged to the sea. Platform A was investigated in previous works from the same authors and more details of the analysis can be found in [10].

- Platform B has been in production for approximately 10 years. It has high reservoir temperature, pressure and gas-to-oil ratio and produces gas and condensate through pressure depletion. The exported gas is not dehydrated. Produced water is injected into another reservoir for disposal.

Power consumption is small because of a relatively low compression demand. There is some heat integration between process streams with cooling- and heating demand.
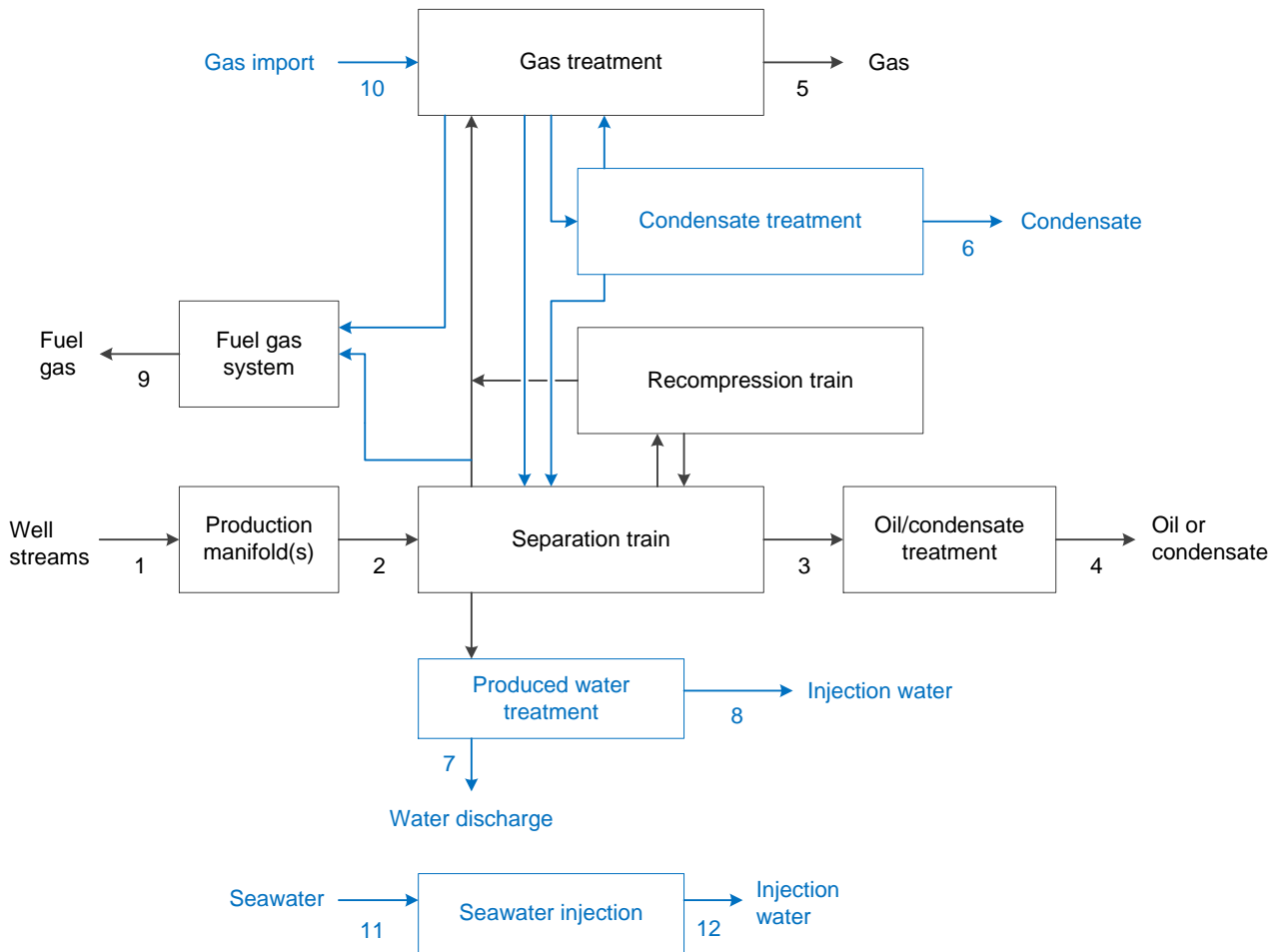

Fig. 1. A generalised overview of the oil and gas processing on a North Sea platform. The arrows represent one or several mass streams while the blocks represent subsystems. Black arrows and blocks are the same for all the studied platforms. Blue arrows and blocks are not present at all four platforms.

- Platform C has also been in production for approximately 10 years. It produces oil with high viscosity, and heating is required for the crude oil-water separation. The heating demand is met by waste heat recovery from the exhaust gases exiting the gas turbines, and by heat integration with other process streams. Gas lifting is used in order to decrease the density of the oil and enhance recovery, and gas is also injected into the reservoir for pressure maintenance. Due to the low gas-to-oil ratio, gas is imported for injection and gas lifting purposes. Produced water is discharged to the sea.
- Platform D has been in production for approximately 20 years, and gas, oil and condensate is exported. The treatment and export of condensate is due to a high propane content in the reservoir fluid, and is done to prevent recirculation of medium-weight alkanes in the recompression train and extra power consumption. Both gas and condensate are dehydrated. Heating is required to enhance separation of oil, gas and water, and for regenerating the glycol used for dehydration. Gas lifting and water injection is used to enhance oil recovery.

The gas-to-oil ratios and product flow rates for each of the studied platforms are given in Table 1.

Table 1. Gas-to-oil ratios and product flow rates for the studied oil and gas platforms. Gas-to-oil ratio is given on a standard volume basis, with a standard temperature of 15°C and pressure of 1.013 bar.

	Platform A	Platform B	Platform C	Platform D
Gas-to-oil ratio, -	2800	3200	350	260
Exported oil, Sm^3/h	133	-	1094	195
Exported condensate, Sm^3/h	-	239	-	7.6
Exported gas, $10^3 Sm^3/h$	-	761	-	7.2
Injected gas, $10^3 Sm^3/h$	369	-	362	-
Lift gas, $10^3 Sm^3/h$	-	-	22	45.2
Produced water, Sm^3/h	67	18	8	1332
Injected water, Sm^3/h	-	-	-	919

2.1.3. Process details

Temperatures and pressures for key streams are given in Table 2. The following points are essential for the outcome of the analysis:

- Pressure is reduced in the production manifold and the separation train. Well stream pressures, P_1, and pressures into the separation train, P_2, vary between the platforms, while pressure out of the separation train, P_3, is between 1.7 and 2.8 bar for all platforms, due to vapor pressure requirements for the oil/condensate export.
- Heating is required in the separation train on Platform C, even if the separation train inlet temperature, T_2, is almost as high as on Platform A. This is in order to avoid problems with emulsions and to enhance separation between oil and water, which might be problematic due to the high viscosity of the crude.
- In the export pumping section the pressure of the produced oil or condensate is increased from P_3 to P_4. The magnitude of P_4 depends on the export pipeline requirements.
- The gas treatment section varies between the platforms, depending on the conditions of the incoming gas, and the planned use of it. On Platforms A, C and D the pressure is increased from P_2 to P_5, since the produced gas is to be injected, used for gas lifting or exported at a pressure higher than P_2. On Platform B the gas is not compressed. Since the well-stream pressure is high, they can allow a pressure at the outlet of the production manifold higher than the pressure required for export, so P_5 is lower than P_2. For a detailed overview of the structural design of this section in each of the platforms, we refer to Figs. A.1 – A.4.
- The imported gas on Platform C is compressed from P_{10} to P_5 in the gas treatment section.
- The produced water on Platforms B and C is compressed from P_7 to the injection pressure, P_8, while on platform D the seawater is compressed from P_{11} (ambient) to P_{12} and injected.

Table 2. Pressures and temperatures in the oil- and gas processing of the studied oil and gas platforms.

Stream number (type)	Platform A p (bar)	Platform A T (°C)	Platform B p (bar)	Platform B T (°C)	Platform C p (bar)	Platform C T (°C)	Platform D p (bar)	Platform D T (°C)
1 (reservoir fluids)	88 – 165	80 – 87	122 – 155	64 – 111	13 – 110	51 – 73	15 – 187	55 – 74
2 (reservoir fluids)	70	74	120	106	46[a] 8[b] 14[c]	61[a] 66[b] 60[c]	8	49 –67 63[c]
3 (oil/condensate)	2.8	55	2.4	63	2.7	96	1.7	45 – 55
4 (oil/condensate)	32	50	107	56	99	76	50	61 – 68
5 (treated gas)	236	78	118	35	184	75	179	81
6 (condensate)	-	-	-	-	-	-	179	68
7 (produced water)	9	73	-	-			1.3	55
8 (produced water)	-	-	61	80	7.2	62	127-147	57
9 (fuel gas)	18	54	37	50	-	-	-	-
10 (gas import)	-	-	-	-	110	4.4	-	-
11 (seawater)	-	-	-	-	-	-	1.0	8
12 (seawater)	-	-	-	-	-	-	127 – 147	57

a) From high pressure manifold

b) From low pressure manifold

c) From test manifold

Since flow rates throughout the process change over the field lifetime, some parts will be run at other flow rates than the process equipment was designed for. To avoid compressor surging in this situation, gas is recycled around the compression stages, to keep a minimum flow rate through the compressor. The recycled gas is also sent through the cooler and the scrubber of the compression stage, to keep a low temperature and to avoid liquid in the compressor. The gas recycling rates around compressor stages in the various compression sections of the four platforms are given in Table 3. There is anti-surge recycling in the recompression trains of all the platforms, while in the gas treatment section there is recycling of the imported gas in Platform B and of the produced gas in Platform D.

Table 3. Anti-surge recycle rates in the various compression sections of the studied oil and gas platforms, given as percentage of the flow through the compressors.

	Platform A	Platform B	Platform C	Platform D
Recompression train	69 – 92%	4 – 33%	19 – 40 %	65 – 75%
Gas treatment, produced gas compression	0%	-	0%	5 – 35%
Gas treatment, import gas compression	-	-	23%	-

2.2. Process simulation

The process simulations of Platforms A and C were carried out with Aspen HYSYS® version 7.3 [12] using the Peng-Robinson equation of state [13], while for Platform B the same software was used, but with the Soave-Redlich-Kwong equation of state [14]. The water purification processes were neglected for Platforms A-C. Platform D was simulated with Aspen Plus® version 7.2 [15] using the Peng-Robinson equation of state and the Non-Random Two Liquid model [16], with the exception of the glycol dehydration system that was simulated using the glycol property package of Aspen HYSYS® [12]. The water purification and injection processes of Platform D were simulated based on the Non-Random Two Liquid model and the dehydration process on the glycol property package of Aspen HYSYS® [12].

The test manifold was merged together with the 1st stage separator in the simulations of Platforms A and B, while it was included as an independent separator in the simulations of Platforms C and D.

The well fluids are complex mixtures of crude oil, gas and water, and in all cases these fluids were simulated using a mix of real chemical components such as water and methane, as well as hypothetical components that describe the heavier oil fractions.

2.3. Exergy analysis

Exergy analysis is a well-established field. However, to facilitate reading we repeat the equations essential to this study. For a thorough introduction to exergy analysis, see for instance the textbook of Kotas [6].

2.3.1 Exergy accounting

An exergy accounting was performed to identify the sources of thermodynamic inefficiencies in the four cases investigated. Internal irreversibilities within the oil and gas processing units are responsible for entropy generation and thus exergy destruction, and can be calculated from an exergy balance [8].

For an open control volume in steady-state conditions, the exergy destruction rate, $\dot{E}_d$, is defined as the difference between the rates of exergy entering a system, $\dot{E}_{in}$, and of exergy leaving it, $\dot{E}_{out}$:

$$\dot{E}_d = \sum \dot{E}_{in} - \sum \dot{E}_{out} = \dot{E}_W + \dot{E}_Q + \sum_j \dot{m}_j e_j, \tag{1}$$

where $\dot{E}_W$ and $\dot{E}_Q$ are the rates of exergy accompanying work and heat, respectively. For simplicity we name these variables power and heat exergy in the rest of this study. The symbols $\dot{m}_j$ and e_j represent the mass flow rate and the specific exergy of the stream of matter j. The exergy balance can also be expressed as [17]:

$$\dot{E}_p = \dot{E}_u - \dot{E}_d - \dot{E}_l, \tag{2}$$

where:

- $\dot{E}_p$ is the rate of product exergy, which corresponds to the desired output of the system;
- $\dot{E}_u$ is the rate of utilised or fuel exergy, representing the resources needed to drive the system;
- $\dot{E}_l$ is the rate of exergy losses, which is associated with the transport of exergy to the surroundings with energy and material streams (external irreversibilities).

2.3.2 Exergy transfer

The exergy transported with a stream of matter, e, can be expressed as the sum of its kinetic, e^{kin}, potential, e^{pot}, physical, e^{ph}, and chemical components, e^{ch} [8]:

$$e = e^{kin} + e^{pot} + e^{ph} + e^{ch}. \tag{3}$$

The specific physical exergy accounts for differences in temperature and pressure in reference to the ambient conditions (T_0, p_0) without changes in chemical composition. It is defined as:

$$e^{ph} = (h - h_0) - T_0(s - s_0), \tag{4}$$

where h and s are the specific enthalpy and entropy calculated at the stream conditions and h_0 and s_0 at ambient temperature, T_0, and pressure, p_0. The specific chemical exergy accounts for differences in chemical composition with a reference environment and can be expressed, on a mass basis, as:

$$e^{ch} = \underbrace{\sum_i x_i \bar{e}_i}_{\text{I}} + \underbrace{\left[\left(h_0 - \sum_i x_i h_{i,0}\right) - T_0\left(s_0 - \sum_i x_i s_{i,0}\right)\right]}_{\text{II}} = \underbrace{\sum_i x_i \bar{\bar{e}}_i}_{\text{III}} \tag{5}$$

where the term I represents the chemical exergy of the pure components, with x_i the mass fraction and $\bar{e}_i$ the specific chemical exergy. The term II corresponds to the decrease of chemical exergy due to mixing effects, with $h_{i,0}$ the chemical enthalpy of the pure component i at ambient conditions, and $s_{i,0}$ the corresponding entropy. The term III denotes the chemical exergy of the components in

7

the mixture, with $\overline{\overline{e_i}}$ the specific chemical exergy of the component i in the mixture. The specific potential and kinetic exergies are equal to the potential and kinetic energies, respectively.

2.3.3. Calculation details

The ambient temperature and pressure used in the calculation of physical exergy and the mixing part of the chemical exergy were 8°C and 1 atm. The chemical exergy of the pure components were taken as presented by Kotas [6] for the real chemical components and calculated following the method of Rivero [18] for the hypothetical components. Potential and kinetic exergy were assumed negligible in comparison with chemical and physical exergy in the present cases.

3. Results

The amounts of exergy exported from each of the platforms as oil, condensate or gas, together with the consumption of exergy in form of heat and power are given in Table 4. The chemical exergy in the oil and gas that passes through the system is very high compared to the exergy changes within the system. The consumption of power and heat exergy is less than 2% of the exergy exported for all the platforms.

Table 4. Exergy exported, and power- and heat exergy consumed on the studied platforms.

		Platform A	Platform B	Platform C	Platform D
Exergy exported	MW	1 400	11 000	12 600	2190
Power exergy consumption	MW	24.6	5.5	29.8	23.3
Heat exergy consumption	MW	0	0.3	4.7	0.9

The power and heat exergy, which are consumed in each subsystem for the four platforms, are presented in absolute numbers and per oil equivalent in Fig. 2 and Fig. 3, respectively. It is shown that:

- Power is mainly used for compression in the recompression sections, gas treatment sections and oil/condensate sections.
- On Platform D a significant amount of power is also used for compression in the water injection system.
- No power is required in the gas treatment section on Platform B, at the difference of the three other platforms, because the feed pressure (P_1) at the inlet of the separation subsystem is high enough to meet the export specifications (P_5).
- In the separation section on Platform C, about a third of the exergy used for crude oil heating comes from heat integration with other product streams, while the remaining two thirds come from waste heat from the power turbines.
- The heating demand of the gas treatment and oil/condensate treatment sections on Platform D (in the dehydration processes) is met by recovering waste heat from the power turbines and to a minor extent by heat integration.
- Power used for heating in the fuel gas systems and for compression in produced water handling is negligible compared to the exergy consumption in other subsystems.
- Power and heat exergy consumed per oil equivalent is highest for Platform A, followed by Platform D, while it is relatively small for Platforms B and C.
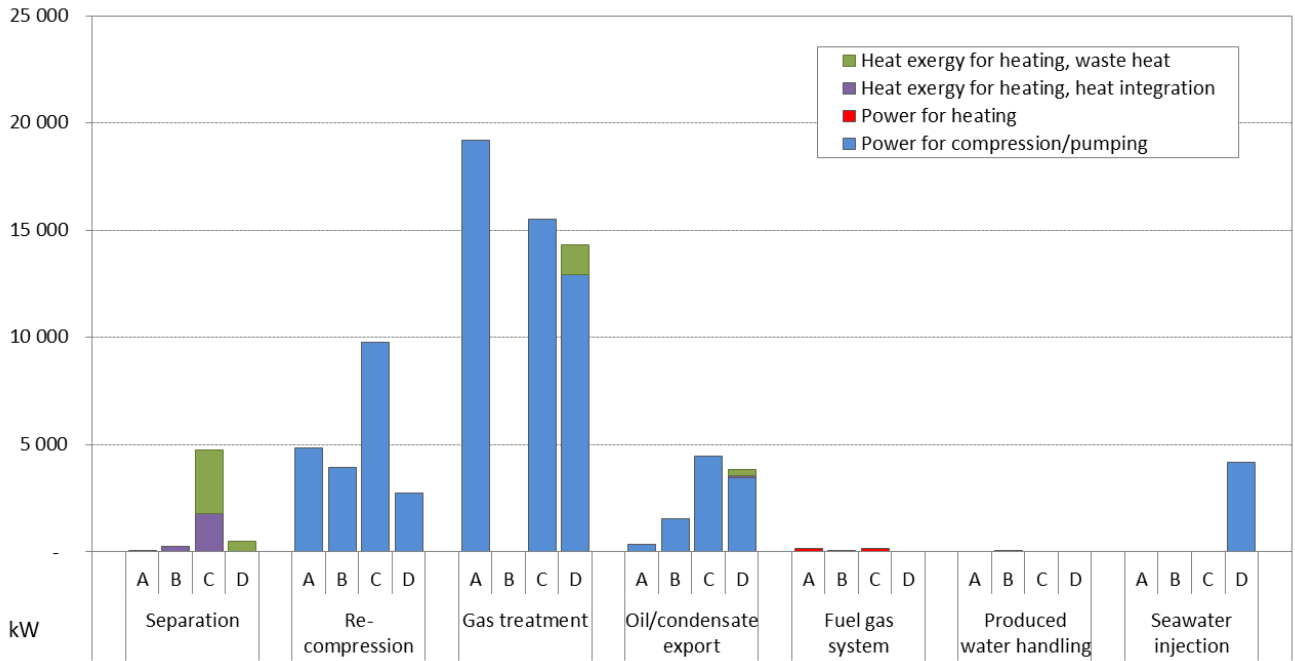
Fig. 2. Power and heat exergy consumed in each subsystem for the studied platforms (Platforms A - D). The production manifolds are not included, since no power and heat exergy is consumed there. The thermal energy labelled 'waste heat' is from a heating medium that is heated with waste heat from the power turbines. The thermal energy labelled 'heat integration' is from heat integration with other process streams.
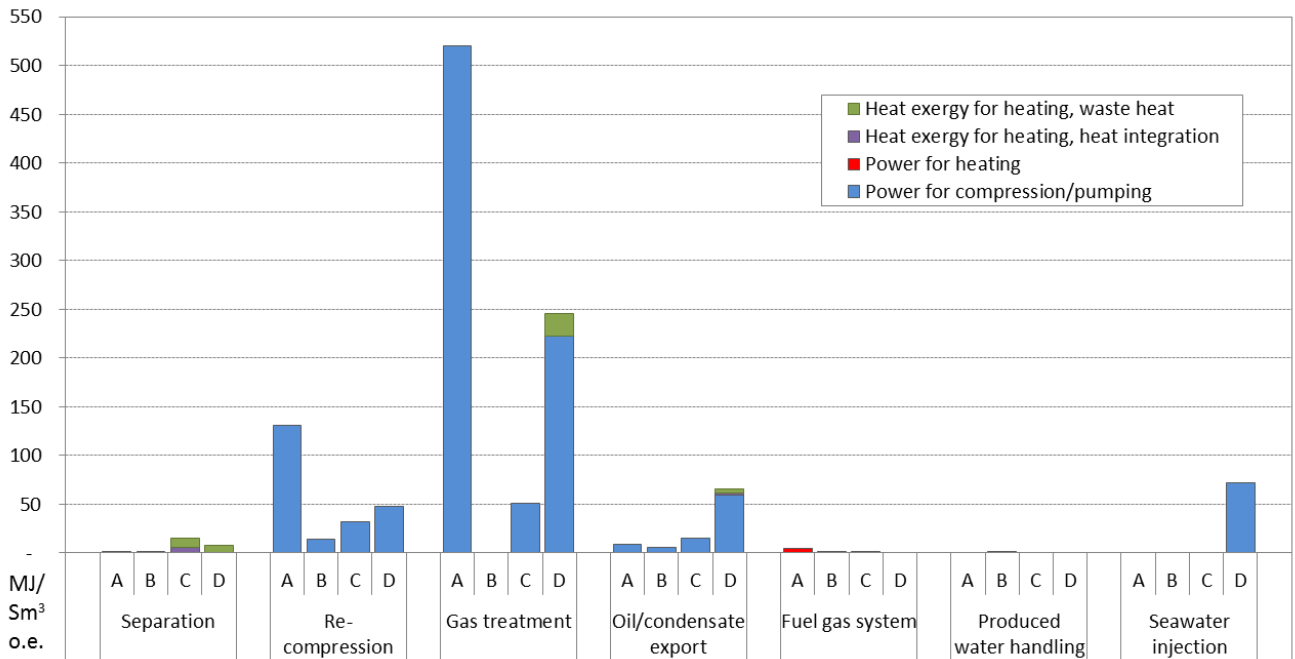

Fig. 3. Power and heat exergy consumed per exported oil equivalent (o.e.) in each subsystem for the studied platforms (Platforms A - D). The production manifolds are not included, since no power and heat exergy is consumed there. The thermal energy labelled 'waste heat' is from a heating medium that is heated with waste heat from the power turbines. The thermal energy labelled 'heat integration' is from heat integration with other process streams. The following conversion factors are used when converting to o.e: 1 Sm^3 oil = 1 Sm^3 condensate = 1000 Sm^3 gas = 1 Sm^3 o.e.

9

In Fig. 4 exergy destruction and exergy lost with cooling water in each subsystem for each of the platforms are given and in Fig. 5 the same values are given as percentage for each platform. In general, the highest contributions to exergy destruction and exergy losses are due to:

▪ throttling in production manifolds and separation trains;
▪ irreversibilities in coolers and losses with cooling medium;
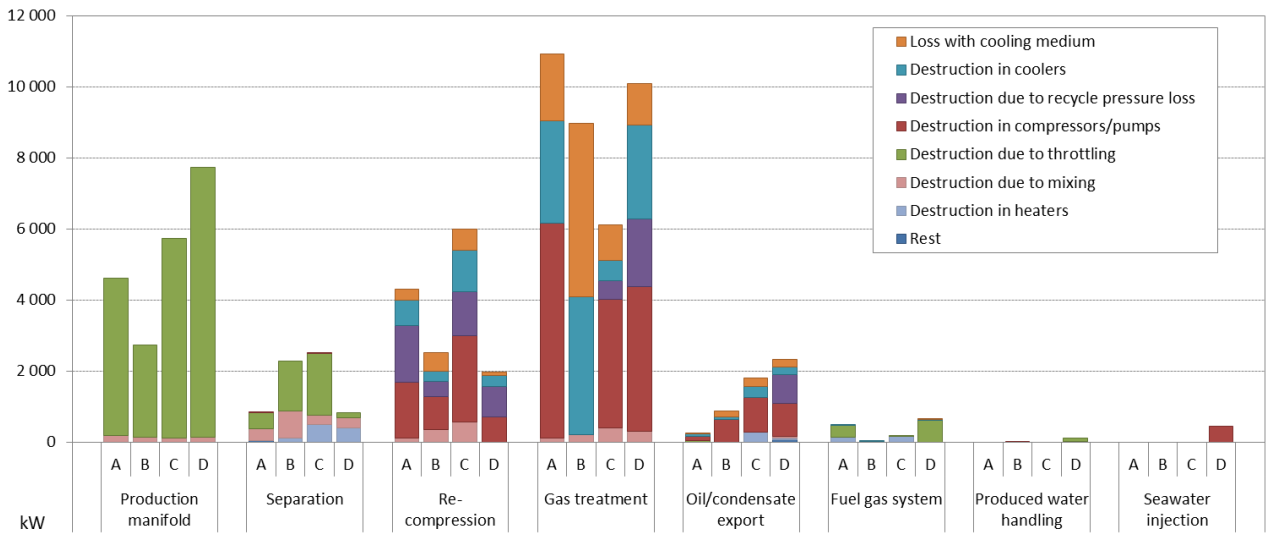▪ inefficiencies in compressors and anti-surge recycling.

Fig. 4. Exergy destruction and loss in each subsystem for the studied platforms (Platforms A – D). The main sources of exergy destruction/loss in each subsystem are indicated with different colours, and smaller sources are lumped into 'rest'.
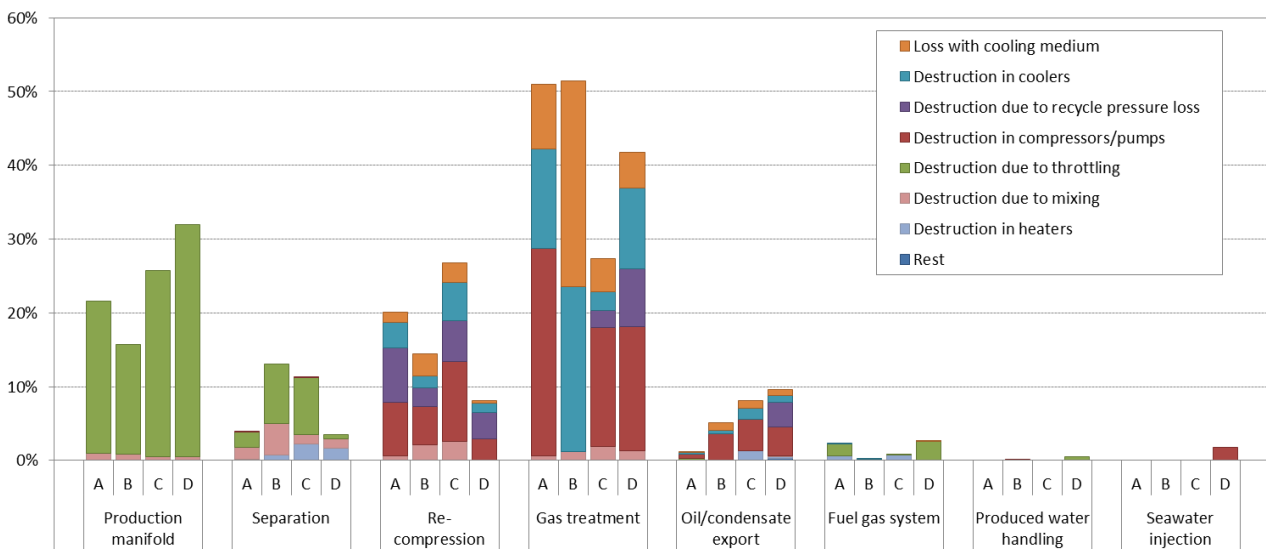
Fig. 5. Percentage of exergy destruction and loss in each subsystem for the studied platforms (Platforms A – D). The main sources of exergy destruction and loss in each subsystem are indicated with different colours, and smaller sources are lumped into 'rest'.

10

A more detailed investigation of Fig. 5 shows the following about the locations and sources of exergy destruction and losses on the four platforms:

- Exergy destruction in production manifolds represents 16–32% of the total exergy destruction at the four platforms.
- Exergy destruction due to throttling in separation trains accounts for 1–8%.
- Exergy destroyed in compressors amounts to 20–35%, with the exception of Platform B where it amounts to only 5%.
- On Platform B, 50% is due to cooling in the gas treatment section.
- Exergy destruction due to pressure loss in recycled streams amounts to 3–15% for the four platforms.
- Exergy destruction in the crude oil heater makes up approximately 2% for both Platforms C and D.
- The exergy destruction and losses in the oil/condensate export system of Platform A accounts for 1%, while for Platforms B − D it accounts for 5−10%.
- Exergy destruction and losses in the fuel gas, produced water handling and seawater injection systems are of minor importance compared to the other studied systems.

The exergy destroyed and lost per exported oil equivalent in each subsystem for the four platforms are shown in Fig. 6. Platforms A and D have clearly more inefficiencies per oil equivalent than Platforms B and C. They are older than the other two platforms and have export flow rates that are low compared to their peak production. Platform A has a high gas-to-oil ratio, injects gas and exports only oil. The injection of gas makes a high oil recovery from the reservoir possible but is responsible for considerable power consumption and exergy destruction:

- The high amount of gas that is not exported gives high exergy destruction per exported oil equivalent in the production manifold.
- In the recompression train, recycling of gas to prevent compressor surging has led to almost constant flow rates, and thus exergy destruction and losses, even if the amount of oil in the separation train has decreased.
- The high exergy destruction and loss per exported oil equivalent in the gas treatment section is because here a significant amount of compression work is done to produce gas that is not exported but used for enhanced oil recovery.

Platform D has a low gas-to-oil ratio, uses gas, produced water and seawater for lift and injection, and exports oil, gas and condensate. The high exergy destruction per exported oil equivalent results both from the large amount of power required to compress the gas and from the depressurisation of the reservoir fluid in the production manifold.
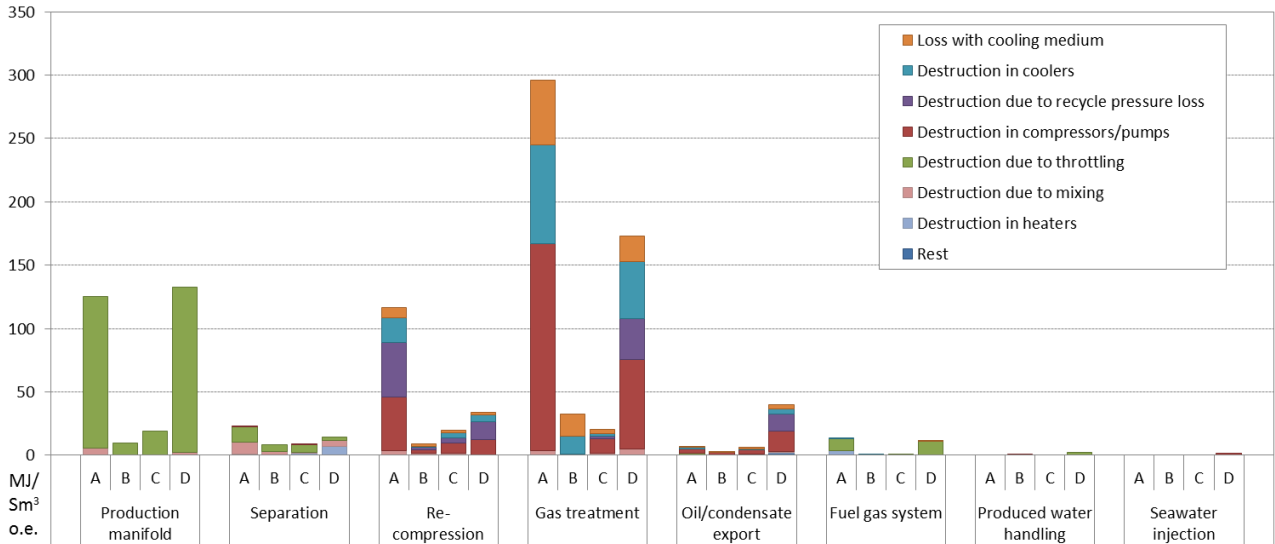
Fig. 6. Exergy destruction and loss per exported oil equivalent (o.e.) in each subsystem for the studied platforms (Platforms A-D). The main sources of exergy destruction/loss in each subsystem are indicated with different colours, and smaller sources are lumped into 'rest'.

4. Discussion

We have mapped exergy consumption and exergy destruction and losses in the oil and gas processing system of four oil and gas platforms. These results can be compared to the previous findings of Bothamley [19] and Svalheim [2,3]. They stressed the great power consumption associated with the gas treatment, recompression and oil pumping steps of various oil and gas facilities located in the North Sea region and in the Gulf of Mexico, which is confirmed by the present analysis. They also stressed the high power demand due to water injection, which was only significant on Platform D, as this is the only facility where it is implemented.

These authors [2,3,19] also suggested several efficiency measures, such as the re-wheeling of the turbo-machinery components, to reduce the power consumption of the processing plant. The same was suggested after the exergy analysis of Platform A [10] and of a generic platform simulation [11]. These studies, together with the present results, indicate the importance of gas compression subsystems when monitoring oil and gas facilities and trying to improve their performance. In the two latter references, production manifolds were also pointed out as sections with high losses, and ways to reduce these losses are discussed.

Oliveira and Van Hombeeck [9] investigated a real-case oil facility located in Brazil. The gas delivery pressure was about 174 bar, which is similar to the pressure requirements of the gas produced on the Platforms A, B and D. In these four cases, the gas treatment step ranks as one of the most exergy-consuming subsystems. This suggests that improvement measures could well focus on this particular part of the processing system and on the subsystems interacting with it. However, they also emphasised the large exergy consumption of the heating operations taking place within the separation system, which was small or inexistent on the four platforms analysed in this work. For the two cases with some crude oil heating in this work, the heating demand was small enough to be covered by waste heat recovery from the exhaust gases exiting the gas turbines, and by heat integration with other process streams, while for the Brazilian case a furnace was required for crude oil heating in addition to a gas turbine heat recovery system. This discrepancy is mainly due to the differences in feed characteristics between the North Sea and the Brazilian Gulf regions. The temperature at the inlet of the separation was 7.4°C in their case, whilst it is between 45°C and 75°C for the four North Sea platforms described here. Seemingly, smaller systems such as the fuel gas, produced water and seawater injection systems contribute only to a minor extent to the total exergy destruction of the processing plant, which was also shown in their work.

Platform B had much lower power consumption per produced oil equivalent than the other three platforms in this study. The first separation stage takes place at a high pressure, avoiding the need for gas compression before export. Operating the first separation stage at as high pressure as possible reduces the exergy destruction in the production manifold, and the power consumption and exergy destruction in the gas treatment system. This illustrates that it is not sufficient to consider a single subsystem for improving the thermodynamic performance of the platform, but to also investigate the interactions and dependences between them.

The four platforms that are compared within this study are all of the North Sea platform type, and they represent some of the variety within this group of platforms, with production of heavy and viscous oil to condensate and gas, and different reservoir pressures and product specifications. The results common for these four platforms, such as high thermodynamic losses due to throttling in production manifolds and inefficient compression when feed conditions change over time, are therefore expected to be typical for a large part of the North Sea oil and gas platforms, which is supported by the findings in the generic analysis conducted by Nguyen et al. [11]. At the same time, the variations in power consumption and exergy destruction in the gas treatment section show the great differences that exist between North Sea platforms. The results depend strongly on factors such as (i) the efficiency and the control strategies of the turbo-machinery components (ii) the integration of additional subsystems such as condensate export and (iii) the outlet specifications of the processing plant. In addition, the differences between the platforms analysed in this study and the Brazilian case shows that caution should be exercised when extending the present conclusions to platforms in other regions of the world. Each oil platform should therefore be analysed individually, to pinpoint major sources of exergy destruction on that specific facility.

5. Conclusion

Exergy analyses were performed on the oil and gas processing systems on four North Sea oil and gas platforms, which differ by their operating conditions and strategies. The comparison of the exergy destruction sources illustrated the large exergy destruction associated with the gas treatment and production manifold systems, ranging above 27% and 16%, respectively. The fuel gas and seawater injection processes represent less than 3% each in every case.

However, the contributions of the recompression, separation and oil export sections vary significantly across the different platforms. Although the precise values of the exergy destruction rates differ from one platform to another, the main causes can be identified with the depressurisation in the production manifold, the compressor inefficiencies, and the heat transfers processes in the coolers.

Acknowledgements

Appendix

This appendix contains process flowsheets for the four platforms, given in Figs. A.1–A.4. Details on process data for Platform A can be found in [10].
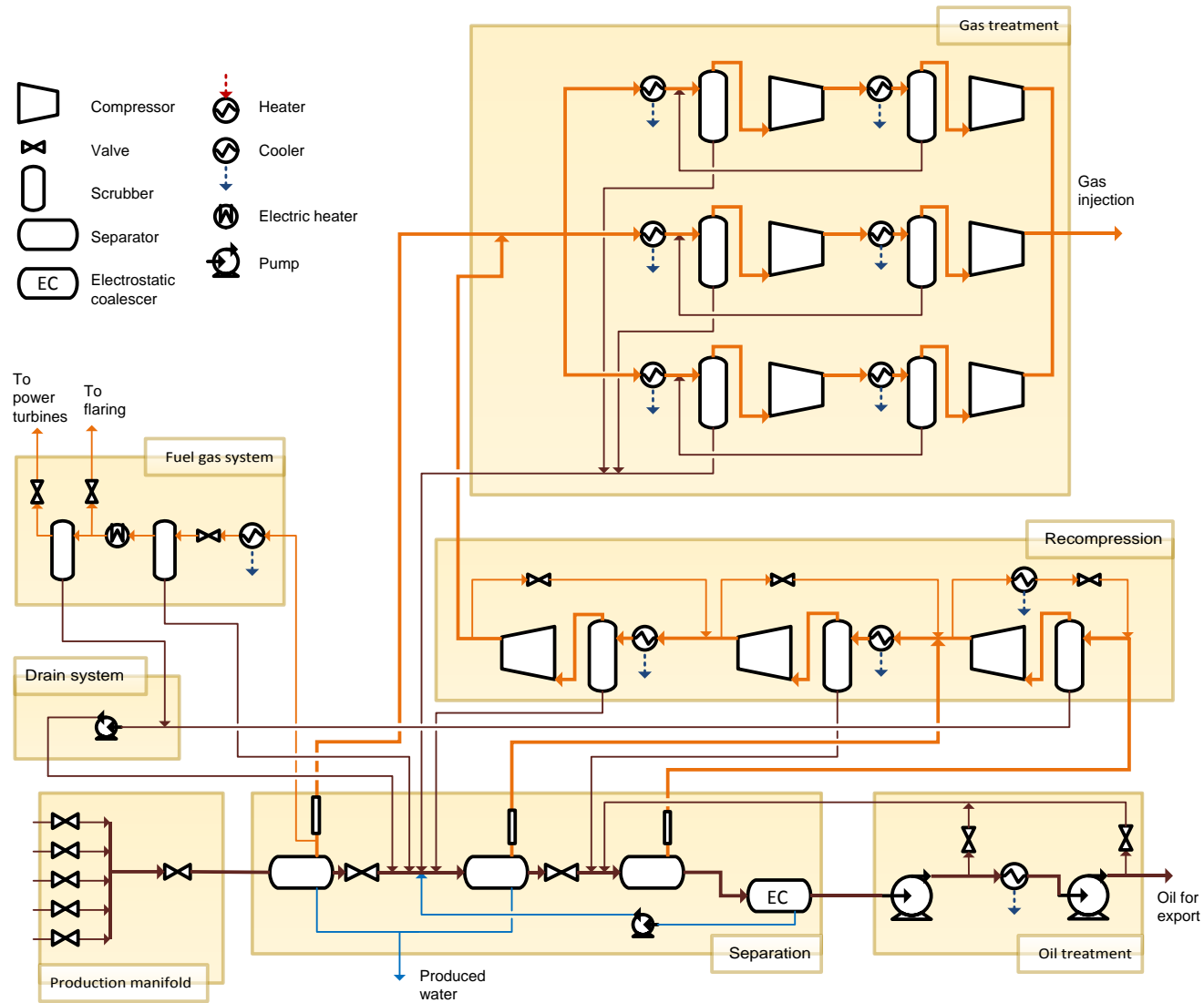
Fig. A.1. Process flowsheet of Platform A. Gas streams are shown with orange arrows, water streams with blue arrows, and oil, condensate and mixed streams are shown with brown arrows.
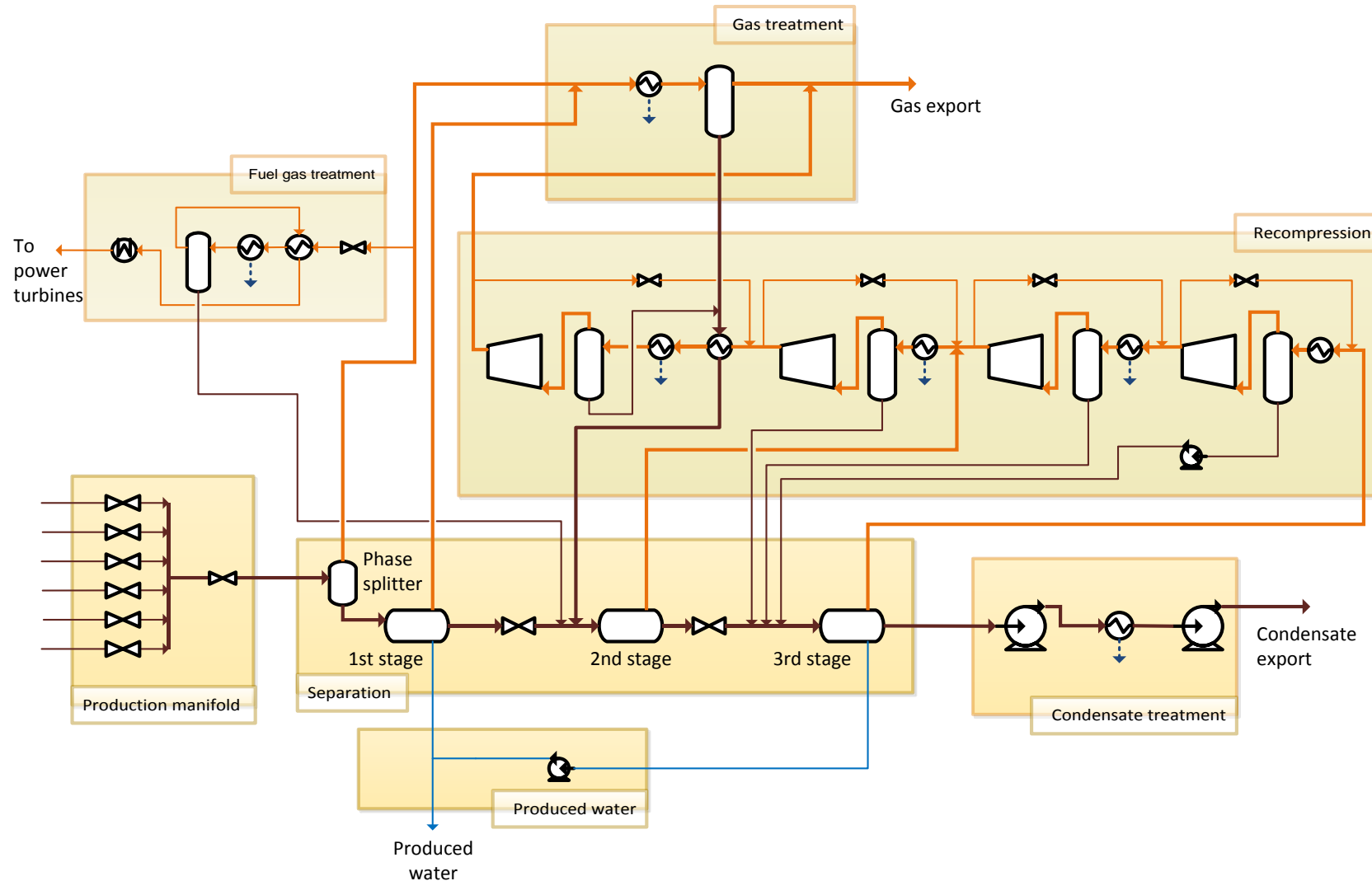
Fig. A.2. Process flowsheet of Platform B Gas streams are shown with orange arrows, water streams with blue arrows, and oil, condensate and mixed streams are shown with brown arrows. Symbol explanations can be found in Fig. A.1.
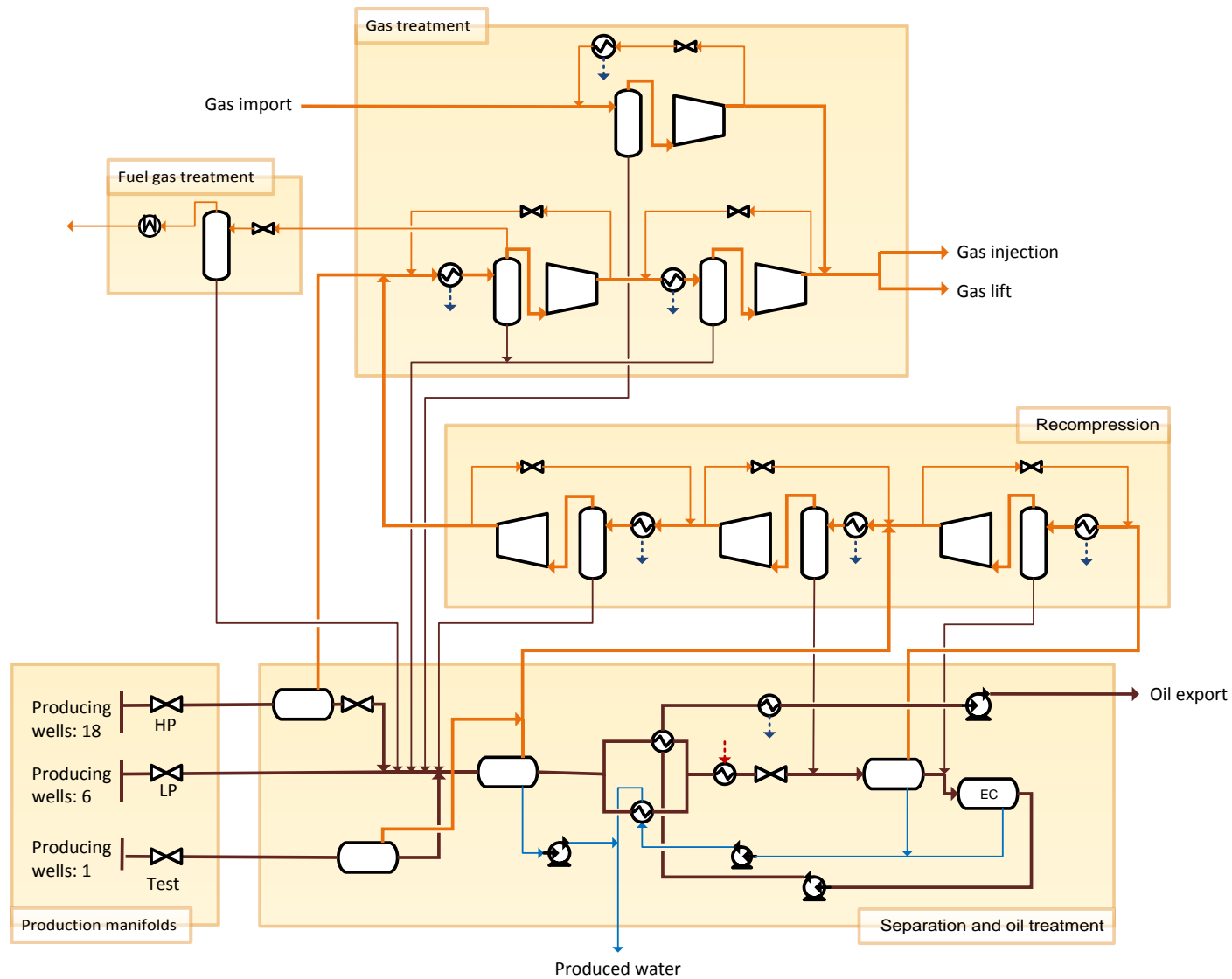
Fig. A.3. Process flowsheet of Platform C. Gas streams are shown with orange arrows, water streams with blue arrows, and oil, condensate and mixed streams are shown with brown arrows. Symbol explanations can be found in Fig. A.1.
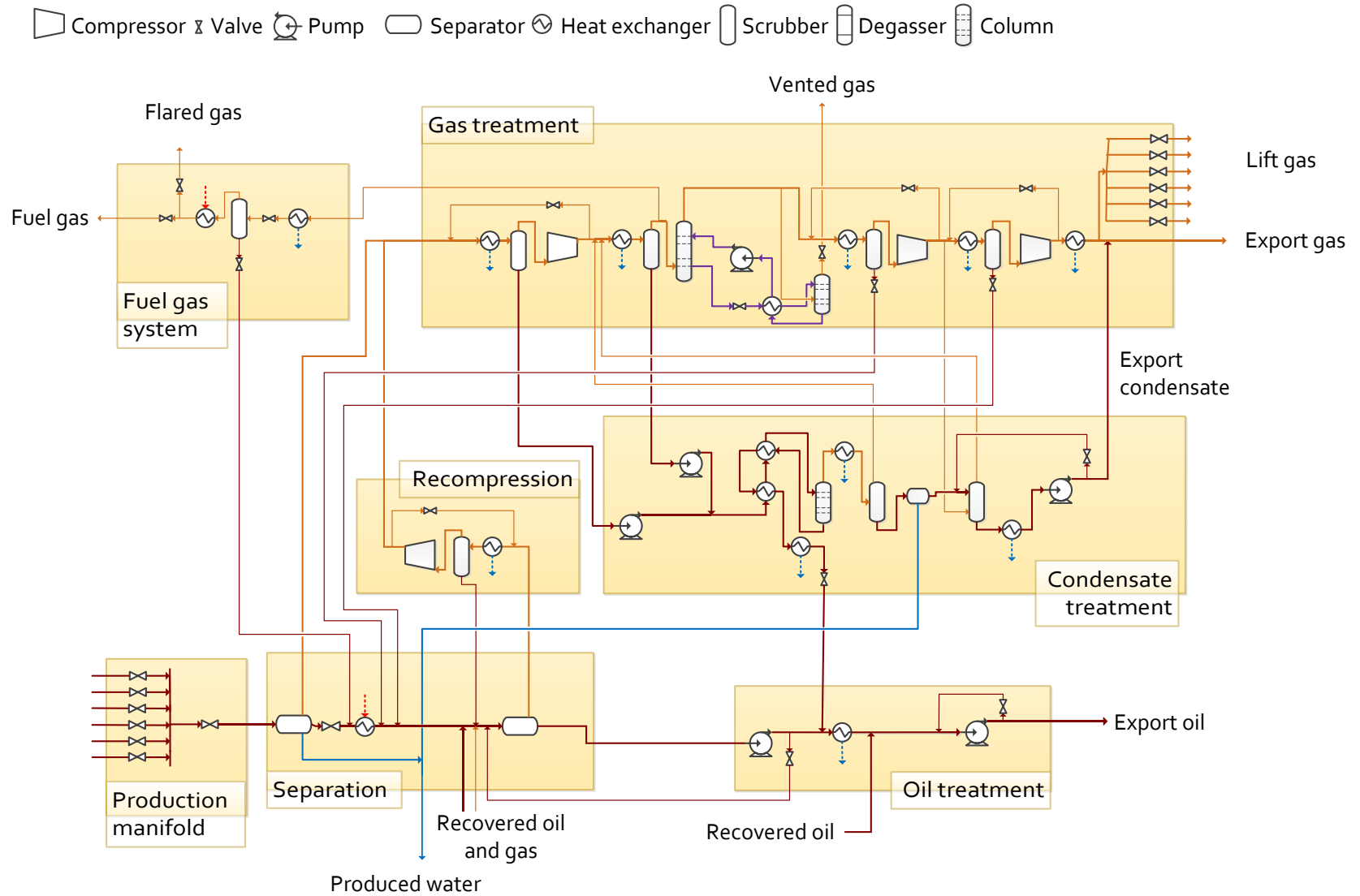
Fig. A.4. Process flowsheet of Platform D. Gas streams are shown with orange arrows, water streams with blue arrows, glycol is shown with purple arrows, and oil, condensate and mixed streams are shown with brown arrows.

References

[1]   Norwegian Ministry of Petroleum and Energy, "Facts 2012 – The Norwegian Petroleum Sector," Norwegian Petroleum Directorate, Oslo, Norway, Tech. Rep., 2012.

[2]   S. M. Svalheim, "Environmental Regulations and Measures on the Norwegian Continental Shelf," in *Proceedings of the SPE International Conference on Health, Safety and Environment in Oil and Gas Exploration and Production*. Kuala Lumpur, Malaysia: Society of Petroleum Engineers, 2002, pp. 1–10 (Paper SPE 73982).

[3]   S. M. Svalheim and D. C. King, "Life of Field Energy Performance," in *Proceedings of the SPE Offshore Europe Conference*, no. July. Aberdeen, United Kingdom: Society of Petroleum Engineers, 2003, pp. 1–10 (Paper SPE 83993).

[4]   P. Kloster, "Energy optimization on offshore installations with emphasis on offshore and combined cycle plants," in *Proceedings of the Offshore Europe Conference*. Aberdeen, United Kingdom: Society of Petroleum Engineers, 1999, pp. 1–9 (Paper SPE 56964).

[5]   P. Kloster, "Reduction of emissions to air through energy optimisation on offshore installations," in *Proceedings of the SPE International Conference on Health, Safety, and the Environment in Oil and Gas Exploration and Production*. Stavanger, Norway: Society of Petroleum Engineers, 2000, pp. 1–7 (Paper SPE 61651).

[6]   T. J. Kotas, *The Exergy Method of Thermal Plant Analysis*. Malabar, USA: Krieger Publishing, 1995.

[7]   T. J. Kotas, "Exergy Criteria of Performance for Thermal Plant: Second of two papers on exergy techniques in thermal plant analysis," *International Journal of Heat and Fluid Flow*, vol. 2, no. 4, pp. 147–163, 1980.

[8]   A. Bejan, G. Tsatsaronis, and M. Moran, *Thermal Design & Optimization*. New York, USA: John Wiley & Sons, 1996.

[9]   S. D. Oliveira Jr. and M. Van Hombeeck, "Exergy Analysis of Petroleum Separation Processes in Offshore Platforms," *Energy Conversion and Management*, vol. 38, no. 15-17, pp. 1577–1584, 1997.

[10]   M. Voldsund, I. S. Ertesvåg, W. He, and S. Kjelstrup, "Exergy analysis of the oil and gas processing a real production day on a north sea oil platform," [Energy, in press], 2013.

[11]   T.-V. Nguyen, L. Pierobon, B. Elmegaard, F. Haglind, P. Breuhaus, and M. Voldsund, "Exergetic assessment of energy systems on north sea oil and gas platforms," [Energy, in press], 2013.

[12]   Aspen Technology, *Aspen Hysys 2004.2 – User Guide*. Cambridge, USA: Aspen Technology, 2004.

[13]   D.-Y. Peng and D. B. Robinson, "A New Two-Constant Equation of State," *Industrial & Engineering Chemistry Fundamentals*, vol. 15, no. 1, pp. 59–64, Feb. 1976.

[14]   G. Soave, "Equilibrium constants from a modified Redlich–Kwong equation of state," *Chemical Engineering Science*, vol. 27, no. 6, pp. 1197–1203, 1972.

[15]   Aspen Technology, *Aspen Plus – Modelling Petroleum Processes*. Burlington, USA: Aspen Technology, 1999.

[16]   H. Renon and J. M. Prausnitz, "Local compositions in thermodynamic excess functions for liquid mixtures," *AIChE Journal*, vol. 14, no. 1, pp. 135–144, Jan. 1968.

[17]   G. Tsatsaronis, "Definitions and nomenclature in exergy analysis and exergoeconomics," *Energy*, vol. 32, no. 4, pp. 249–253, 2007.

[18]   R. Rivero, C. Rendon, and L. Monroy, "The Exergy of Crude Oil Mixtures and Petroleum Fractions: Calculation and Application," *International Journal of Applied Thermodynamics*, vol. 2, no. 3, pp. 115–123, 1999.

[19]   M. Bothamley, "Offshore Processing Options for Oil Platforms," in *Proceedings of the SPE Annual Technical Conference and Exhibition*. Houston, USA: Society of Petroleum Engineers, 2004, pp. 1–17 (Paper SPE 90325).